# Extreme events and warming in the Baltic Sea: relevance for coastal benthic communities

## Dissertation

In fulfilment of the requirements for the doctoral degree in natural sciences

**– Dr. rer. nat. –**

of the Faculty of Mathematics and Natural Sciences
at the Christian-Albrechts-Universität zu Kiel

submitted by

**Fabian Jeldrik Wolf**

Kiel, 2022

First Referee: Prof. Dr. Martin Wahl

Second Referee: Prof. Dr. Olivia Roth

Third Referee: Associate Prof. Dr. Christian Pansch-Hattich

Day of the oral examination: 13.05.2022

# Table of contents

# SUMMARY

Ongoing global climate changes leads to an increased water temperature and thus, an increased probability of critical temperatures during future heatwaves, and an extension of hypoxic areas. While summer upwelling is typically characterised by decreased temperatures, it is accompanied with low oxygen concentration, low pH, and increased salinity. With the projected increase of upwelling events, stressful upwelling with hypoxic and acidic conditions will become more likely. Although, extreme events are typically attributed with negative impacts on marine species and entire ecosystems, a mechanistical understanding of the importance of frequency, duration, and intensity of extreme events is still lacking. Furthermore, the relevance of acclimation and adaptation to changing conditions is not yet well studied, but likely plays a major role of a species response to environmental stress.

Therefore, this thesis focuses on (**i**) the characterisation of heatwaves and cold-spells in the Kiel Fjord, (**ii**) using this characterisation for treatment development, (**iii**) running mesocosm experiments to unravel the importance of frequency, duration, and intensity of environmental stress (i.e., heatwaves, upwelling, and warming) for the impact on the two important species *Asterias rubens* and *Zostera marina*, and (**iv**) the coping mechanisms of these species with (succeeding) environmental stress.

In Chapter I, heatwave and cold-spell events in the Kiel Fjord between 1997 and 2018 were characterised. This extreme event characterisation and another heatwave characterisation of the same area with a similar maximum summer heatwave intensity were used in Chapter I and Chapter II to implement realistic treatment scenarios for mesocosm experiments. Here, common today's heatwaves were simulated in addition to treatments not encompassing any heatwave. Additionally, heatwaves were prolonged, amplified, amplified and prolonged, as well as interrupted, the latter simulating upwelling events. In Chapter I and II, it was tested how these treatments impact the important predator *Asterias rubens*. Starfish were substantially impacted by heatwaves, with stronger and longer-lasting impacts in amplified and prolonged heatwaves. The impacts reached from 100% mortality (simulated future intensity) to an almost 100% decreased feeding rate, 87% reduced growth, and 63% reduced activity (today's intensity with extended duration). Imposed upwelling led to a 93% decreased starfish activity. This indicates that with ongoing warming and increased extreme event magnitude, blue mussels may be relieved from their predator *A. rubens* and may propagate into new habitats. However, the succession of extreme events (i.e., heatwave and heatwave or heatwave and upwelling) led to an alleviated impact during the second event. This indicates the acclimation potential of *A. rubens* through an ecological memory. Such an ecological memory likely plays an important role in the response of this species to changing environmental conditions and has the potential to mitigate impacts of succeeding stress events.

As the increase of heatwave magnitude is mainly driven by warming, in Chapter III the relative importance of heatwaves differing in frequency and duration (based on the heatwave characterisation presented in Chapter I) for the impact on the ecosystem engineer *Zostera marina* in contrast to warming was tested. Furthermore, in Chapter III it was tested if upwelling reduces the performance of eelgrass and if eelgrass populations from shallow habitats may be heat-selected and perform better under warming conditions. Eelgrass was not impacted by short heatwaves or upwelling alone but had 22% less leaves when the heatwave was extended, or a short heatwave was followed by upwelling. The latter combination of stressors also reduced the number of eelgrass shoots by 27%. When exposed to even longer thermal stress (i.e., long-term warming), aboveground and belowground biomass of non-heat-selected eelgrass even decreased by 74 and 80%. This indicates that eelgrass is more tolerant to short-term environmental stress than starfish but accumulates stress over longer time periods, so that eelgrass meadows might decline further with projected increased warm periods. However, eelgrass individuals from a potentially heat-selected population grew more than individuals from a non-heat-selected population. Such heat selection may be used to restore eelgrass meadows with heat-resistant genotypes, and thus alleviate the losses of eelgrasses.

Overall, this thesis highlights that extreme events are important drivers of temperate benthic ecosystems, but that their impact depends on the nature of the event, their succession, duration, and intensity. Furthermore, this thesis demonstrates that species may have the potential to cope with recurring stress events via an ecological memory or via heat-selection *in situ*.

# ZUSAMMENFASSUNG

Die globalen Klimaveränderungen führen zu einem Anstieg der Wassertemperatur, was zu einer erhöhten Wahrscheinlichkeit von kritischen Temperaturen während zukünftigen Hitzewellen führt, und einer Ausdehnung von hypoxischen Gebieten. Während der sommerliche Auftrieb typischerweise durch einen Temperaturabfall gekennzeichnet ist, geht er auch mit einer niedrigen Sauerstoffkonzentration, einem niedrigen pH-Wert und einem erhöhten Salzgehalt einher. Mit der prognostizierten Zunahme von Auftriebsereignissen werden Auftriebserscheinungen mit hypoxischen und sauren Bedingungen wahrscheinlicher. Obwohl Extremereignisse in der Regel mit negativen Auswirkungen auf marine Arten und ganze Ökosysteme in Verbindung gebracht werden, fehlt noch immer ein mechanistisches Verständnis der Bedeutung von Häufigkeit, Dauer und Intensität von Extremereignissen. Darüber hinaus ist die Bedeutung der Akklimatisierung und Anpassung an sich ändernde Bedingungen noch nicht gut untersucht, obwohl sie vermutlich eine wichtige Rolle bei der Reaktion einer Art auf Umweltstress spielt.

Daher konzentriert sich diese Arbeit auf (**i**) die Charakterisierung von Hitzewellen und Kälteperioden in der Kieler Förde, (**ii**) die Nutzung dieser Charakterisierung für die Entwicklung von experimentellen Behandlungen, (**iii**) die Durchführung von Mesokosmen-Experimenten, um die Bedeutung von Häufigkeit, Dauer und Intensität von Umweltstress (d.h. Hitzewellen, Auftrieb und Erwärmung) für die Auswirkungen auf die beiden wichtigen Arten *Asterias rubens* und *Zostera marina* zu entschlüsseln, und (**iv**) die Bewältigungsmechanismen dieser Arten bei (aufeinander folgendem) Umweltstress.

In Kapitel I wurden Hitzewellen- und Kälteereignisse in der Kieler Förde zwischen 1997 und 2018 charakterisiert. Diese Extremereignis-Charakterisierung und eine weitere Hitzewellen-Charakterisierung desselben Gebiets mit einer ähnlichen maximalen sommerlichen Hitzewellenintensität wurden in Kapitel I und Kapitel II verwendet, um realistische Behandlungsszenarien für Mesokosmen-Experimente zu verwenden. Dabei wurden sowohl die heute üblichen Hitzewellen simuliert als auch Behandlungen, die keine Hitzewelle umfassten. Außerdem wurden Hitzewellen verlängert, verstärkt, verstärkt und verlängert, sowie unterbrochen, wobei letzteres Auftriebsereignisse simulierte. In Kapitel I und II wurde untersucht, wie sich diese Behandlungen auf den wichtigen Räuber *Asterias rubens* auswirken. Die Seesterne wurden durch Hitzewellen erheblich beeinträchtigt, wobei die Auswirkungen bei verstärkten und längeren Hitzewellen stärker und länger anhaltend waren. Die Auswirkungen reichten von 100% Mortalität (simulierte zukünftige Intensität) bis zu einer um fast 100%

verringerten Fraßrate, 87% verringertem Wachstum und 63% verringerter Aktivität (heutige Intensität mit verlängerter Dauer). Das experimentelle Auftriebsereignis führte zu einer um 93% verringerten Aktivität der Seesterne. Dies deutet darauf hin, dass Miesmuscheln bei fortschreitender Erwärmung und zunehmender Stärke von Extremereignissen möglicherweise von ihrem Räuber *A. rubens* befreit werden und sich in neuen Lebensräumen ausbreiten kann. Die Abfolge von Extremereignissen (d. h. Hitzewelle und Hitzewelle oder Hitzewelle und Auftrieb) führte jedoch zu einer Abschwächung der Auswirkungen während des zweiten Ereignisses. Dies deutet auf das Akklimatisierungspotenzial von *A. rubens* durch ein ökologisches Gedächtnis hin. Ein solches ökologisches Gedächtnis spielt wahrscheinlich eine wichtige Rolle bei der Reaktion dieser Art auf sich ändernde Umweltbedingungen und hat das Potenzial, die Auswirkungen nachfolgender Stressereignisse zu mildern.

Da die Zunahme von Hitzewellen hauptsächlich auf die Erwärmung zurückzuführen ist, wurde in Kapitel III die relative Bedeutung von Hitzewellen, die sich in Häufigkeit und Dauer unterscheiden (basierend auf der Hitzewellencharakterisierung in Kapitel I) für die Auswirkungen auf den Ökosystemingenieur *Zostera marina* im Vergleich zu Erwärmung untersucht. Darüber hinaus wird in Kapitel III untersucht, ob Auftriebsereignisse das Wachstum von Seegras beeinträchtigt und ob Seegraspopulationen aus flachen Habitaten hitzeselektiert sind und sich unter wärmeren Bedingungen besser entwickeln. Das Seegras wurde durch kurze Hitzewellen oder Auftrieb allein nicht beeinträchtigt, wies aber 22% weniger Blätter auf, wenn die Hitzewelle verlängert wurde oder auf eine kurze Hitzewelle ein Auftrieb folgte. Die letztgenannte Kombination von Stressfaktoren reduzierte auch die Anzahl der Seegras-Triebe um 27%. Bei noch längerem Hitzestress (d. h. bei langfristiger Erwärmung) sank die ober- und unterirdische Biomasse von nicht Wärme-selektiertem Seegras sogar um 74 bzw. 80%. Dies deutet darauf hin, dass Seegras gegenüber kurzfristigem Umweltstress toleranter ist als Seesterne, aber über längere Zeiträume Stress akkumuliert, so dass Seegraswiesen mit den prognostizierten längeren Wärmeperioden weiter zurückgehen könnten. Allerdings wuchsen Seegras Individuen aus einer potenziell Wärme-selektierten Population stärker als Individuen aus einer nicht Wärme-selektierten Population. Eine solche Wärmeselektion könnte genutzt werden, um Seegraswiesen mit hitzeresistenten Genotypen wieder aufzuforsten und so die Verluste an Seegras zu mildern.

Insgesamt zeigt diese Arbeit, dass Extremereignisse wichtige Einflussfaktoren für benthische Ökosysteme der gemäßigten Breiten sind, dass ihre Auswirkungen jedoch von der Art des Ereignisses, seiner Abfolge, Dauer und Intensität abhängen. Darüber hinaus zeigt diese Arbeit,

dass Arten das Potenzial haben, wiederkehrende Stressereignisse durch ein ökologisches Gedächtnis oder durch Wärmeselektion *in situ* zu bewältigen.

# GENERAL INTRODUCTION

## Global climate change

### *Abiotic changes*

Since the industrial revolution, the concentration of greenhouse gases like $CO_2$ has increased 1.5-fold in the atmosphere (NOAA Climate). This growth of greenhouse gas emissions led to an increased air temperature of 1.07 °C until 2010-2019 compared to the reference period of 1850-1900 (IPCC 2021). With ongoing high greenhouse gas emissions (climate scenario SSP3-7.0; IPCC 2021), the earth's surface is projected to have warmed by 3.5 °C until 2100 (IPCC 2021).

Accompanied by atmospheric warming, the world's oceans are warming (IPCC 2021). Indeed, the oceans take up 90% of the excess energy that reaches the earth (Gebbie 2021) and are thus, buffering the atmospheric warming. However, acting as such an energy sink led to an increased ocean temperature by 0.6 °C since the beginning of the 19th century (IPCC 2019) and will reach warming of 3 °C until the end of this century (IPCC 2019, 2021). Along with a warmer globe, the pole caps are melting, which on the one hand leads to a desalination, but on the other hand to an increased sea level (Cazenave and Llovel 2010). Sea level rise is further facilitated by the thermal expansion of water masses under warmer temperatures (Nerem et al. 2006). Furthermore, increased water temperatures lead to lower solubility of gases, e.g., oxygen. Together with a more stratified water column, due to longer warm periods, hypoxic zones are spreading (Diaz 2001). Despite the lower solubility of gases, the increased amount of atmospheric $CO_2$ has diffused into the oceans and thus, led to acidification of all oceans (IPCC 2021).

Most of the above-mentioned changes of abiotic processes in the global oceans are mainly caused by global warming and is thus considered as one of the most important, if not the main, driver of climate change and its impacts on ecosystems (see e.g., Bates and Johnson 2020; Wahl et al. 2020). However, the interaction with other abiotic drivers such as oxygen availability, acidification, or salinity may change the responses of ecosystems (see e.g., Sampaio et al. 2017; Takolander et al. 2017; Wahl et al. 2021).

### *Ecosystem impacts*

Many studies have focused on the impact of ongoing climate change on various ecosystems worldwide (Walther et al. 2002; Doney et al. 2012). Perhaps, the most widely known impact of climate change is coral bleaching in tropical reefs (e.g., Glynn 1991; Hoegh-Guldberg 1999;

Hughes 2003). However, not only coral reefs but likewise other crucial benthic ecosystems like mangroves, seagrass meadows or macrophyte stands have been impacted by climate change across latitudinal ranges (Field 1995; Duarte et al. 2018). Apart from the impacts on benthic communities, climate change also decreased habitat for pelagic species by vertical compression of the suitable habitat due to the extension of hypoxic zones (Gilly et al. 2013). With ongoing warming, some species will, and already do, migrate to higher latitudes to escape unfavourable temperatures (e.g., range shifts; Poloczanska et al. 2013). This migration of species causes changes in the ecosystem at the new location (see also Coping mechanisms in a changing ocean below). Overall, climate change has already visible impacts on various ecosystems, but the impacts will intensify under current projections (IPCC 2019).

### *Environmental variability*

Superimposed on the gradual changes of e.g., temperature are environmental thermal fluctuations. These can range from seasonal changes to day-night shifts (Introduction - Figure 1). The compound effect of succeeding stress events can either have a larger impact (synergistic), the same impact (additive) or a lower impact (antagonistic) on a species than the sum of both single stress events (Gunderson et al. 2016). Environmental fluctuations can either increase or decrease the performance of a species when compared to a constant stress regime (Ruel and Ayres 1999). This direction largely depends on whether the parameter fluctuates below or above the optimum of a performance curve (i.e., Jensen's Inequality; Ruel and Ayres 1999). However, the effect also depends on the intensity, duration or rate of change (as discussed by e.g., Gunderson et al. 2016; Spillman et al. 2021).

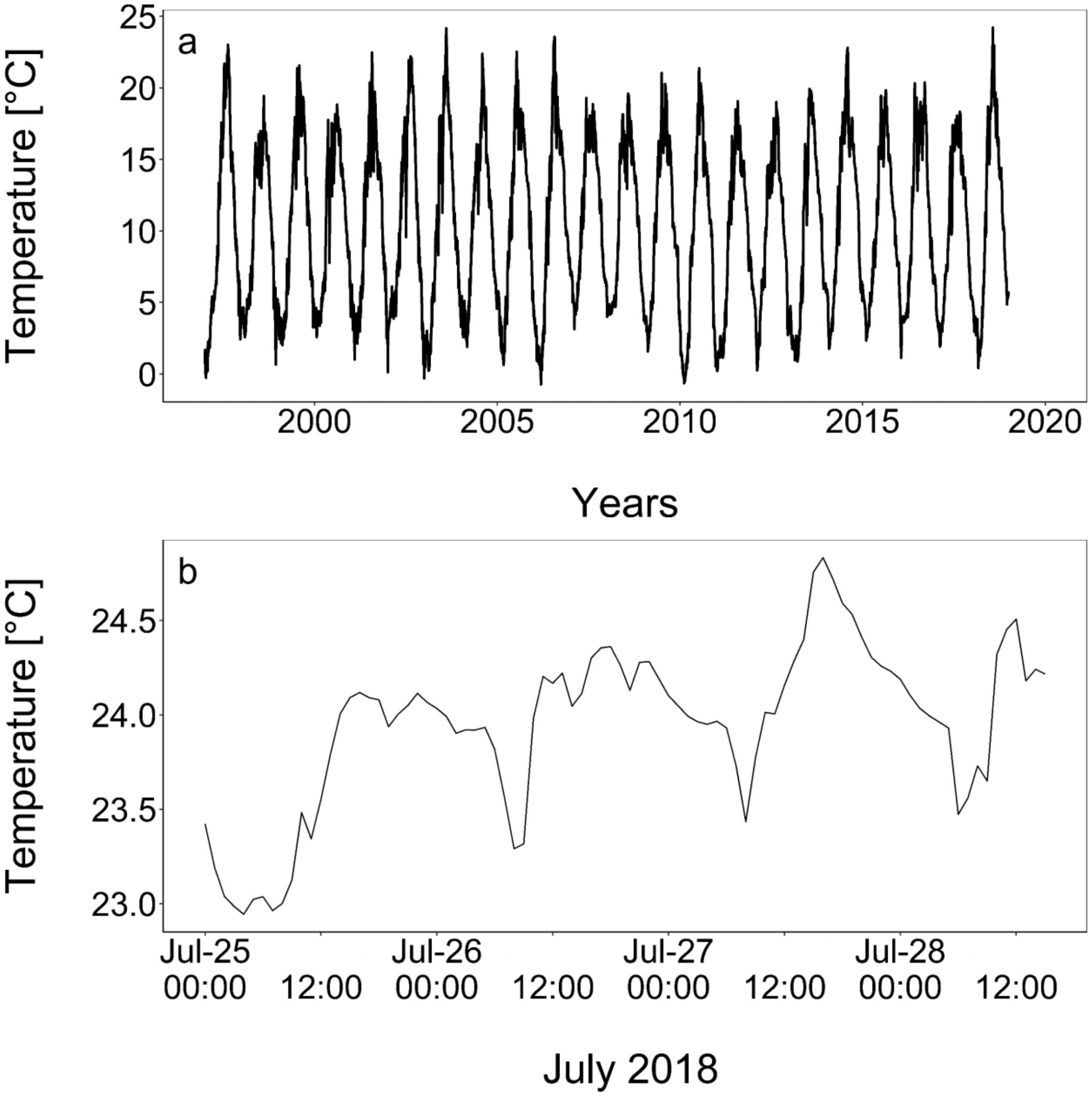

**Introduction - Figure 1:** Water temperatures in the Kiel Fjord, Baltic Sea, Germany typically fluctuate annually between 0 and 20 °C (**a**) and can have daily offsets of 1 °C (**b**). Data were obtained from a 22-year long high resolution (8 min) data set (Wolf et al. 2020).

Despite its obvious relevance in ecology, environmental variability has been neglected in experimental ecology for a long time (Thompson et al. 2013) but is now a central aspect of modern stress ecology (e.g., Benedetti-Cecchi 2003; Estay et al. 2011; Paaijmans et al. 2013; Wahl et al. 2016; Pansch and Hiebenthal 2019; Vajedsamiei et al. 2021a). Although it remains demanding to implement environmental variability in experimental research due to complex experimental set-ups, considering or including environmental variability in experiments is crucial to fully understand the potential future ecosystem changes (as discussed by Vasseur et al. 2014).

## Extreme events

Extreme events are a special case of environmental variability and by extending the definition of Broska et al. (2020) can be defined as follows: An extreme event is a disturbance that can sporadically occur and is in terms of intensity, rate of change, or duration beyond the typical conditions in the respective system. Extreme events, such as heatwaves, droughts, heavy precipitation, or storms are projected to occur more often and with a higher intensity in the future (e.g., Easterling et al. 2000; IPCC 2021). As these events represent untypical conditions in the respective system, such extremes can drive ecosystem changes as performance limits of species are likely exceeded (as discussed by Oliver et al. 2019).

### *Marine heatwaves*

Following the above-described definition of extreme events, heatwaves are temporally limited abnormally high temperatures. As heatwaves occur globally, researchers worldwide started to (**i**) focus on identifying these extreme events (e.g., Hobday et al. 2016, 2018; Oliver et al. 2021), (**ii**) monitoring their impacts (e.g., Frölicher et al. 2018; Thomsen et al. 2019; Wernberg et al. 2021), and (**iii**) experimentally testing their impacts (e.g., Winters et al. 2011; Pansch et al. 2018a; Saha et al. 2019). Although heatwaves occur globally, they can have very different causes (Oliver et al. 2021). Heatwaves can emerge with or without changes of ocean currents (Oliver et al. 2021). Usually, the Humboldt-Current brings cold, nutrient-rich deep water to the surface off Peru (Chavez et al. 2008; see also the section Upwelling and cold-spells below). During the El Niño phase of the El Niño-Southern Oscillation (ENSO) in the equatorial Pacific Ocean, the Humboldt-Current is weakened, so that surface waters off Peru are not cooled anymore by shoaled deep water, but warm up very quickly (Holbrook et al. 2019; Sen Gupta et al. 2020). During the La Niña phase of ENSO heatwaves can emerge in the Southeast Indian Ocean by a strengthening of the Leeuwin Current (Feng et al. 2013) and can lead to drastic losses of e.g., kelp forests (Wernberg et al. 2016). Yet, heatwaves can also emerge from exceptional high atmospheric temperatures (Oliver et al. 2021). These atmospherically driven heatwaves are thought to have more severe impacts on shallow compared to deeper waters (Giraldo-Ospina et al. 2020). Therefore, shallow coastal communities are particularly prone to be impacted by atmospherically driven heatwaves.

There are very different approaches of how marine heatwave are defined in the literature. Heatwaves can be defined as temperatures above a thermal optimum of a single species (e.g., Bertolini & Pastres 2021). The downside of such an approach is that each species in an ecosystem can have different thermal optima as well as critical thermal limits (Wahl et al. 2020), which makes it difficult to test the impact of heatwaves on whole communities. Additionally complicating the story, even within a species, different traits may have different thermal optima and limits (Wahl et al. 2020). However, all species in a community are exposed to the same environmental conditions. Therefore, the analysis of long-term temperature data (i.e., oceanographic heatwave definitions), can be a valuable approach when testing heatwave impacts on species and communities. Even among such oceanographic definitions, different concepts exist on how to define a marine heatwave. A rather established concept is the use of degree heating weeks (i.e., the accumulation of thermal stress over time), which is widely used in coral research (e.g., Kayanne 2017; see Introduction - Figure 2a). However, the field of heatwave research has grown in the past years and new definitions have come up. As such, Pansch et al. (2018a) defined marine heatwaves based on temperature increase rates, as particularly in shallow areas heatwaves emerge quickly (see Introduction - Figure 2b). However, the currently most widely used definition was proposed by Hobday et al. (2016). They define a heatwave, similarly to terrestrial meteorologists, as temperatures above a certain threshold, which itself is based on long-term temperature data (Hobday et al. 2016). Thus, Hobday et al. (2016) define a marine heatwave as water temperatures above the 90th percentile for at least five consecutive days, ideally based on 30-year long temperature data (see Introduction - Figure 2c). Depending on which definition one applies, the heatwave duration can range from 94 days (Introduction - Figure 2a) to only eight days (Introduction - Figure 2b) and the maximum intensity can range from 0.8 (Introduction - Figure 2c) to 5.5 °C (Introduction - Figure 2a). Also, the general occurrence or absence of a heatwave in specific periods changes depending on the heatwave definition (Introduction - Figure 2). Therefore, applying the same heatwave definition is crucial to compare the ecological impacts that stem from the respective heatwave.

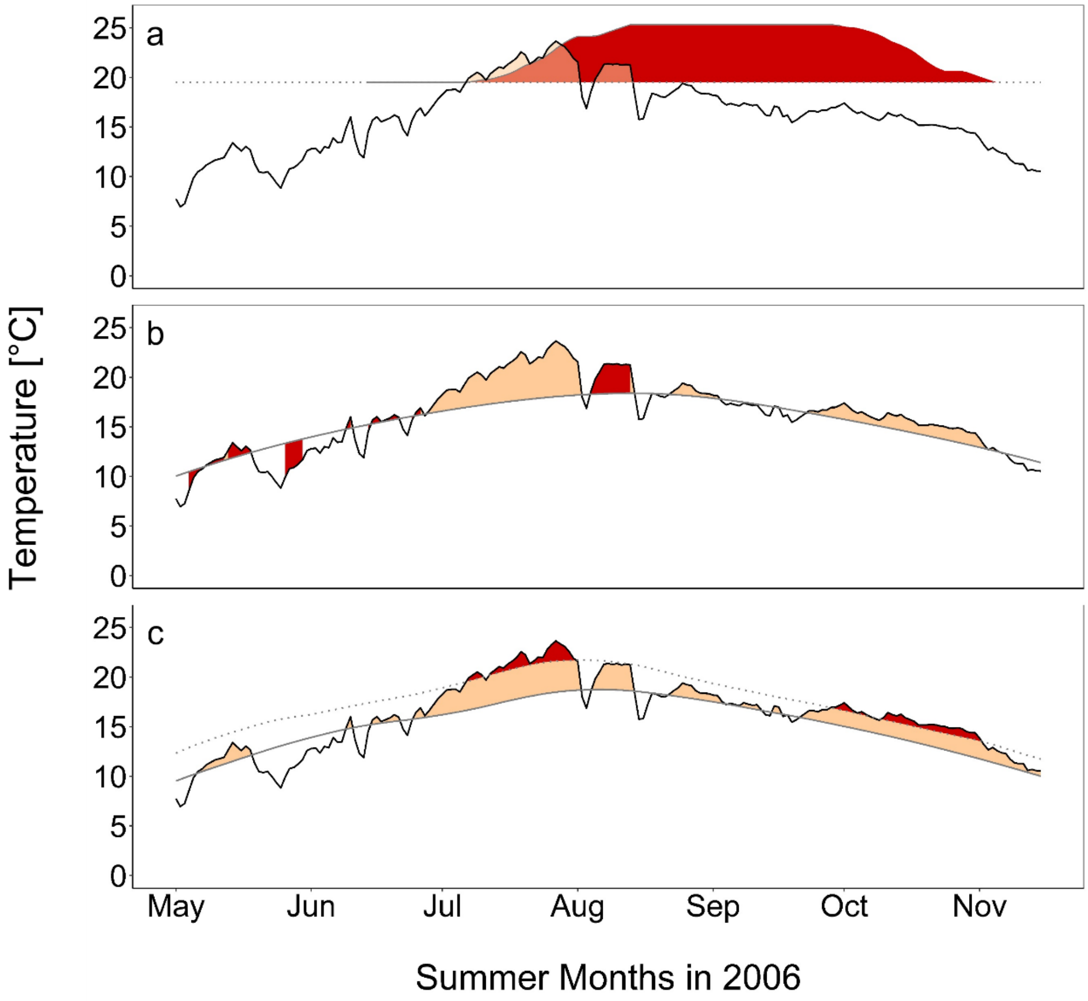

**Introduction - Figure 2:** Temperature in the summer months in 2006 (black solid lines) with indication of heatwaves following different heatwave definitions. Data are based on a 15-year long temperature data set from the Kiel Fjord (Pansch et al. 2018b). (**a**) Degree heating weeks are based on temperatures above the maximum monthly mean temperature (dotted line; Kayanne 2017). Temperatures of at least 1 °C above this threshold (orange) are summed over a rolling window of twelve weeks (Kayanne 2017) and displayed as weekly values (solid grey line, red filling). (**b**) Heatwaves are defined as onset rates of at least 0.7 °C $d^{-1}$ for at least two consecutive days (Pansch et al. 2018a) and are represented as red fillings (note that Pansch et al. 2018a ran this analysis only until end of September). Temperatures above the climatology (grey solid line) are represented as orange filling. (**c**) Heatwaves are defined as temperatures above the 90th percentile (dotted line) for at least five days (Hobday et al. 2016) and are represented as red fillings. Temperatures above the climatology (solid grey line) are represented as orange fillings.

Following the Hobday et al. (2016) heatwave definition, today's heatwaves occur 34% more often and are 17% longer compared to the beginning of the 20th century (Oliver et al. 2018). As this trend is predominantly driven by overall increasing temperatatures (Oliver 2019), critical temperatures experienced during heatwaves are projected to occur more often and endure longer in the future, when compared to today (Meehl and Tebaldi 2004; Oliver et al. 2018; Oliver 2019).

Heatwaves and their impacts have been monitored and experimentally tested globally and revealed ecosystem impacts from the tropics (e.g., Smale et al. 2019; Wernberg et al. 2021) over the subtropics (Arias-Oritz et al. 2018; Thomsen et al. 2019) to the temperate regions (e.g., Reusch et al. 2005; Pansch et al. 2018a). The El Niño event in 2015–2016, for example, has led to a record sea surface temperature in the major coral reefs and caused massive coral bleaching (Hughes et al. 2018). Other studies have revealed that also temperate ecosystems such as large macrophyte stands or seagrass meadows have already been impacted by today's heatwaves (Reusch et al. 2005; Arias-Oritz et al. 2018; Tait et al. 2021). As the overall temperature is projected to increase and heatwaves reach critical temperatures more often, more severe impacts on marine ecosystems are expected (Oliver et al. 2019). Therefore, heatwaves pose a significant and global threat to marine biodiversity.

### *Upwelling and cold-spells*

The Eastern Boundary Upwelling systems are well recognized and studied oceanic areas (see e.g., Chavez and Messié 2009). These upwelling systems change the abiotic conditions in the upper surface waters (i.e., mainly decreased temperature and increased nutrient load; e.g., Chavez and Messié 2009). Due to the nutrient input, these upwelling systems belong to the most productive ecosystems (see e.g., Chavez et al. 2008). However, apart from these large current-driven (Ekman motion theory) upwelling systems, smaller and local upwelling events can occur in coastal areas (e.g., Largier 2020).

In the Baltic Sea, wind-driven upwelling events can occur all year round. However, upwelling in different seasons may lead to different changes of abiotic conditions. In winter, the water column is well mixed, so that upwelling does not lead to significant changes in abiotic conditions (Wahl et al. 2021). However, in spring remineralised nutrients can be transported to the surface and thus, facilitate plankton growth (Wahl et al. 2021). During the warm summer period, the water column in temperate coastal areas stratifies, leaving the deeper waters cooler and more saline than the surface layers (e.g., Raateoja et al. 2010; Karstensen et al. 2014; Wahl et al. 2021). The longer this constant and warm period lasts, the more stable the stratification becomes (Yamaguchi and Suga 2019). The planktonic material that was produced in spring slowly sinks down to the sea floor below the pycnocline, where it is degraded by bacteria (Raateoja et al. 2010). Due to the formation of the two distinct water masses, exchange between those layers is limited (Breitburg et al. 2018). Therefore, the bacterial consumption of oxygen by the degradation of biological material leads to hypoxia in bottom waters with, depending on the definition, oxygen values below 4.6 mg $L^{-1}$ (Vaquer-Sunyer and Duarte 2008) or below

2 mg $L^{-1}$ (Breitburg et al. 2018). Due to overall projected higher sea surface temperatures, such oxygen minimum zones will increase in future (Diaz and Rosenberg 2008). Although, some species are adapted to live in permanent oxygen minimum zones (Levin 2003), species that only experience hypoxia irregularly are particularly threatened by this extension of hypoxic zones (Breitburg et al. 2018). Such irregular exposures can occur by upwelling of hypoxic deep water in late summer and autumn (Wahl et al. 2021). However, these upwelling events are typically not only characterised by low oxygen concentration but also by reduced pH, a drop in temperature, and an increased salinity in surface waters (Wahl et al. 2021). During late summer upwelling events, organisms living in these shallow-water habitats are exposed to abrupt changes in the aforementioned abiotic conditions (Wahl et al. 2021). As discussed by Melzner et al. (2013) and Wahl et al. (2021), the change in oxygen availability and pH during late summer upwelling are likely the two abiotic drivers that may be a threat to shallow benthic organisms.

As mentioned before, late summer upwelling is not only characterised by hypoxic and acidified waters, but also by low temperatures. Therefore, some events may be characterised as cold-spells, analogously to heatwaves (see above; Hobday et al. 2016), only that not the 90th percentile but the 10th percentile of the long-term temperature dataset is applied as threshold (Schlegel et al. 2021). However, not necessarily all upwellings need to be cold-spells. It may be that the temperature during the upwelling does not drop below the cold-spell threshold. Furthermore, it needs to be noted that also not every cold-spell in late summer needs to be caused by upwelling. However, both, upwelling as well as cold-spells may provide relaxation periods from extreme thermal stress in summer. It was shown that corals (Randall et al. 2020) and macroalgae (Lourenço et al. 2016) are partially relieved from thermal stress in upwelling areas. Thus, despite the exposure to hypoxia and other potentially critical abiotic changes, upwelling in late summer might also act as a thermal stress relieve if it interrupts a severe heatwave (Wahl et al. 2021).

## Coping mechanisms in a changing ocean

### *Migration*

When environmental conditions become suboptimal, organisms can migrate to new locations with better conditions (e.g., Poloczanska et al. 2013). Yet, migrating species may lead to ecosystem changes in their new habitats (as discussed by Doney et al. 2012). In the case of ocean warming, the escape from unfavourable high temperatures can be the migration to higher latitudes at which temperatures are more favourable for the respective species (e.g., Poloczanska et al. 2013). For stressors that occur more abruptly (e.g., marine heatwaves), migrating to deeper and thus, colder waters may represent a temporal thermal refuge (e.g., Giraldo-Ospina et al. 2020; Magel et al. 2020). Yet, deeper waters can often be hypoxic in summer when surface temperatures are highest (Introduction - Figure 3), and therefore, might prevent species from such migration.

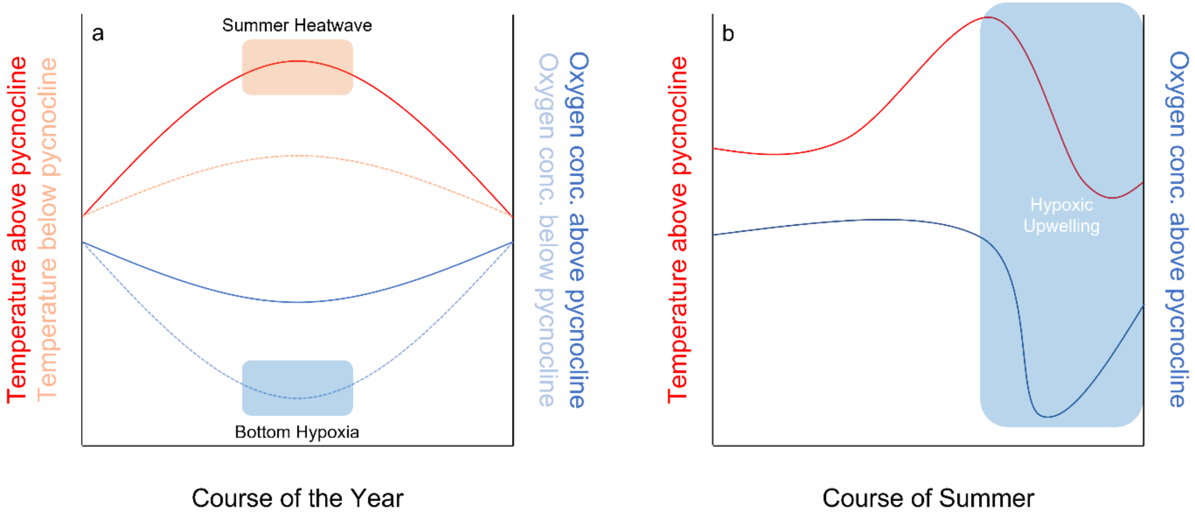

**Introduction - Figure 3:** Schematic representation of the annual course of temperature (red) and oxygen concentration (blue) above (solid line) and below (dotted line) the pycnocline (**a**) and schematic representation of temperature and oxygen concentration changes above the pycnocline during a hypothetical hypoxic upwelling event in late summer (**b**). For more details see Chapter II - Supplementary Figure 13.

### *Adaptation and acclimation*

Furthermore, species can adapt to new environmental conditions via genetic modifications that occur within a population (e.g., Rugiu et al. 2018). However, analogously to long-distance migration, such environmental change cannot occur abrupt but must be gradual so that genetic changes can manifest in the population. However, short but extreme stress events may foster adaptation in the way that such events particularly select on the most resistant genotypes from a standing population (Han et al. 2020).

Environmental stress may also provoke physiological acclimation processes on the cellular level and can involve the development of heat shock proteins (HSPs; Sørensen et al. 2003) or antioxidant enzymes (He et al. 2021). Without acclimation, individuals may also go into metabolic depression (Guppy and Withers 1999) to prevent the organism from severe damages. However, if organisms stop feeding and use up their energy reserves, this may lead to starvation and a lower condition index (e.g., Melzner et al. 2020) as well as reduced reproduction success. Therefore, physiological acclimation processes are only helpful if the stress event is of limited duration.

Besides the aforementioned active acclimation, a form of passive acclimation is the so-called ecological memory (*sensu* Jackson et al. 2021). Jackson et al. (2021) define an ecological memory as “the ability of past stressors to influence the future ecological responses of a population, community, or ecosystem (Hughes et al. 2019; Ogle et al. 2015)”. More precisely, this mechanism is referred to as stress memory if the succeeding events are of the same nature or cross stress tolerance if the events are of different nature (Munné-Bosch and Alegre 2013; Walter et al. 2013).

The mechanism of stress memory is well studied in terrestrial plants (e.g., Walter et al. 2013; Lämke et al. 2016; Tabassum et al. 2017). It was shown that recurring droughts lead to a higher resistance of plants towards future water shortage (e.g., Walter et al. 2013). However, marine ecologists only started to focus on the concept of ecological memory in the recent years (e.g., Jackson et al. 2021). Yet, there are already some examples from the marine realm: corals, for example, became more heat tolerant after being exposed to heatwaves in two consecutive years (Hughes et al. 2019) or seagrasses performed better during a heatwave if they experienced a previous heat event (Nguyen et al. 2020). However, as called for by Jackson et al. (2021), there is a need for experiments testing the resilience of species to future stress events and there is no study testing the concept of succeeding stress events of differing quality in the marine realm. Overall, ecological memory holds the possibility to help organisms or ecosystems to acclimatise to a changing ocean, particularly to respond more adequately to recurring stress events.

## The Baltic Sea

### *Abiotic conditions*

The Baltic Sea is a semi-enclosed marginal sea in Northern Europe (Kautsky and Kautsky 2000). The Baltic is characterised by its salinity gradient decreasing from North to South and West to East. While the Kattegat in the North still experiences almost fully marine conditions, the East in the Gulf of Bothnia is experiencing almost fully freshwater conditions (Kautsky and Kautsky 2000). Along this salinity gradient, the number of marine macrofauna species is decreasing from 1500 species under fully marine conditions to 52 in almost freshwater conditions (Kautsky and Kautsky 2000). The high riverine inflow does not only lead to the low salinity of the Baltic Sea, but also to the input of nutrients from agriculture to the Baltic Sea (Kautsky and Kautsky 2000). The still comparably high eutrophication status of the Baltic Sea favours planktonic growth in spring (Richardson and Heilmann 2012; Murray et al. 2019), which causes, in combination with a stably stratified water column in summer, extended hypoxic or even anoxic zones (Diaz and Rosenberg 2008). This is particularly pronounced in the Baltic Proper (Kautsky and Kautsky 2000) and in sheltered bays (Largier et al. 2020). This enhances the chance of wind-driven hypoxic upwelling in coastal areas as introduced above. As the Baltic Sea has an average depth of only 54 m (Kautsky and Kautsky 2000), the projected temperature increase until 2100 is with circa 4 °C (HELCOM 2013) higher than the global average of around 3 °C (IPCC 2021). In total, the conditions that are found in the Baltic Sea today, together with its future projections, make this marginal sea an ideal study area and is considered as ‘Time Machine’ for coastal stress ecology research (Reusch et al. 2018).

### *Ecosystems*

The Western Baltic Sea is dominated by three major habitat forming species, eelgrass (*Zostera marina*), bladder wrack (*Fucus vesiculosus*), and blue mussels (*Mytilus spp.*; HELCOM 2009). These key species are ecosystem engineers and foundation species as they provide substrate and habitat for many other species (Boström and Bonsdorff 1997; Norling and Kautsky 2007; Wikström and Kautsky 2007). In the following, I will go into further details for the eelgrass *Z. marina* as well as one of the main predators of *Mytilus* mussels, the common starfish *Asterias rubens*.

## The predator *Asterias rubens*

The starfish *Asterias rubens* is an impotant predator in coastal areas of the North-Atlantic region (Vevers 1949; Clark and Downey 1992; Budd 2008; SealifeBase). On its distribution range, this starfish experiences temperatures from -0.4 to 24.1 °C (Schlegel 2020), while its performance optimises at circa 14 °C (Melzner et al., personal communication). Furthermore, *A. rubens* experiences regularly occurring hypoxia in the inhabited regions (Diaz 2001; Fennel and Testa 2019). *A. rubens* distribution within the Baltic Sea is mainly limited by low salinities. Therefore, *A. rubens* does not occur East of the peninsula Rügen below a salinity of 8 (Kautsky and Kautsky 2000). However, the salinities typically occurring in the study area of Kiel Fjord, are not detrimental to this starfish and do not decrease its feeding rate (see Supplementary Introduction to CHAPTER II).

*A. rubens* is an important predator as this starfish controls blue mussel (*Mytilus spp.*) abundances (Reusch and Chapman 1997) and thus, the extend of blue mussel reefs. While *Mytilus* reefs are important ecosystem engineers and provide habitat for many other species (Norling and Kautsky 2007; Sadchatheeswaran et al. 2015), these blue mussels can settle on many different substrata (Dobretsov and Wahl 2001), so that they might outcompete other habitat forming species like *Fucus vesiculosus* or *Zostera marina*. Such monocultures of blue mussels would decrease the overall biodiversity (Reusch and Chapman 1997; Dürr and Wahl 2004) and thus, ecosystem services. Therefore, the study of its main predator *A. rubens* is crucial to evaluate the fate of this ecosystem under global change.

## The ecosystem engineer *Zostera marina*

The eelgrass *Zostera marina* is the most common seagrass on the northern hemisphere and widely distributed (Green and Short 2003). More specifically, *Z. marina* occurs in the Baltic, Black and Mediterranean Sea, from Norway to Roscoff (France) on the East Atlantic coast, from Nova Scotia (Canada) to New Hampshire (USA) on the West Atlantic coast, from Alaska (USA) to Mexico on the East Pacific coast and around the Japanese islands (AlgaeBase). Along its distribution range the eelgrass is experiencing temperatures from -1.6 to 28.6 °C (Schlegel 2020). *Z. marina* is tolerant to low salinities and is found throughout the Baltic Sea down to salinities of 5, albeit with implications on reproduction traits (HELCOM 2009).

As ecosystem engineer, *Z. marina* provides a three-dimensional structure and thus, habitat for many benthic vertebrate and invertebrate species (Boström and Bonsdorff 1997). Apart from its obvious important ecological role, eelgrass provides other ecosystem services that can directly impact humans. *Z. marina* meadows function as a huge carbon sink and can thus, reduce $CO_2$ concentrations in the water and indirectly from the atmosphere (Duarte et al. 2013). Also, eelgrass or their associated community may reduce the number of potential harmful bacteria in the water column (Reusch et al. 2021). Furthermore, eelgrass stabilises the sediment and therefore, reduces sediment erosion (Duarte et al. 2013). However, global warming, turbidity, and the infection with Labyrinthlomycetes are currently leading to a decreased eelgrass distribution (Muehlstein et al. 1988; Giesen et al. 1990; Hammer et al. 2018). To fully understand the impact of global change on *Z. marina*, the adaptational potential of this species as well as its vulnerability to extreme events needs to be assessed.

## AIMS, STUDY QUESTIONS AND MAIN FINDINGS

This thesis constitutes of three chapters and aims to (**i**) characterise extreme events in the Kiel Fjord, Western Baltic Sea, (**ii**) elucidate the impact of these extreme events on the key predator *Asterias rubens* and its acclimation potential to repeated events, and to (**iii**) investigate the relative impact of extreme events in contrast to global warming on the ecosystem engineer *Zostera marina*.

**CHAPTER I** describes the heatwave and cold-spell definition after Hobday et al. (2016) that was applied to a 22-year-long temperature dataset from the Kiel Fjord, Western Baltic Sea (Wolf et al. 2020). In a further step, this characterisation of extreme events was used to design close-to-natural heatwave scenarios, which were applied as treatments to test the impact of summer heatwaves on the performance of the key predator *Asterias rubens*. This study revealed a strong negative impact on *A. rubens* with longer heatwaves having a stronger impact. If the heatwaves were interrupted, simulating sporadic wind-driven (non-hypoxic) upwelling events, starfish could use the period in between heatwaves to recover, which led to an overall better performance of *A. rubens* compared to individuals exposed to continuous heatwaves. In addition, starfish subjected to repeated short-term heatwave events showed signs of acclimation to thermal stress, which might hint towards the development of an ecological memory in form of a stress memory (i.e., acclimation to recurrent events of the same nature; *sensu* Jackson et al. 2021). Overall, I could demonstrate that (**i**) extreme event characterisation is a valuable tool to create most natural treatments and that (**ii**) starfish are strongly negatively impacted by heatwaves of today's intensity but (**iii**) the interruption of heatwaves allow recovery from thermal stress.

**CHAPTER II** tests the hypothesis that heatwaves of longer duration and increased intensity, characteristics projected for the future ocean, impact the performance of the starfish *Asterias rubens* more severely than common heatwaves of today. Furthermore, this chapter tests if the experience of a heatwave in summer modifies the starfish's response to a succeeding upwelling event that may irregularly occur in the study area in late summer and early autumn. Heatwaves of increased intensity (just 1 °C above recorded temperatures) were 100% lethal to starfish. Extended heatwaves led to a strongly reduced overall performance in activity and feeding of *A. rubens*, and this pattern was observed also beyond the heatwave period, leading to a reduced size of individuals. Moreover, starfish that previously experienced a heatwave of today's intensity, significantly improved their activity during the succeeding upwelling conditions, when compared to individuals that never experienced a heatwave event. Thus, this study supports the hypotheses that (**i**) heatwaves projected for the near future have a more severe impact on starfish than heatwaves of today's magnitude and that (**ii**) the response of *A. rubens* in successive stress events may be modified through a cross-stress tolerance.

**CHAPTER III** tests the relative importance of heatwaves and upwelling events on the ecosystem engineer *Zostera marina* in contrast to long-term warming. Furthermore, this study tested if potentially heat-selected eelgrass individuals perform better under a warming scenario than individuals that were not heat-selected. This study reveals that extreme events (heatwaves of today's intensity and subsequent upwelling) have only minor impacts on eelgrass. Long-term warming, applied across seasons and including natural peaks and heatwaves, on the other hand, can strongly reduce overall plant biomass of eelgrass. Noteworthily, eelgrass individuals coming from a potentially heat-selected population performed better than individuals from less thermally stressful habitats. However, with ongoing global warming the probability of critical temperatures during future heatwaves will likely increase. Thus, eelgrass populations are likely threatened by a steady increase in seawater temperature and potentially by heatwave events that exceed eelgrass' capacities in the future Baltic Sea. Yet, the potential for heat-selection may be used in reforestation projects. This study supports the hypotheses that (**i**) *Z. marina* is negatively impacted by warming and heatwaves and that (**ii**) heat selection in extreme habitats may provide population tolerance to future warming.

## Chapters and authors contributions

Some chapters of this doctoral thesis have been published or submitted to peer-reviewed journals.

### *Chapter I: The role of recovery phases in mitigating the negative impacts of marine heatwaves on the sea star Asterias rubens*

Authors: Fabian Wolf, Katja Seebass, Christian Pansch

History: Published in Frontiers in Marine Science (doi: 10.3389/fmars.2021.790241)

Author contributions: FW and CP initiated and designed this study. FW and KS collected the data. FW analyzed the data and wrote the manuscript. All co-authors contributed to the final version of the manuscript.

### *Chapter II: Marine heatwaves and upwelling shape stress responses in a keystone predator*

Authors: Sarah Rühmkorff*, Fabian Wolf*, Jahangir Vajedsamiei, Francisco Rafael Barboza, Claas Hiebenthal, Christian Pansch

* shared first authorship

History: Currently under consideration for publication, Resubmitted (April 6th, 2022) to *Proceedings of the Royal Society B*.

Author contributions: CP and FW initiated and designed this study. FW and SR collected the data. FW, SR, JV and FRB analysed the data. FW and SR wrote the manuscript. All co-authors contributed to the final version of the manuscript.

### *Chapter III: Accumulation of stress drives eelgrass losses in non-heat-selected populations*

Authors: Fabian Wolf, Christian Pansch, Florian Weinberger

History: Not-submitted

Authors contributions: FaW, CP and FlW initiated and designed this study. FaW and FlW collected the data. FaW analysed the data. FaW wrote the manuscript. All co-authors contributed to the final version of the manuscript.

# CHAPTER I

# The role of recovery phases in mitigating the negative impacts of marine heatwaves on the sea star *Asterias rubens*

**Running head:** Heatwave impacts on sea stars

**List of authors:** Fabian Wolf [1*], Katja Seebass[2], Christian Pansch [1, 3]

**Institute or laboratory of origin:** [1] Department of Marine Ecology, GEOMAR Helmholtz Centre for Ocean Research Kiel, 24105 Kiel, Germany; [2] Faculty of Mathematics and Natural Sciences, Christian-Albrechts-University Kiel, 24118 Kiel, Germany; [3] Environmental and Marine Biology, Åbo Akademi University, 20520 Åbo, Finland

[*] **Corresponding author:** Fabian Wolf, GEOMAR Helmholtz Centre for Ocean Research Kiel, Düsternbrooker Weg 20, 24105 Kiel, Germany, telephone: +49 431 600 1599, E-Mail: fabian.wolf.research@gmail.com

**ORCIDs:** FW: 0000-0002-0955-8487, KS: 0000-0001-6520-7369, CP: 0000-0001-8442-4502

**Keywords:** climate change, warming (heating), environmental fluctuation, extreme events, marine heatwaves (MHWs), mitigation, recovery

## Abstract

During recent years, experimental ecology started to focus on regional to local environmental fluctuations in the context of global climate change. Among these, marine heatwaves can pose significant threats to marine organisms. Yet, experimental studies that include fluctuating thermal stress are rare, and if available often fail to base experimental treatments on available long-term environmental data.

We evaluated 22-year high-resolution sea surface temperature data on the occurrence of heatwaves and cold-spells in a temperate coastal marine environment. The absence of a general warming trend in the data may in parts be responsible for a lack of changes in heatwave occurrences (frequency) and their traits (intensity, duration, and rate of change) over time. Yet, the retrieved traits for present-day heatwaves ensured most-natural treatment scenarios, enabling an experimental examination of the impacts of marine heatwaves and phases of recovery on an important temperate predator, the common sea star *Asterias rubens*. In a 68-days long experiment, we compared a 37- and a 28-days long heatwave with a treatment that consisted of three consecutive 12-days long heatwaves with four days of recovery in between. The heatwaves had an intensity of 4.6 °C above climatological records, resulting in a maximum temperature of 23.25 °C.

We demonstrate that heatwaves decrease feeding and activity of *A. rubens*, with longer heatwaves having a more severe and lasting impact on overall feeding pressure (up to 99.7% decrease in feeding rate) and growth (up to 87% reduction in growth rate). Furthermore, heatwaves of similar overall mean temperature, but interrupted, had a minor impact compared to continuous heatwaves, and the impact diminished with repeated heatwave events.

We experimentally demonstrated that mild heatwaves of today’s strength decrease the performance of *A. rubens*. However, this echinoderm may use naturally occurring short interruptions of thermal stress as recovery to persist in a changing and variable ocean. Thus, our results emphasize the significance of thermal fluctuations and especially, the succession and timing of heat-stress events.

## Introduction

Anthropogenically induced climate change alters the abiotic conditions for all marine organisms and ecosystems (IPCC 2021). Thereby, sea surface temperatures (SSTs) are projected to increase by 3 °C until the end of this century (IPCC 2021), which has been shown to negatively impact ecosystems worldwide (Walther et al. 2002; Doney et al. 2012; IPCC 2021).

Thermal fluctuations are superimposed on this gradual change in temperature, reaching from yearly (seasonal) to daily (day-night) or tidal fluctuations. While colder periods may serve as refuge from heat stress in a fluctuating world, peak temperatures cause high thermal stress temporally (Wahl et al. 2015). Therefore, the examination of natural fluctuations and their extremes is key to understand a system's response to a warming ocean. Among the most important thermal fluctuations, heatwave events are projected to increase in frequency, duration, and intensity worldwide (Oliver et al. 2018), with particular intensification in marginal shallow seas, like the Baltic Sea (Gräwe et al. 2013).

Heatwaves have a high potential of impacting marine ecosystems, by exceeding the thermal limits of species (Oliver et al. 2019; Smale et al. 2019). Much research has been done in tropical systems such as coral reefs, as slight temperature deviations can have massive impacts leading to e.g., coral bleaching (Le Nohaïc et al. 2017). In coral reef ecosystems, the accumulation of thermal anomalies is used to assess the bleaching potential (degree heating weeks; e.g., Kayanne 2017). The impact of temperature events on marine ecosystems therefore depends on a heatwave's intensity, but also on traits such as duration (e.g., Oliver et al. 2019) and onset rates (e.g., Genin et al. 2020). Thus, even in temperate regions, with generally higher thermal variability, heatwaves can have strong impacts on marine ecosystems (Pansch et al. 2018; Smale et al. 2019), yet the overall effect strength and direction may strongly depend on the timing of the heatwave event and on the environmental history of the community (Pansch et al. 2018).

Generally, acclimation to environmental change may occur across species, challenging reliable predictions of future ecosystem changes. As shown for multiple simultaneous drivers (Boyd et al. 2018), consecutive stress events (e.g., recurring marine heatwaves) can either have additive, antagonistic or synergistic impacts on species (Gunderson et al. 2016). Antagonistic impacts can mean that a first stressor prepares the organism to respond more adequately when the same stressor recurs, a concept referred to as 'stress memory' or 'ecological memory' (e.g., Walter et al. 2013; Jackson et al. 2021). At the species level, such processes are triggered by, for example, the expression of heat shock proteins (HSPs, e.g., Todgham et al. 2005; Banti et al. 2008; McBryan et al. 2016), while at the population and the community level, genotype, and species sorting as well as changes in dispersal capacities or species interactions can trigger such “lagged” effects, long after a stress event occurred (as discussed by Jackson et al. 2021).

Environmental climate change has the potential to drive ecosystem responses if keystone species are impacted (Sanford 1999). The common sea star (*Asterias rubens*) is such a keystone species in the temperate benthic communities of the Atlantic Ocean, North Sea and Baltic Sea (Vevers 1949; Budd 2008). This species is an important part of the ecosystem as it controls the abundance of mussels and thus, the distribution of mussel beds (Gaymer et al. 2001). Mussels, e.g., blue mussels, (*Mytilus spp.*) play an important role as ecosystem engineers by providing habitat for many other species (Norling and Kautsky 2007; Sadchatheeswaran et al. 2015). Yet, when released from one of their main predators, mussels might outcompete other important structure-forming species like seagrasses and macroalgae by forming large monocultures and thus decreasing overall diversity (Reusch and Chapman 1997; Dürr and Wahl 2004).

Even though the importance of environmental variability, including marine heatwaves, is widely acknowledged in the scientific community (Pincebourde et al. 2012; Gunderson et al. 2016; Smale et al. 2019), this aspect is often neglected in experimental ecology. One major problem may be the lack of a universal characterization of variability such as marine heatwave events. In this study, we used a physical (oceanographic) approach suggested by Hobday et al. (2016), which is now widely used in characterizing marine heatwave events globally (Oliver et al. 2019; Smale et al. 2019; Thomsen et al. 2019), thus allowing for a worldwide comparison of events and their impacts. Hobday et al. (2016) defined a heatwave as temperatures that exceed the 90th percentile of a long-term temperature dataset for at least five consecutive days. Our experimental treatments were designed using a 22-years high-resolution (8 minutes intervals) SST dataset available for the Kiel Fjord (Wolf et al. 2020). We tested the impact of heatwave events of different duration and frequency on the keystone predator *A. rubens*. We expected a decreased performance of *A. rubens* with increasing duration of the heatwave and a mitigation of heatwave impacts in a scenario that applied successive heatwave events and therefore periods for recovery. In contrast to many existing studies, we measured sea star traits, feeding in particular, at high temporal resolution, allowing for a better approximation of the instant responses of this species to the short-term stress events, explaining long-term consequences.

## Methods

### *The study system*

The Baltic Sea as a semi-enclosed marginal shelf sea, is characterized by its shallow waters with an average depth of 54 m (Leppäranta and Myrberg 2009). Here, unlike most of the world's oceans, SST is projected to increase by up to 4 °C by the end of the century (HELCOM 2013; 3 °C worldwide: IPCC 2021). Therefore, the Baltic Sea provides an ideal study area as it already shows conditions today that are projected for 2100 in other regions and may thus be considered as "Time Machine" for climate change research (Reusch et al. 2018).

### *Modelling heatwave traits*

Extreme event identification and calculation of their traits in different seasons (i.e., frequency, duration, maximum intensity, cumulative intensity, onset rate and decline rate), was performed using the "heatwaveR" package (Schlegel and Smit 2018) in R (R Core Team 2021), which is based on the heatwave definition by Hobday et al. (2016). The script uses a moving window of eleven days to provide a climatology as well as 90th and 10th percentile thresholds from which heatwave and cold-spell traits are determined, respectively. We used a 22-years high-resolution (8 minutes intervals) sea surface (1.8 m depth) temperature dataset from the Kiel Fjord provided by GEOMAR weather station (Wolf et al. 2020). We extracted daily means, which were then implemented into R. The longest period with missing data was between May 25th, 1999 and June 16th, 1999. Therefore, the maximum gap length was set to 23 days into the "heatwaveR" package, in which the temperature was linearly extrapolated.

### *Using heatwave traits for defining the experimental treatments*

We applied treatments with summer heatwaves differing in their duration and sequence. The underlying seasonal summer temperature is based on the temperature modelling as described above (i.e., the extracted climatological values) and provided the baseline (*No* heatwave treatment; Chapter I - Figure 1A). The *No* heatwave treatment experiences temperatures starting with 16.57 °C, maximizing to 18.64 °C and ending with 16.69 °C. A mean summer heatwave intensity of 4.6 °C above seasonality and a maximum onset rate of 0.7 °C and decline rate of 1.4 °C per day (see bold values in Chapter I - Supplementary Table 1) were used as baseline for the applied heatwave treatments. The *Interrupted* heatwave consisted of three single heatwave events of 12 days each above seasonality (Chapter I - Figure 1B; 5 or 7 days above the 90th percentile threshold for the first two or the last heatwave, respectively), representing minimum duration as found from the 22-year dataset (see bold values in Chapter I -

Supplementary Table 1). The heatwaves were separated by four relaxation days in between (Chapter I - Figure 1B). Maximum temperatures for each of these three short heatwave events were 22.84, 23.25 and 22.63 °C, respectively (Chapter I - Figure 1B). To achieve the same overall average temperature of 19.2 °C of the *Interrupted* heatwave treatment, the *Present-day* heatwave (Chapter I - Figure 1C) had a duration of 28 days above the seasonality (20 days above the 90th percentile threshold) reaching a maximum temperature of 23.25 °C. This duration lies within the maximum identified summer heatwave duration of 39 days (Chapter I - Supplementary Table 1). The *Extended* heatwave had a duration of 37 days above the seasonality (31 days above the 90th percentile threshold) and is simulating a scenario in which the *Present-day* heatwave is not interrupted by a typical cold-spell (Chapter I - Figure 1D). A typical cold-spell in summer has a duration of at least 6 days below the 10th percentile (Chapter I - Supplementary Table 2). Such a cold-spell would last for a total of nine days, when starting and ending at the temperature of the seasonal baseline. This represents the difference in duration between the *Present-day* and *Extended* heatwave treatment, if starting and closing from the seasonal temperature baseline.

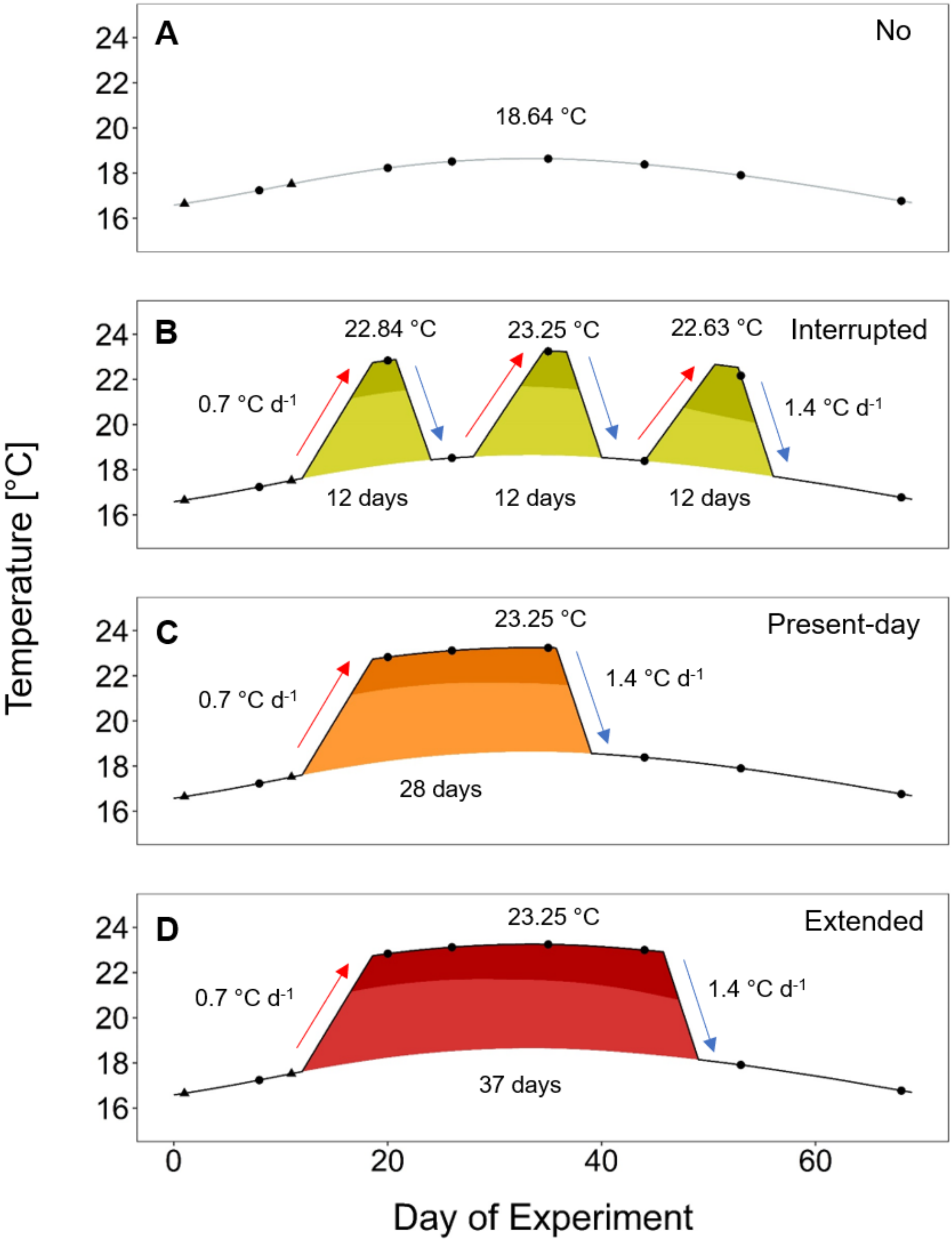

**Chapter I - Figure 1:** Experimental treatments based on the heatwave definition by Hobday et al. 2016. The treatments followed a smoothed natural summer seasonal temperature profile (No heatwave, grey line in **A**; "climatological values" in Hobday et al. 2016) or experienced three short heatwaves of 12 days each (Interrupted, yellow-green filling in **B**), a heatwave of 28 days (Present day, orange filling in **C**) or a heatwave of an extended duration of 37 days (Extended, red filling in **D**). Durations refer to the period with temperatures above the climatological values. Temperatures above the 90th percentile are shown in a darker shade. All heatwaves had a maximum peak of +4.6 °C above the climatological values. Mean temperatures of the Interrupted and Present-day heatwave treatments were equal. Black triangles represent measuring points for wet weight of A. rubens, and black dots indicate additional assessments of righting responses.

### *Experimental set-up*

The treatments were applied in the Kiel Indoor Benthocosms (Pansch and Hiebenthal 2019) from July 5th to September 10th, 2019. The KIBs are a state-of-the-art mesocosm system comprised of twelve 600 L tanks, which served as water baths for each six replicated experimental units (2 L Kautex bottles). Every treatment was applied in two separate and randomly chosen tanks leading to a replication of n=12. Temperature was logged hourly in all ten tanks (EnvLogger, ElectricBlue, Vairão, Portugal; see Chapter I - Supplementary Figure 1 for attained temperatures). Additionally, temperature was monitored by measuring with a handheld thermometer at least every three days (TTX 110 type T, Ebro, Ingolstadt, Germany). Salinity, pH and oxygen concentration were also monitored over the experimental period (Multi 3630 IDS, WTW, Kaiserslautern, Germany; see Chapter I - Supplementary Figure 2). Each of the 72 experimental units contained one separate sea star individual. Though six of the experimental units were placed in the same tank, all of them had a separate water inflow and aeration and were thus considered as independent replicates, yet, potential tank effects were accounted for in the model by including the individual sea star as random factor (see Data analysis below). The temperature in each of the tanks is automatically controlled via chillers and heating elements (Pansch and Hiebenthal 2019). Due to a short malfunctioning of the system, oxygen levels in the experimental units dropped to circa 2 mg $L^{-1}$ (pH down to 7.1) for one out of 68 days in all treatments (Chapter I - Supplementary Figure 2). As this stress was only experienced for a short time, presumably all starfish were impacted equally, and we did not observe any impacts on the sea stars (such short-term hypoxic events are relatively common in the area with 18 days of upwelling favorable winds per summer; Karstensen et al. 2014), we continued with the experiment.

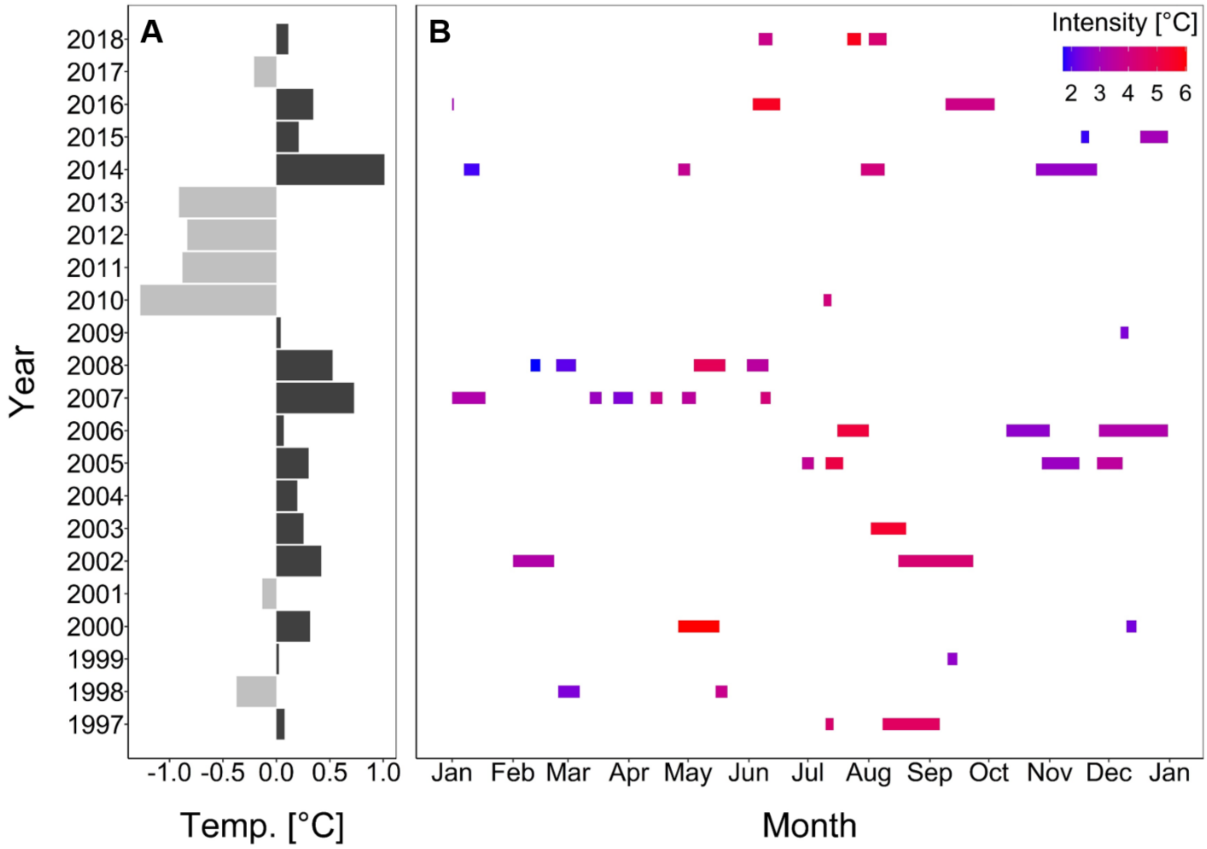

**Chapter I - Figure 2:** Deviations from annual mean seawater temperature from a 22-year mean (**A**; Wolf et al. 2020) and heatwave durations in different months over the 22-year record (B). Colors in **A** represent cold (light grey) or warm (dark grey) years, and in **B** the intensity of the heatwave (i.e., maximum amplitude above the climatological value).

### *The study organism*

We collected *A. rubens* individuals in Möltenort, Kiel, Germany (N54°22'57.5", E010°12'8.8") on July 1st, 2019. Directly after collection, all sea stars were brought to a climate room and placed inside a 600 L tank with a temperature of 18 °C as was measured at the collection site while sampling. The sea stars were fed *ad libitum* with blue mussels. When starting the experiment only sea stars of similar weight (11.3 ± 1.4 g SD) were used.

### *Response variables*

We measured feeding rate (mg mussel dry weight per day), wet weight change (g) and righting time as a measure for the activity of *A. rubens* (min). For feeding rate, blue mussels (*Mytilus* spp.) between 1.5 and 2 cm shell length were collected the day prior to the feeding at piers next to GEOMAR, Kiel, Germany (N54°19'45.8", E010°08'56.4"). At each feeding event, mussels inside each experimental unit were replaced with the freshly collected mussels. At the same time, we measured the shell length of consumed mussels (Dial Caliper DialMax Metric, Wiha Division KWB Switzerland). As previously described, the mussel's shell length and tissue dry weight correlate strongly (Supplementary Material in Morón Lugo et al. 2020). Therefore, we used this correlation to estimate the dry weight of mussels consumed by the sea stars. Wet weight of the sea stars was measured at the start of the experiment, right before the heatwaves started, before the *Present-day* heatwave started to decline, before the *Extended* heatwave started to decline and at the end of the experiment (Chapter I - Figure 1). The righting time was measured by turning the sea star on its aboral side and stopping the time it needed to fully turn back on its oral side (Lawrence and Cowell 1996). These measurements were taken at the same days as weighing (Chapter I - Figure 1) to reduce unnecessary handling stress for the sea stars.

### *Data analysis*

All data were analyzed using R (R Core Team 2021).

The trends of extreme event properties were analyzed using Generalized Additive Models (GAMs), applying the function *bam* from the package “mgcv” (Wood 2017). The models were fitted assuming Gaussian distribution of errors for all parameters, but for frequency of events. As the frequency represents count data, a Poisson distribution of errors was assumed. The smooth terms for all peak dates and months were adjusted using thin plate regression splines, while the smoothing parameters were estimated via Restricted Maximum Likelihood (Wood 2017). For duration and cumulative intensity an additional autocorrelation factor rho was included in the model.

We analyzed the impact of our treatments over time on the performance (feeding rate, wet weight and righting time) of *A. rubens* using sophisticated regression approaches. We used Generalized Additive Mixed-effects Models (GAMMs) for identifying trends in feeding rate and righting time over the course of the experiment. Therefore, the function *bam* from the package “mgcv” (Wood 2017) was used. We chose GAMMs for feeding rate and righting time as the observed pattern was complex and not linear. The models were fitted assuming Gaussian distribution of errors. The smooth terms for all applied treatments over the experimental period were adjusted using thin plate regression splines, while the smoothing parameters were estimated via REML (Wood 2017). As all measurements were repeated through time on the same individuals, identity of the respective individual (i.e., replicate) was included as random effect. The temporal trends of the GAMMs in the different treatments were compared using the function *plot_diff* found in the package “itsadug” (van Rij et al. 2020).

In contrast to feeding rate and righting time, the pattern for wet weight was linear, so we applied a Linear Mixed-effect Model (LMM) showing the growth trends over time. Therefore, the function *lmer* from the package “lme4” (Bates et al. 2015) was used, in which the interaction between time and treatment was included, to elucidate the changes over the experimental period subjected to our applied treatments. To account for the repeated measurements of the same individual, we included individual identity as random effect. Identically as for the GAMMs, REML was used to estimate smoothing parameters.

An LMM using REML was applied to identify the impact of the three consecutive heatwaves in the *Interrupted* heatwave treatment on the average feeding rate during each heatwave event. This was compared to the feeding rate in the *No* heatwave treatment during the same periods. Therefore, we included the interaction between treatment and the heatwave event as fixed effects, as well as identity of individuals as random effect.

For all response variables an additional LMM was applied using REML to identify the treatment's overall impact at the end of the experiment. In these models, only the treatment as fixed effect and the identity of individuals as random effect were included. The output for all LMMs were generated via the function *emmeans* of the equally named package, in which the contrast analysis is based on a Tukey-test (Lenth 2020).

The assumptions for all models were thoroughly checked via visual inspection of residual plots.

## Results

### *Heatwave characteristics and trends*

Between 1997 and 2018, only the onset rate of cold-spells decreased significantly (Chapter I - Supplementary Figure 3E). All other parameter of cold-spells as well as heatwaves did not change significantly during this time (Chapter I - Supplementary Figure 3 and Chapter I - Supplementary Figure 4). Though, cold-spells tended to increase in duration and cumulative intensity (Chapter I - Supplementary Figure 3B and D), while maximum intensity and decline rate tended to decrease (Chapter I - Supplementary Figure 3C and F). Cold-spell frequency and all heatwave characteristics on the other hand, did not show any trend (Chapter I - Supplementary Figure 3A and Chapter I - Supplementary Figure 4A-F). Although, date of occurrence of the extreme events did mostly not significantly explain the given trend, the maximum intensity, onset and decline rate for heatwaves as well as cold-spells differed significantly between months (Chapter I - Supplementary Figure 3C, E, F and Chapter I - Supplementary Figure 4C, E, F). Generally, cold years favored cold-spells, whereas warm years favored heatwaves (Chapter I - Supplementary Figure 5 and Chapter I - Figure 2).

Heatwaves usually occur 1.8 times per year with a mean duration of 14.9 days and an intensity of 3.6 °C. (Chapter I - Supplementary Table 1). At the same time, cold-spells occur twice per year on average with a mean duration and intensity of 12.7 days and 3.7 °C, respectively (Chapter I - Supplementary Table 2). These parameters differ throughout the seasons (Chapter I - Supplementary Table 1 and Chapter I - Supplementary Table 2).

### *Feeding rates over time*

Sea stars (*A. rubens*) increased their feeding rate over the 68-days experiment but stopped feeding immediately as soon as the heatwave started in both, the *Present-day* and *Extended* heatwave treatments (Chapter I - Figure 3A). Yet, sea stars in the *Present-day* heatwave treatment fed on as many mussels as in the *No* heatwave treatment by the end of the experiment (Chapter I - Figure 3A). Feeding rates were also reduced in the *Interrupted* heatwave treatment, but less than in the two continuous heatwave treatments (Chapter I - Figure 3A). This is also indicated by the non-significant reduction of feeding rates during the first heatwave of the *Interrupted* heatwave treatment (Chapter I - Figure 4A). However, the second and third heatwave reduced the feeding rate significantly by 72 and 45%, respectively (Chapter I - Figure 4B and C). The reduced performance during heatwaves is further indicated by an overall diminished feeding rate in heatwave treatments, with a more severe impact the longer the event lasted (up to 99.7% decrease in the *Extended* compared to the *No* heatwave treatment; Chapter I - Figure 3A and B).

### *Wet weights*

Growth rates, as indicated by changes in weight, decreased by 39, 70, and 87% in the *Interrupted*, *Present-day* and *Extended* heatwave treatments when compared to the reference treatment (i.e., the *No* heatwave treatment), respectively (slopes of GAMMs in Chapter I - Figure 3C). Overall, wet weight only decreased significantly in the *Present-day* and *Extended* heatwave treatments (Chapter I - Figure 3D). Similarly to the feeding rates, the effect was more severe in the *Extended* heatwave treatment (Chapter I - Figure 3C and D).

### *Reduced righting time during continuous heatwaves*

Only during the *Present-day* and *Extended* heatwave event the righting time of sea stars (a measure of activity) was significantly increased (i.e., low activity), whereas specimens in the *Interrupted* heatwave treatment did not show a lower activity (Chapter I - Figure 3E). Although sea stars were as active after the *Extended* heatwave had ended as before the heatwave had started, there was an overall negative impact of the *Extended* heatwave on the activity of the sea stars (Chapter I - Figure 3F).

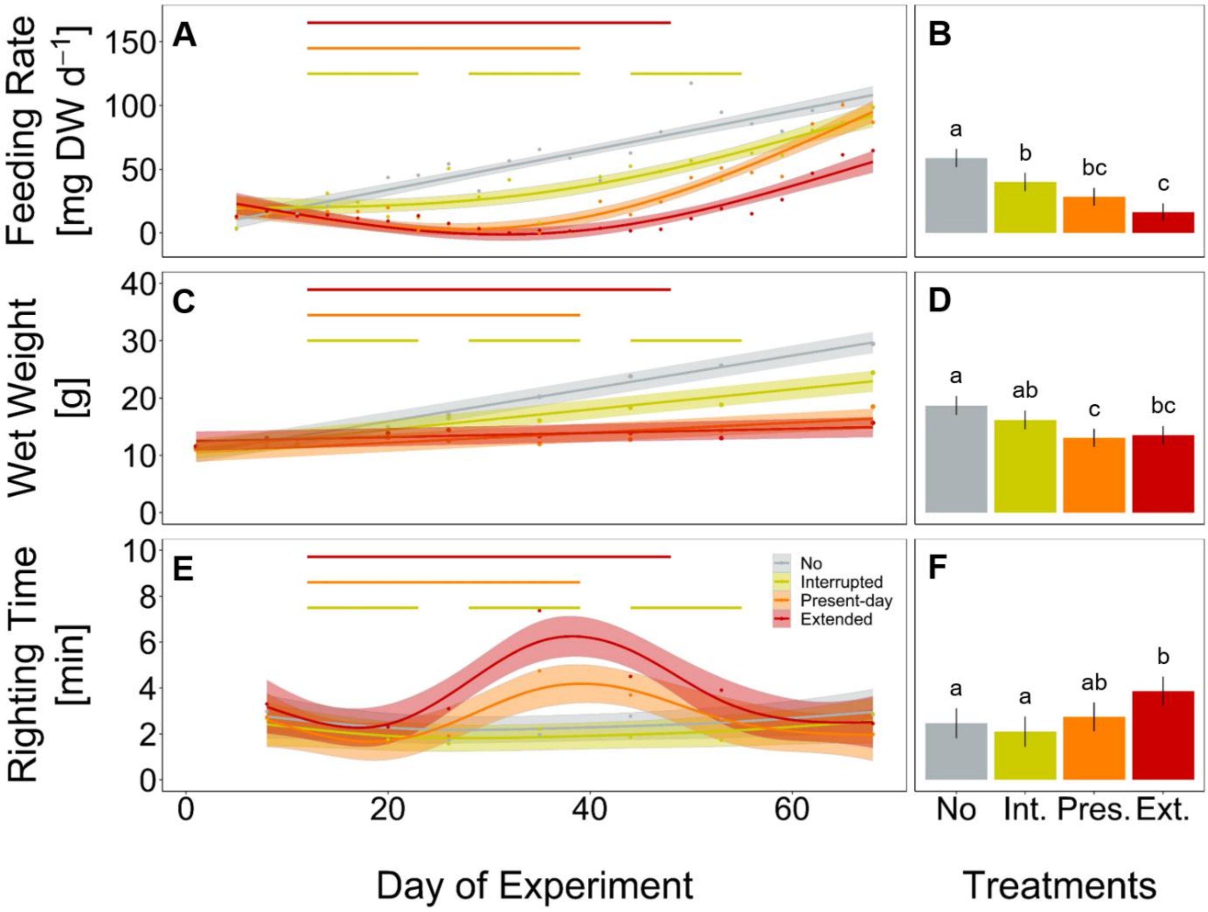

**Chapter I - Figure 3:** Feeding rate (mg mussel dry weight per day, **A** and **B**), wet weight (g, **C** and **D**) and righting time (minutes, **E** and **F**) of *Asterias rubens* during 68 days of incubation, under No (grey), Interrupted (yellow-green), Present day (orange), and Extended (red) heatwave treatments (see Fig. 1 for treatment descriptions). Measured data are represented as means for every measurement point (dots in **A**, **C**, **E**) and as overall means with 95% confidence intervals (bars and whiskers in **B**, **D**, **F**). Temporal trends are modelled using Generalized Additive Mixed-effects Models (GAMM; solid lines in **A** and **E**) or Linear Mixed-effects Models (LMM; solid lines in **B**) and 95% confidence intervals (shaded areas in **A**, **C**, **E**). The horizontal lines (**A**, **C**, **E**) represent the periods of heatwaves (Interrupted, Present day and Extended). Significant differences between treatments for feeding rate and righting time (**A** and **E**) are shown in Chapter I - Supplementary Figure 6 and Chapter I - Supplementary Figure 7). Lower case letters in **B**, **D**, **F** represent significant differences between treatments based on Tukey post-hoc comparisons of LMM. Results shown are based on n=12 (Present day and Extended) or n=11 (No and Interrupted) replicates. Detailed statistical outcomes are given in Chapter I - Table 1, Chapter I - Table 2, and Chapter I - Table 3. See also Chapter I - Supplementary Figure 8, Chapter I - Supplementary Figure 9, and Chapter I - Supplementary Figure 10 for representation of bar plots and 95% confidence intervals over time.

**Chapter I - Table 1:** Generalized Additive Mixed-effect Model (GAMM) and Linear Mixed-effect Model (LMM) results for feeding rate (mg mussel dry weight per day) over 68 days of incubation. The GAMM for feeding rate had an explained deviance of 54.8%. Significant effects are shown in bold.

| **GAMM Feeding Rate** | | | | |
|---|---|---|---|---|
| ***Parametric Coefficients*** | ***Estimate*** | ***Std. Error*** | ***t-value*** | ***p-value*** |
| Intercept | 55.46 | 2.36 | 23.49 | **<0.001** |
| Interrupted | -17.25 | 2.54 | -6.80 | **<0.001** |
| Present-day | -31.33 | 2.42 | -12.93 | **<0.001** |
| Extended | -43.65 | 2.45 | -17.80 | **<0.001** |
| ***Smooth Terms*** | ***Estimated d.f.*** | ***Reference d.f.*** | ***F-value*** | ***p-value*** |
| s (Day of Experiment) | 1.015 | 1.028 | 285.750 | **<0.001** |
| s (Day of Experiment): Interrupted | 1.952 | 1.997 | 15.253 | **<0.001** |
| s (Day of Experiment): Present-day | 1.990 | 2.000 | 54.139 | **<0.001** |
| s (Day of Experiment): Extended | 1.984 | 2.000 | 65.768 | **<0.001** |
| s (Replicate) | 0.808 | 1.000 | 4.195 | **0.023** |

| **LMM Feeding Rate** | | | | | |
|---|---|---|---|---|---|
| ***Contrast*** | ***Estimate*** | ***Std. Error*** | ***d.f.*** | ***t-value*** | ***p-value*** |
| No:Interrupted | 18.700 | 5.220 | 42.000 | 3.585 | **0.005** |
| No:Present-day | 30.400 | 5.110 | 42.000 | 5.952 | **<0.001** |
| No:Extended | 42.500 | 5.110 | 42.000 | 8.306 | **<0.001** |
| Interrupted:Present-day | 11.700 | 5.110 | 42.000 | 2.289 | 0.117 |
| Interrupted:Extended | 23.700 | 5.110 | 42.000 | 4.644 | **<0.001** |
| Present-day:Extended | 12.000 | 5.000 | 42.000 | 2.408 | 0.091 |

**Chapter I - Table 2:** Linear Mixed-effect Model (LMM) results for the wet weight (g) over 68 days of incubation. Significant effects are shown in bold.

| **LMM Wet Weight** | | | | | |
|---|---|---|---|---|---|
| ***Parametric Coefficients*** | ***Estimate*** | ***Std. Error*** | ***d.f.*** | ***t-value*** | ***p-value*** |
| Intercept | 10.195 | 0.899 | 55.088 | 11.346 | **<0.001** |
| Interrupted | 0.789 | 1.271 | 55.088 | 0.621 | 0.537 |
| Present-day | 0.268 | 1.245 | 55.294 | 0.215 | 0.830 |
| Extended | 2.259 | 1.245 | 55.294 | 1.814 | 0.075 |
| Day of Experiment | 0.287 | 0.011 | 362.029 | 26.355 | **<0.001** |
| Interrupted:Day of Exeperiment | -0.111 | 0.015 | 362.029 | -7.225 | **<0.001** |
| Present-day:Day of Experiment | -0.200 | 0.015 | 362.061 | -13.216 | **<0.001** |
| Extended:Day of Experiment | -0.250 | 0.015 | 362.061 | -16.579 | **<0.001** |
| ***Contrast*** | ***Estimate*** | ***Std. Error*** | ***d.f.*** | ***t-value*** | ***p-value*** |
| No:Interrupted | 2.496 | 1.190 | 41.900 | 2.102 | 0.169 |
| No:Present-day | 5.609 | 1.160 | 42.000 | 4.822 | **<0.001** |
| No:Extended | 5.134 | 1.160 | 42.000 | 4.413 | **<0.001** |
| Interrupted:Present-day | 3.114 | 1.160 | 42.000 | 2.677 | **0.050** |
| Interrupted:Extended | 2.638 | 1.160 | 42.000 | 2.268 | 0.122 |
| Present-day:Extended | -0.476 | 1.140 | 42.100 | -0.418 | 0.975 |

**Chapter I - Table 3:** Generalized Additive Mixed-effect Model (GAMM) and Linear Mixed-effect Model (LMM) results for righting time (min) over 68 days of incubation. The GAMM for feeding rate had an explained deviance of 24.9%. Significant effects are shown in bold.

**GAMM Righting Time**

| ***Parametric Coefficients*** | ***Estimate*** | ***Std. Error*** | ***t-value*** | ***p-value*** |
|---|---|---|---|---|
| Intercept | 147.577 | 13.777 | 10.712 | **<0.001** |
| Present-day | -21.904 | 19.483 | -1.124 | 0.262 |
| Interrupted | 17.506 | 19.129 | 0.915 | 0.361 |
| Extended | 83.577 | 19.129 | 4.369 | **<0.001** |
| ***Smooth Terms*** | ***Estimated d.f.*** | ***Reference d.f.*** | ***F-value*** | ***p-value*** |
| s (Day of Experiment) | 2.264 | 2.734 | 1.487 | 0.304 |
| s (Day of Experiment): Interrupted | 1.003 | 1.006 | 0.002 | 0.985 |
| s (Day of Experiment): Present-day | 3.555 | 3.864 | 4.672 | **0.004** |
| s (Day of Experiment): Extended | 3.776 | 3.958 | 9.894 | **<0.001** |
| s (Individual) | 0.000 | 1.000 | 0.000 | 0.943 |

**LMM Righting Time**

| ***Contrast*** | ***Estimate*** | ***Std. Error*** | ***d.f.*** | ***t-value*** | ***p-value*** |
|---|---|---|---|---|---|
| No:Interrupted | 0.365 | 0.473 | 41.700 | 0.771 | 0.867 |
| No:Present-day | -0.283 | 0.464 | 42.000 | -0.611 | 0.928 |
| No:Extended | -1.400 | 0.464 | 42.000 | -3.018 | **0.022** |
| Interrupted:Present-day | -0.648 | 0.464 | 42.000 | -1.398 | 0.508 |
| Interrupted:Extended | -1.765 | 0.464 | 42.000 | -3.805 | **0.003** |
| Present-day:Extended | -1.116 | 0.454 | 42.200 | -2.457 | 0.082 |

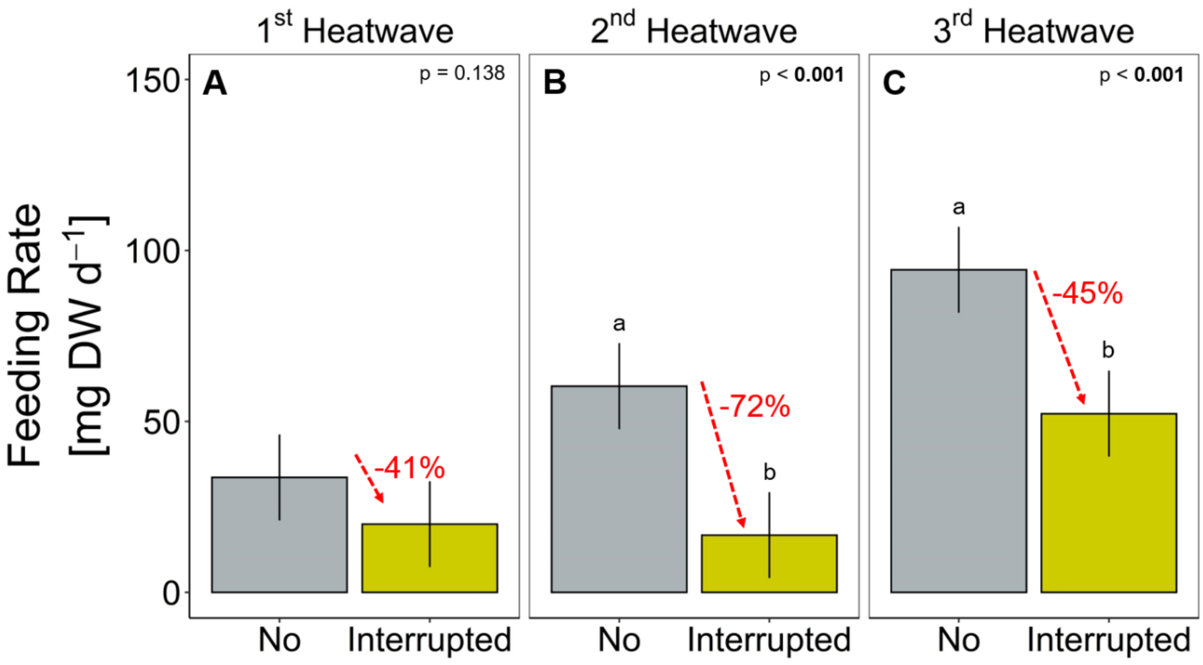

**Chapter I - Figure 4:** Feeding rate (mg mussel dry weight per day) during each of the three heatwaves of the Interrupted heatwave treatment and the respective period in the No heatwave treatment (**A**: 1st, **B**: 2nd and **C**: 3rd heatwave period). Data are presented as means (bars) and 95% confidence intervals (whiskers). Lower case letters represent significant differences between treatments based on Tukey post-hoc comparisons. Percental differences between means are given in red. Detailed statistical outcomes are given in Chapter I - Table 4.

**Chapter I - Table 4:** Linear Mixed-effect Model (LMM) results for feeding rate (mg mussel dry weight per day) over the three heatwave events in the Interrupted heatwave treatment. Significant effects are shown in bold.

| **LMM Feeding Rate** | | | | | |
|---|---|---|---|---|---|
| Parametric Coefficients | Estimate | Std. Error | df | t-value | p-value |
| Intercept | 33.609 | 6.408 | 55.040 | 5.245 | **<0.001** |
| Interrupted | -13.655 | 9.063 | 55.040 | -1.507 | 0.138 |
| Heatwave No. 2 | 26.693 | 8.044 | 40.000 | 3.318 | **0.002** |
| Heatwave No. 3 | 60.729 | 8.044 | 40.000 | 7.550 | **<0.001** |
| Interrupted:Heatwave No. 2 | -29.910 | 11.375 | 40.000 | -2.629 | **0.012** |
| Interrupted:Heatwave No. 3 | -28.413 | 11.375 | 40.000 | -2.498 | **0.017** |

# Discussion

## *Heatwave traits and trends*

Marine species are differently impacted by heat stress (e.g., Pansch et al. 2018; Gómez-Gras et al. 2019; Saha et al. 2020; Wahl et al. 2020). Therefore, defining particular temperature thresholds for marine ecosystems at the local scale and globally remains challenging. Corals have been a major research subject for global warming since the 1990s, so that much information is available to project the impact of heating events on corals (i.e., bleaching) using the concept of degree heating weeks (Liu et al. 2006). However, in order to define species-specific thresholds in diverse communities, one would need thermal performance curves for all species in the system (Schulte et al. 2011). But even if these performance curves were to exist, different traits may have different optima (Wahl et al. 2020). Thus, the whole organism response of the respective species would be a combination from all relevant traits with their potentially different optima resulting in the overall fitness. Therefore, a biology-based methodology for the characterization of heatwaves may not necessarily be the ideal approach. A physical (oceanographic) approach as applied in our study can circumvent the problem by merely focusing on time-series of temperature data and thus, modelling typical vs. extreme conditions in an environment.

Baltic Sea models project an increase in e.g., heatwave duration (Gräwe et al. 2013). Therefore, it is unlikely that the absence of trends in heatwave characteristic in the Kiel Fjord is an actual absence of a trend but rather suggests that our dataset of 22-years may not be sufficient to capture long-term trends in this naturally variable system (Reusch et al. 2018). Fluctuations in the Baltic Sea are not only apparent as extreme events or short-term temperature changes (Pansch and Hiebenthal 2019), but even as fluctuations on an inter-annual scale as our data highlight. The years 2010–2013 were particularly cold years, which compares well to the extremely low North Atlantic Oscillation index around 2010 (Hurell and National Center for Atmospheric Research Staff 2020). This anomalous low index (Osborn 2011) may partly be the reason we did not detect a general warming trend in the time span tested. Yet, warming is the main driver of heatwave trends (Oliver 2019). Therefore, longer (Hobday et al. 2016) datasets may be required in highly fluctuating systems like the Baltic Sea. This does not only mean that we might have missed existing trends, but also that we may have over- or underestimated some of the heatwave properties. A recent publication by Schlegel et al. (2019) investigated how shorter timeseries impact the differently modelled heatwave parameters. Following their findings of the median heatwave properties, our 22-year dataset should likely have 7% more heatwaves, while the duration and maximum intensity should be decreased by 6.4 and 7.3%, respectively. As we chose the heatwave properties for our experiment conservatively, the natural relevance of the study persists, especially as natural heatwaves similar to our *Present-day* and *Extended* heatwave treatment occurred in August 2003 and August 2002, respectively (Chapter I - Supplementary Figure 11). Therefore, our experiment provides unique insights into the performance of a keystone predator in times of extreme (and recurring) events.

### *Heatwaves reduce the performance of Asterias rubens*

Daily temperatures of at least 23.25 °C (maximum temperature reached in our experiment) were already measured 89 times in the Kiel Fjord over the past two decades (Wolf et al. 2020). Though not lethal, continuous heatwaves (i.e., *Present-day* and *Extended* heatwave treatments) reduced the performance of the sea star *A. rubens* in feeding, growth, and activity, which confirms previous findings (Rühmkorff et al., unpublished data). Similar impacts and temperature thresholds were also identified for other sea stars (*Pisaster ochraceus*, Pincebourde et al. 2008) and sea urchins (*Heliocidaris erythrogramma*, Minuti et al. 2021). Melzner et al. (personal communication) showed for echinoderms, that thermal stress causes low coelomic oxygen concentrations. Likely, the heatwaves in our experiment led to such a decreased coelomic oxygen concentration in *A. rubens*, so that activity and feeding rate decreased. Consequently, this reduced the growth rate of individuals. Especially, when the heatwaves were extended by nine days, the impact on sea stars was drastic.

Sea stars in all, but the *Extended* heatwave treatment, fed more at the end compared to the start of the experiment (Chapter I - Figure 3A). On the one hand, this indicates the high recovery potential of *A. rubens*, but is likely also driven by the higher energy need of larger sea stars towards the end of the experiment. This elongation is similar to future extrapolation trends of heatwave duration with an increase of 10.3 days by 2100 (Oliver et al. 2018). Pincebourde et al. (2008) likewise demonstrated that longer exposure to heat stress provokes a lasting effect on sea stars. Even when the stress event may be over, echinoderms still suffer from the experienced heat stress by carry over effects (Minuti et al. 2021).

While the more robust prey of sea stars, blue mussels, were shown to survive weeks of exposure to temperatures up to 26 °C in the Baltic Sea (Vajedsamiei et al. 2021) or even temperatures up to 41 °C for 3 hours air exposure in the eastern English Channel (Seuront et al. 2019), temperatures of already 26 °C were shown to be 100% lethal for *A. rubens* (Rühmkorff et al., unpublished data). Similarly, Petes et al. (2008) could show that sea stars' mortality is more pronounced in mussel beds that lay closer to the warmer water surface at an intertidal rocky shore, whereas their mussel prey proved to be more resistant to that same heat stress.

Bonaviri et al. (2017) showed that the sea star *Pycnopodia helianthoides* can only control its main prey, the sea urchin *Strongylocentrotus purpuratus*, in a non-warming scenario. Considering the fact that blue mussels are thermally more robust (Vajedsamiei et al. 2021) than sea stars and assuming that sea stars cannot adapt or temporarily migrate to deeper and colder waters, *A. rubens* will hardly be able to control blue mussel abundances (Reusch and Chapman

1997) in the future Baltic Sea. Thus, a mussel dominated ecosystem might be formed (Reusch and Chapman 1997), resulting in a restructured benthic community with overall lower diversity. At the same time, we demonstrated that summer heatwaves reduce the weight and thus the size of sea stars. As body size and prey size are strongly correlated in sea stars (Sommer et al. 1999), a heatwave summer would consequently lead to an increased predation on smaller mussels after the heatwaves have ended. This ecosystem-wide impact might be particularly strong for species-poor ecosystems such as the Baltic Sea, unless newcomers add to ecosystem diversity. In this particular case, feeding pressure on similar prey and prey size, as provoked by the recent invader *Hemigrapsus takanoi* (Nour et al. 2020), may add to ecosystem complexity, with yet unknown consequences. Yet, we conclude that heatwaves affect the keystone predator *A. rubens* with likely ecosystem-wide consequences, especially on the distribution and extent of mussel beds.

### *Mitigated impacts by Interrupted heatwaves*

Naturally, an interruption of a heatwave is most likely caused by a cold-spell during an upwelling event at which deeper and colder waters are shoaled to the surface (Lehmann and Myrberg 2008; Wahl et al. 2021). Though, upwelling events in late summer are often hypoxic (Karstensen et al. 2014) and were shown to negatively impact *A. rubens* (Rühmkorff et al., unpublished data), they can still be beneficial when they interrupt lethal temperature extremes during heatwave events. The importance of cooling events, e.g., large-amplitude internal waves, during heat stress was already demonstrated for tropical systems (Schmidt et al. 2016). In our experiment, sea star individuals subjected to the *Interrupted* heatwaves fed more, were more active, and therefore grew faster than individuals exposed to continuous heatwave treatments. Yet, other fitness consequences such as reproductive success were not measured but could have long-term impacts (Melzner et al. 2020). Overall, this demonstrates that sea stars in temperate regions may quickly recover from thermal stress by using the colder periods in between heatwave events. Or in simpler words, sea stars stop feeding during the heat stress events itself, with a more pronounced impact by longer heatwaves, while resuming to feed normally after the event had ended. In contrast, findings by Morón Lugo et al. (2020), show that repeated short-term excursion into stressful conditions can be detrimental for *A. rubens*. Thus, mean stress levels, but also duration and amplitude of stress events and periods of recovery, will act collectively and determine the overall impact of heat stress in in a future ocean. Additionally, we provide strong evidence that environmental variability such as frequent times of stress recovery may provide a short-term refuge for sea stars from heatwave conditions projected for the future.

We show that the interruption of heatwaves did not only increase the overall performance of the temperate predator *A. rubens* compared to more continuous heat events, but also that the interruption has led to a significantly smaller impact of the third heatwave than the previous event, indicating some potential for acclimation. Other studies already showed that recovery time is very important for a species' and community's stress response (e.g., DeCarlo et al. 2019; Hughes et al. 2019; Nguyen et al. 2020) and this seems to play a crucial role also for the response of *A. rubens* to heatwaves. Our results might thus indicate the potential of *A. rubens* to gain benefits through an ecological stress memory (sensu Jackson et al. 2021). Yet, this needs further investigation, especially on the physiological mechanisms that are involved.

## Conclusion

An appropriate heatwave characterization can be an extremely important tool for the design of close-to-nature experiments and can therefore help our understanding of the impact of extreme events on single species up to communities and ecosystems. The decreased performance of a temperate keystone predator in response to such simulated heatwaves has likely effects on the whole benthic ecosystem, as their main prey is an ecosystem engineer that may be released from its main predation pressure. At the same time, distinct recovery phases can play an essential role in the heatwave response of the investigated sea star *A. rubens*. The underlying mechanisms that trigger such acclimation and hardening processes still need to be investigated, as well as the question if long-term acclimation to continuous stressors is possible.

## Data availability

All data obtained from the present study are stored at PANGAEA and can be accessed through the following links: https://doi.org/10.1594/PANGAEA.939981 and https://doi.org/10.1594/PANGAEA.939978.

## Authors Contributions

FW and CP initiated and designed the study. FW and KS collected the data. FW analyzed the data and wrote the manuscript. All authors contributed to the article and approved the submitted version.

## Funding

This study was funded by the Deutsche Forschungsgemeinschaft (DFG; PA2643/2/348431475), through GEOMAR (Helmholtz-Gemeinschaft) and through Deutsche Bundesstiftung Umwelt (DBU; 20018/553).

## Acknowledgements

We would like to thank Mia Großmann and Sean Kearney for their help during the experiment, including mussel collection, feeding and general maintenance, and Björn Buchholz for help in maintaining the experimental facility.

## References

Banti, Valeria; Loreti, Elena; Novi, Giacomo; Santaniello, Antonietta; Alpi, Amedeo; Perata, Pierdomenico (2008): Heat acclimation and cross-tolerance against anoxia in Arabidopsis. In Plant, cell & environment 31 (7), pp. 1029–1037. DOI: 10.1111/j.1365-3040.2008.01816.x.

Bates, Douglas; Mächler, Martin; Bolker, Ben; Walker, Steve (2015): Fitting Linear Mixed-Effects Models Using lme4. In J. Stat. Soft. 67 (1). DOI: 10.18637/jss.v067.i01.

Bonaviri, Chiara; Graham, Michael; Gianguzza, Paola; Shears, Nick T. (2017): Warmer temperatures reduce the influence of an important keystone predator. In The Journal of animal ecology 86 (3), pp. 490–500. DOI: 10.1111/1365-2656.12634.

Boyd, Philip W.; Collins, Sinead; Dupont, Sam; Fabricius, Katharina; Gattuso, Jean-Pierre; Havenhand, Jonathan et al. (2018): Experimental strategies to assess the biological ramifications of multiple drivers of global ocean change-A review. In Glob Change Biol 24 (6), pp. 2239–2261. DOI: 10.1111/gcb.14102.

Budd, G. C. (2008): Asterias rubens Common starfish. Edited by Tyler-Walters H., K. Hiscock. Marine Life Information Network: Biology and Sensitivity Key Infomation Reviews (online). Plymouth: Marine Biological Association of the United Kingdom. Available online at https://dx.doi.org/10.17031/marlinsp.1194.1.

DeCarlo, Thomas M.; Harrison, Hugo B.; Gajdzik, Laura; Alaguarda, Diego; Rodolfo-Metalpa, Riccardo; D'Olivo, Juan et al. (2019): Acclimatization of massive reef-building corals to consecutive heatwaves. In Proceedings. Biological sciences 286 (1898), p. 20190235. DOI: 10.1098/rspb.2019.0235.

Doney, Scott C.; Ruckelshaus, Mary; Duffy, J. Emmett; Barry, James P.; Chan, Francis; English, Chad A. et al. (2012): Climate change impacts on marine ecosystems. In Annual review of marine science 4, pp. 11–37. DOI: 10.1146/annurev-marine-041911-111611.

Dürr, Simone; Wahl, Martin (2004): Isolated and combined impacts of blue mussels (Mytilus edulis) and barnacles (Balanus improvisus) on structure and diversity of a fouling community. In Journal of Experimental Marine Biology and Ecology 306 (2), pp. 181–195. DOI: 10.1016/j.jembe.2004.01.006.

Gaymer, Carlos F.; Himmelman, John H.; Johnson, Ladd E. (2001): Distribution and feeding ecology of the seastars Leptasterias polaris and Asterias vulgaris in the northern Gulf of St Lawrence, Canada. In J. Mar. Biol. Ass. 81 (5), pp. 827–843. DOI: 10.1017/S0025315401004660.

Genin, Amatzia; Levy, Liraz; Sharon, Galit; Raitsos, Dionysios E.; Diamant, Arik (2020): Rapid onsets of warming events trigger mass mortality of coral reef fish. In Proceedings of the National Academy of Sciences of the United States of America 117 (41), pp. 25378–25385. DOI: 10.1073/pnas.2009748117.

Gómez-Gras, Daniel; Linares, Cristina; Caralt, Sonia de; Cebrian, Emma; Frleta-Valić, Maša; Montero-Serra, Ignasi et al. (2019): Response diversity in Mediterranean coralligenous assemblages facing climate change. Insights from a multispecific thermotolerance experiment. In Ecology and evolution 9 (7), pp. 4168–4180. DOI: 10.1002/ece3.5045.

Gräwe, Ulf; Friedland, René; Burchard, Hans (2013): The future of the western Baltic Sea. Two possible scenarios. In Ocean Dynamics 63 (8), pp. 901–921. DOI: 10.1007/s10236-013-0634-0.

Gunderson, Alex R.; Armstrong, Eric J.; Stillman, Jonathon H. (2016): Multiple Stressors in a Changing World. The Need for an Improved Perspective on Physiological Responses to the Dynamic Marine Environment. In Annual review of marine science 8, pp. 357–378. DOI: 10.1146/annurev-marine-122414-033953.

HELCOM (2013): Climate Change in the Baltic Sea Area: A HELMCOM thematic assessment in 2013. In Balt. Sea Environ. Proc. 37.

Hobday, Alistair J.; Alexander, Lisa V.; Perkins, Sarah E.; Smale, Dan A.; Straub, Sandra C.; Oliver, Eric C.J. et al. (2016): A hierarchical approach to defining marine heatwaves. In Progress in Oceanography 141, pp. 227–238. DOI: 10.1016/j.pocean.2015.12.014.

Hughes, Terry P.; Kerry, James T.; Connolly, Sean R.; Baird, Andrew H.; Eakin, C. Mark; Heron, Scott F. et al. (2019): Ecological memory modifies the cumulative impact of recurrent climate extremes. In Nature Clim Change 9 (1), pp. 40–43. DOI: 10.1038/s41558-018-0351-2.

Hurell, James; National Center for Atmospheric Research Staff (2020): The Climate Data Guide: Hurell North Atlantic Oscillation (NAO) Index (station based). Available online at https://climatedataguide.ucar.edu/climate-data/hurrell-north-atlantic-oscillation-nao-index-station-based, updated on 4/24/2020, checked on 7/23/2021.

IPCC (2021): Climate Change 2021: The Physical Science Basis. In V. Masson-Delmotte, P. Zhai, A. Pirani, S. L. Connors, C. Péan, S. Berger et al. (Eds.): Contribution of Working Group I to the Sixth Assessment Report of the Intergovernmental Panel on Climate Change. In press.

Jackson, Michelle C.; Pawar, Samraat; Woodward, Guy (2021): The Temporal Dynamics of Multiple Stressor Effects. From Individuals to Ecosystems. In Trends in Ecology & Evolution 36 (5), pp. 402–410. DOI: 10.1016/j.tree.2021.01.005.

Karstensen, J.; Liblik, T.; Fischer, J.; Bumke, K.; Krahmann, G. (2014): Summer upwelling at the Boknis Eck time-series station (1982 to 2012) – a combined glider and wind data analysis. In Biogeosciences 11 (13), pp. 3603–3617. DOI: 10.5194/bg-11-3603-2014.

Kayanne, Hajime (2017): Validation of degree heating weeks as a coral bleaching index in the northwestern Pacific. In Coral Reefs 36 (1), pp. 63–70. DOI: 10.1007/s00338-016-1524-y.

Lawrence, John M.; Cowell, Bruce C. (1996): The righting response as an indication of stress in stichaster striatus (Echinodermata, asteroidea). In Marine and Freshwater Behaviour and Physiology 27 (4), pp. 239–248. DOI: 10.1080/10236249609378969.

Le Nohaïc, Morane; Ross, Claire L.; Cornwall, Christopher E.; Comeau, Steeve; Lowe, Ryan; McCulloch, Malcolm T.; Schoepf, Verena (2017): Marine heatwave causes unprecedented regional mass bleaching of thermally resistant corals in northwestern Australia. In Scientific reports 7 (1), p. 14999. DOI: 10.1038/s41598-017-14794-y.

Lehmann, Andreas; Myrberg, Kai (2008): Upwelling in the Baltic Sea — A review. In Journal of Marine Systems 74, S3-S12. DOI: 10.1016/j.jmarsys.2008.02.010.

Lenth, Russels V. (2020): emmeans: Estimated Marginal Means, aka Least Squares means. Available online at https://CRAN.R-project.org/package=emmeans.

Leppäranta, Matti; Myrberg, Kai (Eds.) (2009): Physical Oceanography of the Baltic Sea. Berlin, Heidelberg: Springer Berlin Heidelberg.

Liu, G.; Srong, A. E.; Skirving W. J.; Arzayus L. F. (2006): Overview of NOAA coral reef watch program's near-real-time satellite global coral bleaching monitoring activities. In Proceedings of the 10th International Coral Reef Symposium, pp. 1783–1793.

McBryan, Tara L.; Healy, Timothy M.; Haakons, Kristen L.; Schulte, Patricia M. (2016): Warm acclimation improves hypoxia tolerance in Fundulus heteroclitus. In The Journal of experimental biology 219 (Pt 4), pp. 474–484. DOI: 10.1242/jeb.133413.

Melzner, Frank; Buchholz, Björn; Wolf, Fabian; Panknin, Ulrike; Wall, Marlene (2020): Ocean winter warming induced starvation of predator and prey. In Proceedings. Biological sciences 287 (1931), p. 20200970. DOI: 10.1098/rspb.2020.0970.

Minuti, Jay J.; Byrne, Maria; Hemraj, Deevesh A.; Russell, Bayden D. (2021): Capacity of an ecologically key urchin to recover from extreme events. Physiological impacts of heatwaves and the road to recovery. In The Science of the total environment 785, p. 147281. DOI: 10.1016/j.scitotenv.2021.147281.

Morón Lugo, Sonia C.; Baumeister, Moritz; Nour, Ola Mohamed; Wolf, Fabian; Stumpp, Meike; Pansch, Christian (2020): Warming and temperature variability determine the performance of two invertebrate predators. In Scientific reports 10 (1), p. 6780. DOI: 10.1038/s41598-020-63679-0.

Nguyen, Hung Manh; Kim, Mikael; Ralph, Peter J.; Marín-Guirao, Lázaro; Pernice, Mathieu; Procaccini, Gabriele (2020): Stress Memory in Seagrasses. First Insight Into the Effects of Thermal Priming and the Role of Epigenetic Modifications. In Frontiers in plant science 11, p. 494. DOI: 10.3389/fpls.2020.00494.

Norling, P.; Kautsky, N. (2007): Structural and functional effects of Mytilus edulis on diversity of associated species and ecosystem functioning. In Mar. Ecol. Prog. Ser. 351, pp. 163–175. DOI: 10.3354/meps07033.

Nour, Ola; Stumpp, Meike; Morón Lugo, Sonia C.; Barboza, Francisco R.; Pansch, Christian (2020): Population structure of the recent invader Hemigrapsus takanoi and prey size selection on Baltic Sea mussels. In AI 15 (2), pp. 297–317. DOI: 10.3391/ai.2020.15.2.06.

Oliver, Eric C. J. (2019): Mean warming not variability drives marine heatwave trends. In Clim Dyn 53 (3-4), pp. 1653–1659. DOI: 10.1007/s00382-019-04707-2.

Oliver, Eric C. J.; Burrows, Michael T.; Donat, Markus G.; Sen Gupta, Alex; Alexander, Lisa V.; Perkins-Kirkpatrick, Sarah E. et al. (2019): Projected Marine Heatwaves in the 21st Century and the Potential for Ecological Impact. In Front. Mar. Sci. 6, p. 891. DOI: 10.3389/fmars.2019.00734.

Oliver, Eric C. J.; Donat, Markus G.; Burrows, Michael T.; Moore, Pippa J.; Smale, Dan A.; Alexander, Lisa V. et al. (2018): Longer and more frequent marine heatwaves over the past century. In Nature communications 9 (1), p. 1324. DOI: 10.1038/s41467-018-03732-9.

Osborn, Timothy J. (2011): Winter 2009/2010 temperatures and a record-breaking North Atlantic Oscillation index. In Weather 66 (1), pp. 19–21. DOI: 10.1002/wea.660.

Pansch, Christian; Hiebenthal, Claas (2019): A new mesocosm system to study the effects of environmental variability on marine species and communities. In Limnol. Oceanogr. Methods 28, p. 16. DOI: 10.1002/lom3.10306.

Pansch, Christian; Scotti, Marco; Barboza, Francisco R.; Al-Janabi, Balsam; Brakel, Janina; Briski, Elizabeta et al. (2018): Heat waves and their significance for a temperate benthic community. A near-natural experimental approach. In Glob Change Biol. DOI: 10.1111/gcb.14282.

Petes, Laura E.; Mouchka, Morgan E.; Milston-Clements, Ruth H.; Momoda, Tracey S.; Menge, Bruce A. (2008): Effects of environmental stress on intertidal mussels and their sea star predators. In Oecologia 156 (3), pp. 671–680. DOI: 10.1007/s00442-008-1018-x.

Pincebourde, Sylvain; Sanford, Eric; Casas, Jérôme; Helmuth, Brian (2012): Temporal coincidence of environmental stress events modulates predation rates. In Ecology letters 15 (7), pp. 680–688. DOI: 10.1111/j.1461-0248.2012.01785.x.

Pincebourde, Sylvain; Sanford, Eric; Helmuth, Brian (2008): Body temperature during low tide alters the feeding performance of a top intertidal predator. In Limnol. Oceanogr. 53 (4), pp. 1562–1573. DOI: 10.4319/lo.2008.53.4.1562.

R Core Team (2021): R: A language and environment for statistical computing. Version 4.1.1. Vienna, Austria: R Foundation for Statistical Computing. Available online at https://www.R-project.org.

Reusch, Thorsten B. H.; Chapman, Anthony R. O. (1997): Persistence and Space Occupancy by Subtidal Blue Mussel Patches. In Ecological Monographs 67 (1), p. 65. DOI: 10.2307/2963505.

Reusch, Thorsten B. H.; Dierking, Jan; Andersson, Helen C.; Bonsdorff, Erik; Carstensen, Jacob; Casini, Michele et al. (2018): The Baltic Sea as a time machine for the future coastal ocean. In Science advances 4 (5), eaar8195. DOI: 10.1126/sciadv.aar8195.

Sadchatheeswaran, Saachi; Branch, George M.; Robinson, Tamara B. (2015): Changes in habitat complexity resulting from sequential invasions of a rocky shore. Implications for community structure. In Biol Invasions 17 (6), pp. 1799–1816. DOI: 10.1007/s10530-014-0837-4.

Saha, Mahasweta; Barboza, Francisco R.; Somerfield, Paul J.; Al-Janabi, Balsam; Beck, Miriam; Brakel, Janina et al. (2020): Response of foundation macrophytes to near-natural simulated marine heatwaves. In Glob Change Biol 26 (2), pp. 417–430. DOI: 10.1111/gcb.14801.

Sanford (1999): Regulation of keystone predation by small changes in ocean temperature. In Science (New York, N.Y.) 283 (5410), pp. 2095–2097. DOI: 10.1126/science.283.5410.2095.

Schlegel, Robert W.; Oliver, Eric C. J.; Hobday, Alistair J.; Smit, Albertus J. (2019): Detecting Marine Heatwaves With Sub-Optimal Data. In Front. Mar. Sci. 6, p. 165. DOI: 10.3389/fmars.2019.00737.

Schlegel, Robert W.; Smit, Albertus J. (2018): heatwaveR. A central algorithm for the detection of heatwaves and cold-spells. In JOSS 3 (27), p. 821. DOI: 10.21105/joss.00821.

Schmidt, Gertraud M.; Wall, Marlene; Taylor, Marc; Jantzen, Carin; Richter, Claudio (2016): Large-amplitude internal waves sustain coral health during thermal stress. In Coral Reefs 35 (3), pp. 869–881. DOI: 10.1007/s00338-016-1450-z.

Schulte, Patricia M.; Healy, Timothy M.; Fangue, Nann A. (2011): Thermal performance curves, phenotypic plasticity, and the time scales of temperature exposure. In Integrative and comparative biology 51 (5), pp. 691–702. DOI: 10.1093/icb/icr097.

Seuront, Laurent; Nicastro, Katy R.; Zardi, Gerardo I.; Goberville, Eric (2019): Decreased thermal tolerance under recurrent heat stress conditions explains summer mass mortality of the blue mussel Mytilus edulis. In Scientific reports 9 (1), p. 17498. DOI: 10.1038/s41598-019-53580-w.

Smale, Dan A.; Wernberg, Thomas; Oliver, Eric C. J.; Thomsen, Mads; Harvey, Ben P.; Straub, Sandra C. et al. (2019): Marine heatwaves threaten global biodiversity and the provision of ecosystem services. In Nature Clim Change 9, p. 360. DOI: 10.1038/s41558-019-0412-1.

Sommer, Ulrich; Meusel, Bodo; Stielau, Cordula (1999): An experimental analysis of the importance of body-size in the seastar-mussel predator-prey relationship. In Acta Oecologica 20 (2), pp. 81–86. DOI: 10.1016/S1146-609X(99)80019-8.

Thomsen, Mads S.; Mondardini, Luca; Alestra, Tommaso; Gerrity, Shawn; Tait, Leigh; South, Paul M. et al. (2019): Local Extinction of Bull Kelp (Durvillaea spp.) Due to a Marine Heatwave. In Front. Mar. Sci. 6, p. 3126. DOI: 10.3389/fmars.2019.00084.

Todgham, Anne E.; Schulte, Patricia M.; Iwama, George K. (2005): Cross-tolerance in the tidepool sculpin. The role of heat shock proteins. In Physiological and biochemical zoology : PBZ 78 (2), pp. 133–144. DOI: 10.1086/425205.

Vajedsamiei, Jahangir; Wahl, Martin; Schmidt, Andrea Lee; Yazdanpanahan, Maryam; Pansch, Christian (2021): The Higher the Needs, the Lower the Tolerance. Extreme Events May Select Ectotherm Recruits With Lower Metabolic Demand and Heat Sensitivity. In Front. Mar. Sci. 8, p. 672. DOI: 10.3389/fmars.2021.660427.

van Rij, Jacolien; Wieling, Martijn; Baayen, R. Harald; van Rijn, Hedderik (2020): itsadug: Interpreting Time Series and Autocorrelated Data Using GAMMs. Available online at https://CRAN.R-project.org/package=itsadug.

Vevers, H. G. (1949): The Biology of Asterias Rubens L. Growth And Reproduction. In J. Mar. Biol. Ass. 28 (1), pp. 165–187. DOI: 10.1017/S0025315400055272.

Wahl, Martin; Barboza, Francisco R.; Buchholz, Björn; Dobretsov, Sergey; Guy-Haim, Tamar; Rilov, Gil et al. (2021): Pulsed pressure. Fluctuating impacts of multifactorial environmental change on a temperate macroalgal community. In Limnol. Oceanogr. 33, p. 477. DOI: 10.1002/lno.11954.

Wahl, Martin; Buchholz, Björn; Winde, Vera; Golomb, Dar; Guy-Haim, Tamar; Müller, Jens et al. (2015): A mesocosm concept for the simulation of near-natural shallow underwater climates. The Kiel Outdoor Benthocosms (KOB). In Limnol. Oceanogr. Methods 13 (11), pp. 651–663. DOI: 10.1002/lom3.10055.

Wahl, Martin; Werner, Franziska Julie; Buchholz, Björn; Raddatz, Stefanie; Graiff, Angelika; Matthiessen, Birte et al. (2020): Season affects strength and direction of the interactive impacts of ocean warming and biotic stress in a coastal seaweed ecosystem. In Limnol. Oceanogr. 65 (4), pp. 807–827. DOI: 10.1002/lno.11350.

Walter, Julia; Jentsch, Anke; Beierkuhnlein, Carl; Kreyling, Juergen (2013): Ecological stress memory and cross stress tolerance in plants in the face of climate extremes. In Environmental and Experimental Botany 94, pp. 3–8. DOI: 10.1016/j.envexpbot.2012.02.009.

Walther, Gian-Reto; Post, Eric; Convey, Peter; Menzel, Annette; Parmesan, Camille; Beebee, Trevor J. C. et al. (2002): Ecological responses to recent climate change. In Nature 416 (6879), pp. 389–395. DOI: 10.1038/416389a.

Wolf, Fabian; Bumke, Karl; Wahl, Sebastian; Nevoigt, Frauke; Hecht, Ute; Hiebenthal, Claas; Pansch, Christian (2020): High resolution water temperature data between January 1997 and December 2018 at the GEOMAR pier surface. PANGAEA. DOI: 10.1594/PANGAEA.919186

Wood, Simon N. (2017): Generalized Additive Models: Chapman and Hall/CRC.

# CHAPTER II

# Marine heatwaves and upwelling shape stress responses in a keystone predator

**Running head:** Impacts of extreme events on starfish

**List of authors:** Sarah Rühmkorff [1#], Fabian Wolf [2#*], Jahangir Vajedsamiei [2], Francisco Rafael Barboza[3], Claas Hiebenthal[2], Christian Pansch [2,4]

Institute or laboratory of origin: 1 Christian-Albrechts-University Kiel, 24118 Kiel, Germany; 2 Department of Marine Ecology, GEOMAR Helmholtz Centre for Ocean Research Kiel, 24105 Kiel, Germany; 3 Estonian Marine Institute, University of Tartu, 12618 Tallinn, Estonia; 4 Environmental and Marine Biology, Åbo Akademi University, 20520 Åbo, Finland

[#] **Shared lead authorship**

[*] **Corresponding author:** Fabian Wolf, GEOMAR Helmholtz Centre for Ocean Research Kiel, Düsternbrooker Weg 20, 24105 Kiel, Germany, telephone: +49 431 600 1599, E-Mail: fabian.wolf.research@gmail.com

**ORCIDs:** SR: 0000-0003-0215-2190, FW: 0000-0002-0955-8487, JV: 0000-0002-8625-4719, FRB: 0000-0002-9100-2962, CH: 0000-0003-4774-3242, CP: 0000-0001-8442-4502

**Keywords:** climate change, environmental fluctuation, extreme events, ecological memory, cross stress tolerance, starfish

## Abstract

Climate change intensifies the magnitude of marine heatwaves and upwelling events in shallow marine habitats. However, the interplay of these extreme events and the consequences for species and ecosystems remain unknown. We experimentally tested the impacts of summer heatwaves of differing intensities and durations, and a succeeding upwelling event on a temperate keystone predator, the starfish *Asterias rubens*. We recorded feeding rates (mussel consumption) throughout the experiment and assessed activity (righting response) and growth at strategically chosen timepoints to unveil the consequences of the imposed stressors. We found that the low-pH and low-oxygen upwelling event overall impaired starfish feeding and activity while prior exposure to a present-day heatwave (+5 °C above climatology) alleviated upwelling-induced stress on starfish activity (i.e., an indication of cross stress tolerance). Heatwaves of present-day intensity decreased starfish feeding and growth. While the heatwave of limited duration (9 days) caused slight impacts but allowed for recovery, the prolonged (13 days) heatwave impaired overall growth. Yet, projected future heatwaves (+8 °C above climatology) caused 100% mortality of starfish. Our findings indicate that A. rubens can express a cross stress tolerance during successive stressful events. Yet, starfish populations may strongly suffer from extensive mortality during intensified end-of-century heatwave conditions.

## Introduction

Climate change does not only lead to an overall increase in temperature (IPCC 2019) but also increases the frequency, duration, and intensity of marine heatwaves (Oliver et al. 2018; IPCC 2019). Simultaneously, ocean warming intensifies the stratification of the water column. Together with eutrophication, this causes worldwide expansions of hypoxic zones (Diaz and Rosenberg 2008) and facilitates the occurrences of stressful coastal upwelling (Snyder et al. 2003; Bakun et al. 2015). Heatwaves and upwelling events commonly occur consecutively in coastal habitats (Paalme et al. 2020; Suursaar 2020; Wahl et al. 2021) and upwelling itself may represent a driver of multiple simultaneous changes. Upwelling may shoal nutrients in spring (Wahl et al. 2021) and can thus, facilitate primary production (as reviewed in Kämpf and Chapman 2016). Upwelling in late summer, however, may provide release from heat stress, and bring waters of higher salinity, but will typically also be of acidified (reduction in pH, and an increase in $p\mathrm{CO}_2$) and hypoxic (Wahl et al. 2021) nature. The overall impacts of such extreme events range from single-species mortalities (Arias-Ortiz et al. 2018) to restructuring and losses of entire ecosystems (Smale et al. 2019).

Whether the succession or co-occurrence of extreme events results in additive, synergistic or antagonistic responses depends on the nature, their intensity and duration, and timing of these events (Gunderson et al. 2016). Recent publications have called for empirical evidence on the consequences of environmental fluctuations and the impacts of succeeding extreme events on marine ecosystems (Gunderson et al. 2016; Smale et al. 2019; Jackson et al. 2021). Acclimation to an extreme event may modify an individual’s stress response to another succeeding pulse stress, referred to as ecological memory (Jackson et al. 2021) (more precisely, ‘stress memory’ if succeeding events of similar nature are described or ‘cross stress tolerance’ in case of succeeding events of different nature; Munné-Bosch and Alegre 2013; Walter et al. 2013). Thus, in contrast to a common perception of mostly negative synergistic effects imposed by multiple drivers and successive stress events (Gunderson et al. 2016; Przeslawski et al. 2015), an ecological memory may mediate the negative effects on the species to the ecosystem level.

How consecutive stressful events impact marine ecosystems remains mostly unknown (but see Gunderson et al. 2016; Jackson et al. 2021). As the intensity and frequency of extremes are projected to increase (Suursaar 2020), it is of great interest to study the main and interactive effects of such events on resident keystone and habitat-forming species. As an important and widespread benthic predator, the starfish *Asterias rubens* controls bivalve abundances in mussel beds (Gaymer et al. 2001) that provide habitats for numerous associated species (Norling and Kautsky 2007). Disturbances of this predator-prey interaction caused by extreme events

(Dobashi et al. 2018) can affect mussel bed formation and the functioning of associated ecosystems (Reusch and Chapman 1997). *A. rubens* inhabits the inter- and subtidal zones of the North Atlantic region (Vevers 1949; Clark and Downey 1992; Budd 2008). Across its distribution range, *A. rubens* experiences marine heatwaves and upwelling conditions, e.g., in Chesapeake Bay, St. Lawrence Bay, Long Island Sound (Zimmerman et al. 2017; Fennel and Testa 2019) or in the North and Baltic Seas (Diaz 2001; Wolf et al. 2022). The Supplementary Introduction contains further details on the distribution and on temperature, salinity, acidification, and oxygen tolerance of *A. rubens*.

We present an experimental study examining the consequences of the interplay between naturally occurring heatwaves and upwelling events for *A. rubens* performance, measured as feeding on mussel prey as well as their activity and body mass changes. We simulated four types of marine heatwaves, characterized by differences in duration and intensity (maximum intensity was at least 1 °C above the threshold at which feeding ceases, see Supplementary Material 1), imposed on top of a climatological trajectory. After recovery from heatwaves, starfish were exposed to an upwelling event. We hypothesized that (i) the applied heatwaves would reduce the performance of *A. rubens,* with (ii) stronger impacts induced by extended or intensified heatwaves. We further (iii) hypothesized a negative impact induced by the imposed upwelling event (due to low pH and hypoxic conditions), and (iv) an additive effect of both successive stress events (heatwave and upwelling).

## Methods

### *Experimental setup and treatments*

We conducted our experiment using the Kiel Indoor Benthocosms (KIBs) (Pansch and Hiebenthal 2019) from July 10th until September 10th, 2018. 60 2 L experimental units (transparent Kautex® bottles with black lids) were evenly distributed across ten 600 L tanks, which served as water baths. In each tank, a temperature control system (Pansch and Hiebenthal 2019) automatically implemented five different temperature regimes (treatments were always applied in two randomly chosen mesocosms), including heatwaves and upwelling events (see further information below and in Chapter II - Figure 1, Chapter II - Supplementary Figure 4, and Chapter II - Supplementary Figure 5). Each of the 60 experimental units was separately supplied with fresh seawater from Kiel Fjord and received pressurized air for ventilation. Therefore, the experimental units were considered true replicates (n = 12).

Heatwave treatments (i.e., *No*, *Present-day*, *Extended*, *Amplified*, and *Future* heatwaves; Fig. 1) were based on a heatwave characterisation by Pansch et al. (2018) and on the projected future scenarios (Oliver et al. 2018). The subsequent upwelling event, which was applied to all experimental units, mimicked an event that naturally occurred in September 2017 in Kiel Fjord (Chapter II - Figure 1 and Chapter II - Supplementary Figure 5). This upwelling followed an 18 or 14 day-long recovery period from the *Present-day* or *Extended* heatwaves, respectively, and was applied for 10 days. For more details see Supplementary Methods.

Seawater temperature was measured over the entire experimental period in at least three experimental units of each tank (TTX 110 type T, Ebro, Germany). Salinity, pH, and oxygen concentrations were measured along with the simulated upwelling event in all units (Multi 3630 IDS, WTW, Germany). Temperatures in the experimental units matched the targeted treatments with deviations < 0.95 °C from set values and < 0.17 °C among replicates (see Fig. S4 for the entire monitoring period).

During the upwelling treatment, the temperature in the 18 L experimental units decreased from 17.8 ± 0.05 °C (mean and SD) to 13.8 ± 0.07 °C, salinity increased from 17.4 ± 0.04 to 19.6 ± 0.09, pH decreased from 7.9 ± 0.06 to 7.4 ± 0.06 (pHNBS units), and oxygen dropped from 9.4 ± 0.16 mg $L^{-1}$ to 3.1 ± 0.68 mg $L^{-1}$ (Fig. S5). Vaquer-Sunyer and Duarte (2008) argue that 2 mg $L^{-1}$ oxygen concentration, the threshold commonly used for defining hypoxia, is not suitable as thresholds are highly species-specific. Indeed, the 90th percentile threshold for the median lethal oxygen concentration of marine species lies at 4.6 mg $L^{-1}$, and for sublethal effects even at 5.0 mg $L^{-1}$ (Vaquer-Sunyer and Duarte 2008; see also Seibel 2011). Thus, sublethal (below 5.0 mg $L^{-1}$) oxygen levels were experienced for 8 consecutive days in the experiment. During this time, mean temperature conditions were 14.4 ± 0.9 °C (mean over all treatments and SD), with a mean salinity of 19.4 ± 0.3, a mean pH of 7.5 ± 0.1 and a mean oxygen concentration of 4.1 ± 1.0 mg $L^{-1}$.

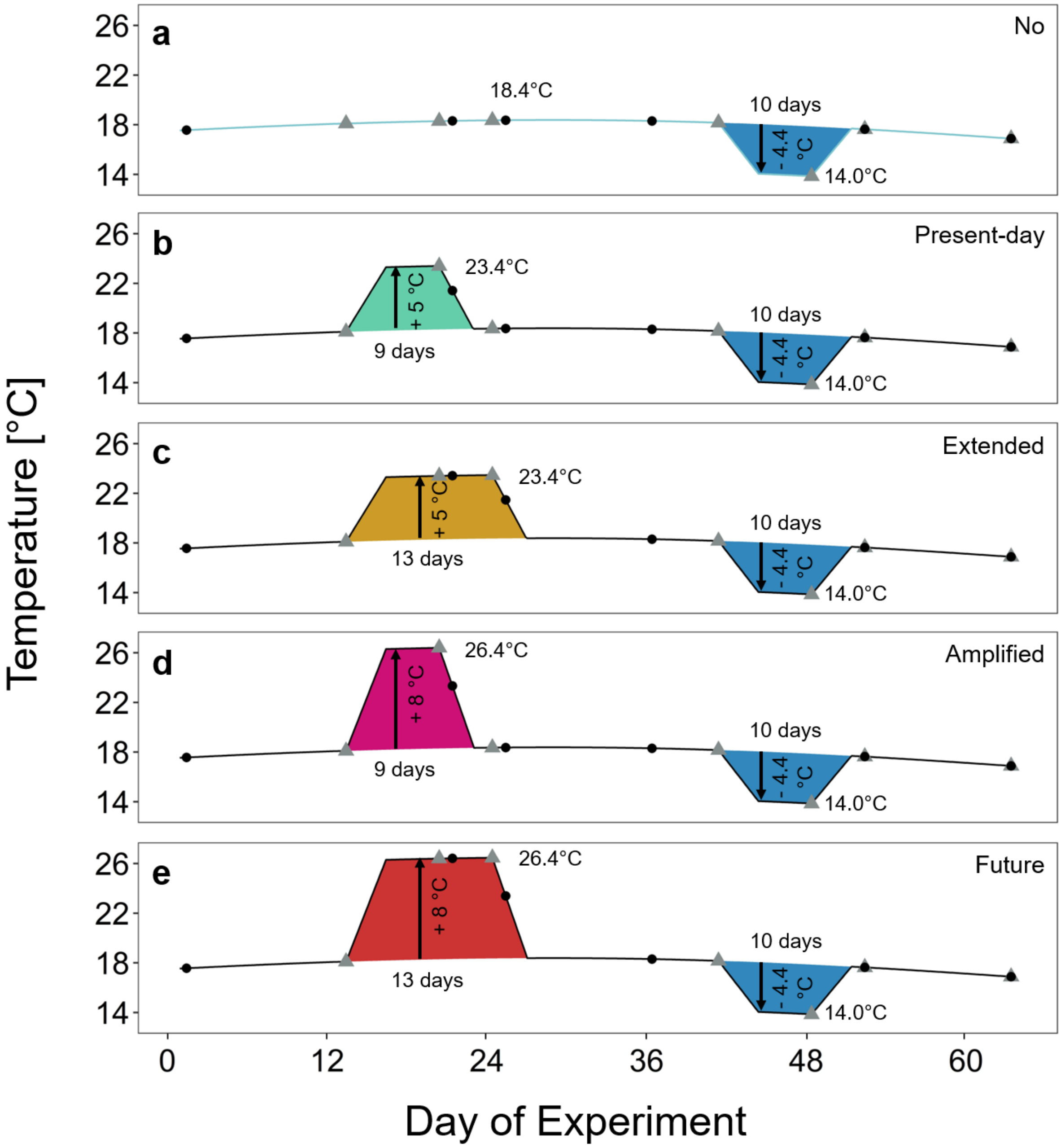

**Chapter II - Figure 1:** Schematic representation of the treatments experienced by individuals of *Asterias rubens* throughout the duration of the experiment. *No* heatwave: followed a smoothed natural mean seasonal temperature profile (blue line in **a**; see methods for further information). *Present day*: experienced a short heatwave with the intensity and duration of present-day events (9 days above the seasonal profile depicted in **a** with a maximum +5 °C, green polygon in **b**). *Extended*: a heatwave of extended duration in comparison to *Present-day* (13 days above seasonal profile with a maximum +5 °C, yellow polygon in **c**). *Amplified*: a heatwave of increased intensity in comparison to *Present-day* (9 days above seasonal profile with a maximum +8 °C, pink polygon in **d**). *Future*: a heatwave with the combined characteristics of those described in c and d (13 days above seasonal profile with a maximum +8 °C, red polygon in **e**). All treatments received anupwelling event (blue polygon) towards the end of the experiment, which was characterised by a drop in temperature (-4.4 °C), oxygen concentration (-6.3 mg $L^{-1}$) and $pH_{NBS}$ (-0.5 units) as well as an increase in salinity (+2.2 units; details in Chapter II - Supplementary Figure 4). Black dots represent measuring events of wet weight, while grey triangles represent assessments of righting responses of *A. rubens*.

### *Starfish collection and measured response variables*

Starfish individuals (*Asterias rubens*) were collected near Möltenort, Kiel (N54° 22’57.54”, E10°12’8.81”) on July 2nd, 2018. Animals were kept in a transitional tank at water temperatures measured at the collection habitat (17.6 °C). After 8 days of acclimation to laboratory conditions, 12 similarly sized starfish per treatment (wet weight: 6.4 ± 1.1 g, size as arm-tip to arm-tip length: 5.5 ± 0.3 cm, mean and SD) were transferred to individual experimental units.

Starfish were fed *ad libitum* every third day with blue mussels (*Mytilus spp.*: 1.5–2.0 cm shell length) freshly collected from Kiel Fjord the day before feeding. After each feeding event, the shell lengths of consumed mussels were measured (Dial Caliper, Wiha Division KWB Switzerland). Based on a previously described relationship between shell size and tissue dry weight for mussels in the study area (Morón Lugo et al. 2020), the dry weight of consumed mussels was estimated.

We weighed each starfish individual at the start of the experiment (day 1), during the heatwaves (day 21 for *Present-day* and day 21 and 25 for *Extended* heatwaves), in between heatwaves and the upwelling event (day 36), directly after the upwelling event (day 52) and at the end of the experiment (day 63; see also Chapter II - Figure 1).

We measured the activity of starfish (i.e., righting response) as the time required by the individuals to turn back onto their oral side after being placed on their aboral side. Righting is an essential response as it maintains the individual’s ability to detect and consume prey (Lawrence and Cowell 1996). Righting measurements were performed before the beginning of the heatwave treatments (day 13), at the end of the heatwaves (day 20 and 24 for the *Present-day* and *Extended* heatwave treatment, respectively), before (day 41), during (day 48) and at the end (day 52) of the upwelling event, and at the end of the experiment (day 63; see also Chapter II - Figure 1).

While feeding the starfish, we also checked for mortality (i.e., every third day). Starfish were considered dead if the bodies had been disintegrated (Chapter II - Supplementary Figure 6c), if they could not move their tube feet in response to physical stimuli, if they lost one or more arm(s) (Chapter II - Supplementary Figure 6d), or if they did not show signs of regeneration.

### *Data analysis*

All analyses were performed using R (R Core Team 2021). Impacts of the applied treatments on the performance of *A. rubens* over time and their interplay were analysed using regression approaches. Changes in the feeding rate and wet weight of A. rubens throughout the experiment and in response to the simulated heatwaves and upwelling events were described through generalised additive mixed models (GAMMs) fitted with the function bam from the R package “mgcv” (Wood 2017). In addition, linear mixed models (LMM) were fitted using the function lmer from the “lme4” package (Bates et al. 2015) to evaluate the impact of heatwave treatments over time on righting time. For feeding rate and wet weight, an additional LMM was applied using REML to test for the overall effect of the applied treatments at the end of the experiment. Supplementary Material 2 contains additional details regarding the statistical analyses and graphing.

## Results

### *Survival*

In our study, survival of the starfish *Asterias rubens* differed strongly between treatments (Chapter II - Supplementary Figure 7). Both *Amplified* treatments that simulated end-of-century heatwaves (Oliver et al. 2019) (amplitude +8 °C, maximum 26.0 °C; Chapter II - Supplementary Figure 4d and e) were lethal to all *A. rubens* individuals (Chapter II - Supplementary Figure 7). By day 21, 83% and 75% of the starfish had died when the temperature reached 25.9 °C for 2 and 3 days in the *Amplified* and the *Future* heatwave treatments, respectively (Chapter II - Supplementary Figure 7). After 3 more days, all remaining individuals in both *Amplified* treatments had died (Chapter II - Supplementary Figure 7). On the contrary, all *A. rubens* individuals survived exposures to *Present-day* and *Extended* heatwaves (intensity +5 °C, maximum 23 °C, and a duration of 9 and 13 days, respectively; Chapter II - Supplementary Figure 4d, b, c and Chapter II - Supplementary Figure 7). The upwelling event, an abrupt change in multiple drivers (Chapter II - Supplementary Figure 5), was not lethal to starfish.

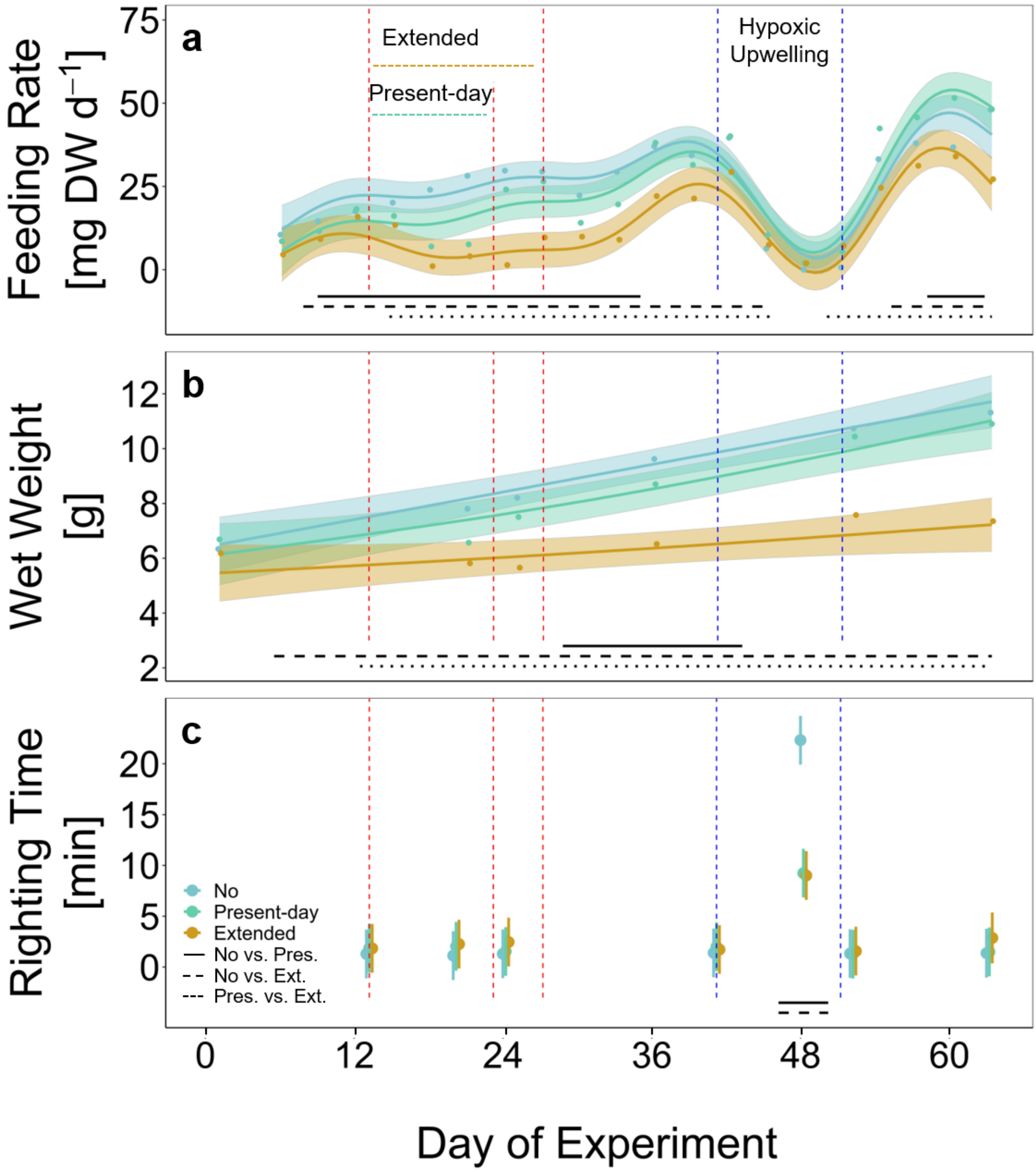

**Chapter II - Figure 2:** Feeding rate (mg mussel dry weight per day, a), wet weight (g, b) and righting time (minutes, c) of *Asterias rubens* throughout 63 days of our experiment, under *No* (blue), *Present-day* (green), and *Extended* (yellow) heatwave treatments (see Chapter II - Figure 1 for treatment descriptions). All treatments received an upwelling event towards the end of the experiment. The red dashed lines represent the periods of heatwaves (*Present-day* and *Extended*) and the blue dashed lines the period of hypoxic upwelling. Data are represented as means (dots) of n=12 experimental units. Trends in a and b were modelled using generalised additive mixed models (GAMM, explained deviance = 37.6% and 40.5%, respectively). Solid lines show the mean fitted trends and the shaded areas the associated 95% confidence intervals (a and b). Whiskers in c represent 95% confidence intervals. Differences between *No* and *Present-day*, between *No* and *Extended* and between *Present-day* and *Extended* are represented by solid, dashed and dotted black lines placed at the bottom of the plots, respectively (see Chapter II - Supplementary Figure 8 for further details). See also Chapter II - Supplementary Figure 9, Chapter II - Supplementary Figure 10, and Chapter II - Supplementary Figure 11 for related bar plots and 95% confidence intervals. Detailed statistical outcomes are presented in Chapter II - Supplementary Table 2, Chapter II - Supplementary Table 3, and Chapter II - Supplementary Table 4. All starfish died after 24 days in the *Amplified* treatments and were therefore excluded from the plots.

### *Feeding Rate*

Feeding rates of starfish subjected to *No* and both present-day amplitude heatwave treatments (*Present-day* and *Extended*) closely followed the trajectories modelled by the fitted generalised additive mixed model (GAMM; Chapter II - Figure 2a; explained deviance of 37.6%). Feeding rates in all treatments generally increased over the course of the experiment until the application of the upwelling event when feeding decreased steeply (Chapter II - Figure 2a). Still, the heatwave events of the Present day and Extended treatments significantly reduced mussel consumption by *A. rubens* (Chapter II - Figure 2a) compared to the feeding of starfish in the *No* heatwave treatment during the same period. Impacts of the *Present-day* heatwaves on *A. rubens*, however, were only transient and the starfish were able to resume feeding after the heatwaves ended. Those individuals that experienced heatwaves of present-day intensity and duration consumed overall as many mussels after the event as starfish that never experienced a heatwave (Chapter II - Figure 3a). In contrast, a pronounced heat-induced reduction of starfish feeding activity during the *Extended* heatwave events (Chapter II - Figure 3a) caused an overall reduction of mussel consumption by 53% compared to starfish in the *No* heatwave treatment (Chapter II - Figure 3a).

Simulated upwelling led to a dramatic decline in feeding rates of *A. rubens* in all treatments (Chapter II - Figure 2a). Yet, interestingly, starfish that had experienced heatwaves before the upwelling event on average consumed slightly (not significantly) more mussel soft tissue, than starfish in the *No* heatwave treatment (Chapter II - Supplementary Figure 12). Also, the negative effect of the upwelling was transient. *A. rubens* could recover from this event and their feeding rate (enormously) increased (Chapter II - Figure 2a).

### *Wet weight change*

Wet weight of *A. rubens* linearly increased over the two-month experimental period in all three treatments as can be seen by the trajectory predicted by the GAMM, which fits the data well (Chapter II - Figure 2b; explained deviance of 40.5%). No significant differences between wet weights of *A. rubens* experiencing a *Present-day* heatwave and *No* heatwave could be detected (Chapter II - Figure 2b). Growth rates of starfish experiencing a *Present-day* heatwave were significantly higher than of those experiencing an *Extended* heatwave (Chapter II - Figure 2b). Accordingly, the starfish's body mass in the *Present-day* heatwave treatment at the end of the summertime was not significantly impacted by the heatwave (Chapter II - Figure 3b), whereas it was significantly reduced in the *Extended* heatwave treatment (Chapter II - Figure 3b). In the

*Extended* heatwave treatment, over the two-month experiment, wet weight of *A. rubens* was reduced by 30% (Chapter II - Figure 3b) compared to the *No* heatwave treatment.

### *Righting Time*

Righting times of *A. rubens* were similar during all three treatments until the application of the upwelling event. The *Present-day* and the *Extended* heatwave had no effect on the activity (righting time) of the starfish (Chapter II - Figure 2c). The upwelling, however, strongly increased the righting time and, therefore, reduced the activity of *A. rubens*. During the upwelling, however, starfish individuals that had previously experienced a heatwave were significantly more active (lower righting time) than individuals of the *No* heatwave treatment (Chapter II - Figure 2c). After the completion of the upwelling event, righting time decreased to values as low as those registered at the beginning of the experiment.

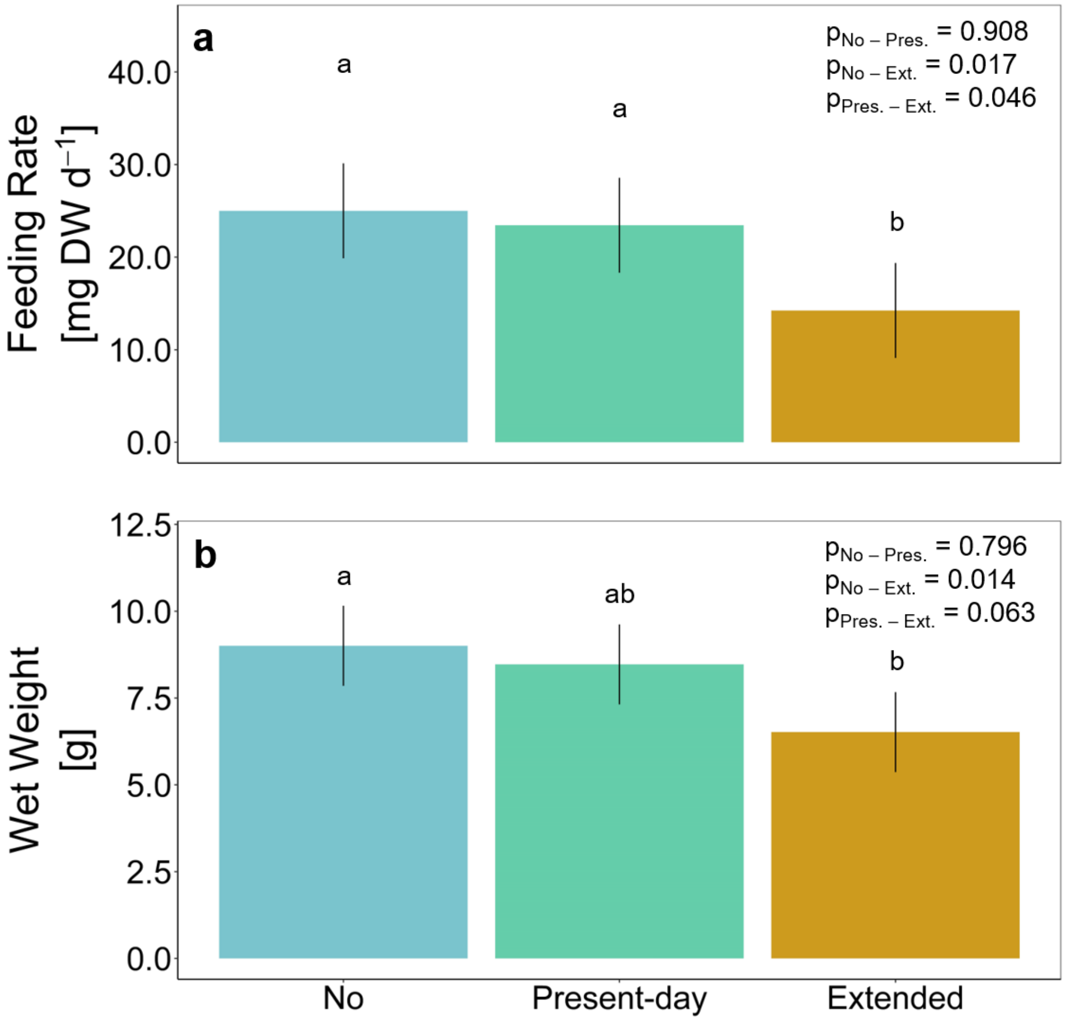

**Chapter II - Figure 3:** Mean feeding rate (mg mussel dry weight day, a) and wet weight (g, b) of *Asterias rubens* during 63 days of incubation, under *No* (blue), *Present-day* (green), and *Extended* (yellow) heatwave treatments (see Chapter II - Figure 1 for treatment descriptions). All treatments received an upwelling event towards the end of the experiment. Data are presented as means and 95% confidence intervals (n=12). Lower case letters represent significant differences between treatments based on linear mixed models (LMM, see Chapter II - Supplementary Table 2 and Chapter II - Supplementary Table 3). All starfish died after 24 days in the *Amplified* treatments and were therefore excluded from the plots.

## Discussion

We demonstrate that heatwaves caused (i) either severe mortality when applying future projected intensities or (ii) temporally decreased feeding and growth of Asterias rubens when exposed to today's intensities, and that (iii) longer heatwaves can lead to stronger overall impacts. Furthermore, starfish (iv) strongly reduced their activity during the seemingly very stressful upwelling event. However, (v) the negative impact imposed by the upwelling event was alleviated in individuals that were previously exposed to heatwaves of today's intensity.

### *Intensity- and duration-specific effects of marine heatwaves on starfish*

This experimental study showed that the performance of *Asterias rubens* was negatively affected by simulated marine heatwaves, and the effect strongly depended on their intensity and duration. The temperatures applied in our *Amplified* heatwave treatments (26 °C) exceeded the upper thermal tolerance limit of *A. rubens* (i.e., 25 °C; F. Melzner, personal communication). At such critical temperatures, the starfish likely suffered from a combination of extremely high cellular demands for oxygen and ATP as well as the constraints to supply those (Melzner et al. 2013), potentially leading to diminished oxygen concentrations in the coelomic fluid and tissues, acute stress, tissue damage and mortality (F. Melzner, personal communication; Vahl 1984; Pörtner 2001; Peck et al. 2008; Sokolova 2013). Extreme temperatures with peaks of 25 °C were recorded in the Kiel Fjord's shallow waters in summer 2018 (Wolf et al. 2021), just when the present experiment was being conducted. Such extreme temperatures were not only measured in the Baltic Sea, but also along the East coast of North America (Schlegel 2020). Thus, experimental temperatures only 1 °C above this historical record in the Baltic Sea, appear to be 100% lethal to *A. rubens*, presenting an emerging risk for this currently common and at places dominant marine predator.

Peak temperatures of 23 °C led to decreased starfish performance, which corroborates other recent findings suggesting that A. rubens feeding performance optimises at temperatures around 14 °C and suppresses at < 2 °C and > 22 °C (F. Melzner, personal communication; Agüera et al. 2012). Such temperatures of the *Present-day* and *Extended* heatwave treatments represented conditions recorded on 18 different days in surface waters of Kiel Fjord between 1997 and 2018 (Wolf et al. 2020). Interestingly, recovery from the heatwaves was possible and compensatory feeding could alleviate the overall negative impact following a present-day marine heatwave. Recovery of marine species following heatwaves was also shown in previous studies (Leung et al. 2017; Wolf et al. 2022), and therefore might represent a very important aspect in species (and ecosystem) responses to climate change (Leung et al. 2017). Although, starfish tended to increase their feeding rate also after an extended heatwave, they could not recover fully. Leung et al. (2019) demonstrated that species may be resistant (i.e., no impact), resilient (i.e., recovery is possible), or sensitive (i.e., no recovery is possible) when exposed to stressful conditions. This indicates that starfish are resilient to heatwaves of today's intensity but become sensitive if the stress persists longer or is of increased intensity.

Our results show that growth rates as well as final size of starfish experiencing a *Present-day heatwave* were significantly increased compared to starfish experiencing an *Extended* heatwave. Therefore, a projected elongation of heatwaves by 0.5 days per decade until 2100 (Oliver et al. 2018) (i.e., from 9 to 13 days) will likely negatively affect growth of *A. rubens* (in the absence of thermal adaptation or the presence of temporal spatial refugia).

### *Late summer upwelling events transiently decrease starfish performance*

The experimental imposition of upwelling conditions (i.e., low temperature, high salinity, low pH, and low oxygen concentrations) reduced the performance of *A. rubens*. As this species optimises its feeding at around 14 °C (F. Melzner, personal communication) the decrease of temperature during the upwelling cannot explain the lower feeding rate, and rather represented a release from the generally warm summer conditions. While the distribution of *A. rubens* is generally limited by very low salinities (Kautsky and Kautsky 2000), experimental feeding rates at a salinity of 20 (i.e., during the applied upwelling) are shown to be similar to those at a salinity of 16 (i.e., conditions throughout the rest of the experiment; Chapter II - Supplementary Figure 3). We therefore conclude that the reduced performance in the applied upwelling event was mainly caused by the low pH (or high $p\mathrm{CO}_2$) and the low oxygen concentrations in the upwelled seawater.

Experiments on the green sea urchin *Strongylocentrotus droebachiensis* have stated sublethal impacts of low oxygen at concentrations between 4.0 and 6.0 mg $L^{-1}$ (Siikavuopio et al. 2007). Fontanini et al. (2018) demonstrated that the combination of low pH (pH 7.6) and hypoxia (2.0 - 3.5 mg $L^{-1}$) led to a decrease in feeding rates of *A. rubens*. Similar negative synergistic effects of acidification and hypoxia were shown other benthic species (Steckbauer et al. 2015). Actually, the low pH during the upwelling potentially had a direct impact on the starfish's tissue as A. rubens cannot regulate coelomic fluid pH (Collard et al. 2013). Hu et al. (2018) could indeed show that a reduction in pH to 7.5 led to decreased feeding rates and growth. Thus, activity and feeding of *A. rubens* are transiently impacted during the upwelling event, most probably triggered by the low pH and low oxygen conditions in the seawater, while immediate recovery from such short-term events seems possible.

As neither acidification nor hypoxia led to mortalities during the applied upwelling, we conclude that the tested *A. rubens* population may generally tolerate moderate and transient acidification and hypoxia (Theede et al. 1969). Other starfish species have also been shown to survive acidified conditions for up to 4 months (Hue et al. 2020) as well as short-term (3 days) hypoxia (Diehl et al. 1979). Hu et al. (2018) discuss that under acidification, *A. rubens* allocates energy to the synthesis of proteins as protection of important physiological processes. Feeding suppression under acidification and hypoxia (Siikavuopio et al. 2007; Huo et al. 2018) (or high critical temperatures) potentially allows ectotherms such as *A. rubens* to allocate metabolic substrates (especially oxygen) to essential cellular processes (Vahl 1984). Yet, while *A. rubens* appears temporally tolerant towards acidified and hypoxic conditions, reduced mussel consumption by the starfish, caused by upwelling (and also by preceding heatwaves) during summer months, may lead to severe reduction of starfish energy reserves, possibly decreasing the probability of long-term (across years) survival and reproduction (Melzner et al. 2020).

### *Upwelling or spatial avoidance may provide refuge from heat stress*

As was shown for other species like corals (Randall et al. 2020) and macrophytes (Lourenço et al. 2016), low-temperature upwelling might act as a refuge from heat stress for *A. rubens*. Therefore, despite the transient adverse effects of upwelling, these events may relieve starfish from intense heat stress (Chapter II - Supplementary Figure 13c). During stressful upwelling events that follow (or interrupt) marine heatwaves, the habitable areas for *A. rubens*, currently in depths of 6.2 – 9.4 m (orange area in Chapter II - Supplementary Figure 1b), would shift towards even shallower zones (Chapter II - Supplementary Figure 1c). However, in the present study, heatwaves reaching the highest temperatures (up to 26 °C) were lethal for *A. rubens*, whereas no mortality was observed during the applied upwelling event that entailed realistic multiple changes in abiotic drivers. As upwelling with acidified and hypoxic conditions leads to reduced activity, and as these events occur unpredictable and fast, *A. rubens* might not be able to move fast enough to escape such sublethal stress.

Maximum temperatures in surface waters (Chapter II - Supplementary Figure 13a) tend to occur at the same time as minimum pH and oxygen concentrations in bottom waters (Chapter II - Supplementary Figure 13b; see also Wahl et al. 2021) for details on the Kiel Fjord). During late summer, oxygen minimum zones regularly form in deeper layers of marginal seas like the Gulf of Mexico (Rakocinski and Menke 2016) or the Baltic Sea (Raateoja et al. 2010). Migrating to these (cooler) waters would, thus, expose organisms to acidification and hypoxia (Chapter II - Supplementary Figure 1b), which may reduce organismal functioning (i.e., secondary production and community maturity; Rakocinski and Menke 2016). In the future, more stable seawater stratification caused by extended warm periods (and heatwaves) as well as a progressing eutrophication (Diaz and Rosenberg 2008; Lennartz et al. 2014; Yamaguchi and Suga 2019) will further foster the formation of a distinct acidified and hypoxic bottom layer. Hence, the size of refuge habitats for mobile species, like *A. rubens*, will, be reduced in many coastal regions (Chapter II - Supplementary Figure 1b).

### *Sub-lethal heatwaves may induce resistance to upcoming upwelling*

In contrary to expectations, starfish during the upwelling event benefited from the stress experienced previously in the form of a sublethal marine heatwave. More precisely, the activity of *A. rubens* that experienced a previous heatwave was 2.4 (*Present-day*) or 2.5 (*Extended*) times higher during the upwelling than that of naive *A. rubens* not experiencing a heatwave prior to the upwelling event. This pattern was also visible (as a strong but insignificant trend, $p = 0.065$) in recorded feeding rates of *A. rubens* (on average 2.5 - *Present-day* - or 2.4 - *Extended* - times higher, Chapter II - Supplementary Figure 12e). Reductions in feeding rates during the upwelling event were dramatic and occurred across treatments, potentially masking parts of the differences between heatwave treatments. In addition, as the period during which starfish experienced acidified and hypoxic conditions was short, higher mean feeding rates did not reverse the overall pattern of smaller individuals found in the Extended heatwave treatment. Typically, smaller-sized benthic invertebrate taxa are found in areas with regularly occurring hypoxia (Levin 2003). A higher surface-to-volume ratio results in a larger diffusive boundary layer through which more oxygen can be acquired in skin-breathing animals like *A. rubens*. Therefore, the smaller sized starfish that resulted from the *Extended* heatwave could have had an advantage during the subsequent upwelling. Furthermore, we qualitatively observed that the starfish's arms became longer and thinner during the upwelling event (Chapter II - Supplementary Figure 6a compared to Supplementary Figure 6b). This morphological change might have affected gas exchange, a finding that requires further investigation.

Theory suggests that the impacts of upwelling as a subsequent natural stressor could be mitigated to some extent by a preceding stress event (Walter et al. 2013; Jackson et al. 2021). As starfish were of similar size in the *No* and the *Present-day* treatments, morphological (size) variation cannot explain the higher activity (and partly feeding rate) of starfish in heatwave versus no heatwave treatments (see discussion above). Starfish previously exposed to heatwaves might have required energy and therefore fed even during the upwelling event. More plausibly, acclimation to heatwaves could have caused physiological and behavioural adjustments that functionally prepared starfish for the upwelling (i.e., ecological memory or cross stress tolerance (Walter et al. 2013; Jackson et al. 2021). In particular, cross stress tolerance enables species after an exposure to an initial stressor to better tolerate a subsequent stressor of different nature (Munné-Bosch and Alegre 2013; Walter et al. 2013).

Several studies have highlighted the role of HSPs in cross stress tolerance in terrestrial plants and fish species (Todgham et al. 2005; Banti et al. 2008; McBryan et al. 2016), although the underlying mechanisms are not yet fully understood. Potentially, genetic and molecular modifications are involved. Activation and upregulation of heat shock factors (e.g., HFS1) but also the hypoxia inducible factor HIF1a lead to an increased expression of HSPs (Hofmann et al. 2002; Ely et al. 2014; Lämke et al. 2016). These interactions between HIF1a and HSPs could explain the cross stress tolerance between heat and hypoxia (Hofmann et al. 2002; Ely et al. 2014; Lämke et al. 2016). HSPs have also been shown to play an important role in the response of marine species to acidification (as reviewed by Yusof et al. 2022). Therefore, the expression of transcription factors activating HSP genes and, thus, upregulation of HSPs during heatwaves could have also been beneficial for the performance of *A. rubens* in response to the applied upwelling event.

## Conclusions

Our work demonstrates that short-term but extreme pulse events can significantly impact marine species. Noteworthy, the strength of the impact from heatwaves strongly depends on amplitude and durations (i.e., overall strength) of the heatwave event. While upwelling entails multiple changes, reduced pH (increased $pCO_2$) and oxygen deficiency likely represent the main drivers reducing *A. rubens* activity. Consequently, heatwaves and upwelling will likely temporally reduce the in situ feeding pressure of this key predator *A. rubens* on mussel beds (Reusch and Chapman 1997), possibly having cascading ecosystem-wide consequences in the Western Baltic Sea and potentially other temperate regions of the Northern Atlantic region (Suchanek 1985; Reusch and Chapman 1997; Sanford 1999). The successive occurrence of stress events of different nature and the concepts of ecological memory and cross stress tolerance are theories already intensively studied in plant ecology (e.g., Munné-Bosch and Alegre 2013; Walter et al. 2013). However, we are only starting to understand such phenomena in the marine realm. The present study highlights such cross stress tolerance enabling starfish to endure and withstand consecutive stressors of differing quality (heatwaves versus upwelling) and to potentially acclimate to changing and fluctuating environments in the future. Overall, this study demonstrates the general importance of considering environmental fluctuations in experimental ecology and stresses the necessity for evaluating the concomitant effect of extreme events to generate realistic projections of how marine ecosystems may be transformed during climate change.

## Data Availability

Data collected during the experiment are available on PANGAEA (https://doi.pangaea.de/10.1594/PANGAEA.930929).

## Funding

This study was funded by the Deutsche Forschungsgemeinschaft (DFG; PA2643/2/348431475), through GEOMAR (Helmholtz-Gemeinschaft) and by Deutsche Bundesstiftung Umwelt (DBU; 20018/553).

## Acknowledgements

We would like to thank Anna-Lena Kolze and Christiane Schulz for their help during the experiment, including mussel collection, feeding and general maintenance, Björn Buchholz for help in maintaining the experimental facility, and Lyndsay Grace Walls for final proof reading and grammar check. We further thank five anonymous reviewers whose comments significantly improved our manuscript.

## References

Agüera, Antonio; Trommelen, Michel; Burrows, Frances; Jansen, Jeroen M.; Schellekens, Tim; Smaal, Aad (2012): Winter feeding activity of the common starfish (Asterias rubens L.). The role of temperature and shading. In Journal of Sea Research 72, pp. 106–112. DOI: 10.1016/j.seares.2012.01.006.

Arias-Ortiz, A.; Serrano, O.; Masqué, P.; Lavery, P. S.; Mueller, U.; Kendrick, G. A. et al. (2018): A marine heatwave drives massive losses from the world’s largest seagrass carbon stocks. In Nature Clim Change 8 (4), pp. 338–344. DOI: 10.1038/s41558-018-0096-y.

Bakun, A.; Black, B. A.; Bograd, S. J.; García-Reyes, M.; Miller, A. J.; Rykaczewski, R. R.; Sydeman, W. J. (2015): Anticipated Effects of Climate Change on Coastal Upwelling Ecosystems. In Curr Clim Change Rep 1 (2), pp. 85–93. DOI: 10.1007/s40641-015-0008-4.

Banti, Valeria; Loreti, Elena; Novi, Giacomo; Santaniello, Antonietta; Alpi, Amedeo; Perata, Pierdomenico (2008): Heat acclimation and cross-tolerance against anoxia in Arabidopsis. In Plant, cell & environment 31 (7), pp. 1029–1037. DOI: 10.1111/j.1365-3040.2008.01816.x.

Bates, Douglas; Mächler, Martin; Bolker, Ben; Walker, Steve (2015): Fitting Linear Mixed-Effects Models Using lme4. In J. Stat. Soft. 67 (1). DOI: 10.18637/jss.v067.i01.

Budd, G. C. (2008): Asterias rubens Common starfish. Edited by Tyler-Walters H., K. Hiscock. Marine Life Information Network: Biology and Sensitivity Key Infomation Reviews (online). Plymouth: Marine Biological Association of the United Kingdom. Available online at https://dx.doi.org/10.17031/marlinsp.1194.1.

Clark, Ailsa M.; Downey, Maureen E. (1992): Starfishes of the Atlantic. 1. ed. London: Chapman & Hall (Natural History Museum publications, 3).

Collard, Marie; Catarino, Ana I.; Bonnet, Stéphanie; Flammang, Patrick; Dubois, Philippe (2013): Effects of CO2-induced ocean acidification on physiological and mechanical properties of the starfish Asterias rubens. In Journal of Experimental Marine Biology and Ecology 446, pp. 355–362. DOI: 10.1016/j.jembe.2013.06.003.

Diaz, R. J. (2001): Overview of hypoxia around the world. In Journal of environmental quality 30 (2), pp. 275–281. DOI: 10.2134/jeq2001.302275x.

Diaz, Robert J.; Rosenberg, Rutger (2008): Spreading dead zones and consequences for marine ecosystems. In Science (New York, N.Y.) 321 (5891), pp. 926–929. DOI: 10.1126/science.1156401.

Diehl, W. J.; McEdward, L.; Proffitt, E.; Rosenberg, V.; Lawrence, J. M. (1979): The response of Luidia clathrata (Echinodermata. Asteroidea) to hypoxia. In Comparative Biochemistry and Physiology Part A: Physiology 62 (3), pp. 669–671. DOI: 10.1016/0300-9629(79)90122-1.

Dobashi, Tomoya; Iida, Midori; Takemoto, Kazuhiro (2018): Decomposing the effects of ocean environments on predator-prey body-size relationships in food webs. In Royal Society open science 5 (7), p. 180707. DOI: 10.1098/rsos.180707.

Ely, Brett R.; Lovering, Andrew T.; Horowitz, Michal; Minson, Christopher T. (2014): Heat acclimation and cross tolerance to hypoxia. Bridging the gap between cellular and systemic responses. In Temperature (Austin, Tex.) 1 (2), pp. 107–114. DOI: 10.4161/temp.29800.

Fennel, Katja; Testa, Jeremy M. (2019): Biogeochemical Controls on Coastal Hypoxia. In Annual review of marine science 11, pp. 105–130. DOI: 10.1146/annurev-marine-010318-095138.

Fontanini, Aisling; Steckbauer, Alexandra; Dupont, Sam; Duarte, Carlos M. (2018): Variable metabolic responses of Skagerrak invertebrates to low O2 and high CO2 scenarios. In Biogeosciences 15 (12), pp. 3717–3729. DOI: 10.5194/bg-15-3717-2018.

Gaymer, Carlos F.; Himmelman, John H.; Johnson, Ladd E. (2001): Distribution and feeding ecology of the seastars Leptasterias polaris and Asterias vulgaris in the northern Gulf of St Lawrence, Canada. In J. Mar. Biol. Ass. 81 (5), pp. 827–843. DOI: 10.1017/S0025315401004660.

Gunderson, Alex R.; Armstrong, Eric J.; Stillman, Jonathon H. (2016): Multiple Stressors in a Changing World. The Need for an Improved Perspective on Physiological Responses to the Dynamic Marine Environment. In Annual review of marine science 8, pp. 357–378. DOI: 10.1146/annurev-marine-122414-033953.

Hofmann, Gretchen E.; Buckley, Bradley A.; Place, Sean P.; Zippay, Mackenzie L. (2002): Molecular chaperones in ectothermic marine animals. Biochemical function and gene expression. In Integrative and comparative biology 42 (4), pp. 808–814. DOI: 10.1093/icb/42.4.808.

Hu, M. Y.; Lein, E.; Bleich, M.; Melzner, F.; Stumpp, M. (2018): Trans-life cycle acclimation to experimental ocean acidification affects gastric pH homeostasis and larval recruitment in the sea star Asterias rubens. In Acta physiologica (Oxford, England) 224 (2), e13075. DOI: 10.1111/apha.13075.

Hue, Thomas; Chateau, Olivier; Lecellier, Gael; Kayal, Mohsen; Lanos, Noeline; Gossuin, Hugues et al. (2020): Temperature affects the reproductive outputs of coral-eating starfish Acanthaster spp. after adult exposure to near-future ocean warming and acidification. In Marine environmental research 162, p. 105164. DOI: 10.1016/j.marenvres.2020.105164.

Huo, Da; Sun, Lina; Ru, Xiaoshang; Zhang, Libin; Lin, Chenggang; Liu, Shilin et al. (2018): Impact of hypoxia stress on the physiological responses of sea cucumber Apostichopus japonicus. Respiration, digestion, immunity and oxidative damage. In PeerJ 6, e4651. DOI: 10.7717/peerj.4651.

IPCC (2019): Summary for Policymakers. In H. O. Pörtner, D. C. Roberts, V. Masson-Delmotte, P. Zhai, M. Tignor, E. Poloczanska et al. (Eds.): IPCC Special Report on the Ocean and Cryosphere in a Changing Climate. In press.

Jackson, Michelle C.; Pawar, Samraat; Woodward, Guy (2021): The Temporal Dynamics of Multiple Stressor Effects. From Individuals to Ecosystems. In Trends in Ecology & Evolution 36 (5), pp. 402–410. DOI: 10.1016/j.tree.2021.01.005.

Kämpf, Jochen; Chapman, Piers (2016): Upwelling Systems of the World. Cham: Springer International Publishing.

Kautsky, Lena; Kautsky, Nils (2000): The Baltic Sea, including Bothnian Sea and Bothnian Bay. In Charles R. C. Sheppard (Ed.): Seas at the Millenium: An environmental Evaluation. Regional Chapters: Europe, The Amicas and West Africa: Pergamon (1).

Lämke, Jörn; Brzezinka, Krzysztof; Altmann, Simone; Bäurle, Isabel (2016): A hit-and-run heat shock factor governs sustained histone methylation and transcriptional stress memory. In The EMBO journal 35 (2), pp. 162–175. DOI: 10.15252/embj.201592593.

Lawrence, John M.; Cowell, Bruce C. (1996): The righting response as an indication of stress in stichaster striatus (Echinodermata, asteroidea). In Marine and Freshwater Behaviour and Physiology 27 (4), pp. 239–248. DOI: 10.1080/10236249609378969.

Lennartz, S. T.; Lehmann, A.; Herrford, J.; Malien, F.; Hansen, H.-P.; Biester, H.; Bange, H. W. (2014): Long-term trends at the Boknis Eck time series station (Baltic Sea), 1957–2013. Does climate change counteract the decline in eutrophication? In Biogeosciences 11 (22), pp. 6323–6339. DOI: 10.5194/bg-11-6323-2014.

Leung, Jonathan Y. S.; Connell, Sean D.; Russell, Bayden D. (2017): Heatwaves diminish the survival of a subtidal gastropod through reduction in energy budget and depletion of energy reserves. In Scientific reports 7 (1), p. 17688. DOI: 10.1038/s41598-017-16341-1.

Leung, Jonathan Y.S.; Russell, Bayden D.; Connell, Sean D. (2019): Adaptive Responses of Marine Gastropods to Heatwaves. In One Earth 1 (3), pp. 374–381. DOI: 10.1016/j.oneear.2019.10.025.

Levin, L. A. (2003): Oxygen minimum zone benthos: Adaptation and community response to hypoxia. In Oceanography and Marine Biologie 41, pp. 1–45.

Lourenço, Carla R.; Zardi, Gerardo I.; McQuaid, Christopher D.; Serrão, Ester A.; Pearson, Gareth A.; Jacinto, Rita; Nicastro, Katy R. (2016): Upwelling areas as climate change refugia for the distribution and genetic diversity of a marine macroalga. In J. Biogeogr. 43 (8), pp. 1595–1607. DOI: 10.1111/jbi.12744.

McBryan, Tara L.; Healy, Timothy M.; Haakons, Kristen L.; Schulte, Patricia M. (2016): Warm acclimation improves hypoxia tolerance in Fundulus heteroclitus. In The Journal of experimental biology 219 (Pt 4), pp. 474–484. DOI: 10.1242/jeb.133413.

Melzner, Frank; Buchholz, Björn; Wolf, Fabian; Panknin, Ulrike; Wall, Marlene (2020): Ocean winter warming induced starvation of predator and prey. In Proceedings. Biological sciences 287 (1931), p. 20200970. DOI: 10.1098/rspb.2020.0970.

Melzner, Frank; Thomsen, Jörn; Koeve, Wolfgang; Oschlies, Andreas; Gutowska, Magdalena A.; Bange, Hermann W. et al. (2013): Future ocean acidification will be amplified by hypoxia in coastal habitats. In Mar Biol 160 (8), pp. 1875–1888. DOI: 10.1007/s00227-012-1954-1.

Morón Lugo, Sonia C.; Baumeister, Moritz; Nour, Ola Mohamed; Wolf, Fabian; Stumpp, Meike; Pansch, Christian (2020): Warming and temperature variability determine the performance of two invertebrate predators. In Scientific reports 10 (1), p. 6780. DOI: 10.1038/s41598-020-63679-0.

Munné-Bosch, Sergi; Alegre, Leonor (2013): Cross-stress tolerance and stress “memory” in plants. An integrated view. In Environmental and Experimental Botany 94, pp. 1–2. DOI: 10.1016/j.envexpbot.2013.02.002.

Norling, P.; Kautsky, N. (2007): Structural and functional effects of Mytilus edulis on diversity of associated species and ecosystem functioning. In Mar. Ecol. Prog. Ser. 351, pp. 163–175. DOI: 10.3354/meps07033.

Oliver, Eric C. J.; Burrows, Michael T.; Donat, Markus G.; Sen Gupta, Alex; Alexander, Lisa V.; Perkins-Kirkpatrick, Sarah E. et al. (2019): Projected Marine Heatwaves in the 21st Century and the Potential for Ecological Impact. In Front. Mar. Sci. 6, p. 891. DOI: 10.3389/fmars.2019.00734.

Oliver, Eric C. J.; Donat, Markus G.; Burrows, Michael T.; Moore, Pippa J.; Smale, Dan A.; Alexander, Lisa V. et al. (2018): Longer and more frequent marine heatwaves over the past century. In Nature communications 9 (1), p. 1324. DOI: 10.1038/s41467-018-03732-9.

Paalme, Tiina; Torn, Kaire; Martin, Georg; Kotta, Ilmar; Suursaar, Ülo (2020): Littoral Benthic Communities Under Effect of Heat Wave and Upwelling Events in the Ne Baltic Sea. In Journal of Coastal Research 95 (sp1), p. 133. DOI: 10.2112/SI95-026.1.

Pansch, Christian; Hiebenthal, Claas (2019): A new mesocosm system to study the effects of environmental variability on marine species and communities. In Limnol. Oceanogr. Methods 28, p. 16. DOI: 10.1002/lom3.10306.

Pansch, Christian; Scotti, Marco; Barboza, Francisco R.; Al-Janabi, Balsam; Brakel, Janina; Briski, Elizabeta et al. (2018): Heat waves and their significance for a temperate benthic community. A near-natural experimental approach. In Glob Change Biol. DOI: 10.1111/gcb.14282.

Peck, L. S.; Webb, K. E.; Miller, A.; Clark, M. S.; Hill, T. (2008): Temperature limits to activity, feeding and metabolism in the Antarctic starfish Odontaster validus. In Mar. Ecol. Prog. Ser. 358, pp. 181–189. DOI: 10.3354/meps07336.

Pörtner, H. O. (2001): Climate change and temperature-dependent biogeography. Oxygen limitation of thermal tolerance in animals. In Die Naturwissenschaften 88 (4), pp. 137–146. DOI: 10.1007/s001140100216.

Przeslawski, Rachel; Byrne, Maria; Mellin, Camille (2015): A review and meta-analysis of the effects of multiple abiotic stressors on marine embryos and larvae. In Glob Change Biol 21 (6), pp. 2122–2140. DOI: 10.1111/gcb.12833.

R Core Team (2021): R: A language and environment for statistical computing. Version 4.1.1. Vienna, Austria: R Foundation for Statistical Computing. Available online at https://www.R-project.org.

Raateoja, M.; Kuosa, H.; Flinkman, J.; Pääkkönen, J.-P.; Perttilä, M. (2010): Late summer metalimnetic oxygen minimum zone in the northern Baltic Sea. In Journal of Marine Systems 80 (1-2), pp. 1–7. DOI: 10.1016/j.jmarsys.2009.06.005.

Rakocinski, Chet F.; Menke, Daneen P. (2016): Seasonal hypoxia regulates macrobenthic function and structure in the Mississippi Bight. In Marine pollution bulletin 105 (1), pp. 299–309. DOI: 10.1016/j.marpolbul.2016.02.006.

Randall, Carly J.; Toth, Lauren T.; Leichter, James J.; Maté, Juan L.; Aronson, Richard B. (2020): Upwelling buffers climate change impacts on coral reefs of the eastern tropical Pacific. In Ecology 101 (2), e02918. DOI: 10.1002/ecy.2918.

Reusch, Thorsten B. H.; Chapman, Anthony R. O. (1997): Persistence and Space Occupancy by Subtidal Blue Mussel Patches. In Ecological Monographs 67 (1), p. 65. DOI: 10.2307/2963505.

Sanford (1999): Regulation of keystone predation by small changes in ocean temperature. In Science (New York, N.Y.) 283 (5410), pp. 2095–2097. DOI: 10.1126/science.283.5410.2095.

Schlegel, Robert W. (2020): Marine Heatwave Tracker. Available online at http://www.marineheatwaves.org/tracker.

Seibel, Brad A. (2011): Critical oxygen levels and metabolic suppression in oceanic oxygen minimum zones. In The Journal of experimental biology 214 (Pt 2), pp. 326–336. DOI: 10.1242/jeb.049171.

Siikavuopio, Sten Ivar; Dale, Trine; Mortensen, Atle; Foss, Atle (2007): Effects of hypoxia on feed intake and gonad growth in the green sea urchin, Strongylocentrotus droebachiensis. In Aquaculture 266 (1-4), pp. 112–116. DOI: 10.1016/j.aquaculture.2007.02.028.

Smale, Dan A.; Wernberg, Thomas; Oliver, Eric C. J.; Thomsen, Mads; Harvey, Ben P.; Straub, Sandra C. et al. (2019): Marine heatwaves threaten global biodiversity and the provision of ecosystem services. In Nature Clim Change 9, p. 360. DOI: 10.1038/s41558-019-0412-1.

Snyder, Mark A.; Sloan, Lisa C.; Diffenbaugh, Noah S.; Bell, Jason L. (2003): Future climate change and upwelling in the California Current. In Geophys. Res. Lett. 30 (15), p. 198. DOI: 10.1029/2003GL017647.

Sokolova, Inna M. (2013): Energy-limited tolerance to stress as a conceptual framework to integrate the effects of multiple stressors. In Integrative and comparative biology 53 (4), pp. 597–608. DOI: 10.1093/icb/ict028.

Steckbauer, Alexandra; Ramajo, Laura; Hendriks, Iris E.; Fernandez, Miriam; Lagos, Nelson A.; Prado, Luis; Duarte, Carlos M. (2015): Synergistic effects of hypoxia and increasing CO2 on benthic invertebrates of the central Chilean coast. In Front. Mar. Sci. 2. DOI: 10.3389/fmars.2015.00049.

Suchanek, T. H. (1985): Mussels and their role in structuring rocky shore communities. In P. G. Moore, R. Seed (Eds.): The ecology of rocky coasts. Sevenoaks, pp. 70–96.

Suursaar, Ülo (2020): Combined impact of summer heat waves and coastal upwelling in the Baltic Sea. In Oceanologia 62 (4), pp. 511–524. DOI: 10.1016/j.oceano.2020.08.003.

Theede, H.; Ponat, A.; Hiroki, K.; Schlieper, C. (1969): Studies on the resistance of marine bottom invertebrates to oxygen-deficiency and hydrogen sulphide. In Mar Biol 2 (4), pp. 325–337. DOI: 10.1007/BF00355712.

Todgham, Anne E.; Schulte, Patricia M.; Iwama, George K. (2005): Cross-tolerance in the tidepool sculpin. The role of heat shock proteins. In Physiological and biochemical zoology : PBZ 78 (2), pp. 133–144. DOI: 10.1086/425205.

Vahl, Ola (1984): The relationship between specific dynamic action (SDA) and growth in the common starfish, Asterias rubens L. In Oecologia 61 (1), pp. 122–125. DOI: 10.1007/BF00379097.

Vaquer-Sunyer, Raquel; Duarte, Carlos M. (2008): Thresholds of hypoxia for marine biodiversity. In Proceedings of the National Academy of Sciences of the United States of America 105 (40), pp. 15452–15457. DOI: 10.1073/pnas.0803833105.

Vevers, H. G. (1949): The Biology of Asterias Rubens L. Growth And Reproduction. In J. Mar. Biol. Ass. 28 (1), pp. 165–187. DOI: 10.1017/S0025315400055272.

Wahl, Martin; Barboza, Francisco R.; Buchholz, Björn; Dobretsov, Sergey; Guy-Haim, Tamar; Rilov, Gil et al. (2021): Pulsed pressure. Fluctuating impacts of multifactorial environmental change on a temperate macroalgal community. In Limnol. Oceanogr. 33, p. 477. DOI: 10.1002/lno.11954.

Walter, Julia; Jentsch, Anke; Beierkuhnlein, Carl; Kreyling, Juergen (2013): Ecological stress memory and cross stress tolerance in plants in the face of climate extremes. In Environmental and Experimental Botany 94, pp. 3–8. DOI: 10.1016/j.envexpbot.2012.02.009.

Wolf, Fabian; Bumke, Karl; Wahl, Sebastian; Nevoigt, Frauke; Hecht, Ute; Hiebenthal, Claas; Pansch, Christian (2020): High resolution water temperature data between January 1997 and December 2018 at the GEOMAR pier surface. PANGAEA. Available online at https://doi.org/10.1594/PANGAEA.919186.

Wolf, Fabian; Clemmesen, Catriona; Hiebenthal, Claas (2021): Continuous water temperature, salinity, oxygen and pH data in front of GEOMAR Pier, Kiel, Germany (2014-2019). PANGAEA. Available online at https://doi.org/10.1594/PANGAEA.930979.

Wolf, Fabian; Seebass, Katja; Pansch, Christian (2022): The Role of Recovery Phases in Mitigating the Negative Impacts of Marine Heatwaves on the Sea Star Asterias rubens. In Front. Mar. Sci. 8, p. 1029. DOI: 10.3389/fmars.2021.790241.

Wood, Simon N. (2017): Generalized Additive Models: Chapman and Hall/CRC.

Yamaguchi, Ryohei; Suga, Toshio (2019): Trend and Variability in Global Upper-Ocean Stratification Since the 1960s. In J. Geophys. Res. Oceans 124 (12), pp. 8933–8948. DOI: 10.1029/2019JC015439.

Yusof, Nur Athirah; Masnoddin, Makdi; Charles, Jennifer; Thien, Ying Qing; Nasib, Farhan Nazaie; Wong, Clemente Michael Vui Ling et al. (2022): Can heat shock protein 70 (HSP70) serve as biomarkers in Antarctica for future ocean acidification, warming and salinity stress? In Polar Biol 45 (3), pp. 371–394. DOI: 10.1007/s00300-022-03006-7.

Zimmerman, R. C.; Hill, V. J.; Jinuntuya, M.; Celebi, B.; Ruble, D.; Smith, M. et al. (2017): Experimental impacts of climate warming and ocean carbonation on eelgrass Zostera marina. In Mar. Ecol. Prog. Ser. 566, pp. 1–15. DOI: 10.3354/meps12051.

# CHAPTER III

# Accumulation of stress drives eelgrass losses in non-heat-selected populations

**Running head:** Impact of warming vs. heatwaves on seagrass

**List of authors:** Fabian Wolf [1*], Christian Pansch [2], Florian Weinberger [1]

**Institute or laboratory of origin:** [1] Department of Marine Ecology, GEOMAR Helmholtz Centre for Ocean Research Kiel, 24105 Kiel, Germany; [2] Environmental and Marine Biology, Åbo Akademi University, 20520 Åbo, Finland

[*] **Corresponding author:** Fabian Wolf, GEOMAR Helmholtz Centre for Ocean Research Kiel, Düsternbrooker Weg 20, 24105 Kiel, Germany, telephone: +49 431 600 1599, E-Mail: fabian.wolf.research@gmail.com

**ORCIDs:** FaW: 0000-0002-0955-8487, CP: 0000-0001-8442-4502, FlW: 0000-0003-3366-6880

**Keywords:** climate change, environmental fluctuation, extreme events, acclimation, populations, *Zostera marina*, foundation species

## Abstract

Global climate change does not only lead to warming oceans but also increases probability of extreme marine heatwaves. Both, warming and heatwaves can impact coastal benthic ecosystems globally. However, heat-selection may mitigate those impacts. To entangle the relevance of long-term warming effects and the short-term effects of marine heatwaves and late summer upwelling on the foundation species *Zostera marina*, we conducted two experiments with either heat-selected or non-heat-selected individuals. While both, extended heatwaves and warming, reduced the number of leaves, warming also reduced the eelgrass height and number of shoots. Late summer upwelling only reduced the number of shoots and leaves if preceded by a typical heatwave of today's intensity. Heat-selected individuals generally grew more under warming conditions than non-heat-selected individuals. Our results indicate that *Zostera marina* is generally rather tolerant to short exposures of stressful events but accumulates negative impacts. With ongoing warming, stressful high temperatures will occur for longer times and thus, impact the important eelgrass with potential cascading effects on the whole ecosystem. However, heat-selection may actually mitigate the biomass losses of eelgrass and could be used for reforestation projects.

## Introduction

Global greenhouse gas emissions result in a projected increase of the world oceans’ temperature of 3 °C until 2100 (IPCC 2021). Ongoing warming has already impacted many species worldwide (Walther et al. 2002; Poloczanska et al. 2016) and will exacerbate in the future (IPCC 2019). Marginal seas, like the Baltic Sea, are characterized by an enclosure of shallow seawater by landmasses (Leppäranta and Myrberg 2009). This combination leads to a projected temperature increase of 4 °C until 2100 in the Baltic Sea (HELCOM 2013). Therefore, the Baltic Sea is considered as ‘Time Machine’ (Reusch et al. 2018) providing insights into future scenarios projected for other coastal areas, such as Delaware Bay or Chesapeake Bay.

Superimposed on this gradual warming are thermal fluctuations. Temperature fluctuates on very different scales, ranging from day-night fluctuations to seasonal variation (Bates et al. 2018; supplementary material to Pansch and Hiebenthal 2019). Although environmental fluctuations are crucial for the understanding of ecosystem impacts by climate change, only in recent years, variability has been implemented in experimental studies (e.g., Winters et al. 2011; Pansch et al. 2018; Vajedsamiei et al. 2021; Wahl et al. 2021).

Among different environmental fluctuations, extreme events are particularly of interest as they can push species beyond their optimal limits for a critical time and can therefore cause dramatic ecosystem changes (Easterling et al. 2000). Heatwaves, for example, (i.e., thermal anomalies; Hobday et al. 2016) are of particular relevance for marine ecosystems (e.g., Gray et al. 2002; Diaz and Rosenberg 2008; Neumann et al. 2012; Breitburg et al. 2018; Pansch et al. 2018; Smale et al. 2019; Sampaio et al. 2021; Wernberg et al. 2021). Such events have already caused great losses in seagrass populations in different areas worldwide (Reusch et al. 2005; Arias-Ortiz et al. 2018). Heatwaves are projected to increase in magnitude and frequency (Oliver et al. 2018). However, this trend is mainly driven by the general increase of temperatures (Oliver et al. 2019), implying an overriding effect of global warming. Thus, maximum temperatures during future heatwaves will likely have more severe impacts on marine ecosystems worldwide (Oliver et al. 2019).

Stress events, however, do not occur in isolation and recent literature suggests the importance of recurring stress events for species and ecosystem resilience (Gunderson et al. 2016; Jackson et al. 2021). Upwelling events in summer (i.e., stratification of the water column), for example, can bring relaxation from heat stress (e.g., Randall et al. 2020), while imposing (additional) stress from hypoxia (i.e., oxygen concentrations below 4 or 2 mg $L^{-1}$, depending on the species;

Vaquer-Sunyer and Duarte 2008), also bringing acidic and often increased salinity conditions to coastal habitats (e.g., Wahl et al. 2021). Such conditions can cause mortality, decreased growth or altered behaviour in coastal communities (e.g., Pedersen et al. 2004; Appelhans et al. 2014; Zimmerman et al. 2017; Breitburg et al. 2018; Wahl et al. 2021). Yet, the direct interaction of marine heatwaves and summer upwelling events has not been investigated to date (but see Wahl et al. 2021).

*Zostera marina* is the most common seagrass in the northern hemisphere (Green and Short 2003). Seagrass meadows provide various ecosystem services, by being a breeding area for vertebrate (Cole and Moksnes 2016) and invertebrate species (Boström and Bonsdorff 1997), reducing the amount of potentially harmful bacteria in the seawater (Reusch et al. 2021), functioning as a carbon sink (Cole and Moksnes 2016), and stabilizing the sediment and thus, reducing the intensity of coastal erosion (Duarte et al. 2013). Yet, the biomass of *Z. marina* is decreasing worldwide, which has been attributed to the infection of eelgrass with the Labyrinthulomycetes *Labyrinthula zosterae*, to coastal darkening (see e.g., Aksnes et al. 2009), and to higher temperatures (Muehlstein et al. 1988; Giesen et al. 1990; Hammer et al. 2018). Furthermore, hypoxia can induce sulphide intrusion in eelgrass and thus, facilitate mortality (Pedersen et al. 2004). Acidification, on the other hand, can be beneficial for eelgrass due to an enhanced $CO_2$ concentration which is available for photosynthesis (Zimmerman et al. 2017).

A recent study showed that across their latitudinal range, *Z. marina* populations are locally adapted to site-specific temperatures (i.e., ecotypes; Beca-Carretero et al. 2018), which might indicate a potential for acclimation, potentially providing advantages in a rapidly changing ocean (e.g., Morikawa and Palumbi 2019; Caruso et al. 2021; Pazzaglia et al. 2022).

Although *Z. marina* is known for its sensitivity towards thermal stress and hypoxia, a mechanistic understanding of the impacts of extreme events (i.e., heatwaves and summer upwelling) and warming impacts across all seasons is still lacking. Therefore, this study provides detailed insights into the response of this important foundation species towards long-term warming as well as short, but extreme temperatures. Furthermore, we tested for the adaptational potential of this seagrass species and individual differences in the resilience of populations to warming on a small geographic scale. We hypothesized that heat stress (heatwaves and long-term warming) decreases the performance of the eelgrass *Z. marina*. We further hypothesize that upwelling in late summer if preceded by a heatwave further decreases the performance of eelgrass. Furthermore, we hypothesized that heat-selection of *Z. marina* may already exist by microclimatic differences between natural habitats that are only a few hundred metres apart.

## Methods

### *Experiment 1: Outdoor warming experiment*

#### Collection of *Zostera marina* individuals

Two populations of *Zostera marina* were collected at Falckenstein Beach in the outer Kiel Fjord, Western Baltic Sea (Chapter III - Supplementary Figure 1). This part of Falckenstein Beach is characterized by a sand bank separating two populations that are in a distance of less than 200 m. One population (54°23'37.9"N, 010°11'24.4"E) is in shallower water, more protected from waves and currents and for this reason potentially heat-selected whereas the second *Z. marina* population in deeper, more exposed waters behind the sandbank is likely not heat-selected (54°23'37.9"N, 010°11'34.9"E; Chapter III - Supplementary Figure 1 and Chapter III - Supplementary Figure 2). The population from the shallow habitat (ca. 0.5 – 1 m; *Inside* population) was collected by wading, whereas the population from deeper areas (ca. 3 m; *Outside* population) was collected by scuba diving. Shortly after collecting, all individuals were brought back to GEOMAR, where they were planted into 28x19x13 cm (Length x Width x Height) plastic boxes. The boxes were filled with sand that was collected at the same location in the previous year and stored dry. Each box contained six individual plants of the same population. Three boxes of each population were placed into each tank.

#### Experimental setup and treatments

To examine the impact of long-term warming (i.e., across seasons) on the seagrass *Z. marina*, we conducted an experiment in the Kiel Outdoor Benthocosms (KOBs) from April 9th, 2019 until September 22nd, 2020. The KOBs are a state-of-the-art outdoor mesocosm facility in which naturally occurring fluctuation under different temperature scenarios can be tested under natural light and constant high-throughput natural water supply (Wahl et al. 2015). Therefore, seawater from the Kiel Fjord is constantly pumped from 1 m depth into the 12 tanks of 1,500 L capacity each. During this experiment, the water inside each tank was replaced circa six times per day. Thus, the tank abiotic conditions capture all changes that are naturally occurring in the Kiel Fjord (Wahl et al. 2015). Half of the tanks were run at the exact temperature of the Kiel Fjord with its natural fluctuations (*Ambient*), whereas the other half was run with the same fluctuations, but under a warming scenario of +3 °C (*Warming*; IPCC 2021; Chapter III - Figure 1). The KOBs are standing on a floating dock with 12 tanks standing in one line behind each other (Wahl et al. 2015). Eelgrass trays were always placed on the bottom of the western side of the tanks (see Chapter III - Supplementary Figure 3). To avoid any effects of the eelgrass position on the eelgrass performance (i.e., potentially different light and shadow regimes), the treatments were assigned to the tanks in an alternating way and were replicated with n=6 (N=12; Chapter III - Supplementary Figure 3). Temperature, salinity, pH, and oxygen concentration (see Wahl et al. 2015 for sensor details) were measured daily in each tank before sunrise (except weekends; Chapter III - Supplementary Figure 4).

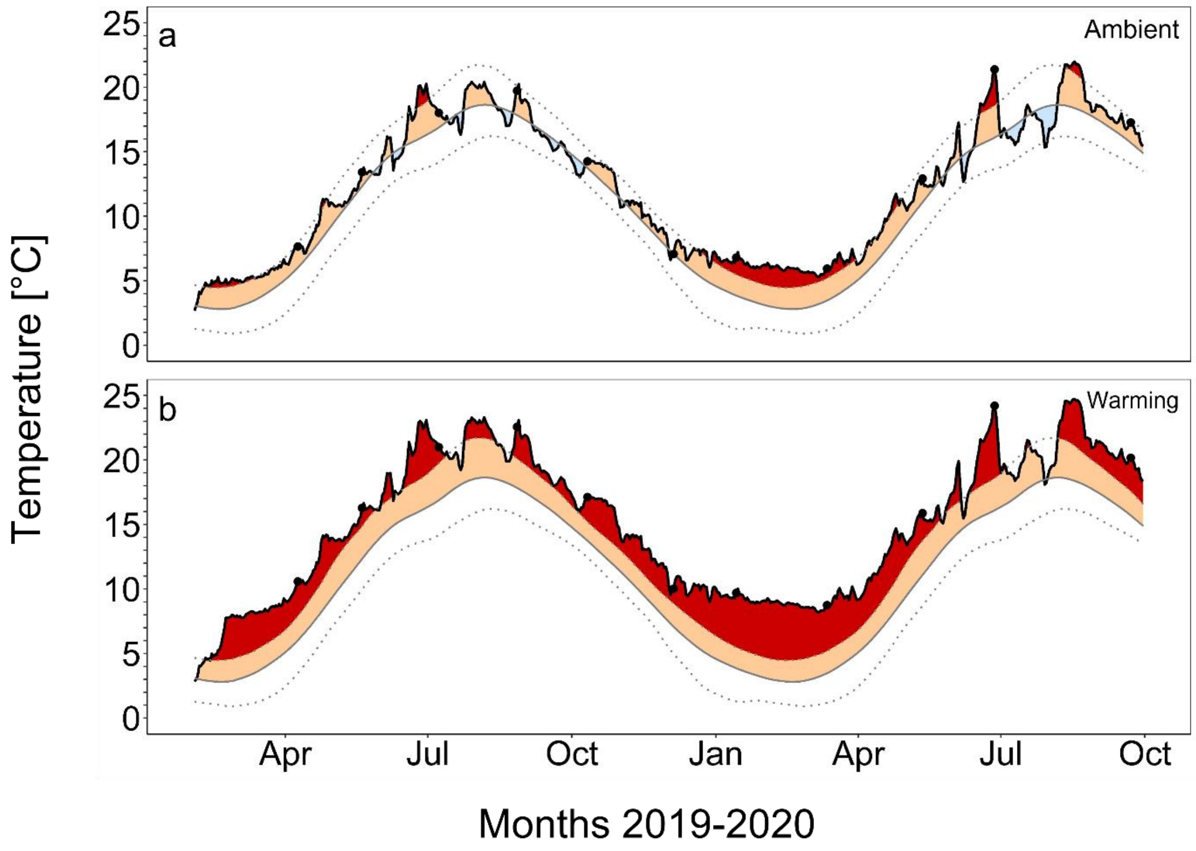

**Chapter III - Figure 1:** The experimental treatments in the Kiel Outdoor Benthocosms were based on the ambient Kiel Fjord temperatures from February 2019 until September 2020. The *Ambient* temperature treatment (**a**) was mirroring the natural fluctuations of the Kiel Fjord. The *Warming* temperature treatment (**b**) was also following the natural fluctuations of the Kiel Fjord, but with a future projected increase in temperature of 3 °C. Shown are daily mean temperatures (black solid line), a climatological trajectory (grey solid line), and thresholds for particularly warm (i.e., 90th percentile, upper black dotted line) and particularly cold temperatures (i.e., 10th percentile, lower black dotted line). Both, the climatological trajectory as well as the thresholds are based on a 22-year water temperature dataset of the Kiel Fjord (N54° 19' 46.0" E10° 8' 58.6"; Wof et al. 2020; Wolf et al. 2022) and were analysed following Hobday et al. (2016). Temperatures above the climatological trend, but below the 90th percentile are shown in orange, whereas temperatures above the 90th percentile are shown in red. Temperatures below the climatological trend, but above the 10th percentile are shown in light-blue, whereas temperatures below the 10th percentile are shown in dark-blue. As eelgrass individuals in the *Ambient* as well as in the *Warming* treatment experienced the same temperature conditions before collection, the climatological trajectoroy and thresholds of the recent past (i.e., 22 years) are shown and were not adjusted to the applied warming of 3 °C. Black dots indicate growth measurements of *Zostera marina*.

The stocking of each tank resembled the typical ecosystems of the Baltic Sea and included a mussel reef with sea stars, *Fucus* beds, soft sediment with polychaetes and the *Z. marina* populations studied here (see e.g., Saha et al. 2020; Sawall et al. 2021). Furthermore, the common periwinkle Littorina littorea was added as important grazer. Due to the constant water inflow, other typical grazers like crustaceans (*Idotea spp.* and *Gammarus spp.*) and gastropods (*Hydrobia spp.* and *Rissoa spp.*) settled in the tanks (see e.g., Pansch et al. 2018). In this paper, however, we will only present the impacts of warming on *Z. marina*.

Response variables

We measured three different growth parameters: number of shoots, number of leaves and longest leaf (i.e., length from sediment to tip of longest leaf) per plastic box. We conducted these measurements at least every two months (on average every 49 days; see black dots in Chapter III - Figure 1). Parts of the larger experiment were terminated already on June 27th, 2020. Therefore, the water in the tanks was drained, all mobile species collected, and the tank cleaned. Afterwards the tanks were refilled again. In the meantime, eelgrass individuals were stored in water baths. The species collection led to a grazer removal, which caused temporal high epiphytic cover on the eelgrass. Therefore, eelgrass growth was only evaluated until June 27th, 2020. At the end of the experiment (i.e., September 22nd, 2020) all eelgrass individuals present in each plastic box were counted and frozen, separated by leaf and root biomass, and freeze dried (Christ Freeze Drier Alpha 1-4 LSC, Osterode am Harz, Germany) and then weighed (Ohaus Scout Pro SPU402, Parsippany, USA).

Data analysis

To elucidate the impact of the interaction between temperature treatment and population on the growth of eelgrass over time, we used generalized additive mixed models (GAMMs). Therefore, the function *bam* of the package “mgcv” (Wood 2017) was applied. The smooth terms of the treatment and population were adjusted using thin plate regression splines and estimated by REML (Wood 2017). A Gaussian distribution of errors was assumed for all models. To account for the repeated measurements of growth over the course of the experiment, the replicated tanks were included in the model as random effect. As growth is highly autocorrelated, the models were checked using ACF and PACF. To account for the found autocorrelation, the function *start_value_rho* from the package “itsadug” (van Rij et al. 2020) was applied and the computed autoregressive model correlation parameter included in the GAMM. To identify temporal differences of the GAMMs, the estimates of each treatment were compared using the function *plot_diff* of the package “itsadug” (van Rij et al. 2020).

LMMs were applied to test for significant differences between the treatment and population at the end of the experiment in eelgrass survival, the weight of leaves and roots. Treatment and population were included as interaction in the model, whereas the replicated tank was included as random effect. Smoothing parameters were estimated via REML. To test for significant impacts of the applied warming treatment and the two eelgrass populations, ANOVAs were applied to the LMMs.

For all models the assumptions were visually checked by the thorough inspection of the residual plots. To meet these assumptions, the weight of leaves and roots of eelgrass individuals at the end of the experiment were transformed by applying a natural logarithmic function.

### *Experiment 2: Indoor heatwave experiment*

#### Collection of *Zostera marina* individuals

Eelgrass was collected by divers off Falckenstein Beach in the outer Kiel Fjord, Western Baltic Sea (54°24'23.2"N, 010°11'31.3"E; Chapter III - Supplementary Figure 1) in a depth of circa 3 m. In shallower water at the same site, we collected bare sand. After collection, eelgrasses and the sand were brought to a climate room and the eelgrass was planted into white plastic buckets (2.8 L volume) filled with sand and two *Z. marina* individuals (to identify the individuals, one side of the bucket was marked). Each individual *Z. marina* plant had one shoot. Buckets were randomly assigned to the 72 experimental units. After one week of acclimation at 18 °C, the experimental treatments were started.

#### Experimental setup

During the summer of 2019 (July 3rd – September 12th) we conducted a second experiment examining the impacts of heatwaves differing in frequency and duration on the seagrass *Z. marina* (see Chapter III - Figure 2). Furthermore, we tested whether a heatwave interruption caused by an upwelling event leads to an additive, antagonistic or synergistic impact on *Z. marina* (see Chapter III - Figure 2). To address these questions, we used the Kiel Indoor Benthocosms (KIBs). This infrastructure represents a state-of-the-art mesocosm system designed to test fluctuating environmental conditions on benthic communities (Pansch and Hiebenthal 2019) and is comprised of 12 600 L tanks in which temperatures can be adjusted automatically. We implemented six treatments, leaving two randomly chosen tanks per treatment, each tank holding six experimental units (Acrylic Glass Cylinders of 18 L volume; see Chapter III - Figure 3a). As each of the experimental units had a separate supply of fresh seawater from the Kiel Fjord and separate aeration, we had a total replication of n=12 per treatment (N=72). The tanks are equipped with two sets of LEDs: one yellow light simulating conditions at sun rise/set and one blue light which is additionally turned on throughout the day. Both LED intensities were linearly increased at sun rise (i.e., the yellow light was turned on at 4:45 and reached maximum intensity at 5:45 while the blue light was turned on one hour later) and decreased linearly at sun set (i.e., the blue light started to decrease at 20:00 and was turned off at 21:00 while the yellow light started to decrease one hour later). The light intensity in the KIBs is similar to the light intensity in 1 m depth of the Kiel Fjord during a cloud-free summer day (Pansch and Hiebenthal 2019).

### Experimental treatments

To ensure that our experimental treatments reflected natural relevant scenarios, we used the characterization of extreme events (heatwaves and cold-spells) after Hobday et al. (2016) based on the analysis of a 22-year high-resolution temperature dataset from the Kiel Fjord (Wolf et al. 2022).

The *No* heatwave treatment followed the climatological trajectory of summer months (Chapter III - Figure 2a; Wolf et al. 2022). All heatwave treatments were designed by applying the average maximum summer amplitude of 4.6 °C and the maximum onset and decline rate of 0.7 and 1.4 °C per day, respectively (Wolf et al. 2022). For the *Interrupted* heatwave treatment, three heatwaves of each 12 days above the climatological trajectory were separated by four relaxation days (Chapter III - Figure 2b; 90th percentile threshold was exceeded for five or seven days for the first two or the last heatwave, respectively). The *Present-day* heatwave had a duration of 28 days above the climatological trajectory (Chapter III - Figure 2c; 90th percentile was exceeded for 20 days). Both, *Present-day* and *Interrupted* heatwave treatments, had an average temperature of 19.2 °C. Duration, intensity, and onset as well as decline rate of the upwelling event were based on the characteristics of marine cold-spells (Wolf et al. 2022). Therefore, the upwelling event that we simulated during our experiment lasted for nine days with an intensity of 4.3 °C and an onset or decline rate of 2.5 or 0.8 °C per day, respectively (*Upwelling*; Chapter III - Figure 2d). In the *Present-day & Upwelling* treatment (Chapter III - Figure 2e), the heatwave is succeeded by the upwelling event, representing a common summer scenario (Pansch and Hiebenthal 2019; Wahl et al. 2021; Wolf et al. 2022). The *Extended* heatwave treatment (Chapter III - Figure 2f) represents conditions during which the *Present-day* heatwave is not interrupted by the upwelling event. Therefore, the *Extended* heatwave had a duration of 37 days above the seasonality (90th percentile was exceeded for 31 days; Wolf et al. 2022).

During the upwelling, water flow-through and aeration were stopped. In cylinders with the upwelling treatment, half the water was exchanged daily with deep Fjord water (from 18 m water depths, i.e., below the pycnocline). In all other cylinders, half the water was exchanged daily with surface water of the Fjord (i.e., the water that was used before and after the upwelling event). Temperature was logged hourly in the tanks (EnvLogger, ElectricBlue, Vairão, Portugal; Chapter III - Supplementary Figure 5) and was additionally measured with a handheld thermometer at least every three days in at least three experimental units (TTX 110 type T, Ebro, Ingolstadt, Germany). During the upwelling event, temperature, salinity, pH and oxygen concentration were measured daily (Multi 3630 IDS, WTW, Kaiserslautern, Germany; Chapter III - Supplementary Figure 6).

### Response variables

We measured the photosynthetic activity of *Z. marina* using a pulse-amplitude modulation device (Underwater Fluorometer Diving PAM, Heinz Walz GmbH, Effeltrich, Germany). The electronical signal gain was set to 6 whereas the intensity of measuring light was set to 3 for the first two measurements and to 4 for all other measurements. We recorded the fluorescence yield shortly before the light pulse, as well as the overall yield as measured by the Underwater PAM. PAM measurements were taken before each heatwave of the *Interrupted* heatwave treatment, at the maximum intensity of each heatwave of the *Interrupted* heatwave treatment and twice after the last heatwave of the *Interrupted* heatwave treatment (Chapter III - Figure 2, black triangles). In addition to the photosynthetic response of *Z. marina*, we measured three growth parameters: number of shoots, number of leaves and the length of the longest leaf of each eelgrass individual using a ruler (Chapter III - Figure 2, black dots).

### Data analysis

Linear mixed effect models (LMMs) using lmer function from the package “lme4” (Bates et al. 2015) were applied to evaluate the growth of eelgrass individuals in terms of height, number of shoots, and number of leaves. The applied treatments were included as fixed effect in the model. The individual cylinders (i.e., replicated experimental units) were included as random effect as measurements were repeated over time on the same cylinders. Smoothing parameters were estimated using Restricted Maximum Likelihood (REML). To test for significant impacts of the applied treatments, analyses of variance (ANOVA) were applied to the LMMs. If the ANOVAs showed a significant effect of the treatments, a Tukey post-hoc test was applied using the function emmeans of the equally named package (Lenth 2020). Residual plots of all models were thoroughly inspected to check for the underlying assumptions.

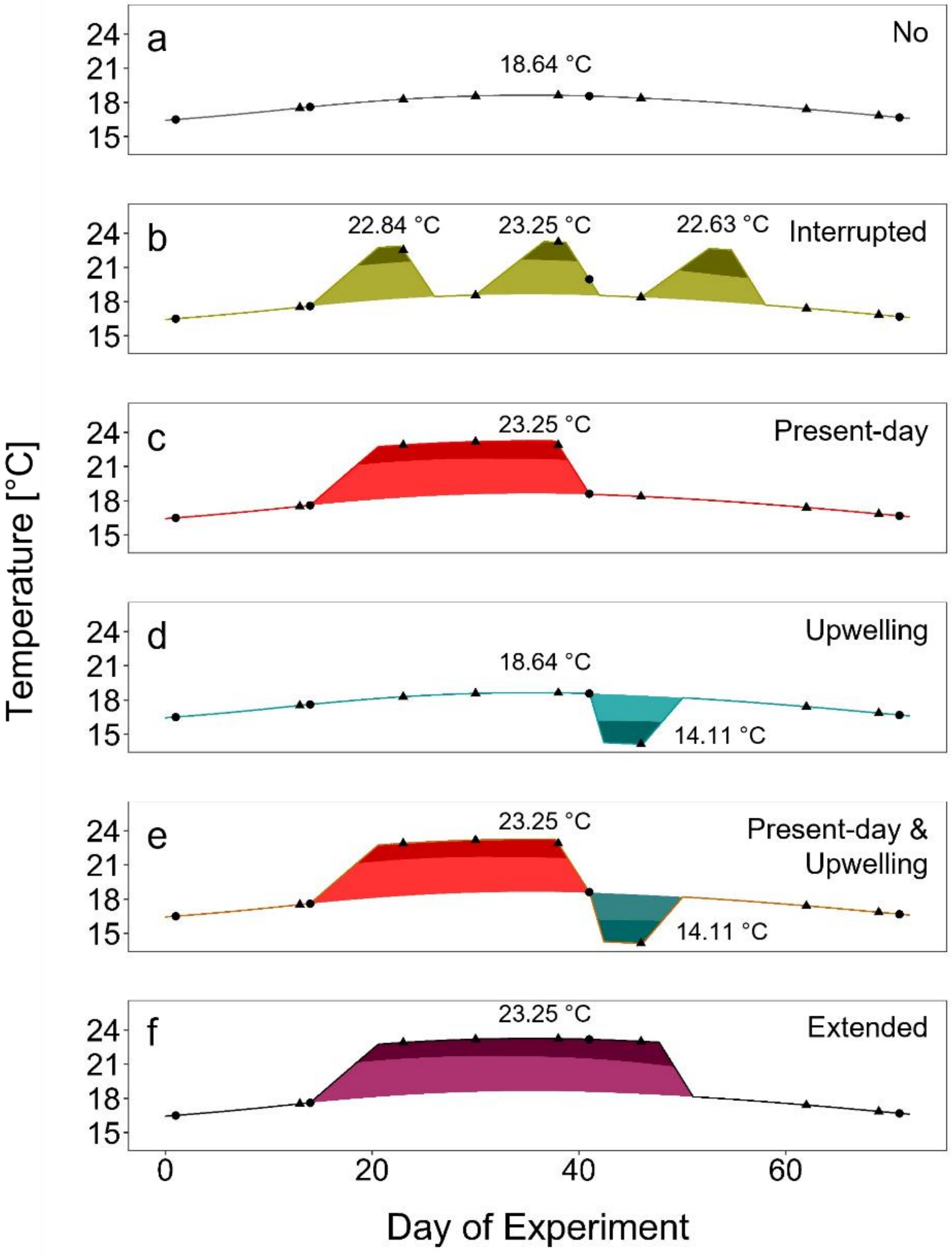

**Chapter III - Figure 2:** The experimental treatments in the Kiel Indoor Benthocosms were based on the heatwave definition by Hobday et al. (2016). The experimental treatments followed a smoothed natural summer seasonal temperature profile (*No* heatwave, grey line in **a**), experienced three short heatwaves of recent amplitude (*Interrupted*, 12 days above seasonality with max. + 4.6 °C, green filling in **b**), a heatwave of recent amplitude and duration (28 days above seasonality with max. + 4.6 °C, *Present-day*, red filling in **c**), an upwelling event (*Upwelling*, 8 days below seasonality with min. – 4.3 °C, blue filling in **d**), a heatwave of recent amplitude and duration with a succeeding upwelling event (*Present-day & Upwelling*, combination of treatments c and d, red and blue filling with orange line in **e**), and a heatwave of extended duration (37 days above seasonality with max. + 4.6 °C, *Extended*, purple filling in **f**). Temperatures above the 90th percentile are shown in a darker shade. Mean temperature of the *Interrupted* and *Present-day* heatwave treatment was equal. Black triangles represent measuring points for Pulse-Amplitude-Modulation (PAM) measurements of *Zosterea marina*, whereas black dots indicate assessments of growth (i.e., height, number of shoots, and number of leaves).

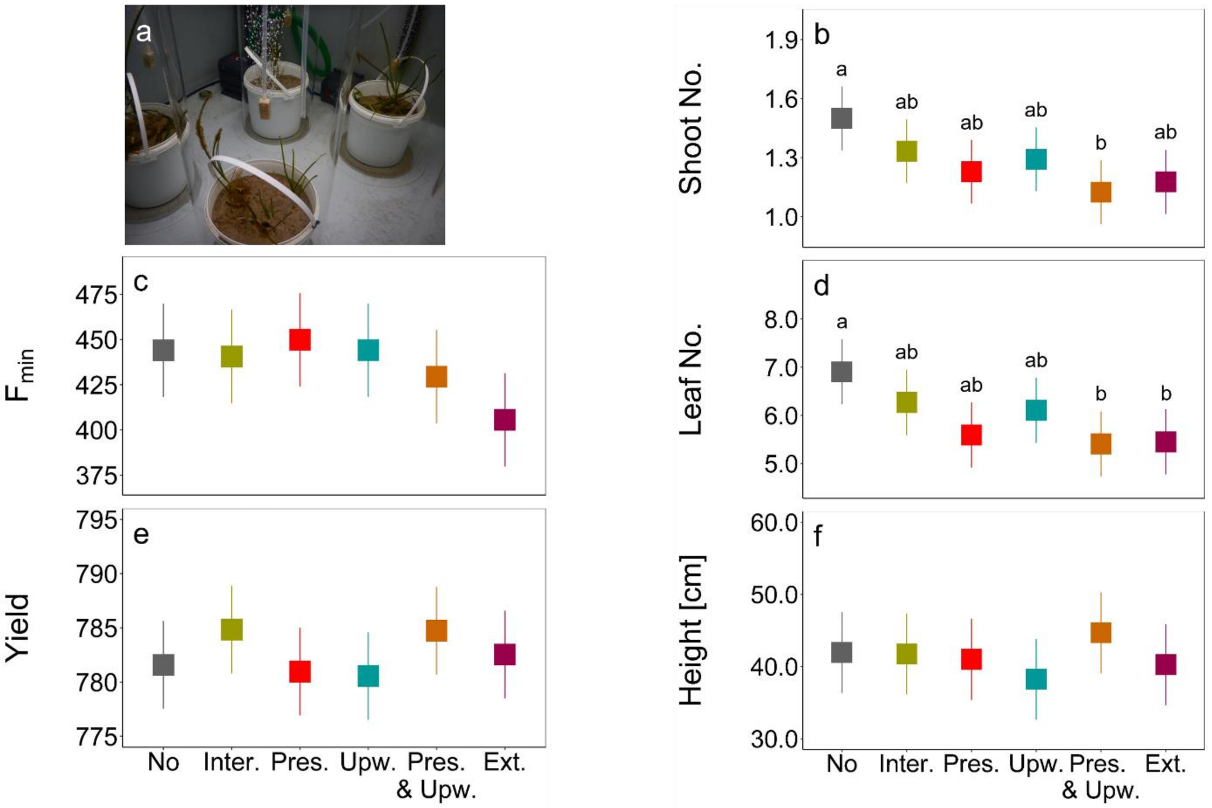

**Chapter III - Figure 3:** Experimental setup (**a**), Number of shoots (**b**), $F_{min}$ (**c**), number of leaves (**d**), yield (**e**), and height (cm, **f**), and of *Zostera marina* during 68 days of incubation in the Kiel Indoor Benthocosms, under *No* (grey), *Interrupted* (green), *Present-day* (red), and *Extended* (purple) heatwave treatments and additional upwelling treatments without a preceding heatwave (*Upwelling*, blue) or with a preceding present-day heatwave (*Present-day & Upwelling*, orange) (see Chapter III - Figure 2 for treatment descriptions). $F_{min}$ (**c**) and yield (**e**) are based on Pulse-Amplitude-Modulation (PAM). Data are presented as means and 95% confidence intervals (n=12) based on Linear Mixed Effect Models (LMM). Lower case letters indicate significant differences between treatments based on Tukey post-hoc tests. For statistical details see Chapter III - Supplementary Table 1, Chapter III - Supplementary Table 2, and Chapter III - Supplementary Table 3).

## Results

### *Outdoor warming experiment*

After 1.5 years of incubation, the survival of *Zostera marina* was on average 2.3 times higher under the *Ambient* compared to the *Warming* temperature scenario as well as it was 1.3 times higher in the *Inside* population compared to the *Outside* population (Chapter III - Figure 4a and b). However, due to huge variations, the trend between the temperature treatments was only marginally significant (Chapter III - Figure 4a and b; Treatment: F-value = 4.349, p-value = 0.064) and not significant for population differences Chapter III - Figure 4a and b; F-value = 0.678, p-value = 0.430). The dry weight (DW) of *Z. marina* leaves and roots was significantly reduced under *Warming* conditions in the *Outside* population (Chapter III - Figure 4c-f; Leaf DW: F-value = 4.518, p-value = 0.042; Root DW: F-value = 4.667, p-value = 0.039). For the *Inside* population no significant effect was found, but individuals subjected to *Warming* conditions tended to have a smaller leaf and root biomass (Chapter III - Figure 4c-f). The generalised additive mixed models (GAMMs) for the number of shoots, the number of leaves and the height of eelgrass fitted the data very well (i.e., explained deviance of 86.6, 78.0, and 78.9%, respectively; Chapter III - Figure 5). The GAMM for the number of eelgrass shoots differed between temperature treatments from July 15th (20.1 °C, *Outside* population) and June 17th, 2019 (18.8 °C, *Inside* population) until the end of the experiment. The GAMM for the number of eelgrass leaves differed between temperature treatments from June 29th (22.8 °C, *Outside* population) and May 31st, 2019 (16.1 °C, *Inside* population) until the end of the experiment. The GAMM for eelgrass height differed among temperature treatments from April 24th (13.7 °C, *Inside* population) and May 3rd, 2019 (13.7 °C, *Inside* Population) until July 3rd (21.7 °C, *Outside* population) and June 25th, 2019 (22.9 °C) for the *Outside* and *Inside* population, respectively. The GAMM for eelgrass height differed again from August 28th (23.1 °C) and August 24th (20.7 °C) for the *Outside* and *Inside* population until the end of the experiment, respectively.  Generally, the differences between temperature treatments occurred earlier in individuals from the *Inside* population compared to the *Outside* population. Furthermore, under *Warming* conditions, the eelgrass biomass peaked on average 37 days earlier (August 17th, 2019; 21.1 °C) than under *Ambient* temperatures (September 24th, 2019; 15.8 °C; Chapter III - Figure 5). Not only the temperature treatment, but also the population had an impact on the timing of peak eelgrass biomass. *Z. marina* individuals from the *Outside* population on average maximized their biomass 11 days earlier (September 18th, 2019; 15.4 and 18.3 ° for *Ambient* and *Warming* temperatures, respectively) than individuals from the *Inside* population (September 29th, 2019; 14.7 and 17.6 °C for *Ambient* and *Warming* temperatures, respectively). However, growth rates (i.e., the slopes of the generalized additive mixed models in Chapter III - Figure 5 and Chapter III - Supplementary Figure 8) peaked already in July, irrespective of the treatment. The growth season of eelgrass generally lasted longer without warming (Chapter III - Figure 5 and Chapter III - Supplementary Figure 8). New leaves and shoots were formed faster by eelgrass individuals that experienced *Ambient* compared to individuals that experienced *Warming* temperature conditions (Chapter III - Figure 5c-f). Significant differences between eelgrass individuals subjected to *Ambient* or *Warming* temperature conditions started to persist after the first summer in 2019 (Chapter III - Figure 5). The *Inside* population had a higher growth compared to the *Outside* population (Chapter III - Figure 5).

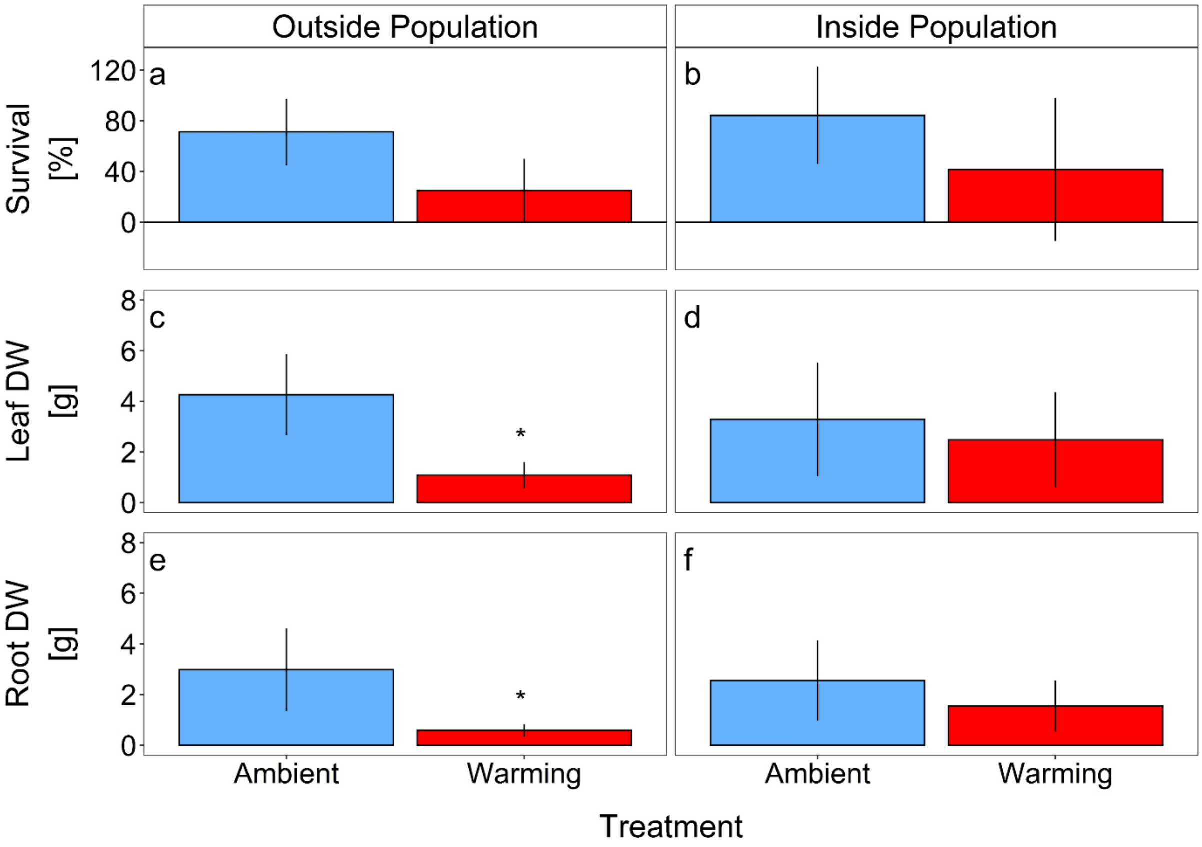

**Chapter III - Figure 4:** Loss of *Zostera marina* individuals (**a** and **b**, in %) and dry weight (DW, in gram) of *Zostera marina* leaves (**c** and **d**) and roots (**e** and **f**) coming from a population outside and a population inside a sandbank over 1.5 years of experiment in the Kiel Outdoor Benthocosms, under *Ambient* Kiel Fjord temperatures (blue) and a *Warming* scenario projected for Kiel Fjord (red). See Chapter III - Figure 1 for temperature profiles. Shown are means and 95% confidence intervals (n=6). Lower case letters indicate significant differences between treatments based on analyses of variance (ANOVA). Detailed statistical outcomes are presented in Chapter III - Supplementary Table 4.

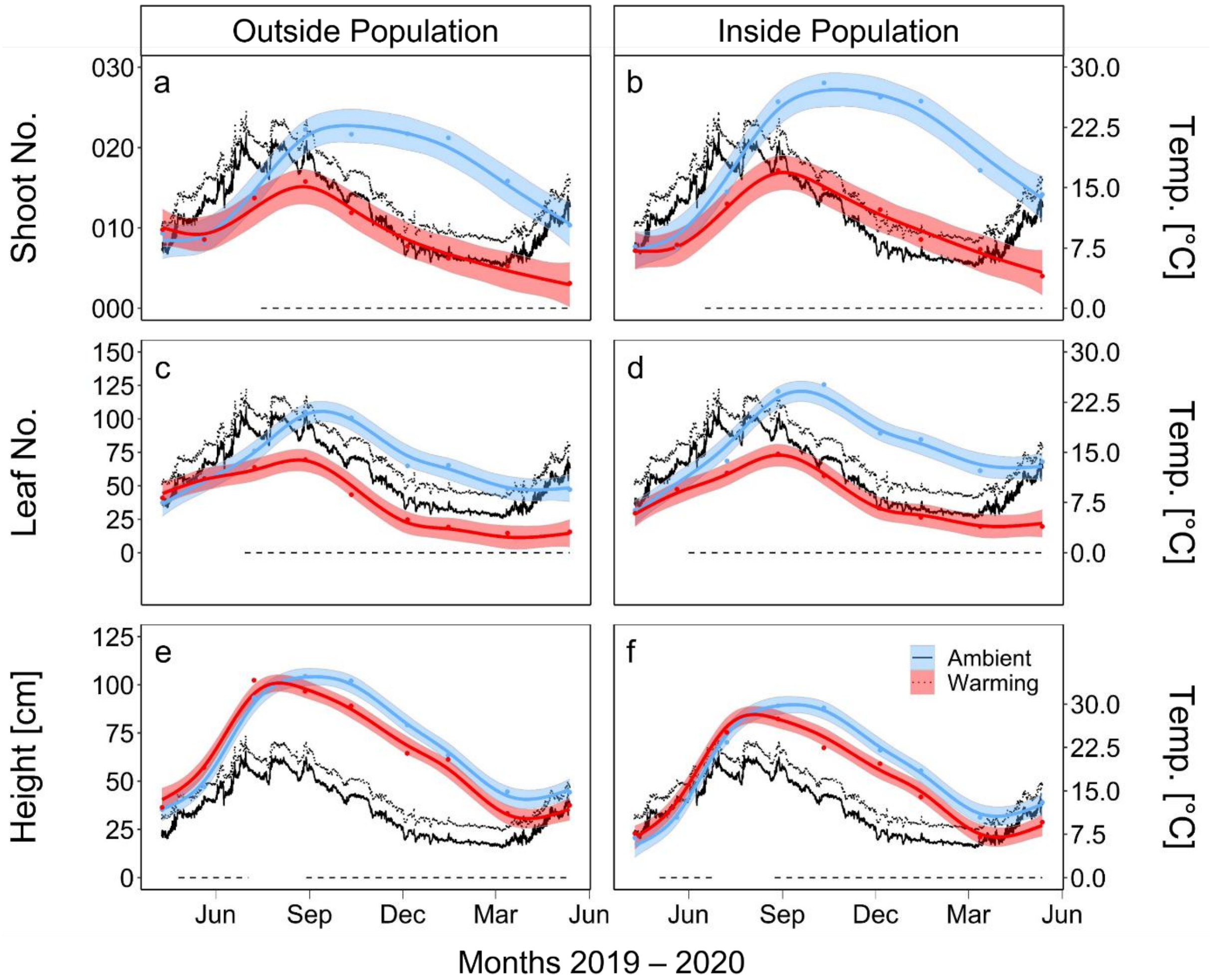

**Chapter III - Figure 5:** Shoot number (**a** and **b**), leaf number (**c** and **d**) and Height (cm, **e** and **f**), of two *Zostera marina* populations coming from outside (**a**, **c**, **e**) and inside a sandbank (**b**, **d**, **f**) throughout 1.5 years of experiment in the Kiel Outdoor Benthocosms, under *Ambient* Kiel Fjord temperatures (blue for response variable and black solid line for temperature profile in °C) and a *Warming* scenario projected for the Kiel Fjord (red for response variable and black dotted line for temperature profile in °C). Data are represented as means (dots) of n=6 experimental tanks. Trends were modelled using generalized additive mixed models (GAMM, explained deviance for shoot number (**a-b**) = 79.7%, leaf number (**c-d**) = 80.3%, and height (**e-f**) = 86.6%,). Solid lines show the mean fitted trends and the shaded areas the associated 95% confidence intervals. Differences between *Z. marina* responses subjected to *Ambient* or *Warming* temperature conditions are represented by dashed black lines placed at the bottom of the plots (see Chapter III - Supplementary Figure 7 for further details). Detailed statistical outcomes are presented in Chapter III - Supplementary Table 5.

### *Indoor heatwave experiment*

Shoot and leaf number were significantly impacted by the imposed treatments (Chapter III - Figure 3a and b; Shoot No.: F-value = 2.578, p-value = 0.034; Leaf No.: F-value = 2.887, p-value = 0.020). The *Present-day & Upwelling* treatment significantly reduced shoot number compared to those individuals that were not subjected to heatwaves or upwelling (Chapter III - Figure 3b). The *Present-day & Upwelling* and the *Extended* heatwave treatments significantly reduced the leaf number of *Z. marina* individuals compared to those individuals that did not experience any extreme event Chapter III - Figure 3d). Noteworthy, the number of shoots and leaves of *Z. marina* individuals decreased on average in all heatwave and upwelling treatments compared to individuals that did not experience any heatwaves or upwelling events (Chapter III - Figure 3b and d).

The height (Chapter III - Figure 3f; F-value = 0.553, p-value = 0.736) and photosynthetic activity (Chapter III - Figure 3c and e; f-min: F-value = 1.508, p-value = 0.185; Yield: F-value = 0.821, p-value = 0.539) of *Z. marina* were both not significantly impacted by the exposure to the applied treatments.

## Discussion

By now, many experiments have focused on short-term responses of seagrasses to elevated temperatures (e.g., Ehlers et al. 2008; Bergmann et al. 2010; Winters et al. 2011; Franssen et al. 2011), but only a few studies investigated the long-term effects (e.g., Sawall et al. 2021). Our approach of combining the short-term impact by summer extreme events (i.e., heatwaves and summer upwelling) and long-term impacts of global warming following all seasons is a novel approach.

### *Accumulation of stressful conditions reduce the growth of Zostera marina*

The applied upwelling decreased the temperature, pH, and oxygen concentration while salinity was increased (see Chapter III - Supplementary Figure 6). While lower temperatures and higher salinities, in the range that were applied during the upwelling, do not impact the growth of *Zostera marina* (Nejrup and Pedersen 2008) and acidification can even be beneficial (Zimmerman et al. 2017), hypoxia was shown to be detrimental (Pedersen et al. 2004). As hypothesized, stressful upwelling alone did not significantly impact the growth of *Z. marina* but only decreased the number of shoots and leaves when preceded by a present-day heatwave. This indicates that when not previously thermally stressed, the increased salinity and $CO_2$ concentration as well as the decreased temperature mitigate the negative impacts of hypoxia. Furthermore, we demonstrated that extended heatwaves decreased the number of leaves in *Z. marina* individuals. However, this decreased leaf number was not caused by a reduced photosynthetic capacity (see Chapter III - Figure 3c and e) but may be caused by the reallocation of energy in essential cellular processes (Somero 2020). This indicates that eelgrass is rather tolerant to shorter extreme events (i.e., summer heatwaves and upwelling), while growth is decreased when the stress is accumulated. A study by Moreno-Marín et al. (2018) already demonstrated that the negative impacts of single stressors were accumulated when the stressors were combined. This proves again the high relevance of studying the succession of stress events as proposed by Jackson et al. (2021).

As accumulation of stress seems to be very important in eelgrass, it is not surprising that long-term warming (i.e., across seasons) also strongly reduced growth of *Z. marina*. Starting with peak temperatures during summer months, growth was reduced, and eelgrass individuals did not recover during the winter months. Interestingly, the timespan until the growth of eelgrass started to differ between temperature treatments was with 75 days almost twice as long as the duration of the extended heatwave in the indoor experiment (i.e., 37 days). The cumulative temperature over the period until the GAMMs of shoots and leaves (both populations) started to differ between temperature treatment is with 1159 °C day in a similar range as for the extended heatwave (i.e., 823 °C day). Likely, the gap between these two values comes from the much higher mean temperature of the heatwave (i.e., 22.2 °C) compared to elevated temperature in the outdoor experiment (15.3 °C).

Warming did not only reduce overall growth by the end of the 1.5-year experiment but also led to an earlier peak in maximum growth. In a similar experiment covering three seasons, Sawall et al. (2021) could demonstrate that the number of reproductive shoots peaked earlier when heated. Also other studies indicate an earlier vegetation period in populations coming from warmer waters (Phillips et al. 1983; Silberhorn et al. 1983; Blok et al. 2018). Therefore, we conclude that eelgrass is susceptible to thermal stress depending on the duration and intensity of the stress. Such an impact of cumulative temperatures on species responses was already demonstrated for a wide range of species and responses, e.g., coral bleaching (i.e., degree heating weeks; Kayanne 2017), gamete release of macroalga (Bacon and Vadas 1991) or hatching of lobster eggs (Haarr et al. 2020).

Negative impacts of high temperature on eelgrass growth are likely attributed to increased metabolic rates (see e.g., Brown et al. 2004) leading to higher energy demands. However, not only temperature, but also light intensity is one important factor that limits the growth of seagrasses (Lee et al. 2007). This may explain why the applied heatwaves in our study only led to a small effect size, while Reusch et al. (2005) showed a substantial loss of eelgrass biomass during a natural heatwave in 2003. The study by Reusch et al. (2005) was carried out in a very shallow bay with high turbidity, so that the strongly reduced biomass during the heatwave may be the combination of low light intensity and high temperatures. As the oceans are warming (IPCC 2021) and water in the Baltic Sea has become more turbid (Dupont and Aksnes 2013), the finding by Reusch et al. (2005) may represent a more accurate scenario than our heatwave experiment. Ongoing warming (IPCC 2021) associated with a higher probability of critical temperatures during future heatwaves (Oliver et al. 2018) and the expansion of hypoxic areas

(Diaz 2001) will likely facilitate the negative impacts on eelgrasses and thus, potentially lead to cascading ecosystem impacts.

### *Heat-selected vs. non-selected eelgrass individuals*

Interestingly, heat-selected individuals were impacted earlier from warming than the non-heat-selected individuals. Several studies suggest a trade-off between the production of heat shock proteins (HSP) and reproduction (e.g., Silbermann and Tatar 2000) or growth (e.g., Fitzgerald-Dehoog et al. 2012). Likely, the heat-selected eelgrass individuals started earlier to decrease the energy input for growth to reallocate the energy to protect their basic functions, via e.g., the production of HSPs. As the non-heat-selected *Z. marina* individuals were likely not exposed to high thermal stress before, it took more time to react to the applied stress. However, individuals from inside the sheltered sandbanks (experiencing higher thermal variability; see Chapter III - Supplementary Figure 2), peaked later in biomass compared to individuals from deeper waters. Thus, individuals from the potentially heat-selected population could grow far into the heat period, while such conditions were already too high for the reference population that normally experiences lower thermal variability. This may have led to a compensation of the earlier decreased growth.

Furthermore, the heat-selected population tended to have a larger underground to aboveground biomass ratio. The underground biomass may represent energy reserves as discussed by Olesen and Sand-Jensen (1993) or Lee et al. (2005) and may be an important source of energy during thermal stress.

Generally, heat-selected individuals showed a higher growth than those coming from outside sandbanks. However, this was not dependent on the initial height as heat-selected eelgrasses also grew more in relative measures (i.e., compared to their start height, start number of leaves and shoots; Chapter III - Supplementary Figure 8). Furthermore, the number of shoots and leaves among populations were comparable at the start of the experiment. Supporting this, differences in growth were not only observed in the first, but also in the second growth season toward the end of the experiment. This indicates a cross-season effect or potentially a genetic foundation for such heat-tolerance traits. High thermal resistance was shown, e.g., in the congener species, *Zostera noltei*, typically growing in shallower habitats than *Z. marina* (Franssen et al. 2011). In combination with the potential for local adaptation of *Z. marina* (Hämmerli and Reusch 2002), this strengthens the hypothesis that the shallow eelgrass population represents a heat-resistant genotype, despite the fact that these populations were only collected <200 m apart (see Chapter III - Supplementary Figure 1). Undisturbed and established eelgrass populations were shown to majorly reproduce vegetatively (Reusch et al. 1999), so that seed dispersal from the non-heat-selected established population is not likely. As water temperature in shallow coastal areas is highly correlated with air temperature (Cho and Lee 2012), shallow habitats are prone to experience extreme temperatures (see e.g., Ganning 1971; Huggett and Griffiths 1986). Therefore, if seeds are dispersed from the deeper to the shallower area, we conclude that only those genotypes survived that are heat-tolerant.

## Conclusion

We experimentally demonstrated that *Zostera marina* is negatively affected by high temperatures with an accumulation of thermal stress the longer the stress event lasted. However, heat-selected eelgrass populations might withstand future temperatures and may be used in restoration projects to provide the important eelgrass habitats also in a warmed ocean. Interestingly, our observations indicate that microclimatic differences between geographically (<200 m) close natural habitats can potentially already result in a selection of differently resilient ecotypes. Ecotypes that are more resilient to warming could then potentially replace less resilient ecotypes in their vicinity in the years to come. However, heatwaves that will occur in a warmed ocean might still pose a significant threat also to heat adapted *Z. marina* populations.

## Funding

This study was funded through Deutsche Bundesstiftung Umwelt (DBU; 20018/553), by the Deutsche Forschungsgemeinschaft (DFG; PA 2643/2/348431475), and through GEOMAR (Helmholtz-Gemeinschaft).

## Acknowledgements

We want to thank the scientific divers from GEOMAR who collected the deeper eelgrass individuals. We further want to thank Luisa Düsedau, Laura Hennigs, Nadja Stärk, and Yue Xiao for their help in measuring the growth of eelgrass in the outdoor experiment on sunny and warm, but also on rainy and cold days. A special thank goes to Mia Großmann, Sean Kerney, and Katja Seebass who did not only help in the measurements of the outdoor but also of the indoor experiment. We also want to thank Björn Buchholz for the maintenance of the mesocosm facilities.

## References

Aksnes, D. L.; Dupont, N.; Staby, A.; Fiksen, Ø.; Kaartvedt, S.; Aure, J. (2009): Coastal water darkening and implications for mesopelagic regime shifts in Norwegian fjords. In Mar. Ecol. Prog. Ser. 387, pp. 39–49. DOI: 10.3354/meps08120.

Appelhans, Y. S.; Thomsen, J.; Opitz, S.; Pansch, C.; Melzner, F.; Wahl, M. (2014): Juvenile sea stars exposed to acidification decrease feeding and growth with no acclimation potential. In Mar. Ecol. Prog. Ser. 509, pp. 227–239. DOI: 10.3354/meps10884.

Arias-Ortiz, A.; Serrano, O.; Masqué, P.; Lavery, P. S.; Mueller, U.; Kendrick, G. A. et al. (2018): A marine heatwave drives massive losses from the world’s largest seagrass carbon stocks. In Nature Clim Change 8 (4), pp. 338–344. DOI: 10.1038/s41558-018-0096-y.

Bacon, Linda C.; Vadas, Robert L. (1991): A MODEL FOR GAMETE RELEASE IN ASCOPHYLLUM NODOSUM (PHAEOPHYTA)1. In Journal of Phycology 27 (2), pp. 166–173. DOI: 10.1111/j.0022-3646.1991.00166.x.

Bates, Amanda E.; Helmuth, Brian; Burrows, Michael T.; Duncan, Murray I.; Garrabou, Joaquim; Guy-Haim, Tamar et al. (2018): Biologists ignore ocean weather at their peril. In Nature 560 (7718), pp. 299–301. DOI: 10.1038/d41586-018-05869-5.

Bates, Douglas; Mächler, Martin; Bolker, Ben; Walker, Steve (2015): Fitting Linear Mixed-Effects Models Using lme4. In J. Stat. Soft. 67 (1). DOI: 10.18637/jss.v067.i01.

Beca-Carretero, P.; Olesen, B.; Marbà, N.; Krause-Jensen, D. (2018): Response to experimental warming in northern eelgrass populations. Comparison across a range of temperature adaptations. In Mar. Ecol. Prog. Ser. 589, pp. 59–72. DOI: 10.3354/meps12439.

Bergmann, Nina; Winters, Gidon; Rauch, Gisep; Eizaguirre, Christophe; Gu, Jenny; Nelle, Peter et al. (2010): Population-specificity of heat stress gene induction in northern and southern eelgrass Zostera marina populations under simulated global warming. In Molecular ecology 19 (14), pp. 2870–2883. DOI: 10.1111/j.1365-294X.2010.04731.x.

Blok, S. E.; Olesen, B.; Krause-Jensen, D. (2018): Life history events of eelgrass Zostera marina L. populations across gradients of latitude and temperature. In Mar. Ecol. Prog. Ser. 590, pp. 79–93. DOI: 10.3354/meps12479.

Boström, Christoffer; Bonsdorff, Erik (1997): Community structure and spatial variation of benthic invertebrates associated with Zostera marina (L.) beds in the northern Baltic Sea. In Journal of Sea Research 37, pp. 153–166.

Breitburg, Denise; Levin, Lisa A.; Oschlies, Andreas; Grégoire, Marilaure; Chavez, Francisco P.; Conley, Daniel J. et al. (2018): Declining oxygen in the global ocean and coastal waters. In Science (New York, N.Y.) 359 (6371). DOI: 10.1126/science.aam7240.

Brown, James H.; Gillooly, James F.; Allen, Andrew P.; van Savage, M.; West, Geoffrey B. (2004): TOWARD A METABOLIC THEORY OF ECOLOGY. In Ecology 85 (7), pp. 1771–1789. DOI: 10.1890/03-9000.

Caruso, Carlo; Hughes, Kira; Drury, Crawford (2021): Selecting Heat-Tolerant Corals for Proactive Reef Restoration. In Front. Mar. Sci. 8, p. 367. DOI: 10.3389/fmars.2021.632027.

Cho, Hong-Yeon; Lee, Khil-Ha (2012): Development of an Air–Water Temperature Relationship Model to Predict Climate-Induced Future Water Temperature in Estuaries. In J. Environ. Eng. 138 (5), pp. 570–577. DOI: 10.1061/(ASCE)EE.1943-7870.0000499.

Cole, Scott G.; Moksnes, Per-Olav (2016): Valuing Multiple Eelgrass Ecosystem Services in Sweden. Fish Production and Uptake of Carbon and Nitrogen. In Front. Mar. Sci. 2, p. 7390. DOI: 10.3389/fmars.2015.00121.

Diaz, R. J. (2001): Overview of hypoxia around the world. In Journal of environmental quality 30 (2), pp. 275–281. DOI: 10.2134/jeq2001.302275x.

Diaz, Robert J.; Rosenberg, Rutger (2008): Spreading dead zones and consequences for marine ecosystems. In Science (New York, N.Y.) 321 (5891), pp. 926–929. DOI: 10.1126/science.1156401.

Duarte, Carlos M.; Losada, Iñigo J.; Hendriks, Iris E.; Mazarrasa, Inés; Marbà, Núria (2013): The role of coastal plant communities for climate change mitigation and adaptation. In Nature Clim Change 3 (11), pp. 961–968. DOI: 10.1038/NCLIMATE1970.

Dupont, N.; Aksnes, D. L. (2013): Centennial changes in water clarity of the Baltic Sea and the North Sea. In Estuarine, Coastal and Shelf Science 131 (Suppl), pp. 282–289. DOI: 10.1016/j.ecss.2013.08.010.

Easterling, D. R.; Meehl, G. A.; Parmesan, C.; Changnon, S. A.; Karl, T. R.; Mearns, L. O. (2000): Climate extremes. Observations, modeling, and impacts. In Science (New York, N.Y.) 289 (5487), pp. 2068–2074. DOI: 10.1126/science.289.5487.2068.

Ehlers, A.; Worm, B.; Reusch, T. B.H. (2008): Importance of genetic diversity in eelgrass Zostera marina for its resilience to global warming. In Mar. Ecol. Prog. Ser. 355, pp. 1–7. DOI: 10.3354/meps07369.

Fitzgerald-Dehoog, Lindsay; Browning, Jeremy; Allen, Bengt J. (2012): Food and heat stress in the California mussel. Evidence for an energetic trade-off between survival and growth. In The Biological bulletin 223 (2), pp. 205–216. DOI: 10.1086/BBLv223n2p205.

Franssen, Susanne U.; Gu, Jenny; Bergmann, Nina; Winters, Gidon; Klostermeier, Ulrich C.; Rosenstiel, Philip et al. (2011): Transcriptomic resilience to global warming in the seagrass Zostera marina, a marine foundation species. In Proceedings of the National Academy of Sciences of the United States of America 108 (48), pp. 19276–19281. DOI: 10.1073/pnas.1107680108.

Ganning, Björn (1971): Studies on chemical, physical and biological conditions in Swedish rockpool ecosystems. In Ophelia 9 (1), pp. 51–105. DOI: 10.1080/00785326.1971.10430090.

Giesen, W.B.J.T.; van Katwijk, M. M.; den Hartog, C. (1990): Eelgrass condition and turbidity in the Dutch Wadden Sea. In Aquatic Botany 37 (1), pp. 71–85. DOI: 10.1016/0304-3770(90)90065-S.

Gray, J. S.; Wu, R. S.; Or, Y. Y. (2002): Effects of hypoxia and organic enrichment on the coastal marine environment. In Mar. Ecol. Prog. Ser. 238, pp. 249–279. DOI: 10.3354/meps238249.

Green, Edmund P.; Short, Frederick T. (2003): World atlas of seagrasses. Berkeley, Calif.: Univ. of California Press. Available online at http://www.loc.gov/catdir/bios/ucal052/2004298124.html.

Gunderson, Alex R.; Armstrong, Eric J.; Stillman, Jonathon H. (2016): Multiple Stressors in a Changing World. The Need for an Improved Perspective on Physiological Responses to the Dynamic Marine Environment. In Annual review of marine science 8, pp. 357–378. DOI: 10.1146/annurev-marine-122414-033953.

Haarr, Marthe Larsen; Comeau, Michel; Chassé, Jöel; Rochette, Rémy; Fields, David (2020): Early spring egg hatching by the American lobster (Homarus americanus) linked to rising water temperature in autumn. In ICES Journal of Marine Science 77 (5), pp. 1685–1697. DOI: 10.1093/icesjms/fsaa027.

Hammer, K. J.; Borum, J.; Hasler-Sheetal, H.; Shields, E. C.; Sand-Jensen, K.; Moore, K. A. (2018): High temperatures cause reduced growth, plant death and metabolic changes in eelgrass Zostera marina. In Mar. Ecol. Prog. Ser. 604, pp. 121–132. DOI: 10.3354/meps12740.

Hämmerli, A.; Reusch, T. B.H. (2002): Local adaptation and transplant dominance in genets of the marine clonal plant Zostera marina. In Mar. Ecol. Prog. Ser. 242, pp. 111–118. DOI: 10.3354/MEPS242111.

HELCOM (2013): Climate Change in the Baltic Sea Area: A HELMCOM thematic assessment in 2013. In Balt. Sea Environ. Proc. 37.

Hobday, Alistair J.; Alexander, Lisa V.; Perkins, Sarah E.; Smale, Dan A.; Straub, Sandra C.; Oliver, Eric C.J. et al. (2016): A hierarchical approach to defining marine heatwaves. In Progress in Oceanography 141, pp. 227–238. DOI: 10.1016/j.pocean.2015.12.014.

Huggett, J.; Griffiths, C. L. (1986): Some relationships between elevation, physico-chemical variables and biota of intertidal rock pools. In Mar. Ecol. Prog. Ser. 29, pp. 189–197. DOI: 10.3354/MEPS029189.

IPCC (2019): Summary for Policymakers. In H. O. Pörtner, D. C. Roberts, V. Masson-Delmotte, P. Zhai, M. Tignor, E. Poloczanska et al. (Eds.): IPCC Special Report on the Ocean and Cryosphere in a Changing Climate. In press.

IPCC (2021): Climate Change 2021: The Physical Science Basis. In V. Masson-Delmotte, P. Zhai, A. Pirani, S. L. Connors, C. Péan, S. Berger et al. (Eds.): Contribution of Working Group I to the Sixth Assessment Report of the Intergovernmental Panel on Climate Change. In press.

Jackson, Michelle C.; Pawar, Samraat; Woodward, Guy (2021): The Temporal Dynamics of Multiple Stressor Effects. From Individuals to Ecosystems. In Trends in Ecology & Evolution 36 (5), pp. 402–410. DOI: 10.1016/j.tree.2021.01.005.

Kayanne, Hajime (2017): Validation of degree heating weeks as a coral bleaching index in the northwestern Pacific. In Coral Reefs 36 (1), pp. 63–70. DOI: 10.1007/s00338-016-1524-y.

Lee, Kun-Seop; Park, Sang Rul; Kim, Jung-Bae (2005): Production dynamics of the eelgrass, Zostera marina in two bay systems on the south coast of the Korean peninsula. In Mar Biol 147 (5), pp. 1091–1108. DOI: 10.1007/s00227-005-0011-8.

Lee, Kun-Seop; Park, Sang Rul; Kim, Young Kyun (2007): Effects of irradiance, temperature, and nutrients on growth dynamics of seagrasses. A review. In Journal of Experimental Marine Biology and Ecology 350 (1-2), pp. 144–175. DOI: 10.1016/j.jembe.2007.06.016.

Lenth, Russels V. (2020): emmeans: Estimated Marginal Means, aka Least Squares means. Available online at https://CRAN.R-project.org/package=emmeans.

Leppäranta, Matti; Myrberg, Kai (Eds.) (2009): Physical Oceanography of the Baltic Sea. Berlin, Heidelberg: Springer Berlin Heidelberg.

Moreno-Marín, Francisco; Brun, Fernando Guillermo; Pedersen, Morten Foldager (2018): Additive response to multiple environmental stressors in the seagrass Zostera marina L. In Limnol. Oceanogr. 63 (4), pp. 1528–1544. DOI: 10.1002/lno.10789.

Morikawa, Megan K.; Palumbi, Stephen R. (2019): Using naturally occurring climate resilient corals to construct bleaching-resistant nurseries. In Proceedings of the National Academy of Sciences of the United States of America 116 (21), pp. 10586–10591. DOI: 10.1073/pnas.1721415116.

Muehlstein, L. K.; Porter, D.; Short, F. T. (1988): Labyrinthula sp., a marine slime mold producing the symptoms of wasting disease in eelgrass, Zostera marina. In Mar Biol 99 (4), pp. 465–472. DOI: 10.1007/BF00392553.

Nejrup, Lars Brammer; Pedersen, Morten Foldager (2008): Effects of salinity and water temperature on the ecological performance of Zostera marina. In Aquatic Botany 88 (3), pp. 239–246. DOI: 10.1016/j.aquabot.2007.10.006.

Neumann, Thomas; Eilola, Kari; Gustafsson, Bo; Müller-Karulis, Bärbel; Kuznetsov, Ivan; Meier, H. E. Markus; Savchuk, Oleg P. (2012): Extremes of temperature, oxygen and blooms in the Baltic sea in a changing climate. In Ambio 41 (6), pp. 574–585. DOI: 10.1007/s13280-012-0321-2.

Olesen, B.; Sand-Jensen, K. (1993): Seasonal acclimatization of eelgrass Zostera marina growth to light. In Mar. Ecol. Prog. Ser. 94, pp. 91–99. DOI: 10.3354/meps094091.

Oliver, Eric C. J. (2019): Mean warming not variability drives marine heatwave trends. In Clim Dyn 53 (3-4), pp. 1653–1659. DOI: 10.1007/s00382-019-04707-2.

Oliver, Eric C. J.; Burrows, Michael T.; Donat, Markus G.; Sen Gupta, Alex; Alexander, Lisa V.; Perkins-Kirkpatrick, Sarah E. et al. (2019): Projected Marine Heatwaves in the 21st Century and the Potential for Ecological Impact. In Front. Mar. Sci. 6, p. 891. DOI: 10.3389/fmars.2019.00734.

Oliver, Eric C. J.; Donat, Markus G.; Burrows, Michael T.; Moore, Pippa J.; Smale, Dan A.; Alexander, Lisa V. et al. (2018): Longer and more frequent marine heatwaves over the past century. In Nature communications 9 (1), p. 1324. DOI: 10.1038/s41467-018-03732-9.

Pansch, Christian; Hiebenthal, Claas (2019): A new mesocosm system to study the effects of environmental variability on marine species and communities. In Limnol. Oceanogr. Methods 28, p. 16. DOI: 10.1002/lom3.10306.

Pansch, Christian; Scotti, Marco; Barboza, Francisco R.; Al-Janabi, Balsam; Brakel, Janina; Briski, Elizabeta et al. (2018): Heat waves and their significance for a temperate benthic community. A near-natural experimental approach. In Glob Change Biol. DOI: 10.1111/gcb.14282.

Pazzaglia, Jessica; Badalamenti, Fabio; Bernardeau-Esteller, Jaime; Ruiz, Juan M.; Giacalone, Vincenzo Maximiliano; Procaccini, Gabriele; Marín-Guirao, Lazaro (2022): Thermo-priming increases heat-stress tolerance in seedlings of the Mediterranean seagrass P. oceanica. In Marine pollution bulletin 174, p. 113164. DOI: 10.1016/j.marpolbul.2021.113164.

Pedersen, O.; BIinzer, T.; Borum, J. (2004): Sulphide intrusion in eelgrass (Zostera marina L.). In Plant, cell & environment 27 (5), pp. 595–602. DOI: 10.1111/j.1365-3040.2004.01173.x.

Phillips, Ronald C.; McMillan, Calvin; Bridges, Kent W. (1983): Phenology of eelgrass, Zostera marina L., along latitudinal gradients in North America. In Aquatic Botany 15 (2), pp. 145–156. DOI: 10.1016/0304-3770(83)90025-6.

Poloczanska, Elvira S.; Burrows, Michael T.; Brown, Christopher J.; García Molinos, Jorge; Halpern, Benjamin S.; Hoegh-Guldberg, Ove et al. (2016): Responses of Marine Organisms to Climate Change across Oceans. In Front. Mar. Sci. 3 (28), p. 515. DOI: 10.3389/fmars.2016.00062.

Randall, Carly J.; Toth, Lauren T.; Leichter, James J.; Maté, Juan L.; Aronson, Richard B. (2020): Upwelling buffers climate change impacts on coral reefs of the eastern tropical Pacific. In Ecology 101 (2), e02918. DOI: 10.1002/ecy.2918.

Reusch, Thorsten B. H.; Baums, Iliana B.; Werner, Benjamin (2021): Evolution via somatic genetic variation in modular species. In Trends in Ecology & Evolution 36 (12), pp. 1083–1092. DOI: 10.1016/j.tree.2021.08.011.

Reusch, Thorsten B.H.; Boström, Christoffer; Stam, Wytze T.; Olsen, Jeanine (1999): An ancient eelgrass clone in the Baltic. In Marine Ecology Progress Series 183, pp. 301–304.

Reusch, Thorsten B. H.; Dierking, Jan; Andersson, Helen C.; Bonsdorff, Erik; Carstensen, Jacob; Casini, Michele et al. (2018): The Baltic Sea as a time machine for the future coastal ocean. In Science advances 4 (5), eaar8195. DOI: 10.1126/sciadv.aar8195.

Reusch, Thorsten B. H.; Ehlers, Anneli; Hämmerli, August; Worm, Boris (2005): Ecosystem recovery after climatic extremes enhanced by genotypic diversity. In Proceedings of the

National Academy of Sciences of the United States of America 102 (8), pp. 2826–2831. DOI: 10.1073/pnas.0500008102.

Saha, Mahasweta; Barboza, Francisco R.; Somerfield, Paul J.; Al-Janabi, Balsam; Beck, Miriam; Brakel, Janina et al. (2020): Response of foundation macrophytes to near-natural simulated marine heatwaves. In Glob Change Biol 26 (2), pp. 417–430. DOI: 10.1111/gcb.14801.

Sampaio, Eduardo; Santos, Catarina; Rosa, Inês C.; Ferreira, Verónica; Pörtner, Hans-Otto; Duarte, Carlos M. et al. (2021): Impacts of hypoxic events surpass those of future ocean warming and acidification. In Nature ecology & evolution 5 (3), pp. 311–321. DOI: 10.1038/s41559-020-01370-3.

Sawall, Yvonne; Ito, Maysa; Pansch, Christian (2021): Chronically elevated sea surface temperatures revealed high susceptibility of the eelgrass Zostera marina to winter and spring warming. In Limnol. Oceanogr. 66 (12), pp. 4112–4124. DOI: 10.1002/lno.11947.

Silberhorn, G. M.; Orth, R. J.; Moore, K. A. (1983): Anthesis and seed production in Zostera marina L. (eelgrass) from the chesepeak by. In Aquatic Botany 15 (2), pp. 133–144. DOI: 10.1016/0304-3770(83)90024-4.

Silbermann, R.; Tatar, M. (2000): Reproductive costs of heat shock protein in transgenic Drosophila melanogaster. In Evolution; international journal of organic evolution 54 (6), pp. 2038–2045. DOI: 10.1111/j.0014-3820.2000.tb01247.x.

Smale, Dan A.; Wernberg, Thomas; Oliver, Eric C. J.; Thomsen, Mads; Harvey, Ben P.; Straub, Sandra C. et al. (2019): Marine heatwaves threaten global biodiversity and the provision of ecosystem services. In Nature Clim Change 9, p. 360. DOI: 10.1038/s41558-019-0412-1.

Somero, George N. (2020): The cellular stress response and temperature. Function, regulation, and evolution. In Journal of experimental zoology. Part A, Ecological and integrative physiology 333 (6), pp. 379–397. DOI: 10.1002/jez.2344.

Vajedsamiei, Jahangir; Melzner, Frank; Raatz, Michael; Kiko, Rainer; Khosravi, Maral; Pansch, Christian (2021): Simultaneous recording of filtration and respiration in marine organisms in response to short-term environmental variability. In Limnol. Oceanogr. Methods 6, p. 341. DOI: 10.1002/lom3.10414.

van Rij, Jacolien; Wieling, Martijn; Baayen, R. Harald; van Rijn, Hedderik (2020): itsadug: Interpreting Time Series and Autocorrelated Data Using GAMMs. Available online at https://CRAN.R-project.org/package=itsadug.

Vaquer-Sunyer, Raquel; Duarte, Carlos M. (2008): Thresholds of hypoxia for marine biodiversity. In Proceedings of the National Academy of Sciences of the United States of America 105 (40), pp. 15452–15457. DOI: 10.1073/pnas.0803833105.

Wahl, Martin; Barboza, Francisco R.; Buchholz, Björn; Dobretsov, Sergey; Guy-Haim, Tamar; Rilov, Gil et al. (2021): Pulsed pressure. Fluctuating impacts of multifactorial environmental change on a temperate macroalgal community. In Limnol. Oceanogr. 33, p. 477. DOI: 10.1002/lno.11954.

Wahl, Martin; Buchholz, Björn; Winde, Vera; Golomb, Dar; Guy-Haim, Tamar; Müller, Jens et al. (2015): A mesocosm concept for the simulation of near-natural shallow underwater climates. The Kiel Outdoor Benthocosms (KOB). In Limnol. Oceanogr. Methods 13 (11), pp. 651–663. DOI: 10.1002/lom3.10055.

Walther, Gian-Reto; Post, Eric; Convey, Peter; Menzel, Annette; Parmesan, Camille; Beebee, Trevor J. C. et al. (2002): Ecological responses to recent climate change. In Nature 416 (6879), pp. 389–395. DOI: 10.1038/416389a.

Wernberg, Thomas; Smale, Dan A.; Frölicher, Thomas L.; Smith, A. J. P. (2021): ScienceBrief Review: Climate change increases marine heatwaves harming marine ecosystems. In Critical Issues in Climate Change.

Winters, G.; Nelle, P.; Fricke, B.; Rauch, G.; Reusch, T. B.H. (2011): Effects of a simulated heat wave on photophysiology and gene expression of high- and low-latitude populations of Zostera marina. In Mar. Ecol. Prog. Ser. 435, pp. 83–95. DOI: 10.3354/meps09213.

Wolf, Fabian; Bumke, Karl; Wahl, Sebastian; Nevoigt, Frauke; Hecht, Ute; Hiebenthal, Claas; Pansch, Christian (2020): High resolution water temperature data between January 1997 and December 2018 at the GEOMAR pier surface. PANGAEA. Available online at https://doi.org/10.1594/PANGAEA.919186.

Wolf, Fabian; Seebass, Katja; Pansch, Christian (2022): The Role of Recovery Phases in Mitigating the Negative Impacts of Marine Heatwaves on the Sea Star Asterias rubens. In Front. Mar. Sci. 8, p. 1029. DOI: 10.3389/fmars.2021.790241.

Wood, Simon N. (2017): Generalized Additive Models: Chapman and Hall/CRC.

Zimmerman, R. C.; Hill, V. J.; Jinuntuya, M.; Celebi, B.; Ruble, D.; Smith, M. et al. (2017): Experimental impacts of climate warming and ocean carbonation on eelgrass Zostera marina. In Mar. Ecol. Prog. Ser. 566, pp. 1–15. DOI: 10.3354/meps12051.

# GENERAL DISCUSSION

## Summary of the main findings

The findings of the presented three chapters of this thesis show that

**i.** extreme event properties do not change over time in the Kiel Fjord, but the number of heatwaves and cold-spells correlate with the mean temperature of the respective year.

**ii.** the characterisation of heatwaves, mimicking stressful upwelling of the recent past, and warming in combination with ambient fluctuation enabled close-to-natural experimental treatments.

**iii.** heatwaves negatively impact starfish performance depending on the frequency, duration, and intensity of the applied event.

**iv.** long exposure to heat stress (i.e., extended heatwave or long-term warming) reduces the growth of eelgrass but depends on the environmental history of the individuals at their collection site.

**v.** the impact of late summer upwelling depends on

  a. the species (i.e., starfish are less active, while eelgrass is not impacted) and

  b. the environmental history of the species (i.e., previous exposure to heatwaves alleviates the impact of the upwelling on starfish but adds to the upwelling stress of eelgrass).

## Characterising environmental variability

As described in the GENERAL INTRODUCTION, environmental variability was neglected for a long time in experimental ecology (Thompson et al. 2013) but came into focus of many researchers in the recent years (e.g., Winters et al. 2011; Wahl et al. 2016; Pansch and Hiebenthal 2019; Vajedsamiei et al. 2021a). Fluctuations on short time scales can be very extreme (7 °C drop of temperature in only one day or an increase by 7 °C in five days; Supplementary Material to Pansch and Hiebenthal 2019). With ongoing global warming (IPCC 2021), increases in temperature are likely more stressful to many species than cooling. Acknowledging that diurnal or unpredictable stochastic variability may play strong roles in the response of an organism to ocean warming (e.g., Shama 2017; Vajedsamiei et al. 2021a), this study focusses on marine heatwave events. However, warming itself also plays a major role as it leads to a higher probability of critical temperatures during future heatwaves (Oliver 2019). Apart from local environmental variability, environmental conditions can also vary between different depths or between sites that are less than 200 m apart from each other (see Chapter II

- Supplementary Figure 13, Chapter III - Supplementary Figure 1, and Chapter III - Supplementary Figure 2). Here, surface waters and shallow sheltered areas that are separated from deeper areas are more exposed to heat stress (see Chapter II - Supplementary Figure 13 and Chapter III - Supplementary Figure 2).

### *Trends in means and in extreme events*

Although, I could not detect a general trend of extreme events over the last 22-years in the Kiel Fjord, models suggest a global increase in extreme events (Oliver et al. 2018). As the Baltic Sea is highly variable across diverse temporal (Bradtke et al. 2010; Pansch and Hiebenthal 2019) and spatial (Bradtke et al. 2010) scales (also discussed by Reusch et al. 2018), it is likely that the dataset I used, did not cover a sufficiently long-time span (22 years). Indeed, Hobday et al. (2016) suggest using data sets of 30 years to detect marine heatwaves. Furthermore, the years 2010–2013 were particularly cold, which is also reflected in (and likely driven by) a low North Atlantic Oscillation (NAO) index around 2010 (Hurell and National Center for Atmospheric Research Staff 2020). In combination, the highly variable Baltic Sea, the shorter time-series, and the low NAO index have likely led to the absence of extreme event trends in the Kiel Fjord.

With three additional years of temperature data from the same location (GEOMAR meteorology department, Sebastian Wahl), I could recently extend the long-term data set to 25 years in total. The additional years were analysed on heatwaves and cold-spells based on the existing analysis in CHAPTER I (Discussion - Figure 1). However, the three additional years did not change the fact that there was no trend in heatwave or cold-spell characteristics (Discussion - Supplementary Figure 1 and Discussion - Supplementary Figure 2; analysis equivalent to Methods in CHAPTER I). Baltic Sea wide measurements from 1970 to 2008 showed an overall warming trend of 0.4 °C per decade (Lehmann et al. 2011). In addition, for the Baltic Sea, a warming by 4 °C (HELCOM 2013) by the end of the ecentury is projected. As warming is the main driver of the observed increase in marine heatwave magnitude (Oliver 2019), an increase of heatwave characteristics was expected.

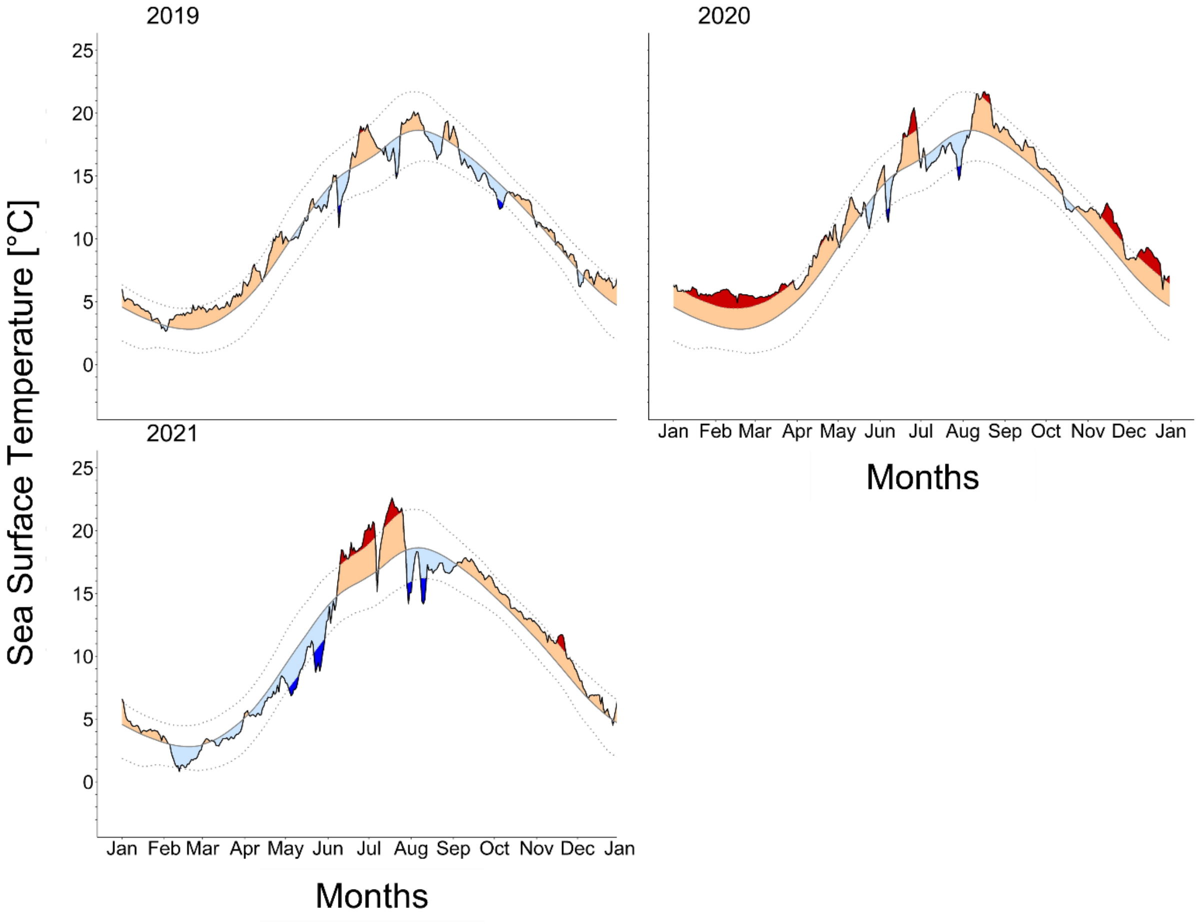

**Discussion - Figure 1:** Recorded temperatures (°C; solid black lines) in 1.8 m depth in the Kiel Fjord, Germany at the GEOMAR pier (N54° 19' 45.97" E10° 8' 58.582"; temperature data from 2019-2021 obtained from GEOMAR meteorology department, Sebastian Wahl) of the years 2019 until 2021. This dataset was analysed on the occurrences of heatwaves and cold-spells after Hobday et al. (2016) based on a 22-year temperature data set (Wolf et al. 2020). Based on this modelling (CHAPTER I) the 22-year climatological values are represented as grey solid line, whereas the thresholds for heatwaves (i.e., 90th percentile) and cold-spells (i.e., 10th percentile) are represented as dotted lines. Temperatures above the climatological values, but below the 90th percentile are shown in orange, whereas temperatures above the 90th percentile are shown in red. Temperatures below the climatological trend, but above the 10th percentile are shown in light-blue, whereas temperatures below the 10th percentile are shown in dark-blue.

Including the three additonal years in the climatology and threshold analysis (after Methods in CHAPTER I) did only slightly change the climatological and threshold results (Discussion - Supplementary Figure 3). Thus, also the heatwave and cold-spell characteristics did only slightly change (Discussion - Figure 2 and Discussion - Figure 3). However, with the inclusion of the three additional years, the frequency of heatwave changes significantly over time with the tendency to increase (Discussion - Figure 2a). Thus, getting closer to the requested length of time-series (i.e., 30 years; Hobday et al. 2016) increases the probability to detect changes in heatwave characteristics over time. Actually, the annual mean temperature in the Kiel Fjord based on 22 years (i.e., 1997-2018) tends to decrease (Discussion - Figure 4a), while it increases when including the years 2019-2021 (Discussion - Figure 4b). This confirms the findings of Oliver (2019) who revealed that the increasing magnitude of marine heatwaves is mainly driven by the warming trend. Therefore, the found trends do not represent an increase in the actual number of events or their magnitude but are an artefact of the heatwave definition of identifying heatwaves based on the past 30-years. Thus, the detection of heatwave trends depends mainly on the presence or absence of a temperature trend, which itself appears to primarily depend on the length of the given dataset (Discussion - Figure 4).

However, it seems that the length of the analysed dataset is less important in retrieving mean characteristics of heatwaves or cold-spells (compare Discussion - Supplementary Table 5 and Discussion - Supplementary Table 6 with Chapter I - Supplementary Table 1 and Chapter I - Supplementary Table 2). Although, there will not be actually more heatwaves with an increased magnitude, the probability of heatwaves reaching critical temperatures for species and ecosystems will increase solely due to the fact that the baseline temperature will be higher. Thus, future heatwaves still pose a significant threat to marine ecosystems. Therefore, the experimental treatments that use future projections of heatwaves (CHAPTER I, CHAPTER II, and CHAPTER III) remain valid and with this the ecological relevance of the respective findings. Yet, as implemented in CHAPTER III, the impact of heatwaves on any species should always include a warming scenario as both are correlated to each other.

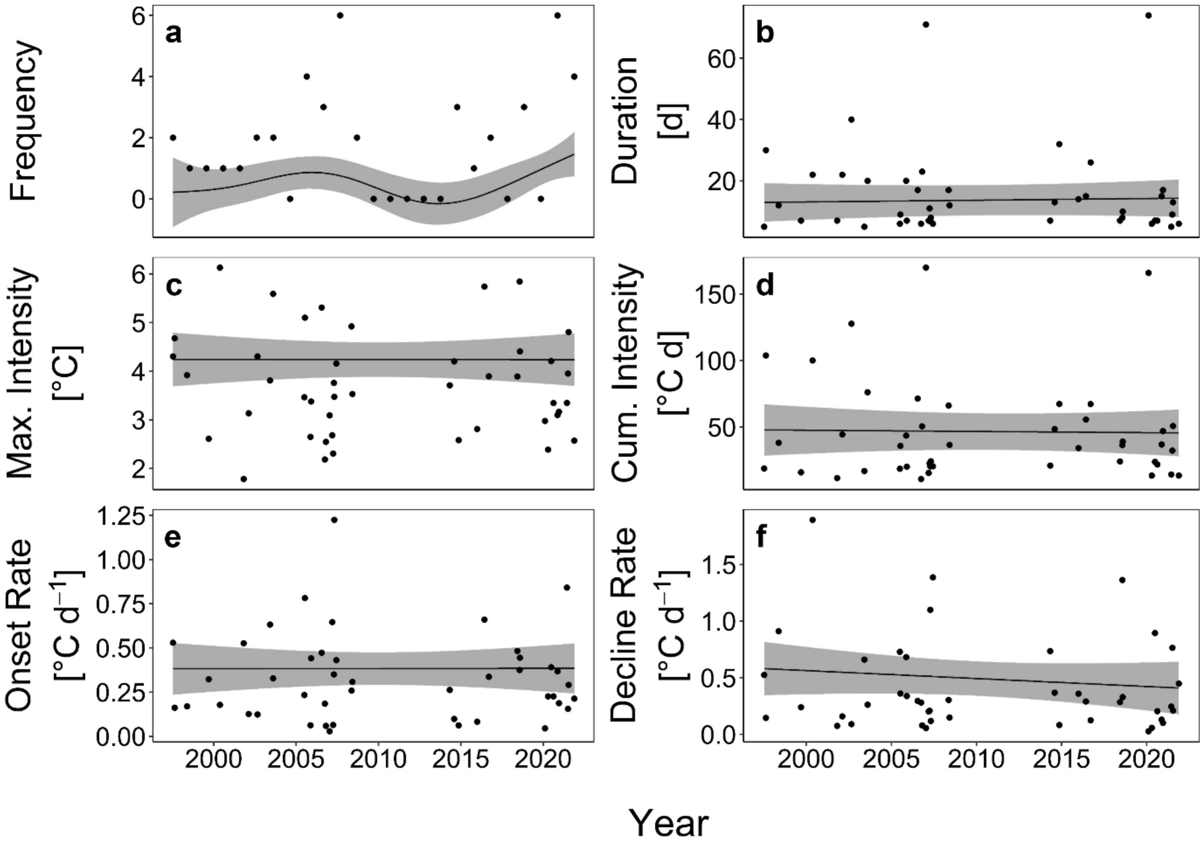

**Discussion - Figure 2:** Modelled yearly heatwave frequency (**a**), duration (**b**), maximal intensity (**c**), cumulative intensity (**d**), onset (**e**) and decline rate (**f**) after Hobday et al. (2016), using published data (Wolf et al. 2020) and additional temperature data from 2019-2021 obtained from GEOMAR meteorology department, Sebastian Wahl. The heatwave threshold is based on all years (1997-2021). Trends were modelled using Generalized Additive Models (GAMs). Shaded areas represent the 95% confidence intervals. Detailed statistic results are given in Discussion - Supplementary Table 3.

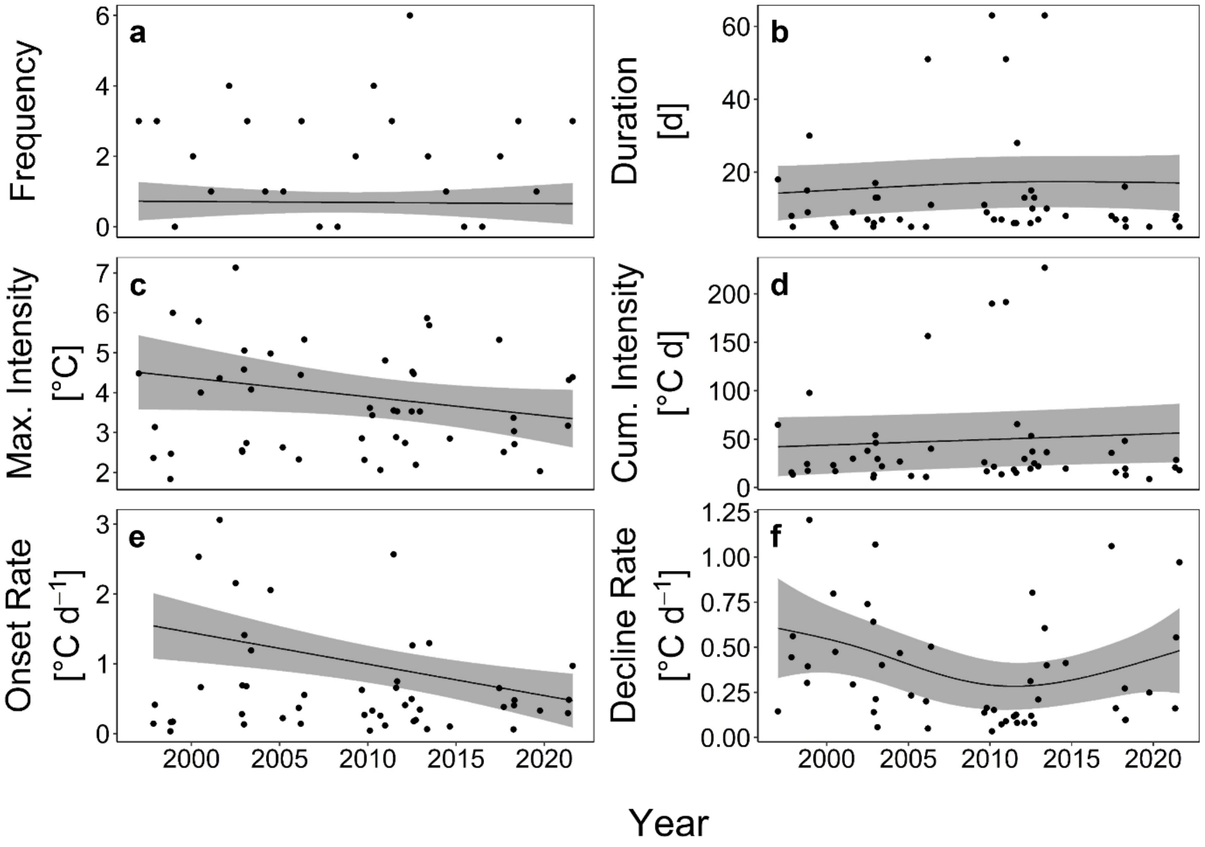

**Discussion - Figure 3:** Modelled yearly cold-spell frequency (**a**), duration (**b**), maximal intensity (**c**), cumulative intensity (**d**), onset (**e**) and decline rate (**f**) after Hobday et al. (2016), using published data (Wolf et al. 2020**)** and additional temperature data from 2019-2021 obtained from GEOMAR meteorology department, Sebastian Wahl. The cold-spell threshold is based on all years (1997-2021). Trends were modelled using Generalized Additive Models (GAMs). Shaded areas represent the 95% confidence intervals. Detailed statistic results are given in Discussion - Supplementary Table 4.

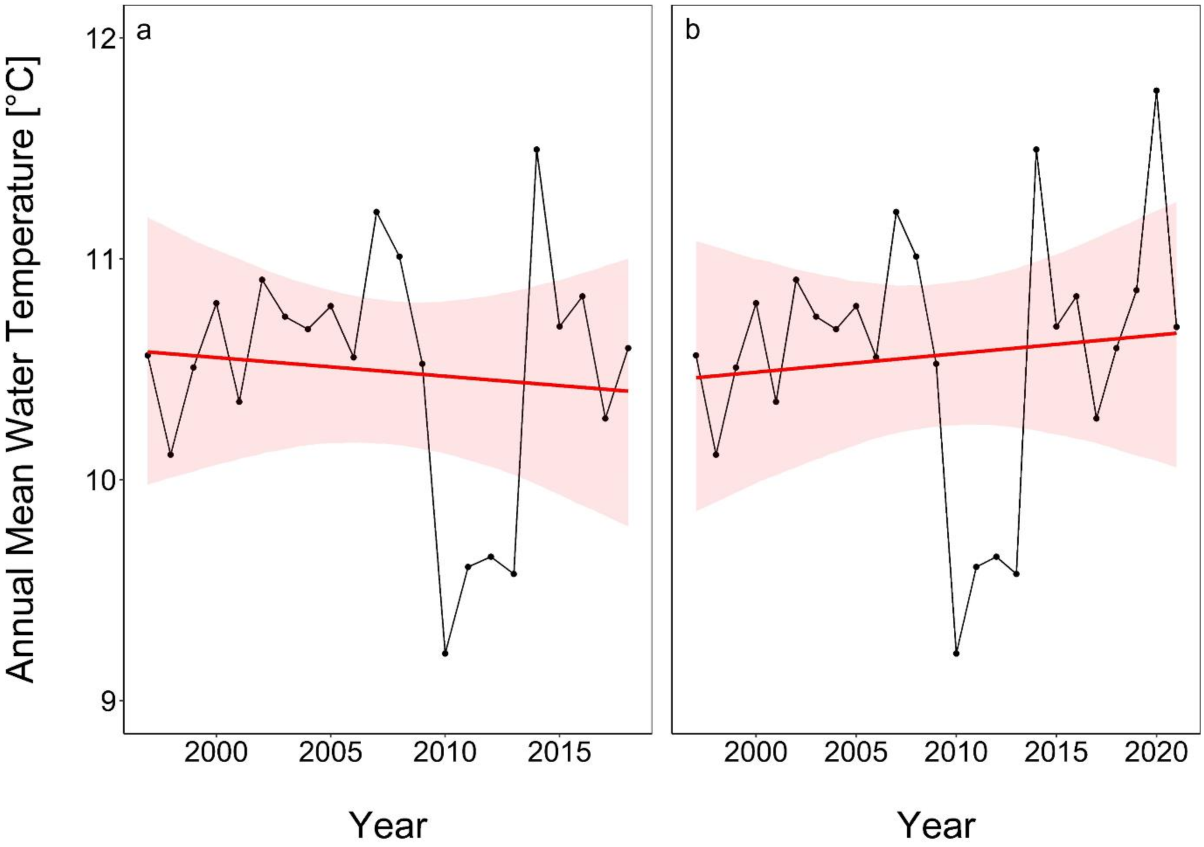

**Discussion - Figure 4:** Annual mean water temperatures (°C) from 1997-2018 (**a**) and from 1997-2021 (**b**) in 1.8 m depth in the Kiel Fjord, Germany. The red line and the 95% confidence interval (red shaded area) represent the trend over time. The trendline was modelled using a linear model using an autocorrelation-moving average function. Data are based on a 22-year temperature data set (1997-2018; Wolf et al. 2020) and temperature data from 2019-2021 obtained from GEOMAR meteorology department, Sebastian Wahl. Detailed statistical outcomes are presented in Discussion - Supplementary Table 7.

### *Characterisation of environmental variability as tool for experimental ecologists*

While extreme event characterisation is mainly used to elucidate the changes of these events over time (e.g., Meehl and Tebaldi 2004; Oliver et al. 2018; Oliver 2019), Thompson et al. (2013) called for experiments that include environmental variability as this can change the understanding of climate change impact on different species.

Some experiments justify their constant temperature treatments with a temperature observed in a long-term dataset (e.g., Leach et al. 2021; Schoen et al. 2021). Other experiments mimic a natural event that happened in the past as, e.g., the heatwave in northern Europe in 2003 (e.g., Ehlers et al. 2008; Bergmann et al. 2010; Winters et al. 2011; Franssen et al. 2014). However, a thorough analysis of environmental variability as presented in this thesis is to date not yet commonly applied. Some scientists, though, did analyse long-term datasets to define their treatment scenarios (e.g., Pansch et al. 2018; Atkinson et al. 2020). While Pansch et al. (2018) came up with a different heatwave characterisation (i.e., an temperature increase of 0.7 °C per day for at least two consecutive days), Atkinson et al. (2020) applied the same heatwave definition after Hobday et al. (2016) as applied in CHAPTER I and CHAPTER III. Irrespective of the applied heatwave definition, both studies implement a for the region typical heatwave (Pansch et al. 2018; Atkinson et al. 2020), which allows a transfer of the found effect to natural ecosystems. Therefore, experiments with treatments based on long-term data represent the advantages of laboratory (controlled environment) and field (natural conditions) experiments. Thus, extreme event characterisation can be an extremely valuable tool in modern stress ecology.

## Implications of environmental stress for Baltic Sea ecosystems

### *Impacts from a global warming scenario*

Negative impacts of long-term warming (+3 °C over 1.5 years) on Baltic eelgrass as presented in CHAPTER III is mostly in line with findings of Sawall et al. (2021), who tested how warming through three seasons (i.e., winter until summer) impacts *Zostera marina*. They found an earlier peak of flowering in spring (Sawall et al. 2021), which corroborates the findings as presented in CHAPTER III, also indicating a shift in phenology as eelgrass reached a peak biomass earlier under the warming scenario. However, while Sawall et al. (2021) found that shoot numbers decreased substantially in spring under the warming scenario (i.e., temperature just below 10 °C) the findings of CHAPTER III show that warming reduces eelgrass shoots only in July when temperatures reached 20 °C. This may be attributed to the time of eelgrass collection. Eelgrasses that were used by Sawall et al. (2021) were collected in November, when energy reserves of eelgrass are lowest (Vichkovitten et al. 2007), while the eelgrasses of the study presented in CHAPTER III were collected in spring, when eelgrass started to accumulate energy reserves again (Vichkovitten et al. 2007). Overall, both, the study by Sawall et al. (2021), as well as the study presented in CHAPTER III show negative impacts of warming on *Z. marina*. In contrast to Sawall et al. (2021), CHAPTER III combines the aforementioned study of long-term warming with (**i**) the systematic investigation of extreme event impacts (i.e., heatwaves and upwelling; as discussed below in Impacts from heatwaves scenarios and Upwelling events in late summer) as well as (**ii**) the potential heat selection of eelgrass (as discussed below in Heat selection in a naturally variable habitat).

Apart from the direct negative impacts of global warming on eelgrasses, essential ecosystem services (Boström and Bonsdorff 1997; Duarte et al. 2013; Cole and Moksnes 2016; Reusch et al. 2021) provided by eelgrass meadows may be impaired as well. The loss of ecosystem engineers in other regions have led to a dramatic ecosystem change (e.g., Reed et al. 2006;

Pillay et al. 2010; Githaiga et al. 2019). Pillay et al. (2010) showed that the decline of *Zostera capensis* led to cascading ecosystem impacts. The invertebrate richness decreased by up to 50%, while the number of wading birds that usually feed in the tidal seagrass meadows declined (Pillay et al. 2010). While I did not investigate the invertebrate diversity of Baltic eelgrass meadows, the above mentioned suggests that the biomass losses of eelgrass meadows in a warming Baltic Sea will likely also lead to a reduced biodiversity.

Apart from the direct climate change impacts on *Z. marina*, eelgrass faces several indirect consequences of anthropogenic changes. Eutrophication enhances epiphytic growth on *Z. marina* (Vinther et al. 2008) as well as macroalgal growth (Hauxwell et al. 2001). Both, epiphytic cover (Vinther et al. 2008) as well as macroalgal growth (Hauxwell et al. 2001) lead to a reduced growth of eelgrass and subsequently to a reduced biomass of *Z. marina*, which is either attributed to light-limitation (Vinther et al. 2008) or to biogeochemical changes of the surrounding water in combination with light-limitation (Hauxwell et al. 2001).

The loss of biodiversity due to declining eelgrass meadows is probably the most dramatic loss of the many ecosystem services that *Z. marina* provides. However, the loss of eelgrass meadows will likely directly impact humans due to enhanced erosion of coastal areas (as discussed by e.g., Barbier et al. 2011; Duarte et al. 2013). Furthermore, ecosystems also provide cultural services such as recreation, which is positively correlated with biodiversity (Harrison et al. 2014). Therefore, the loss of eelgrass biomass may impact tourist's activity in the respective areas. Overall, when neglecting the possible adaptational capacity of eelgrass in the Baltic Sea (as discussed below in Heat selection in a naturally variable habitat) a warming ocean may lead to drastic impacts on the benthic ecosystems of the Baltic Sea.

### *Impacts from heatwaves scenarios*

Including warming scenarios, the intensity of marine heatwaves is projected to increase by 3 °C until 2100 (Oliver et al. 2019), which represents the general warming trend (IPCC 2021). Such future heatwaves in the Kiel Fjord would reach 26 °C and may locally eradicate starfish populations (CHAPTER II). As presented in CHAPTER I and CHAPTER II, even heatwaves of today's intensity decrease the performance of the key predator *Asterias rubens*. However, starfish could recover from heatwave induced thermal stress if the event was not prolonged. Leung et al. (2019) demonstrated that different intertidal gastropods showed three different responses to marine heatwaves: they either did not change their feeding (i.e., resistant), their feeding was reduced during the heatwave but recovered (i.e., resilient), or their feeding was reduced but remained low (i.e., sensitive). If heatwaves are not prolonged, starfish show a resilient type of response as they returned to their initial feeding rate after the heatwave had ended (CHAPTER I and CHAPTER II). If, on the other hand, the heatwave is extended, starfish show a sensitive type of response as they cannot fully recover from the heat stress (CHAPTER I and CHAPTER II). However, although the starfish could not fully recover from the prolonged heatwaves, their feeding rate still increased after the heatwaves had ended. This suggests that a longer recovery period may have led to a full recovery of starfish from the extended heatwaves. Yet, Leung et al. (2017) showed that heatwaves reduced the wet weight of gastropods and thus, their energy reserves. In *A. rubens* high temperatures in winter reduced their energy reserves, which may cause a reduced reproductive capacity in the following spring (Melzner et al. 2020). Therefore, despite the recovery potential of *A. rubens*, heatwaves of today's intensity may reduce the long-term fitness of starfish.

As described above, feeding of *A. rubens* on its main prey *Mytilus spp.* can already today be reduced in times of summer heatwaves. Non-native species like the recent invader *Hemigrapsus takanoi* (Nour et al. 2020) could potentially fill the predation gap that *A. rubens* would leave and thus, be beneficial for the ecosystem services. However, larvae of *H. takanoi* cannot fully develop under global warming and the prevailing salinities (Nour 2020), so that this particular predator will likely not be able to control blue mussel abundances in the future. Thus, if starfish cannot acclimate or migrate to deeper waters (see Spatial-temporal refugia from extreme conditions), a strong decline of feeding pressure of *A. rubens* on *Mytilus* mussels can be expected for the future Kiel Fjord and very likely for large areas of the Western Baltic Sea with likely drastic ecosystem changes.

The planktonic larvae of *Mytilus* mussels can spread 30–60 km (Gilg and Hilbish 2003), so that they could easily propagate to new habitats. Blue mussels are further shown to be thermally very robust and can withstand water (Vajedsamiei et al. 2021b) and air (Seuront et al. 2019) temperatures of 30 and 40 °C for short time, respectively. Thus, blue mussels are more heat tolerant than starfish and likely less impacted by warming and heatwaves. Although, blue mussel reefs provide a diverse community (Norling and Kautsky 2007; Sadchatheeswaran et al. 2015), it is discussed that *Mytilus spp.* can form monocultures (Reusch and Chapmann 1997; Dürr and Wahl 2004) if they are released from their predation pressure (i.e., strong thermal stress on starfish).

If these mussels would spread uncontrolled, other ecosystems like eelgrass meadows might be replaced. Apart from simple replacement, Vinther et al. (2008) showed that *Mytilus* mussels within *Z. marina* meadows function as nitrogen sources for epiphytes growing on eelgrass, which in turn reduces the eelgrass' growth. Such indirect effects alone may be tolerable if eelgrass was temperature tolerant and an uncontrolled spread of blue mussels could be prevented. However, I could demonstrate that heatwaves reduced the growth of eelgrass, yet the effect size on this trait was rather small. A marine heatwave in Western Australia led to 90% loss of the local seagrass (Thomson et al. 2015). Also in *Z. marina*, heatwaves led to 50% mortality (Reusch et al. 2005). However, these results stem from field observations and experiments instead of mesocosm experiments. Naturally, dark-respiration of eelgrass can decrease the oxygen concentration during night to almost 0 mg $L^{-1}$ (as discussed by Rasmusson et al. 2020). In combination with high temperatures, Rasmusson et al. (2020) showed that low oxygen during night leads to reduced photosynthesis during daytime. Therefore, the impacts of heatwaves (CHAPTER III) might have been even more severe if the water inside the experimental units would not have been oxygenated during night. Therefore, I conclude that in a more natural setting (as e.g., discussed above in Impacts from a global warming scenario) allowing for low oxygen during night, a stronger impact of heatwaves can be expected, so that eelgrass meadows may actually not be able to withstand the uncontrolled spread of blue mussels.

### *Upwelling events in late summer*

In the Baltic Sea, the combination of an increasing number of upwelling events (Lehmann et al. 2012) and extending hypoxic areas (Diaz 2001), will likely lead to more hypoxic upwelling events in the future. However, late summer upwelling is not only characterised by low oxygen, but also by low temperature, pH, and increased salinity (Wahl et al. 2021). In the Kiel Fjord, upwelling events typically occur when the wind blows from south-west (Box 1), as this is the orientation of the Kiel Fjord. In the nearby Eckernförde bay, such winds that favour upwelling occur on average 18 times a year (Karstensen et al. 2014). Therefore, upwelling events are a typical phenomenon in the area and can represent another stressor for benthic ecosystems.

**Box 1:** The occurrence of coastal wind-driven upwelling events strongly depends on the wind direction, wind speed, and duration of the wind stress (Lehmann and Myrberg 2008). 56 potential upwelling events were visually identified (i.e., strong temperature drops, e.g., Discussion - Figure 5a; for exact dates see Discussion - Supplementary Table 8) at the GEOMAR Westshore building (N54° 19' 45.97" E10° 8' 58.582"), using the graphical representation of temperatures in Chapter I - Supplementary Figure 11. After the identification of those events, the wind speed and direction (data were provided by the GEOMAR meteorology department, Karl Bumke, Frauke Nevoigt) was analysed using the function *windRose* from the R package “openair”. I assumed that the wind direction during upwelling events would typically reflect the orientation of the Kiel Fjord. The analysis confirmed that the wind in the Kiel Fjord during potential upwelling events is mainly from South-West (Discussion - Figure 5b) which is the overall orientation of the Kiel Fjord.

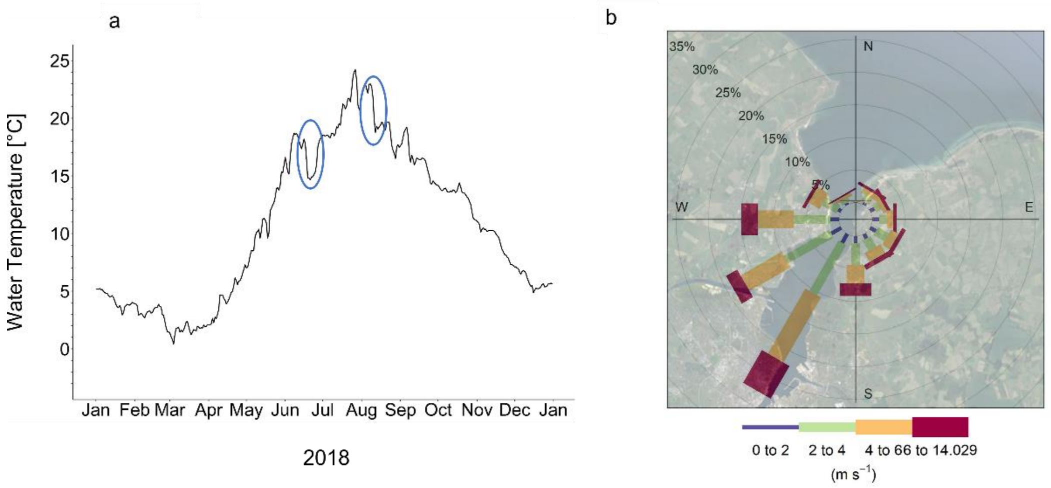

**Discussion - Figure 5:** Recorded temperatures (°C; **a**) in 1.8 m depth in the Kiel Fjord, Germany at the GEOMAR pier (N54° 19' 45.97" E10° 8' 58.582"; Wolf et al. 2020) in 2018 with indication of potential upwelling events (blue circles) and frequency of wind directions (%, **b**) and wind speed (m s$^{-1}$, **b**) at GEOMAR during all potential upwelling events from 1997 until 218. The underlying map (© Google Earth) in **b** shows the orientation of the Kiel Fjord.

While I could demonstrate that the photosynthetic species *Z. marina* was not impacted (i.e., long- and short-term response growth and photosynthetic indicators, respectively) by low oxygen (50% $O_2$ saturation) during upwelling conditions (CHAPTER III), other studies showed that hypoxia affects eelgrass (Pedersen et al. 2004; Rasmusson et al. 2020). Pedersen et al. (2004) and Rasmussen et al. (2020) however, exposed *Z. marina* to lower oxygen saturations (below 30% and 10% oxygen saturation, respectively). Furthermore, this contrasting finding may be caused by antagonistic effects of elevated $p\text{CO}_2$ during the upwelling event (CHAPTER III). Indeed, a study by Zimmerman et al. (2017) demonstrated a positive effect of high $CO_2$

concentrations on growth of *Z. marina*. Overall, the findings of CHAPTER III indicate that the applied upwelling alone was not severe enough to cause any harm to eelgrass.

Mobile species like *A. rubens* on the other hand, can be strongly impacted by late summer upwelling, being less active during an upwelling event (CHAPTER II). Likely, the low activity is caused by a combination of hypoxia and acidification effects as found by Fontanini et al. (2018). As stress response requires energy (Somero 2020), starfish may, during low oxygen and pH, reallocate their energy to critical cellular processes and thus, have less energy left for other processes like moving or feeding.

Although upwelling was not lethal for starfish or eelgrass, oxygen concentration has decreased in bottom waters from 1957–2013 (Lennartz et al. 2014) and will likely continue to decrease, so that future upwelling events in late summer may still pose a significant threat to *A. rubens* and *Z. marina*.

## Spatial-temporal refugia from extreme conditions

### *Thermal relaxiation by the interruption of heatwaves or vertical migration*

As heatwaves in shallow areas like the Baltic Sea are atmospherically driven (Oliver et al. 2021), the interruption of heatwaves by sudden atmospheric temperature changes may provide thermal relaxation (see e.g., August 2018 in Discussion - Figure 6). Such cold phases may solely be driven by atmospheric cold temperature (i.e., cold-spells) but may also be attributed to upwelling with associated changes in salinity, pH, and oxygen concentration. Upwelling can indeed provide thermal relaxation for different species (e.g., Lourenço et al. 2016; Randall et al. 2020). As starfish can survive the exposure to the abiotic changes imposed by upwelling, but projected future heatwaves appear 100% lethal, late summer upwelling may act as thermal relaxation for this species.

Apart from temporal changes of abiotic conditions, abiotic conditions can also vary over small spatial scales, e.g., from shallow to deeper habitats (see Chapter II - Supplementary Figure 1, Chapter II - Supplementary Figure 13, and Chapter III - Supplementary Figure 2). Deep water masses in summer are typically colder than the surface waters (see Chapter II - Supplementary Figure 13). Thus, migration to these deeper waters can represent thermal refugia in times of heat stress (e.g., Giraldo-Ospina et al. 2020; Magel et al. 2020). However, migrating to colder water masses in the Baltic Sea during summer likely exposes these individuals to bottom hypoxia (see Chapter II - Supplementary Figure 13). Therefore, vertical migration as escape from extreme heat stress in summer is often only possible for such species that are also tolerant to hypoxia, as well as the other stress effects from parameters such as low pH.

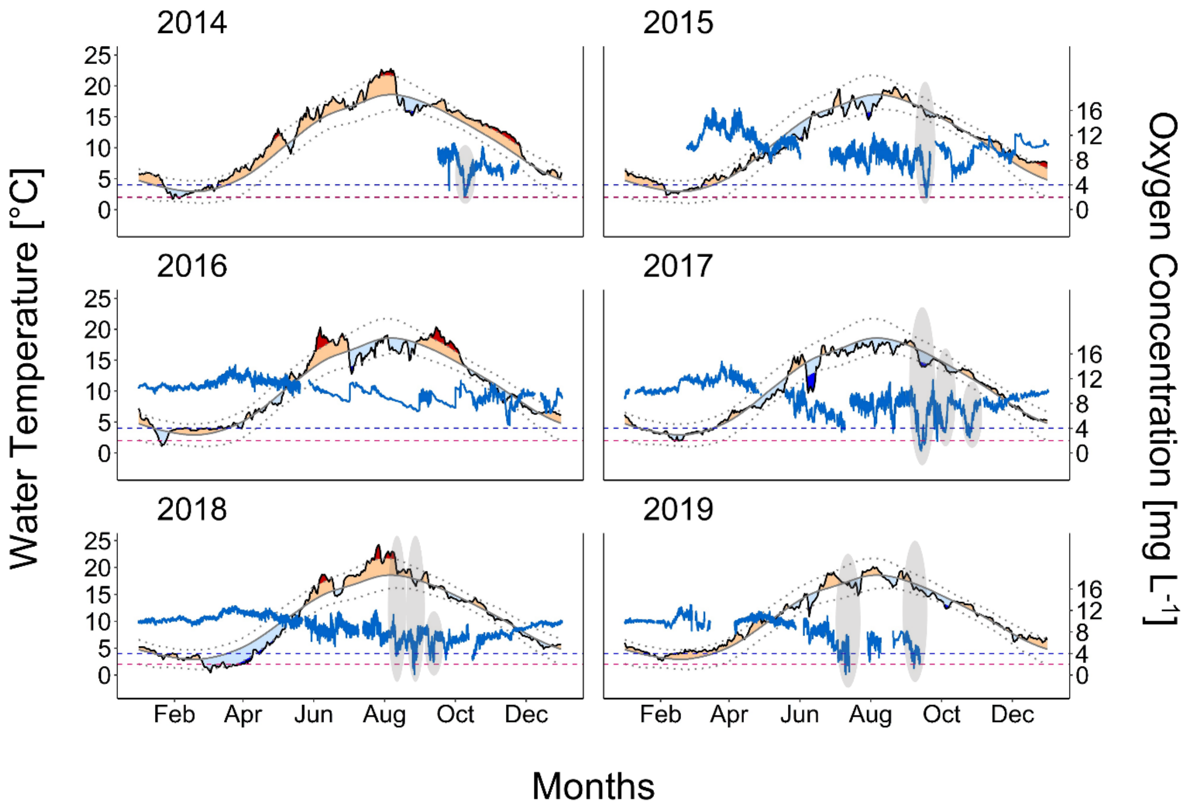

**Discussion - Figure 6:** Recorded Temperatures of the years 2014 until 2019 (°C; solid black lines) in 1.8 m depth in the Kiel Fjord, Germany at the GEOMAR pier (N54° 19' 45.97" E10° 8' 58.582"; Wolf et al. 2020 and additional temperature data from 2019 obtained from GEOMAR meteorology department, Sebastian Wahl). The 25-year temperature dataset (1997-2018: Wolf et al. 2020 and 2019-2021: additional temperature data obtained from GEOMAR meteorology department, Sebastian Wahl) was analysed on the occurrences of heatwaves and cold spells after Hobday et al. (2016). Based on this modelling the 25-year climatological values are represented as grey solid line, whereas the thresholds for heatwaves (i.e., 90th percentile) and cold-spells (i.e., 10th percentile) are represented as dotted lines. Temperatures above the climatological values, but below the 90th percentile are shown in orange, whereas temperatures above the 90th percentile are shown in red. Temperatures below the climatological trend, but above the 10th percentile are shown in light-blue, whereas temperatures below the 10th percentile are shown in dark-blue. Furthermore, oxygen concentration (mg $L^{-1}$; solid blue line) in 1 m depth at an adjacent pier (N54° 19' 48.7" E10° 08' 59.7"; Wolf et al. 2021) is shown. Dashed blue and pink lines represent hypoxia thresholds of 4 mg $L^{-1}$ (Vaquer-Sunyer and Duarte 2008) and 2 mg $L^{-1}$ (Breitburg et al. 2018). Grey ellipses represent hypoxic conditions alone or in combination with steep temperature decreases.

## *Ecological Memory*

Ecological memory (i.e., cross-stress tolerance and stress memory effects) can play a key role in the response of marine organisms to frequent stress events (e.g., Hughes et al. 2018; Jackson et al. 2021). While it was often proposed that more frequent extreme events such as marine heatwaves threaten ecosystems globally (Frölicher et al. 2018; Stillmann 2019; Wernberg et al. 2021), the possibility of acclimation to these events are to this date rarely considered in the marine realm.

One would expect that sessile species and species with restricted mobility living in highly variable environments would benefit most from an ecological memory as they cannot escape the stress. Eelgrasses are such sessile organisms, while starfish are principally mobile. However, Miyoshi et al. (2018) could show that a congener of *A. rubens* can only move about 4 m a day in summer, which implies that the starfish's mobility is restricted to a rather small area. Yet, while starfish could benefit from recurring stress events of different nature (i.e., heatwave and upwelling; CHAPTER II), eelgrasses, were negatively impacted by such a succession of heatwave and upwelling (CHAPTER III).

However, a study from Australia revealed that the local seagrasses *Posidonia australis* and *Zostera muelleri* show signs of a stress memory during a heatwave in those individuals that already experienced a previous heatwave (Nguyen et al. 2020). Similarly, Pazzaglia et al. (2022) could show that seedlings of the Mediterranean seagrass *Posidonia oceanica* can be thermally primed by succeeding heatwaves. These findings suggest that seagrasses generally can acclimate through an ecological memory. However, in contrast to the studies by Nguyen et al. (2020) and Pazzaglia et al. (2022), the experiment presented in CHAPTER III did not test the effects of succeeding stress events of the same (i.e., heatwave and heatwave) but of different nature (i.e., heatwave and upwelling). This may indicate that seagrasses can either acclimate to succeeding stressors of the same nature only or acclimate to heat stress only.

The starfish *A. rubens*, on the other hand, was more active during an upwelling event if it was previously exposed to a heatwave and thus, showed signs of an ecological memory (CHAPTER II). For other echinoderms, such as the sea urchin *Evechinus chloroticus*, a higher lethal temperature was demonstrated in those individuals that were acclimated to higher temperatures (Delorme et al. 2020), which also suggests the importance of succeeding stress events in understanding the response of echinorderms to such events. Yet, while it seems to be clear that the life history of eelgrasses as well as starfish seem to play an important role in their response to environmental stress, it needs to be further investigated why only starfish show an acclimation to stressors of different nature.

### *Physiological mechanisms*

Furthermore, the physiological background of an ecological memory is also not yet fully understood and requires more research efforts in the future. Potentially, heat shock proteins are involved in the ecological memory (Todgham et al. 2005; McBryan et al. 2016; Banti et al. 2008). A recent study by Delorme et al. (2020) demonstrated that sea urchins that were acclimated to high temperatures and then exposed to a thermal shock produced higher amounts of heat shock proteins (HSPs) compared to individuals that were acclimated at lower temperatures. However, Delorme et al. (2020) could not relate this enhanced HSP production to a change in righting time, a measure of individual instant fitness. Yet, this proves that the thermal history of an echinoderm is crucial for the production of HSPs. For this, additional experiments are needed that test the timing of marine heatwaves or additional stress events, measuring responses on the physiological level, including HSPs. Such species-specific measurements are needed to upscale the ecological memory from species to ecosystems (Jackson et al. 2021), so that the impact of environmental stress on the entire community can be unravelled.

### *Heat selection in a naturally variable habitat*

As presented in CHAPTER III, *Z. marina* biomass decreases significantly under a warming scenario of 3 °C (IPCC 2021). However, these results also reveal that eelgrass plants that were collected from a sandbank at the Falckenstein beach (Kiel Fjord, Germany) were less impacted by warming than individuals from adjacent slightly deeper waters just less than 200 m apart. Previous comparisons of the thermal performance of *Zostera noltei* inhabiting shallow areas and *Z. marina* inhabiting deeper habitats showed higher thermal resistance of *Z. noltei* (Franssen et al. 2014), suggesting an adaption of *Z. noltei* to the warmer shallow habitat. Using transplant experiments (Maasholm and Falckenstein populations), Hämmerli and Reusch (2002) could show that *Z. marina* performs better at its original habitat and thus, suggests local adaptation. A study from Maasholm, around 35 km North-West of Kiel, showed that different genotypes reacted differently to a heatwave in 2003 (Reusch et al. 2005). The authors discussed that this difference between genotypes likely indicates a potential of *Z. marina* for an evolutionary response to thermal stress (Reusch et al. 2005).

As the eelgrass population that was collected for the experiment presented in CHAPTER III were less than 200 m apart, one could argue that due to the short distance, gene flow is very high and thus, the populations not genetically different. Eelgrass' sexual reproduction can result in high gene flow by pollen distribution (Ruckelshaus 1996), seed dispersal via currents (Ruckelshaus 1996), or via biotic transport (Sumoski and Orth 2012). However, eelgrass in the Baltic Sea has been shown to mainly grow vegetatively when established (Robertson and Mann 1984; Olesen and Sand-Jensen 1994; Reusch et al. 1999b) and thus, can form large clones of about 6400 $m^2$ (Reusch et al. 1999a). Therefore, it may be that the established *Z. marina* population outside the sandbank is reproducing rather vegetatively than sexually, which limits the gene flow to the neighbouring shallow population. Yet, it cannot be ruled out that the eelgrass population in the shallow area is maintained by seed dispersal from the deep population. Either way, one or several heat resistant genotypes may be selected for at the shallow location, which could explain the different growth rates I found between shallow and deeper eelgrass population (CHAPTER III). If the two populations are not genetically different, a fact that needs to be evaluated in further efforts (see also below Perspectives on future fruitful research in experimental ecology), the higher growth rate of the sandbank population could be attributed to a high phenotypic plasticity of that species or to acclimation through an ecological memory (as discussed above in Ecological Memory). In the shallow regions of Brittany, eelgrass typically grows in high densities with small shoots and leaves, while investing in belowground biomass (Boyé et al. 2022). In deeper areas of the same region, eelgrass rather grows high shoots in low densities (Boyé et al. 2022). This highlights the phenotypic plasticity of this species and their adaptation to different habitats. Actually, the biomass of the sandbank population could maintain more belowground biomass under the warming scenario than the deeper population (CHAPTER III). As responses to environmental stress requires energy (Somero 2020) and as belowground biomass can serve as energy reserves (e.g., Olesen and Sand-Jensen 1993; Lee et al. 2005), investment in belowground biomass can be beneficial in habitats with high environmental stress.

Regardless of the mechanism behind the better performance of the heat-selected population under heat stress, the results suggest that *Z. marina* has the potential for heat adaptation and this knowledge may possibly be applied in restoration efforts. A study on the Mediterranean seagrass *Posidonia oceanica* could show an enhanced performance of seedlings under high temperatures if they previously had been exposed to elevated temperatures (Pazzaglia et al. 2022). Not only for seagrasses (Pazzaglia et al. 2022) but also for corals (Morikawa and Palumbi 2019; Caruso et al. 2021) artificial thermal hardening has been proposed for restoration projects. Currently, the project SeaStore[1] aims for the restoration and afforestation of eelgrass at the German coast of the Baltic Sea. While this project will surely improve the status of *Z. marina* in German coastal areas, ongoing warming might prevent a full recovery of regions that were formerly covered with eelgrass. Therefore, future afforestation projects should consider the possibility to use artificial thermal hardening (Pazzaglia et al. 2022) or natural resistant genotypes or phenotypes (as discussed above) for restoration of eelgrass meadows.

---

[1] https://www.lufi.uni-hannover.de/de/forschung/forschungsschwerpunkte/oekohydraulik-und-oekosystemleistungen/seastore

## Conclusions

In this work I could improve the mechanistic understanding of how the frequency, intensity, and duration of environmental stress (i.e., heatwaves, upwelling, and warming) impacts the two important marine species, *Asterias rubens* and *Zostera marina*. Extreme event characterisation can be a powerful tool to identify typical extremes that can be used to ensure close-to natural experimental treatments that still allow for a mechanistical understanding of extreme event impacts. Mesocosm experiments with realistic treatments based on this extreme event characterisation revealed a strong negative impact of heatwaves on the starfish *Asterias rubens* ranging from decreased feeding rates (today's heatwave intensity) to severe mortalities (future heatwave intensity). Impacts on key predators like starfish will likely have impacts on the whole ecosystems, especially on the extend of mussel beds (Discussion - Figure 7). As blue mussels are more temperature tolerant than starfish and eelgrass lost substantial biomass when exposed to future projected temperatures, *Mytilus* mussels could form large monocultures and thus, decrease overall biodiversity (Discussion - Figure 7). Yet, I could demonstrate that an improved performance under thermal stress or upwelling conditions is possible. Heat-selection, phenotypic plastic responses, or acclimation in *Z. marina* from locally heat-exposed habitats as well as the development of an ecological memory in *A. rubens* seem to play a major role in the response of these species to thermal stress and upwelling conditions. Including the potential stress-resistance may mitigate the impact of warming and future heatwaves (Discussion - Figure 7). However, it needs to be further investigated which physiological mechanisms are involved to fully understand the responses of starfish and eelgrass in the face of global climate change. The results of my thesis answer many urgent questions in stress ecology, but also open new directions for further fruitful research (see Perspectives on future fruitful research in experimental ecology below).

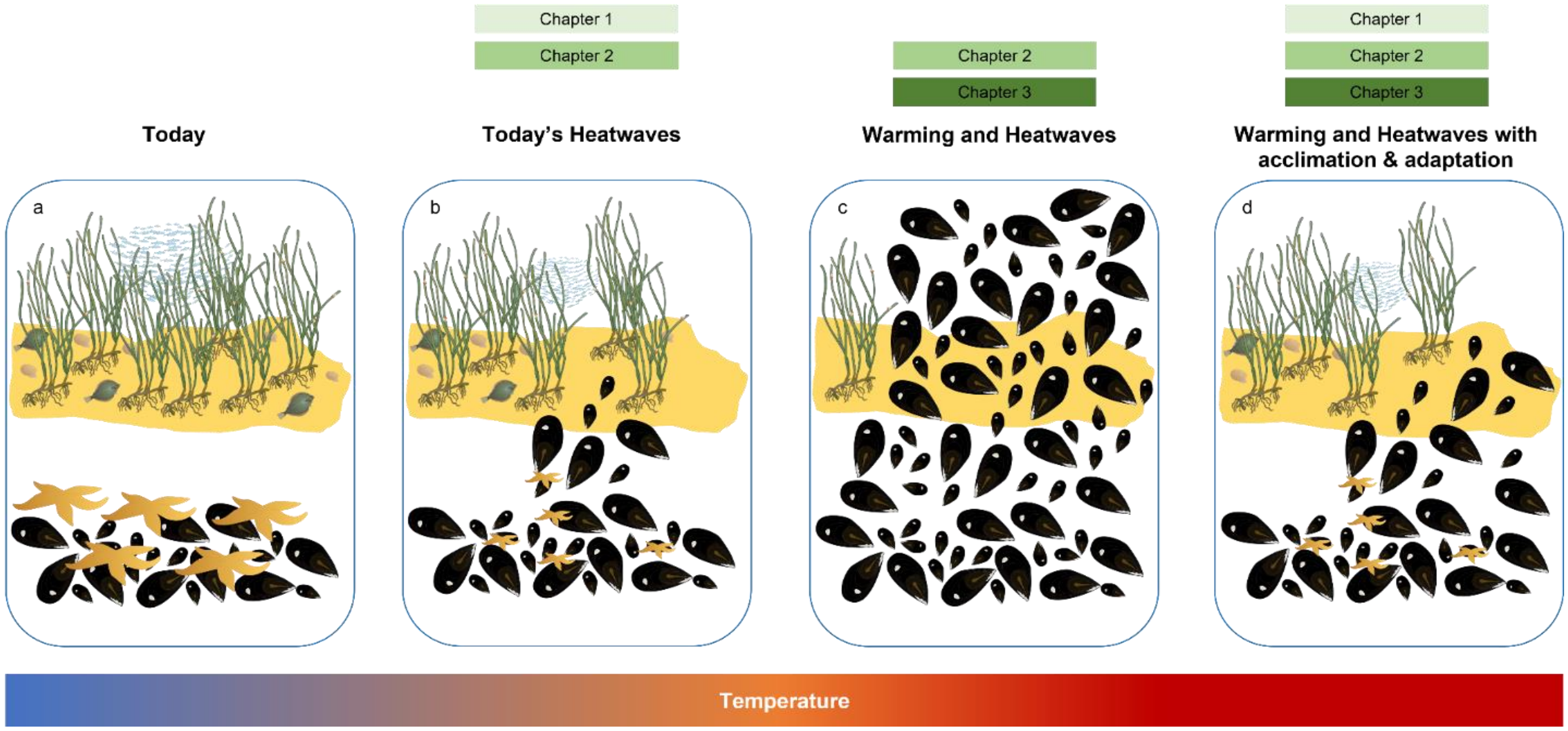

**Discussion - Figure 7:** Summary of all results and implications of my thesis. The investigated species (*Zostera marina* and *Asterias rubens*) change performance along different levels of heat stress (increasing heat stress from blue to red) with and without acclimation and adaptation. As keystone species, associated communities are likely to change as well. Under today's conditions (**a**) eelgrass meadows provide habitat for many associated species and mussel reefs are controlled by starfish. With heatwaves of today's intensity (**b**) starfish are smaller as they feed less. This may enable blue mussels to propagate into eelgrass meadows and partly replace *Z. marina*. With future warming (**c**), heatwaves will lead to high mortalities among starfish, and thus to predator-release of the more heat-tolerant blue mussel. At the same time, eelgrass loses biomass due to increased temperatures, so that blue mussels may replace large part of eelgrass meadows. Acclimation and adaption of eelgrass and starfish may mitigate the impact of future warming and heatwaves (**d**), so that both ecosystems can still co-exist. The contributing chapters are highlighted in different shades of green above the four panels of the graph. Species symbols are taken from https://ian.umces.edu/media-library/symbols/#download.

## Perspectives on future fruitful research in experimental ecology

My research gave detailed insights into the stress response of two important species of the Baltic Sea and a mechanistical understanding of the role of frequency, duration, and intensity of environmental stress. However, the results lead to further questions and open new directions in stress ecology research. I identified three main research lines that I propose for future research:

### *Real-time extreme event detector*

As shown in this thesis, extreme events can negatively impact marine species and as discussed above, likely impacts the entire community or ecosystem (see also Discussion - Figure 7). However, a mechanistical analysis of extreme events is still rather rare. Therefore, the water temperature dataset as well as the heatwave characterisation of the Kiel Fjord is publicly available at the PANGAEA data repository (Wolf et al. 2020, Wolf 2022). Although everyone could access such data, they are mainly accessed by the scientific community. However, in my opinion such data need to be easily accessible and understandable also for people outside the scientific community. Otherwise, rising awareness about heatwaves in the marine area is very difficult. In coral reef systems, early warning systems have been implemented[2] that are not only of interest for conservation efforts but also help in communicating coral bleaching among people outside science. Based on this approach, a real-time extreme event detector was developed (Discussion - Figure 8). This simple tool puts the ambient water temperature of the Kiel Fjord in relation to the extreme event analysis presented in CHAPTER I. Therefore, a recognition of the ambient seawater temperature in relation to long-term climatological values and thresholds for marine heatwave and cold-spells can be made by everyone. This tool may, e.g., be used by tourists, who want to know if the experienced water temperature while swimming was rather typical, too cold, or too warm for the respective time of the year. Furthermore, also scientists can profit from this tool, as they can get an immidiate idea of the environmental conditions in the field that may be important for the timing of a field experiment.

---

[2] https://www.coris.noaa.gov/activities/projects/bleach_events/#two

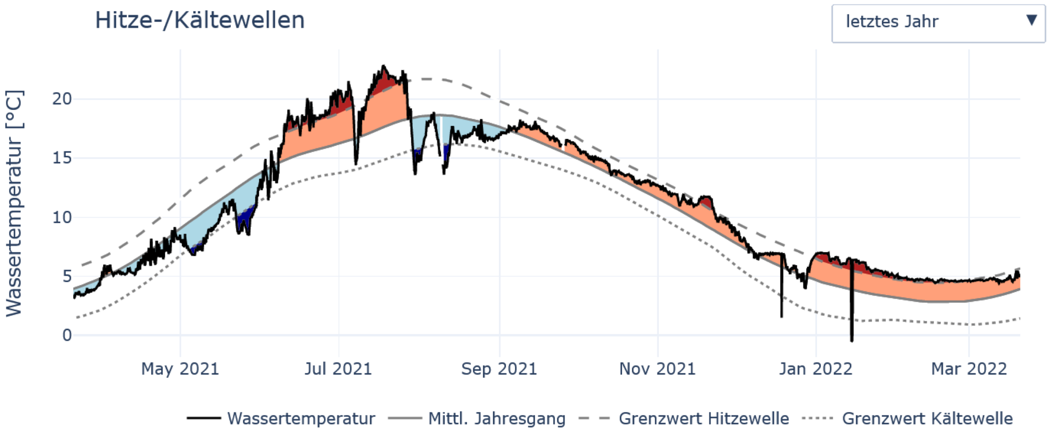

**Discussion - Figure 8:** Ambient (real-time) water temperature (solid black line), climatological values (solid grey line) and thresholds for heatwaves (dashed grey line) and cold-spells (dotted grey line) in the Kiel Fjord following the extreme event characterisation after Hobday et al. (2016) presented in CHAPTER I. Note that the graph was taken from https://solarisheppa.geomar.de/heatwave.html on March 20th, 2022 and is therefore in German. The beta-version of this website was developed together with the GEOMAR meteorology department (Dr. Sebastian Wahl). In a further step it is planned to incorporate this website to the official GEOMAR website, which would make this extreme event characterisation available to everyone.

In late summer, steep temperature decreases are particularly interesting to scientists or aquacultures (e.g., Kieler Lachsforelle[3]) if these are caused by hypoxic upwelling events. Therefore, the existing website could be extended to also show the abiotic conditions of the deep Kiel Fjord water, i.e., water bodies below the pycnocline. This could be realised by using the existing deep-water monitoring at the Kiel Outdoor Benthocosms, GEONAR, Kiel (Wahl et al. 2015, 2021). Ideally, these logged data would be shown on the same website as the heatwave and cold-spell detector[4] and identify if the deep-water is moderately (i.e., below 4 mg $L^{-1}$ oxygen concentration; Vaquer-Dunyer and Duarte 2008) or severely (i.e., below 2 mg $^{-1}$ oxygen concentration; Breitburg et al. 2018) hypoxic.

In collaboration with meteorologists and modellers it may be possible to even predict marine heatwaves or hypoxic upwelling. In combination with the ambient water temperature (i.e., real-time extreme event detector; see Discussion - Figure 8) and the atmospheric weather forecasts[5], it may be possible to predict the occurrence of marine heatwaves in the Kiel Fjord. Above, I also showed that the wind during potential upwelling events in the Kiel Fjord typically blows from south-western direction (see Box 1). Thus, if one knows the wind forecasts and the current state of the deep Kiel Fjord water (i.e., using the existing monitoring of water masses below the

---

[3] https://www.kieler-lachsforelle.de

[4] https://solarisheppa.geomar.de/heatwave.html

[5] https://www.dwd.de/DE/forschung/wettervorhersage/num_modellierung/05_verifikation/verifikation_node.html#doc19956bodyText4

pycnocline), one may on very short-term predict hypoxic upwelling in the future. If these forecasts were available, in case of an upcoming potential hypoxic upwelling event, aquacultures could react on time to ventilate their systems to prevent mass mortalities. Furthermore, such forecasts of extreme events in the Kiel Fjord would also be interesting to scientists who want to test the impact of extreme events in field experiments and thus, rely on the ambient water conditions.

### *Predators in the Mytilus reefs*

My work has focused on one important predator in the *Mytilus spp.* reef ecosystem. However, to identify the whole predator-prey community response to extreme events, future experiments need to include all three main predators (*A. rubens*, *C. maenas*, and *H. takanoi*; see Reusch and Chapman 1997; Nour et al. 2020), as well as the mussel prey (*Mytilus spp.*). These common-garden experiments (see Discussion - Figure 9) need to identify the impact of extreme events of different intensity, duration and frequency on (**i**) the feeding rate of all three predator species separately (e.g., assessing the number of mussels of different size classes that have been fed via methods as outlined above), (**ii**) the performance of the prey *Mytilus spp.* (e.g., by testing the strength of the muscle closing the two shells and by testing the stability of the mussel shell itself), and (**iii**) the direct interaction (e.g., preying on each other, or territorial behaviour) of the three predator species (e.g., via video analysis of species interaction). When all these information are available, a complete predator-prey model could be created that projects how *Mytilus* reefs in the Baltic Sea will change with increasing extreme events under a changing climate.

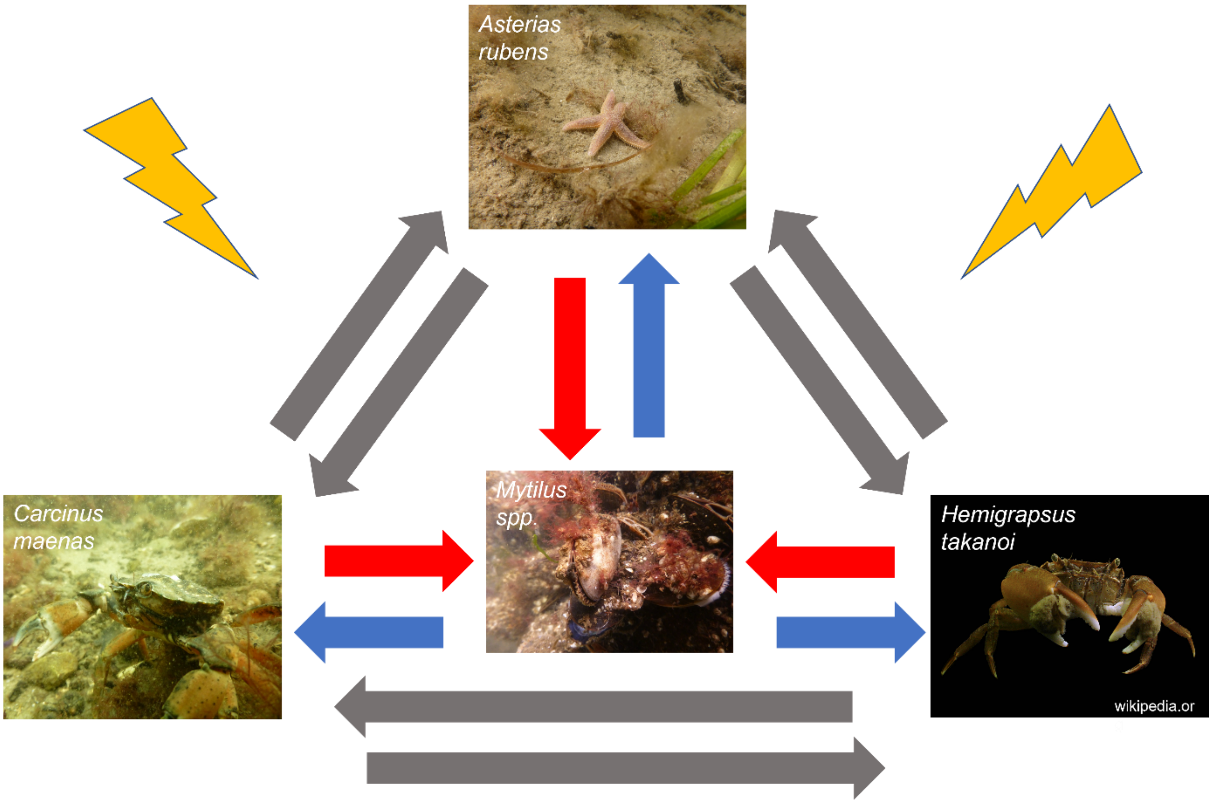

**Discussion - Figure 9:** Schematic illustration of the potential interactions that may be altered under environmental stress (yellow lightning symbols) in the predator-prey system, crabs and starfish feeding on blue mussels: (i) red arrows indicate feeding of predators *Asterias rubens*, *Hemigrapsus takanoi*, and *Carcinus maenas* on *Mytilus spp*. (ii) blue arrows indicate responses of the prey *Mytilus*. (iii) grey arrows represent the interactions among the predator species.

### *Stress-tolerance in benthic key species*

My work demonstrated that heat-selected *Z. marina* individuals could cope better with a warming scenario than non-heat-selected individuals. As mentioned above, this natural heat-selection could be used for restoration projects, but before applied, this needs more research to understand the background of the higher performance of heat-selected individuals.

First of all, it needs to be identified if the sandbank individuals are actually genetically distinct from the deeper individuals (e.g., genotyping-by-sequencing based on single nucleotide polymorphisms as reviewed by Pazzaglia et al. 2021). Regardless of the outcome of such genotyping, further physiological and genetical measurements should be implemented to reveal why the sandbank individuals perform better. Such measurements should include analyses of photosynthesis and respiration rates (see e.g., Beca-Carretero et al. 2018) and energy reserves in the belowground biomass (e.g., Olesen and Sand-Jensen 1993; Lee et al. 2005). Bergmann et al. (2010) could show that several target genes, e.g., sequences for HSPs, are involved in the response of *Z. marina* to marine heatwaves. Furthermore, Bergmann et al. (2010) proposed to use these target genes to identify the potential for local adaptation of *Z. marina*. Hence, the target genes identified by Bergmann et al. (2010) should be measured via qPCR in both populations, inside and outside the sandbank. In combination, these measurements will reveal in more detail how the two populations differ from each other.

Once, the physiological and genetical background of the heat-selected individuals is revealed, experiments need to investigate if thermally robust *Z. marina* individuals can be cultivated in laboratory mesocosm facilities. Depending on if the heat-selected individuals only show a plastic response or if the two populations are genetically different, two different kinds of experiments should be performed. If it was a plastic response, the experiment should aim for artificial hardening (i.e., ecological memory; as discussed above) as implemented by Pazzaglia et al. 2022. If, on the other hand, it proves that the two populations are actually genetically different, it needs to be investigated if the heat-tolerant genotype can be cultivated and reproduced in the laboratory. When the laboratory experiments were successful, long-term field experiments on the natural response of eelgrass in habitats with naturally high temperatures (e.g., sandbanks) need to be performed. These experiments need to investigate (**i**) if the heat-selected eelgrass is also performing better in the field compared to non-heat-selected eelgrass, (**ii**) if the population can be maintained perennially, and (**iii**) if the associated species community is impacted. Finally, the heat-tolerant individuals could be used in large-scale reforestation projects (as proposed by Pazzaglia et al. 2022).

Beyond the heat tolerant eelgrass, my results show that an ecological memory seems to be relevant in the response of starfish to extreme events. However, similar to the heat-tolerant eelgrasses, we do not know what physiological processes are involved. As discussed above, likely heat shock proteins and their transcription factors are involved. However, other physiological mechanisms like the expression of antioxidant enzymes might be involved as well. Therefore, transcriptomics like qPCR (as proposed by Sørensen et al. 2003) should be applied in future experiments. Such experiments should identify (**i**) which genes are involved in the response to extreme events, (**ii**) if the response depends on the intensity or duration of the applied event, (**iii**) if the response depends on the identity of the event (i.e., either heatwave or upwelling), and (**iv**) if the response changes with the frequency of the applied events. Once the genes are identified, it needs to be verified that the respective protein concentrations are actually increased as response to the applied stress. The gained knowledge about how an ecological memory can function in marine benthic ecosystems, needs to be transferred to other key species, such as eelgrass (as presented above), macroalgae (e.g., *Fucus vesiculosus*) or *Mytilus* mussels. Such community experiments are time demanding and difficult to interpret. However, only with the focus on entire communities or ecosystems, we will be able to fully understand and project their future responses to changing conditions.

## References for General Introduction and Discussion

AlgaeBase: Listing the World's Algae. Available online at https://www.algaebase.org/.

Arias-Ortiz, A.; Serrano, O.; Masqué, P.; Lavery, P. S.; Mueller, U.; Kendrick, G. A. et al. (2018): A marine heatwave drives massive losses from the world's largest seagrass carbon stocks. In Nature Clim Change 8 (4), pp. 338–344. DOI: 10.1038/s41558-018-0096-y.

Atkinson, James; King, Nathan G.; Wilmes, Sophie B.; Moore, Pippa J. (2020): Summer and Winter Marine Heatwaves Favor an Invasive Over Native Seaweeds. In Journal of Phycology 56 (6), pp. 1591–1600. DOI: 10.1111/jpy.13051.

Banti, Valeria; Loreti, Elena; Novi, Giacomo; Santaniello, Antonietta; Alpi, Amedeo; Perata, Pierdomenico (2008): Heat acclimation and cross-tolerance against anoxia in Arabidopsis. In Plant, cell & environment 31 (7), pp. 1029–1037. DOI: 10.1111/j.1365-3040.2008.01816.x.

Barbier, Edward B.; Hacker, Sally D.; Kennedy, Chris; Koch, Evamaria W.; Stier, Adrian C.; Silliman, Brian R. (2011): The value of estuarine and coastal ecosystem services. In Ecological Monographs 81 (2), pp. 169–193. DOI: 10.1890/10-1510.1.

Bates, Nicholas Robert; Johnson, Rodney J. (2020): Acceleration of ocean warming, salinification, deoxygenation and acidification in the surface subtropical North Atlantic Ocean. In Commun Earth Environ 1 (1), p. 351. DOI: 10.1038/s43247-020-00030-5.

Beca-Carretero, P.; Olesen, B.; Marbà, N.; Krause-Jensen, D. (2018): Response to experimental warming in northern eelgrass populations. Comparison across a range of temperature adaptations. In Mar. Ecol. Prog. Ser. 589, pp. 59–72. DOI: 10.3354/meps12439.

Benedetti-Cecchi, Lisandro (2003): THE IMPORTANCE OF THE VARIANCE AROUND THE MEAN EFFECT SIZE OF ECOLOGICAL PROCESSES. In Ecology 84 (9), pp. 2335–2346. DOI: 10.1890/02-8011.

Bergmann, Nina; Winters, Gidon; Rauch, Gisep; Eizaguirre, Christophe; Gu, Jenny; Nelle, Peter et al. (2010): Population-specificity of heat stress gene induction in northern and southern eelgrass Zostera marina populations under simulated global warming. In Molecular ecology 19 (14), pp. 2870–2883. DOI: 10.1111/j.1365-294X.2010.04731.x.

Bertolini, C.; Pastres, R. (2021): Tolerance landscapes can be used to predict species-specific responses to climate change beyond the marine heatwave concept. Using tolerance landscape models for an ecologically meaningful classification of extreme climate events. In Estuarine, Coastal and Shelf Science 252 (3), p. 107284. DOI: 10.1016/j.ecss.2021.107284.

Boström, Christoffer; Bonsdorff, Erik (1997): Community structure and spatial variation of benthic invertebrates associated with Zostera marina (L.) beds in the northern Baltic Sea. In Journal of Sea Research 37, pp. 153–166.

Boyé, Aurélien; Gauthier, Olivier; Becheler, Ronan; Le Garrec, Vincent; Hily, Christian; Maguer, Marion; Grall, Jacques (2022): Drivers and limits of phenotypic responses in vulnerable seagrass populations. Zostera marina in the intertidal. In J Ecology 110 (1), pp. 144–161. DOI: 10.1111/1365-2745.13791.

Bradtke, Katarzyna; Herman, Agnieszka; Urbański, Jacek A. (2010): Spatial and interannual variations of seasonal sea surface temperature patterns in the Baltic Sea. In Oceanologia 52 (3), pp. 345–362. DOI: 10.5697/oc.52-3.345.

Breitburg, Denise; Levin, Lisa A.; Oschlies, Andreas; Grégoire, Marilaure; Chavez, Francisco P.; Conley, Daniel J. et al. (2018): Declining oxygen in the global ocean and coastal waters. In Science (New York, N.Y.) 359 (6371). DOI: 10.1126/science.aam7240.

Broska, Lisa Hanna; Poganietz, Witold-Roger; Vögele, Stefan (2020): Extreme events defined—A conceptual discussion applying a complex systems approach. In Futures 115 (6), p. 102490. DOI: 10.1016/j.futures.2019.102490.

Budd, G. C. (2008): Asterias rubens Common starfish. Edited by Tyler-Walters H., K. Hiscock. Marine Life Information Network: Biology and Sensitivity Key Infomation Reviews (online). Plymouth: Marine Biological Association of the United Kingdom. Available online at https://dx.doi.org/10.17031/marlinsp.1194.1.

Caruso, Carlo; Hughes, Kira; Drury, Crawford (2021): Selecting Heat-Tolerant Corals for Proactive Reef Restoration. In Front. Mar. Sci. 8, p. 367. DOI: 10.3389/fmars.2021.632027.

Cazenave, Anny; Llovel, William (2010): Contemporary sea level rise. In Annual review of marine science 2, pp. 145–173. DOI: 10.1146/annurev-marine-120308-081105.

Chavez, Francisco P.; Bertrand, Arnaud; Guevara-Carrasco, Renato; Soler, Pierre; Csirke, Jorge (2008): The northern Humboldt Current System. Brief history, present status and a view towards the future. In Progress in Oceanography 79 (2-4), pp. 95–105. DOI: 10.1016/j.pocean.2008.10.012.

Chavez, Francisco P.; Messié, Monique (2009): A comparison of Eastern Boundary Upwelling Ecosystems. In Progress in Oceanography 83 (1-4), pp. 80–96. DOI: 10.1016/j.pocean.2009.07.032.

Clark, Ailsa M.; Downey, Maureen E. (1992): Starfishes of the Atlantic. 1. ed. London: Chapman & Hall (Natural History Museum publications, 3).

Cole, Scott G.; Moksnes, Per-Olav (2016): Valuing Multiple Eelgrass Ecosystem Services in Sweden. Fish Production and Uptake of Carbon and Nitrogen. In Front. Mar. Sci. 2, p. 7390. DOI: 10.3389/fmars.2015.00121.

Delorme, Natalí J.; Frost, Emily J.; Sewell, Mary A. (2020): Effect of acclimation on thermal limits and hsp70 gene expression of the New Zealand sea urchin Evechinus chloroticus. In Comparative biochemistry and physiology. Part A, Molecular & integrative physiology 250, p. 110806. DOI: 10.1016/j.cbpa.2020.110806.

Diaz, R. J. (2001): Overview of hypoxia around the world. In Journal of environmental quality 30 (2), pp. 275–281. DOI: 10.2134/jeq2001.302275x.

Diaz, Robert J.; Rosenberg, Rutger (2008): Spreading dead zones and consequences for marine ecosystems. In Science (New York, N.Y.) 321 (5891), pp. 926–929. DOI: 10.1126/science.1156401.

Dobretsov, Sergey; Wahl, Martin (2001): Recruitment preferences of blue mussel spat (Mytilus edulis) for different substrata and microhabitats in the White Sea (Russia). In Hydrobiologia 445 (1/3), pp. 27–35. DOI: 10.1023/A:1017502126707.

Doney, Scott C.; Ruckelshaus, Mary; Duffy, J. Emmett; Barry, James P.; Chan, Francis; English, Chad A. et al. (2012): Climate change impacts on marine ecosystems. In Annual review of marine science 4, pp. 11–37. DOI: 10.1146/annurev-marine-041911-111611.

Duarte, Bernardo; Martins, Irene; Rosa, Rui; Matos, Ana R.; Roleda, Michael Y.; Reusch, Thorsten B. H. et al. (2018): Climate Change Impacts on Seagrass Meadows and Macroalgal Forests. An Integrative Perspective on Acclimation and Adaptation Potential. In Front. Mar. Sci. 5, p. 1117. DOI: 10.3389/fmars.2018.00190.

Duarte, Carlos M.; Losada, Iñigo J.; Hendriks, Iris E.; Mazarrasa, Inés; Marbà, Núria (2013): The role of coastal plant communities for climate change mitigation and adaptation. In Nature Clim Change 3 (11), pp. 961–968. DOI: 10.1038/NCLIMATE1970.

Dürr, Simone; Wahl, Martin (2004): Isolated and combined impacts of blue mussels (Mytilus edulis) and barnacles (Balanus improvisus) on structure and diversity of a fouling community. In Journal of Experimental Marine Biology and Ecology 306 (2), pp. 181–195. DOI: 10.1016/j.jembe.2004.01.006.

Easterling, D. R.; Meehl, G. A.; Parmesan, C.; Changnon, S. A.; Karl, T. R.; Mearns, L. O. (2000): Climate extremes. Observations, modeling, and impacts. In Science (New York, N.Y.) 289 (5487), pp. 2068–2074. DOI: 10.1126/science.289.5487.2068.

Ehlers, A.; Worm, B.; Reusch, T. B.H. (2008): Importance of genetic diversity in eelgrass Zostera marina for its resilience to global warming. In Mar. Ecol. Prog. Ser. 355, pp. 1–7. DOI: 10.3354/meps07369.

Estay, Sergio A.; Clavijo-Baquet, Sabrina; Lima, Mauricio; Bozinovic, Francisco (2011): Beyond average. An experimental test of temperature variability on the population dynamics of Tribolium confusum. In Popul Ecol 53 (1), pp. 53–58. DOI: 10.1007/s10144-010-0216-7.

Feng, Ming; McPhaden, Michael J.; Xie, Shang-Ping; Hafner, Jan (2013): La Niña forces unprecedented Leeuwin Current warming in 2011. In Scientific reports 3, p. 1277. DOI: 10.1038/srep01277.

Fennel, Katja; Testa, Jeremy M. (2019): Biogeochemical Controls on Coastal Hypoxia. In Annual review of marine science 11, pp. 105–130. DOI: 10.1146/annurev-marine-010318-095138.

Field, C. D. (1995): Impact of expected climate change on mangroves. In Hydrobiologia 295 (1-3), pp. 75–81. DOI: 10.1007/BF00029113.

Fontanini, Aisling; Steckbauer, Alexandra; Dupont, Sam; Duarte, Carlos M. (2018): Variable metabolic responses of Skagerrak invertebrates to low O2 and high CO2 scenarios. In Biogeosciences 15 (12), pp. 3717–3729. DOI: 10.5194/bg-15-3717-2018.

Franssen, Susanne U.; Gu, Jenny; Winters, Gidon; Huylmans, Ann-Kathrin; Wienpahl, Isabell; Sparwel, Maximiliane et al. (2014): Genome-wide transcriptomic responses of the seagrasses Zostera marina and Nanozostera noltii under a simulated heatwave confirm functional types. In Marine genomics 15, pp. 65–73. DOI: 10.1016/j.margen.2014.03.004.

Frölicher, Thomas L.; Fischer, Erich M.; Gruber, Nicolas (2018): Marine heatwaves under global warming. In Nature 560 (7718), pp. 360–364. DOI: 10.1038/s41586-018-0383-9.

Gebbie, Geoffrey (2021): Combining Modern and Paleoceanographic Perspectives on Ocean Heat Uptake. In Annual review of marine science 13, pp. 255–281. DOI: 10.1146/annurev-marine-010419-010844.

Giesen, W.B.J.T.; van Katwijk, M. M.; den Hartog, C. (1990): Eelgrass condition and turbidity in the Dutch Wadden Sea. In Aquatic Botany 37 (1), pp. 71–85. DOI: 10.1016/0304-3770(90)90065-S.

Gilg, Matthew R.; Hilbish, Thomas J. (2003): THE GEOGRAPHY OF MARINE LARVAL DISPERSAL. COUPLING GENETICS WITH FINE-SCALE PHYSICAL OCEANOGRAPHY. In Ecology 84 (11), pp. 2989–2998. DOI: 10.1890/02-0498.

Gilly, William F.; Beman, J. Michael; Litvin, Steven Y.; Robison, Bruce H. (2013): Oceanographic and biological effects of shoaling of the oxygen minimum zone. In Annual review of marine science 5, pp. 393–420. DOI: 10.1146/annurev-marine-120710-100849.

Giraldo-Ospina, Ana; Kendrick, Gary A.; Hovey, Renae K. (2020): Depth moderates loss of marine foundation species after an extreme marine heatwave. Could deep temperate reefs act as a refuge? In Proceedings. Biological sciences 287 (1928), p. 20200709. DOI: 10.1098/rspb.2020.0709.

Githaiga, Michael N.; Frouws, Anna M.; Kairo, James G.; Huxham, Mark (2019): Seagrass Removal Leads to Rapid Changes in Fauna and Loss of Carbon. In Front. Ecol. Evol. 7, p. 1038. DOI: 10.3389/fevo.2019.00062.

Glynn, Peter W. (1991): Coral reef bleaching in the 1980s and possible connections with global warming. In Trends in Ecology & Evolution 6 (6), pp. 175–179. DOI: 10.1016/0169-5347(91)90208-F.

Green, Edmund P.; Short, Frederick T. (2003): World atlas of seagrasses. Berkeley, Calif.: Univ. of California Press. Available online at http://www.loc.gov/catdir/bios/ucal052/2004298124.html.

Gunderson, Alex R.; Armstrong, Eric J.; Stillman, Jonathon H. (2016): Multiple Stressors in a Changing World. The Need for an Improved Perspective on Physiological Responses to the Dynamic Marine Environment. In Annual review of marine science 8, pp. 357–378. DOI: 10.1146/annurev-marine-122414-033953.

Guppy, Michael; Withers, Philip (1999): Metabolic depression in animals. Physiological perspectives and biochemical generalizations. In Biological Reviews 74 (1), pp. 1–40. DOI: 10.1111/j.1469-185X.1999.tb00180.x.

Hammer, K. J.; Borum, J.; Hasler-Sheetal, H.; Shields, E. C.; Sand-Jensen, K.; Moore, K. A. (2018): High temperatures cause reduced growth, plant death and metabolic changes in eelgrass Zostera marina. In Mar. Ecol. Prog. Ser. 604, pp. 121–132. DOI: 10.3354/meps12740.

Hämmerli, A.; Reusch, T. B.H. (2002): Local adaptation and transplant dominance in genets of the marine clonal plant Zostera marina. In Mar. Ecol. Prog. Ser. 242, pp. 111–118. DOI: 10.3354/MEPS242111.

Han, Guodong; Wang, Wei; Dong, Yunwei (2020): Effects of balancing selection and microhabitat temperature variations on heat tolerance of the intertidal black mussel Septifer virgatus. In Integrative zoology 15 (5), pp. 416–427. DOI: 10.1111/1749-4877.12439.

Harrison, P. A.; Berry, P. M.; Simpson, G.; Haslett, J. R.; Blicharska, M.; Bucur, M. et al. (2014): Linkages between biodiversity attributes and ecosystem services. A systematic review. In Ecosystem Services 9 (9), pp. 191–203. DOI: 10.1016/j.ecoser.2014.05.006.

Hauxwell, Jennifer; Cebrián, Just; Furlong, Christopher; Valiela, Ivan (2001): MACROALGAL CANOPIES CONTRIBUTE TO EELGRASS (ZOSTERA MARINA ) DECLINE IN TEMPERATE ESTUARINE ECOSYSTEMS. In Ecology 82 (4), pp. 1007–1022. DOI: 10.1890/0012-9658(2001)082[1007:MCCTEZ]2.0.CO;2.

He, Guixiang; Liu, Xiaolong; Xu, Yang; Liang, Jian; Deng, Yuewen; Zhang, Yuehuan; Zhao, Liqiang (2021): Repeated exposure to simulated marine heatwaves enhances the thermal tolerance in pearl oysters. In Aquatic toxicology (Amsterdam, Netherlands) 239, p. 105959. DOI: 10.1016/j.aquatox.2021.105959.

HELCOM (2009): Biodiversity in the Baltic Sea - An integrated thematic assessment on biodiversity and nature conservation in the Baltic Sea. In Balt. Sea Environ. Proc. 116B.

HELCOM (2013): Climate Change in the Baltic Sea Area: A HELMCOM thematic assessment in 2013. In Balt. Sea Environ. Proc. 37.

Hobday, Alistair J.; Alexander, Lisa V.; Perkins, Sarah E.; Smale, Dan A.; Straub, Sandra C.; Oliver, Eric C.J. et al. (2016): A hierarchical approach to defining marine heatwaves. In Progress in Oceanography 141, pp. 227–238. DOI: 10.1016/j.pocean.2015.12.014.

Hobday, Alistair; Oliver, Eric; Sen Gupta, Alex; Benthuysen, Jessica; Burrows, Michael; Donat, Markus et al. (2018): Categorizing and Naming Marine Heatwaves. In Oceanog 31 (2). DOI: 10.5670/oceanog.2018.205.

Hoegh-Guldberg, Ove (1999): Climate change, coral bleaching and the future of the world's coral reefs. In Mar. Freshwater Res. DOI: 10.1071/MF99078.

Holbrook, Neil J.; Scannell, Hillary A.; Sen Gupta, Alexander; Benthuysen, Jessica A.; Feng, Ming; Oliver, Eric C. J. et al. (2019): A global assessment of marine heatwaves and their drivers. In Nature communications 10 (1), p. 2624. DOI: 10.1038/s41467-019-10206-z.

Hughes, Brent B.; Lummis, Sarah C.; Anderson, Sean C.; Kroeker, Kristy J. (2018): Unexpected resilience of a seagrass system exposed to global stressors. In Glob Change Biol 24 (1), pp. 224–234. DOI: 10.1111/gcb.13854.

Hughes, Lesley (2003): Climate change and Australia. Trends, projections and impacts. In Austral Ecology 28 (4), pp. 423–443. DOI: 10.1046/j.1442-9993.2003.01300.x.

Hughes, Terry P.; Kerry, James T.; Connolly, Sean R.; Baird, Andrew H.; Eakin, C. Mark; Heron, Scott F. et al. (2019): Ecological memory modifies the cumulative impact of recurrent climate extremes. In Nature Clim Change 9 (1), pp. 40–43. DOI: 10.1038/s41558-018-0351-2.

Hurell, James; National Center for Atmospheric Research Staff (2020): The Climate Data Guide: Hurell North Atlantic Oscillation (NAO) Index (station based). Available online at https://climatedataguide.ucar.edu/climate-data/hurrell-north-atlantic-oscillation-nao-index-station-based, updated on 4/24/2020, checked on 7/23/2021.

IPCC (2019): Summary for Policymakers. In H. O. Pörtner, D. C. Roberts, V. Masson-Delmotte, P. Zhai, M. Tignor, E. Poloczanska et al. (Eds.): IPCC Special Report on the Ocean and Cryosphere in a Changing Climate. In press.

IPCC (2021): Climate Change 2021: The Physical Science Basis. In V. Masson-Delmotte, P. Zhai, A. Pirani, S. L. Connors, C. Péan, S. Berger et al. (Eds.): Contribution of Working Group I to the Sixth Assessment Report of the Intergovernmental Panel on Climate Change. In press.

Jackson, Michelle C.; Pawar, Samraat; Woodward, Guy (2021): The Temporal Dynamics of Multiple Stressor Effects. From Individuals to Ecosystems. In Trends in Ecology & Evolution 36 (5), pp. 402–410. DOI: 10.1016/j.tree.2021.01.005.

Karstensen, J.; Liblik, T.; Fischer, J.; Bumke, K.; Krahmann, G. (2014): Summer upwelling at the Boknis Eck time-series station (1982 to 2012) – a combined glider and wind data analysis. In Biogeosciences 11 (13), pp. 3603–3617. DOI: 10.5194/bg-11-3603-2014.

Kautsky, Lena; Kautsky, Nils (2000): The Baltic Sea, including Bothnian Sea and Bothnian Bay. In Charles R. C. Sheppard (Ed.): Seas at the Millenium: An environmental Evaluation. Regional Chapters: Europe, The Amicas and West Africa: Pergamon (1).

Kayanne, Hajime (2017): Validation of degree heating weeks as a coral bleaching index in the northwestern Pacific. In Coral Reefs 36 (1), pp. 63–70. DOI: 10.1007/s00338-016-1524-y.

Lämke, Jörn; Brzezinka, Krzysztof; Altmann, Simone; Bäurle, Isabel (2016): A hit-and-run heat shock factor governs sustained histone methylation and transcriptional stress memory. In The EMBO journal 35 (2), pp. 162–175. DOI: 10.15252/embj.201592593.

Largier, John L. (2020): Upwelling Bays. How Coastal Upwelling Controls Circulation, Habitat, and Productivity in Bays. In Annual review of marine science 12, pp. 415–447. DOI: 10.1146/annurev-marine-010419-011020.

Leach, Terence S.; BuyanUrt, Buyanzaya; Hofmann, Gretchen E. (2021): Exploring impacts of marine heatwaves. Paternal heat exposure diminishes fertilization success in the purple sea urchin (Strongylocentrotus purpuratus). In Mar Biol 168 (7), p. 8. DOI: 10.1007/s00227-021-03915-x.

Lee, Kun-Seop; Park, Sang Rul; Kim, Jung-Bae (2005): Production dynamics of the eelgrass, Zostera marina in two bay systems on the south coast of the Korean peninsula. In Mar Biol 147 (5), pp. 1091–1108. DOI: 10.1007/s00227-005-0011-8.

Lehmann, A.; Getzlaff, K.; Harlaß, J. (2011): Detailed assessment of climate variability in the Baltic Sea area for the period 1958 to 2009. In Clim. Res. 46 (2), pp. 185–196. DOI: 10.3354/cr00876.

Lehmann, Andreas; Myrberg, Kai (2008): Upwelling in the Baltic Sea — A review. In Journal of Marine Systems 74, S3-S12. DOI: 10.1016/j.jmarsys.2008.02.010.

Lehmann, Andreas; Myrberg, Kai; Höflich, Katharina (2012): A statistical approach to coastal upwelling in the Baltic Sea based on the analysis of satellite data for 1990–2009. In Oceanologia 54 (3), pp. 369–393. DOI: 10.5697/oc.54-3.369.

Lennartz, S. T.; Lehmann, A.; Herrford, J.; Malien, F.; Hansen, H.-P.; Biester, H.; Bange, H. W. (2014): Long-term trends at the Boknis Eck time series station (Baltic Sea), 1957–2013. Does climate change counteract the decline in eutrophication? In Biogeosciences 11 (22), pp. 6323–6339. DOI: 10.5194/bg-11-6323-2014.

Leung, Jonathan Y. S.; Connell, Sean D.; Russell, Bayden D. (2017): Heatwaves diminish the survival of a subtidal gastropod through reduction in energy budget and depletion of energy reserves. In Scientific reports 7 (1), p. 17688. DOI: 10.1038/s41598-017-16341-1.

Leung, Jonathan Y.S.; Russell, Bayden D.; Connell, Sean D. (2019): Adaptive Responses of Marine Gastropods to Heatwaves. In One Earth 1 (3), pp. 374–381. DOI: 10.1016/j.oneear.2019.10.025.

Levin, L. A. (2003): Oxygen minimum zone benthos: Adaptation and community response to hypoxia. In Oceanography and Marine Biologie 41, pp. 1–45.

Lourenço, Carla R.; Zardi, Gerardo I.; McQuaid, Christopher D.; Serrão, Ester A.; Pearson, Gareth A.; Jacinto, Rita; Nicastro, Katy R. (2016): Upwelling areas as climate change refugia for the distribution and genetic diversity of a marine macroalga. In J. Biogeogr. 43 (8), pp. 1595–1607. DOI: 10.1111/jbi.12744.

Magel, Jennifer M. T.; Dimoff, Sean A.; Baum, Julia K. (2020): Direct and indirect effects of climate change-amplified pulse heat stress events on coral reef fish communities. In Ecological applications : a publication of the Ecological Society of America 30 (6), e02124. DOI: 10.1002/eap.2124.

McBryan, Tara L.; Healy, Timothy M.; Haakons, Kristen L.; Schulte, Patricia M. (2016): Warm acclimation improves hypoxia tolerance in Fundulus heteroclitus. In The Journal of experimental biology 219 (Pt 4), pp. 474–484. DOI: 10.1242/jeb.133413.

Meehl, Gerald A.; Tebaldi, Claudia (2004): More intense, more frequent, and longer lasting heat waves in the 21st century. In Science (New York, N.Y.) 305 (5686), pp. 994–997. DOI: 10.1126/science.1098704.

Melzner, Frank; Buchholz, Björn; Wolf, Fabian; Panknin, Ulrike; Wall, Marlene (2020): Ocean winter warming induced starvation of predator and prey. In Proceedings. Biological sciences 287 (1931), p. 20200970. DOI: 10.1098/rspb.2020.0970.

Melzner, Frank; Thomsen, Jörn; Koeve, Wolfgang; Oschlies, Andreas; Gutowska, Magdalena A.; Bange, Hermann W. et al. (2013): Future ocean acidification will be amplified by hypoxia in coastal habitats. In Mar Biol 160 (8), pp. 1875–1888. DOI: 10.1007/s00227-012-1954-1.

Miyoshi, Koji; Kuwahara, Yasuhiro; Miyashita, Kazushi (2018): Tracking the Northern Pacific sea star Asterias amurensis with acoustic transmitters in the scallop mariculture field of Hokkaido, Japan. In Fish Sci 84 (2), pp. 349–355. DOI: 10.1007/s12562-017-1162-5.

Morikawa, Megan K.; Palumbi, Stephen R. (2019): Using naturally occurring climate resilient corals to construct bleaching-resistant nurseries. In Proceedings of the National Academy of Sciences of the United States of America 116 (21), pp. 10586–10591. DOI: 10.1073/pnas.1721415116.

Muehlstein, L. K.; Porter, D.; Short, F. T. (1988): Labyrinthula sp., a marine slime mold producing the symptoms of wasting disease in eelgrass, Zostera marina. In Mar Biol 99 (4), pp. 465–472. DOI: 10.1007/BF00392553.

Munné-Bosch, Sergi; Alegre, Leonor (2013): Cross-stress tolerance and stress “memory” in plants. An integrated view. In Environmental and Experimental Botany 94, pp. 1–2. DOI: 10.1016/j.envexpbot.2013.02.002.

Murray, Ciarán J.; Müller-Karulis, Bärbel; Carstensen, Jacob; Conley, Daniel J.; Gustafsson, Bo G.; Andersen, Jesper H. (2019): Past, Present and Future Eutrophication Status of the Baltic Sea. In Front. Mar. Sci. 6, p. 137. DOI: 10.3389/fmars.2019.00002.

Nerem, Robert Steven; Leuliette, Éric; Cazenave, Anny (2006): Present-day sea-level change. A review. In Comptes Rendus Geoscience 338 (14-15), pp. 1077–1083. DOI: 10.1016/j.crte.2006.09.001.

Nguyen, Hung Manh; Kim, Mikael; Ralph, Peter J.; Marín-Guirao, Lázaro; Pernice, Mathieu; Procaccini, Gabriele (2020): Stress Memory in Seagrasses. First Insight Into the Effects of Thermal Priming and the Role of Epigenetic Modifications. In Frontiers in plant science 11, p. 494. DOI: 10.3389/fpls.2020.00494.

NOAA Climate: Climate Change: Atmospheric Carbon Dioxide. Available online at https://www.climate.gov/news-features/understanding-climate/climate-change-atmospheric-carbon-dioxide.

Norling, P.; Kautsky, N. (2007): Structural and functional effects of Mytilus edulis on diversity of associated species and ecosystem functioning. In Mar. Ecol. Prog. Ser. 351, pp. 163–175. DOI: 10.3354/meps07033.

Nour, Ola (2020): The non-native crab Hemigrapsus takanoi in the south-western Baltic Sea: Population structure and sensitivity to salinity and temperature shifts. Doctoral Thesis. Christian-Albrechts Universität zu Kiel, Kiel.

Nour, Ola; Stumpp, Meike; Morón Lugo, Sonia C.; Barboza, Francisco R.; Pansch, Christian (2020): Population structure of the recent invader Hemigrapsus takanoi and prey size selection on Baltic Sea mussels. In AI 15 (2), pp. 297–317. DOI: 10.3391/ai.2020.15.2.06.

Ogle, Kiona; Barber, Jarrett J.; Barron-Gafford, Greg A.; Bentley, Lisa Patrick; Young, Jessica M.; Huxman, Travis E. et al. (2015): Quantifying ecological memory in plant and ecosystem processes. In Ecology letters 18 (3), pp. 221–235. DOI: 10.1111/ele.12399.

Olesen, B.; Sand-Jensen, K. (1993): Seasonal acclimatization of eelgrass Zostera marina growth to light. In Mar. Ecol. Prog. Ser. 94, pp. 91–99. DOI: 10.3354/meps094091.

Olesen, B.; Sand-Jensen, K. (1994): Patch dynamics of eelgrass Zostera marina. In Mar. Ecol. Prog. Ser. 106, pp. 147–156. DOI: 10.3354/meps106147.

Oliver, Eric C. J. (2019): Mean warming not variability drives marine heatwave trends. In Clim Dyn 53 (3-4), pp. 1653–1659. DOI: 10.1007/s00382-019-04707-2.

Oliver, Eric C. J.; Benthuysen, Jessica A.; Darmaraki, Sofia; Donat, Markus G.; Hobday, Alistair J.; Holbrook, Neil J. et al. (2021): Marine Heatwaves. In Annual review of marine science 13, pp. 313–342. DOI: 10.1146/annurev-marine-032720-095144.

Oliver, Eric C. J.; Burrows, Michael T.; Donat, Markus G.; Sen Gupta, Alex; Alexander, Lisa V.; Perkins-Kirkpatrick, Sarah E. et al. (2019): Projected Marine Heatwaves in the 21st Century and the Potential for Ecological Impact. In Front. Mar. Sci. 6, p. 891. DOI: 10.3389/fmars.2019.00734.

Oliver, Eric C. J.; Donat, Markus G.; Burrows, Michael T.; Moore, Pippa J.; Smale, Dan A.; Alexander, Lisa V. et al. (2018): Longer and more frequent marine heatwaves over the past century. In Nature communications 9 (1), p. 1324. DOI: 10.1038/s41467-018-03732-9.

Paaijmans, Krijn P.; Heinig, Rebecca L.; Seliga, Rebecca A.; Blanford, Justine I.; Blanford, Simon; Murdock, Courtney C.; Thomas, Matthew B. (2013): Temperature variation makes ectotherms more sensitive to climate change. In Glob Change Biol 19 (8), pp. 2373–2380. DOI: 10.1111/gcb.12240.

Pansch, Christian; Hiebenthal, Claas (2019): A new mesocosm system to study the effects of environmental variability on marine species and communities. In Limnol. Oceanogr. Methods 28, p. 16. DOI: 10.1002/lom3.10306.

Pansch, Christian; Scotti, Marco; Barboza, Francisco R.; Al-Janabi, Balsam; Brakel, Janina; Briski, Elizabeta et al. (2018a): Heat waves and their significance for a temperate benthic community. A near-natural experimental approach. In Glob Change Biol. DOI: 10.1111/gcb.14282.

Pansch, Christian; Scotti, Marco; Nevoigt, Frauke; Hecht, Ute; Bumke, Karl (2018b): Daily mean water temperatures between January 2000 and December 2014 in 1.5 m water depths of the GEOMAR pier. PANGAEA.

Pazzaglia, Jessica; Badalamenti, Fabio; Bernardeau-Esteller, Jaime; Ruiz, Juan M.; Giacalone, Vincenzo Maximiliano; Procaccini, Gabriele; Marín-Guirao, Lazaro (2022): Thermo-priming increases heat-stress tolerance in seedlings of the Mediterranean seagrass P. oceanica. In Marine pollution bulletin 174, p. 113164. DOI: 10.1016/j.marpolbul.2021.113164.

Pazzaglia, Jessica; Nguyen, Hung Manh; Santillán-Sarmiento, Alex; Ruocco, Miriam; Dattolo, Emanuela; Marín-Guirao, Lázaro; Procaccini, Gabriele (2021): The Genetic Component of Seagrass Restoration. What We Know and the Way Forwards. In Water 13 (6), p. 829. DOI: 10.3390/w13060829.

Pedersen, O.; BIinzer, T.; Borum, J. (2004): Sulphide intrusion in eelgrass (Zostera marina L.). In Plant, cell & environment 27 (5), pp. 595–602. DOI: 10.1111/j.1365-3040.2004.01173.x.

Pillay, D.; Branch, G. M.; Griffiths, C. L.; Williams, C.; Prinsloo, A. (2010): Ecosystem change in a South African marine reserve (1960–2009). Role of seagrass loss and anthropogenic disturbance. In Mar. Ecol. Prog. Ser. 415, pp. 35–48. DOI: 10.3354/meps08733.

Poloczanska, Elvira S.; Brown, Christopher J.; Sydeman, William J.; Kiessling, Wolfgang; Schoeman, David S.; Moore, Pippa J. et al. (2013): Global imprint of climate change on marine life. In Nature Clim Change 3 (10), pp. 919–925. DOI: 10.1038/NCLIMATE1958.

Raateoja, M.; Kuosa, H.; Flinkman, J.; Pääkkönen, J.-P.; Perttilä, M. (2010): Late summer metalimnetic oxygen minimum zone in the northern Baltic Sea. In Journal of Marine Systems 80 (1-2), pp. 1–7. DOI: 10.1016/j.jmarsys.2009.06.005.

Randall, Carly J.; Toth, Lauren T.; Leichter, James J.; Maté, Juan L.; Aronson, Richard B. (2020): Upwelling buffers climate change impacts on coral reefs of the eastern tropical Pacific. In Ecology 101 (2), e02918. DOI: 10.1002/ecy.2918.

Rasmusson, Lina M.; Buapet, Pimchanok; George, Rushingisha; Gullström, Martin; Gunnarsson, Pontus C. B.; Björk, Mats; Norkko, Joanna (2020): Effects of temperature and hypoxia on respiration, photorespiration, and photosynthesis of seagrass leaves from contrasting temperature regimes. In ICES Journal of Marine Science 77 (6), pp. 2056–2065. DOI: 10.1093/icesjms/fsaa093.

Reed, B. J.; Hovel, K. A. (2006): Seagrass habitat disturbance. How loss and fragmentation of eelgrass Zostera marina influences epifaunal abundance and diversity. In Mar. Ecol. Prog. Ser. 326, pp. 133–143. DOI: 10.3354/meps326133.

Reusch, Thorsten B. H.; Boström, Christoffer; Stam, Wytze T.; Olsen, Jeanine (1999a): An ancient eelgrass clone in the Baltic. In Marine Ecology Progress Series 183, pp. 301–304.

Reusch, Thorsten B. H.; Chapman, Anthony R. O. (1997): Persistence and Space Occupancy by Subtidal Blue Mussel Patches. In Ecological Monographs 67 (1), p. 65. DOI: 10.2307/2963505.

Reusch, Thorsten B. H.; Dierking, Jan; Andersson, Helen C.; Bonsdorff, Erik; Carstensen, Jacob; Casini, Michele et al. (2018): The Baltic Sea as a time machine for the future coastal ocean. In Science advances 4 (5), eaar8195. DOI: 10.1126/sciadv.aar8195.

Reusch, Thorsten B. H.; Ehlers, Anneli; Hämmerli, August; Worm, Boris (2005): Ecosystem recovery after climatic extremes enhanced by genotypic diversity. In Proceedings of the National Academy of Sciences of the United States of America 102 (8), pp. 2826–2831. DOI: 10.1073/pnas.0500008102.

Reusch, Thorsten B. H.; Schubert, Philipp R.; Marten, Silke-Mareike; Gill, Diana; Karez, Rolf; Busch, Kathrin; Hentschel, Ute (2021): Lower Vibrio spp. abundances in Zostera marina leaf canopies suggest a novel ecosystem function for temperate seagrass beds. In Mar Biol 168 (10), p. 1937. DOI: 10.1007/s00227-021-03963-3.

Reusch, Thorsten B. H.; Stam, W. T.; Olsen, J. L. (1999b): Size and estimated age of genets in eelgrass, Zostera marina, assessed with microsatellite markers. In Mar Biol 133 (3), pp. 519–525. DOI: 10.1007/s002270050492.

Richardson, Katherine; Heilmann, J. P. (2012): Primary production in the Kattegat. Past and present. In Ophelia 41 (1), pp. 317–328. DOI: 10.1080/00785236.1995.10422050.

Robertson, A. I.; Mann, K. H. (1984): Disturbance by ice and life-history adaptations of the seagrassZostera marina. In Mar Biol 80 (2), pp. 131–141. DOI: 10.1007/BF02180180.

Ruckelshaus, Mary H. (1996): ESTIMATION OF GENETIC NEIGHBORHOOD PARAMETERS FROM POLLEN AND SEED DISPERSAL IN THE MARINE ANGIOSPERM ZOSTERA MARINA L. In Evolution; international journal of organic evolution 50 (2), pp. 856–864. DOI: 10.1111/j.1558-5646.1996.tb03894.x.

Ruel, Jonathan J.; Ayres, Matthew P. (1999): Jensen’s inequality predicts effects of environmental variation. In Trends in Ecology & Evolution 14 (9), pp. 361–366. DOI: 10.1016/S0169-5347(99)01664-X.

Rugiu, Luca; Manninen, Iita; Rothäusler, Eva; Jormalainen, Veijo (2018): Tolerance and potential for adaptation of a Baltic Sea rockweed under predicted climate change conditions. In Marine environmental research 134, pp. 76–84. DOI: 10.1016/j.marenvres.2017.12.016.

Sadchatheeswaran, Saachi; Branch, George M.; Robinson, Tamara B. (2015): Changes in habitat complexity resulting from sequential invasions of a rocky shore. Implications for community structure. In Biol Invasions 17 (6), pp. 1799–1816. DOI: 10.1007/s10530-014-0837-4.

Saha, Mahasweta; Barboza, Francisco R.; Somerfield, Paul J.; Al-Janabi, Balsam; Beck, Miriam; Brakel, Janina et al. (2020): Response of foundation macrophytes to near-natural simulated marine heatwaves. In Glob Change Biol 26 (2), pp. 417–430. DOI: 10.1111/gcb.14801.

Sampaio, E.; Rodil, I. F.; Vaz-Pinto, F.; Fernández, A.; Arenas, F. (2017): Interaction strength between different grazers and macroalgae mediated by ocean acidification over warming gradients. In Marine environmental research 125, pp. 25–33. DOI: 10.1016/j.marenvres.2017.01.001.

Sawall, Yvonne; Ito, Maysa; Pansch, Christian (2021): Chronically elevated sea surface temperatures revealed high susceptibility of the eelgrass Zostera marina to winter and spring warming. In Limnol. Oceanogr. 66 (12), pp. 4112–4124. DOI: 10.1002/lno.11947.

Schlegel, Robert W. (2020): Marine Heatwave Tracker. Available online at http://www.marineheatwaves.org/tracker.

Schlegel, Robert W.; Darmaraki, Sofia; Benthuysen, Jessica A.; Filbee-Dexter, Karen; Oliver, Eric C.J. (2021): Marine cold-spells. In Progress in Oceanography 198 (6), p. 102684. DOI: 10.1016/j.pocean.2021.102684.

Schoen, Alexandra N.; Bouyoucos, Ian A.; Anderson, W. Gary; Wheaton, Catharine J.; Planes, Serge; Mylniczenko, Natalie D.; Rummer, Jodie L. (2021): Simulated heatwave and fishing stressors alter corticosteroid and energy balance in neonate blacktip reef sharks, Carcharhinus melanopterus. In Conservation Physiology 9 (1), coab067. DOI: 10.1093/conphys/coab067.

SealifeBase: Asterias rubens (Linnaeus, 1758). Available online at https://www.sealifebase.se/summary/Asterias-rubens.html.

Sen Gupta, Alex; Thomsen, Mads; Benthuysen, Jessica A.; Hobday, Alistair J.; Oliver, Eric; Alexander, Lisa V. et al. (2020): Drivers and impacts of the most extreme marine heatwaves events. In Scientific reports 10 (1), p. 19359. DOI: 10.1038/s41598-020-75445-3.

Seuront, Laurent; Nicastro, Katy R.; Zardi, Gerardo I.; Goberville, Eric (2019): Decreased thermal tolerance under recurrent heat stress conditions explains summer mass mortality of the blue mussel Mytilus edulis. In Scientific reports 9 (1), p. 17498. DOI: 10.1038/s41598-019-53580-w.

Shama, Lisa N. S. (2017): The mean and variance of climate change in the oceans. Hidden evolutionary potential under stochastic environmental variability in marine sticklebacks. In Scientific reports 7 (1), p. 8889. DOI: 10.1038/s41598-017-07140-9.

Smale, Dan A.; Wernberg, Thomas; Oliver, Eric C. J.; Thomsen, Mads; Harvey, Ben P.; Straub, Sandra C. et al. (2019): Marine heatwaves threaten global biodiversity and the provision of ecosystem services. In Nature Clim Change 9, p. 360. DOI: 10.1038/s41558-019-0412-1.

Somero, George N. (2020): The cellular stress response and temperature. Function, regulation, and evolution. In Journal of experimental zoology. Part A, Ecological and integrative physiology 333 (6), pp. 379–397. DOI: 10.1002/jez.2344.

Sørensen, Jesper Givskov; Kristensen, Torsten Nygaard; Loeschcke, Volker (2003): The evolutionary and ecological role of heat shock proteins. In Ecology letters 6 (11), pp. 1025–1037. DOI: 10.1046/j.1461-0248.2003.00528.x.

Spillman, Claire M.; Smith, Grant A.; Hobday, Alistair J.; Hartog, Jason R. (2021): Onset and Decline Rates of Marine Heatwaves. Global Trends, Seasonal Forecasts and Marine Management. In Front. Clim. 3, p. 411. DOI: 10.3389/fclim.2021.801217.

Stillman, Jonathon H. (2019): Heat Waves, the New Normal. Summertime Temperature Extremes Will Impact Animals, Ecosystems, and Human Communities. In Physiology (Bethesda, Md.) 34 (2), pp. 86–100. DOI: 10.1152/physiol.00040.2018.

Sumoski, S. E.; Orth, R. J. (2012): Biotic dispersal in eelgrass Zostera marina. In Mar. Ecol. Prog. Ser. 471, pp. 1–10. DOI: 10.3354/meps10145.

Tabassum, Tahira; Farooq, Muhammad; Ahmad, Riaz; Zohaib, Ali; Wahid, Abdul (2017): Seed priming and transgenerational drought memory improves tolerance against salt stress in bread wheat. In Plant physiology and biochemistry : PPB 118, pp. 362–369. DOI: 10.1016/j.plaphy.2017.07.007.

Tait, Leigh W.; Thoral, François; Pinkerton, Matthew H.; Thomsen, Mads S.; Schiel, David R. (2021): Loss of Giant Kelp, Macrocystis pyrifera, Driven by Marine Heatwaves and Exacerbated by Poor Water Clarity in New Zealand. In Front. Mar. Sci. 8, p. 499. DOI: 10.3389/fmars.2021.721087.

Takolander, Antti; Cabeza, Mar; Leskinen, Elina (2017): Climate change can cause complex responses in Baltic Sea macroalgae. A systematic review. In Journal of Sea Research 123, pp. 16–29. DOI: 10.1016/j.seares.2017.03.007.

Thompson, Ross M.; Beardall, John; Beringer, Jason; Grace, Mike; Sardina, Paula (2013): Means and extremes. Building variability into community-level climate change experiments. In Ecology letters 16 (6), pp. 799–806. DOI: 10.1111/ele.12095.

Thomsen, Mads S.; Mondardini, Luca; Alestra, Tommaso; Gerrity, Shawn; Tait, Leigh; South, Paul M. et al. (2019): Local Extinction of Bull Kelp (Durvillaea spp.) Due to a Marine Heatwave. In Front. Mar. Sci. 6, p. 3126. DOI: 10.3389/fmars.2019.00084.

Thomson, Jordan A.; Burkholder, Derek A.; Heithaus, Michael R.; Fourqurean, James W.; Fraser, Matthew W.; Statton, John; Kendrick, Gary A. (2015): Extreme temperatures, foundation species, and abrupt ecosystem change. An example from an iconic seagrass ecosystem. In Glob Change Biol 21 (4), pp. 1463–1474. DOI: 10.1111/gcb.12694.

Todgham, Anne E.; Schulte, Patricia M.; Iwama, George K. (2005): Cross-tolerance in the tidepool sculpin. The role of heat shock proteins. In Physiological and biochemical zoology : PBZ 78 (2), pp. 133–144. DOI: 10.1086/425205.

Vajedsamiei, Jahangir; Melzner, Frank; Raatz, Michael; Kiko, Rainer; Khosravi, Maral; Pansch, Christian (2021a): Simultaneous recording of filtration and respiration in marine organisms in response to short-term environmental variability. In Limnol. Oceanogr. Methods 6, p. 341. DOI: 10.1002/lom3.10414.

Vajedsamiei, Jahangir; Wahl, Martin; Schmidt, Andrea Lee; Yazdanpanahan, Maryam; Pansch, Christian (2021b): The Higher the Needs, the Lower the Tolerance. Extreme Events May Select Ectotherm Recruits With Lower Metabolic Demand and Heat Sensitivity. In Front. Mar. Sci. 8, p. 672. DOI: 10.3389/fmars.2021.660427.

Vaquer-Sunyer, Raquel; Duarte, Carlos M. (2008): Thresholds of hypoxia for marine biodiversity. In Proceedings of the National Academy of Sciences of the United States of America 105 (40), pp. 15452–15457. DOI: 10.1073/pnas.0803833105.

Vasseur, David A.; DeLong, John P.; Gilbert, Benjamin; Greig, Hamish S.; Harley, Christopher D. G.; McCann, Kevin S. et al. (2014): Increased temperature variation poses a greater risk to species than climate warming. In Proceedings. Biological sciences 281 (1779), p. 20132612. DOI: 10.1098/rspb.2013.2612.

Vevers, H. G. (1949): The Biology of Asterias Rubens L. Growth And Reproduction. In J. Mar. Biol. Ass. 28 (1), pp. 165–187. DOI: 10.1017/S0025315400055272.

Vichkovitten, Tritep; Holmer, Marianne; Frederiksen, Morten S. (2007): Spatial and temporal changes in non-structural carbohydrate reserves in eelgrass (Zostera marina L.) in Danish coastal waters. In botm 50 (2), pp. 75–87. DOI: 10.1515/BOT.2007.009.

Vinther, Hanne Fogh; Laursen, Jens Sund; Holmer, Marianne (2008): Negative effects of blue mussel (Mytilus edulis) presence in eelgrass (Zostera marina) beds in Flensborg fjord, Denmark. In Estuarine, Coastal and Shelf Science 77 (1), pp. 91–103. DOI: 10.1016/j.ecss.2007.09.007.

Wahl, Martin; Barboza, Francisco R.; Buchholz, Björn; Dobretsov, Sergey; Guy-Haim, Tamar; Rilov, Gil et al. (2021): Pulsed pressure. Fluctuating impacts of multifactorial environmental change on a temperate macroalgal community. In Limnol. Oceanogr. 33, p. 477. DOI: 10.1002/lno.11954.

Wahl, Martin; Buchholz, Björn; Winde, Vera; Golomb, Dar; Guy-Haim, Tamar; Müller, Jens et al. (2015): A mesocosm concept for the simulation of near-natural shallow underwater climates. The Kiel Outdoor Benthocosms (KOB). In Limnol. Oceanogr. Methods 13 (11), pp. 651–663. DOI: 10.1002/lom3.10055.

Wahl, Martin; Saderne, Vincent; Sawall, Yvonne (2016): How good are we at assessing the impact of ocean acidification in coastal systems? Limitations, omissions and strengths of commonly used experimental approaches with special emphasis on the neglected role of fluctuations. In Mar. Freshwater Res. 67 (1), p. 25. DOI: 10.1071/MF14154.

Wahl, Martin; Werner, Franziska Julie; Buchholz, Björn; Raddatz, Stefanie; Graiff, Angelika; Matthiessen, Birte et al. (2020): Season affects strength and direction of the interactive impacts of ocean warming and biotic stress in a coastal seaweed ecosystem. In Limnol. Oceanogr. 65 (4), pp. 807–827. DOI: 10.1002/lno.11350.

Walter, Julia; Jentsch, Anke; Beierkuhnlein, Carl; Kreyling, Juergen (2013): Ecological stress memory and cross stress tolerance in plants in the face of climate extremes. In Environmental and Experimental Botany 94, pp. 3–8. DOI: 10.1016/j.envexpbot.2012.02.009.

Walther, Gian-Reto; Post, Eric; Convey, Peter; Menzel, Annette; Parmesan, Camille; Beebee, Trevor J. C. et al. (2002): Ecological responses to recent climate change. In Nature 416 (6879), pp. 389–395. DOI: 10.1038/416389a.

Wernberg, Thomas; Bennett, Scott; Babcock, Russell C.; Bettignies, Thibaut de; Cure, Katherine; Depczynski, Martial et al. (2016): Climate-driven regime shift of a temperate marine ecosystem. In Science (New York, N.Y.) 353 (6295), pp. 169–172. DOI: 10.1126/science.aad8745.

Wernberg, Thomas; Smale, Dan A.; Frölicher, Thomas L.; Smith, A. J. P. (2021): ScienceBrief Review: Climate change increases marine heatwaves harming marine ecosystems. In Critical Issues in Climate Change.

Wikström, Sofia A.; Kautsky, Lena (2007): Structure and diversity of invertebrate communities in the presence and absence of canopy-forming Fucus vesiculosus in the Baltic Sea. In Estuarine, Coastal and Shelf Science 72 (1-2), pp. 168–176. DOI: 10.1016/j.ecss.2006.10.009.

Winters, G.; Nelle, P.; Fricke, B.; Rauch, G.; Reusch, T. B.H. (2011): Effects of a simulated heat wave on photophysiology and gene expression of high- and low-latitude populations of Zostera marina. In Mar. Ecol. Prog. Ser. 435, pp. 83–95. DOI: 10.3354/meps09213.

Wolf, Fabian (2022): Climatological analysis of 22-year temperature data on extreme events, Kiel Fjord (1997-2018). PANGAEA.

Wolf, Fabian; Bumke, Karl; Wahl, Sebastian; Nevoigt, Frauke; Hecht, Ute; Hiebenthal, Claas; Pansch, Christian (2020): High resolution water temperature data between January 1997 and December 2018 at the GEOMAR pier surface. PANGAEA. Available online at https://doi.org/10.1594/PANGAEA.919186.

Wolf, Fabian; Clemmesen, Catriona; Hiebenthal, Claas (2021): Continuous water temperature, salinity, oxygen and pH data in front of GEOMAR Pier, Kiel, Germany (2014-2019). PANGAEA. Available online at https://doi.org/10.1594/PANGAEA.930979.

Yamaguchi, Ryohei; Suga, Toshio (2019): Trend and Variability in Global Upper-Ocean Stratification Since the 1960s. In J. Geophys. Res. Oceans 124 (12), pp. 8933–8948. DOI: 10.1029/2019JC015439.

Zimmerman, R. C.; Hill, V. J.; Jinuntuya, M.; Celebi, B.; Ruble, D.; Smith, M. et al. (2017): Experimental impacts of climate warming and ocean carbonation on eelgrass Zostera marina. In Mar. Ecol. Prog. Ser. 566, pp. 1–15. DOI: 10.3354/meps12051.

# SUPPLEMENTARY MATERIAL

## Supplement to Chapter I

### *Supplementary Figures*

**Chapter I - Supplementary Figure 1:** Continuously logged treatment temperatures (°C) in *No* (**A**, grey), *Interrupted* (**B**, yellow-green), *Present-day* (**C**, orange) and *Extended* (**D**, red) heatwave treatments (see Chapter I - Figure 1 for treatment descriptions). Shown are means over the two tanks with the same applied treatment (hourly means). Dotted lines show the anticipated temperatures.

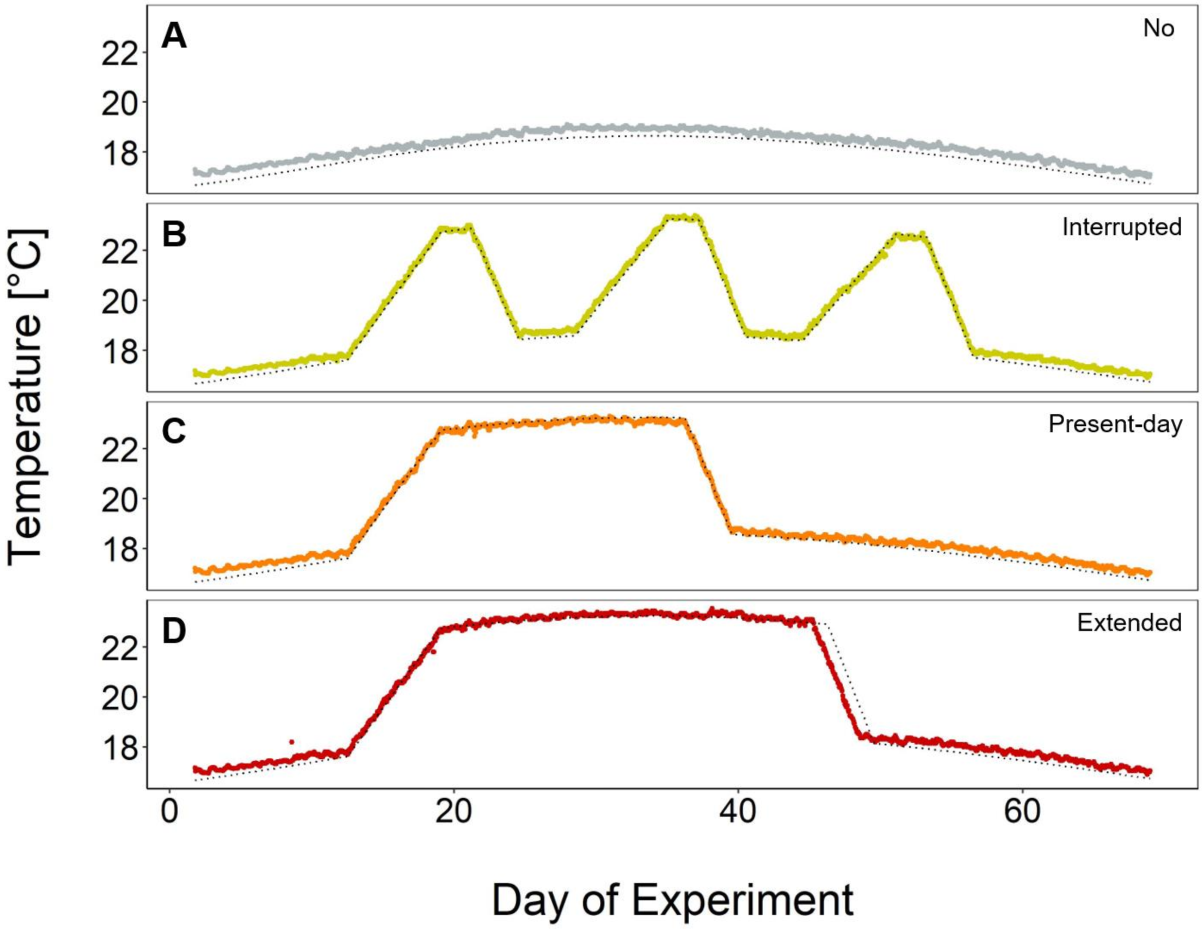

**Chapter I - Supplementary Figure 2:** Point measurements of temperature (°C, **A**), salinity (**B**), pH (**C**) and oxygen concentration (mg $L^{-1}$, **D**), in *No* (grey), *Interrupted* (yellow-green), *Present-day* (orange), and *Extended* (red) heatwave treatments (see Chapter I - Figure 1 for treatment descriptions). Shown are means and standard deviations for n=12 (*Present-day* and *Extended*) and for n=11 (*No* and *Interrupted*).

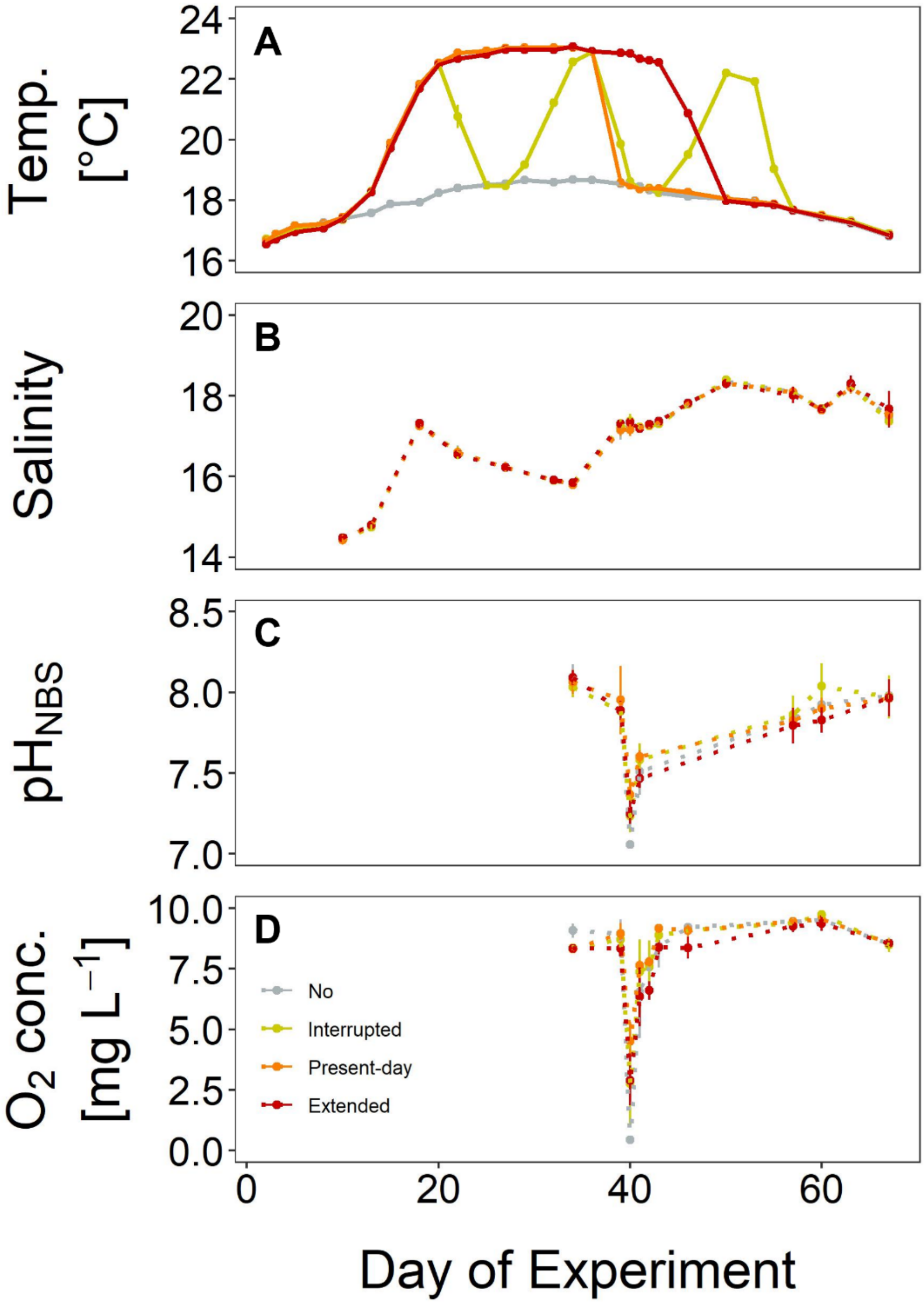

**Chapter I - Supplementary Figure 3:** Modelled yearly cold-spell frequency (**A**), duration (**B**), maximal intensity (**C**), cumulative intensity (**D**), onset (**E**) and decline rate (**F**) after Hobday et al. (2016), using published data (Wolf et al. 2020). Trends were modelled using Generalized Additive Models (GAMs). Shaded areas represent the 95% confidence intervals. Detailed statistic results are given in Chapter I - Supplementary Table 3.

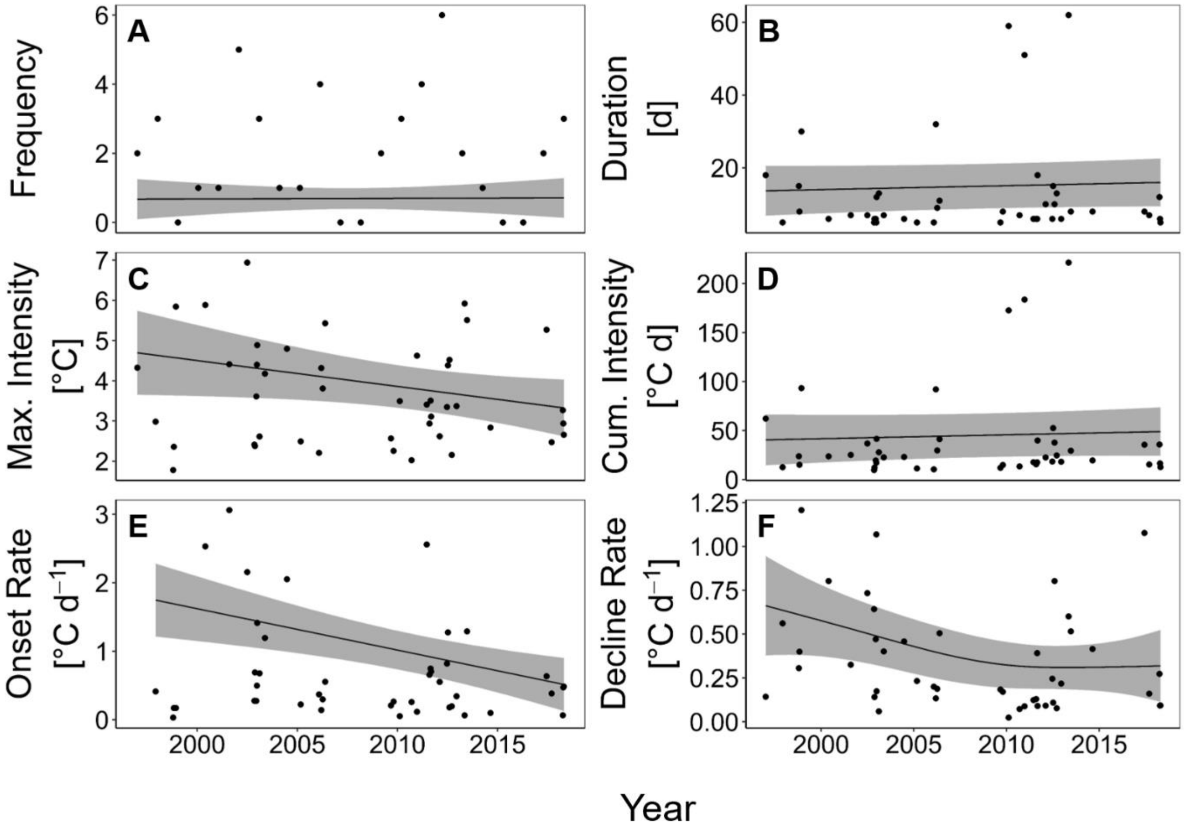

**Chapter I - Supplementary Figure 4:** Modelled yearly heatwave frequency (**A**), duration (**B**), maximal intensity (**C**), cumulative intensity (**D**), onset (**E**) and decline rate (**F**) after Hobday et al. (2016), using published data (Wolf et al. 2020). Trends were modelled using Generalized Additive Models (GAMs). Shaded areas represent 95% confidence intervals. Detailed statistical results are given in Chapter I - Supplementary Table 4.

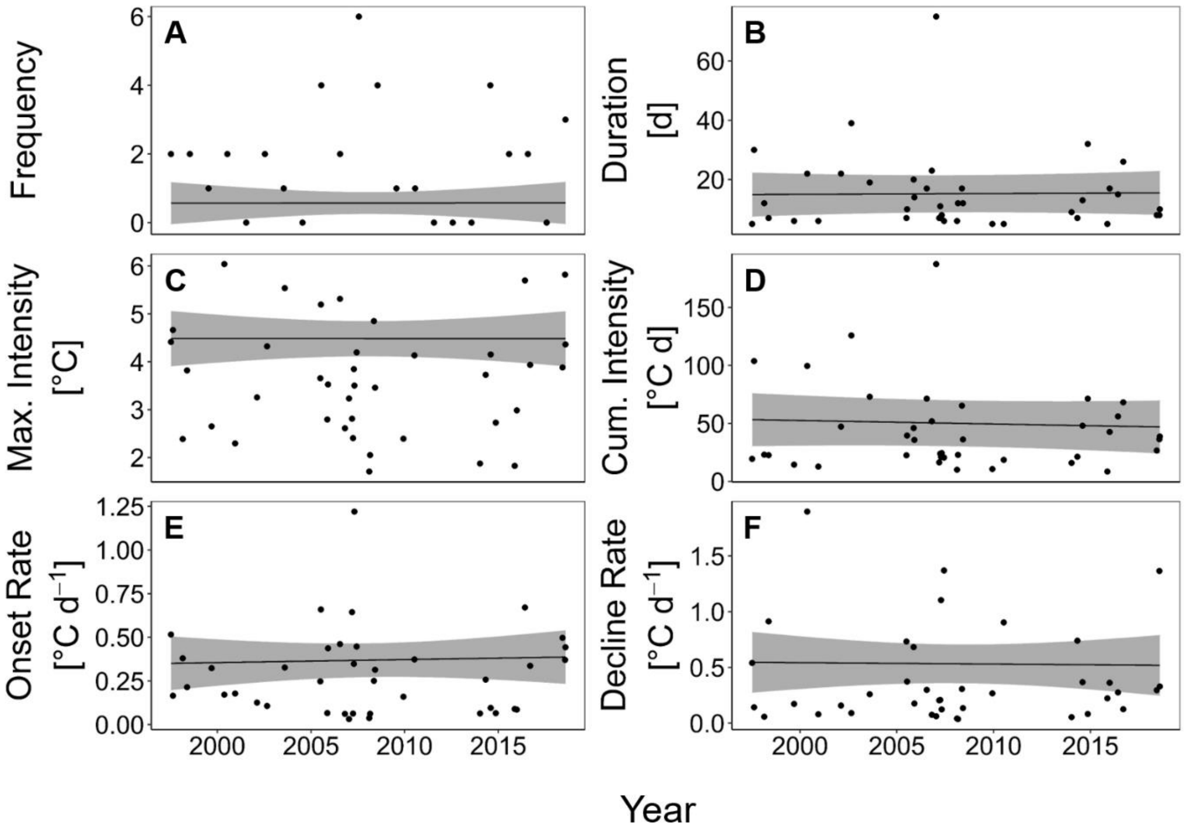

**Chapter I - Supplementary Figure 5:** Deviations from annual mean seawater temperature from a 22-year mean (**A**; Wolf et al. 2020) and cold-spell durations in different months over the 22-year record (**B**). Colors in A represent cold (light grey) or warm years (dark grey) and in **B** the intensity of the cold-spells (i.e. maximal amplitude below the climatological value).

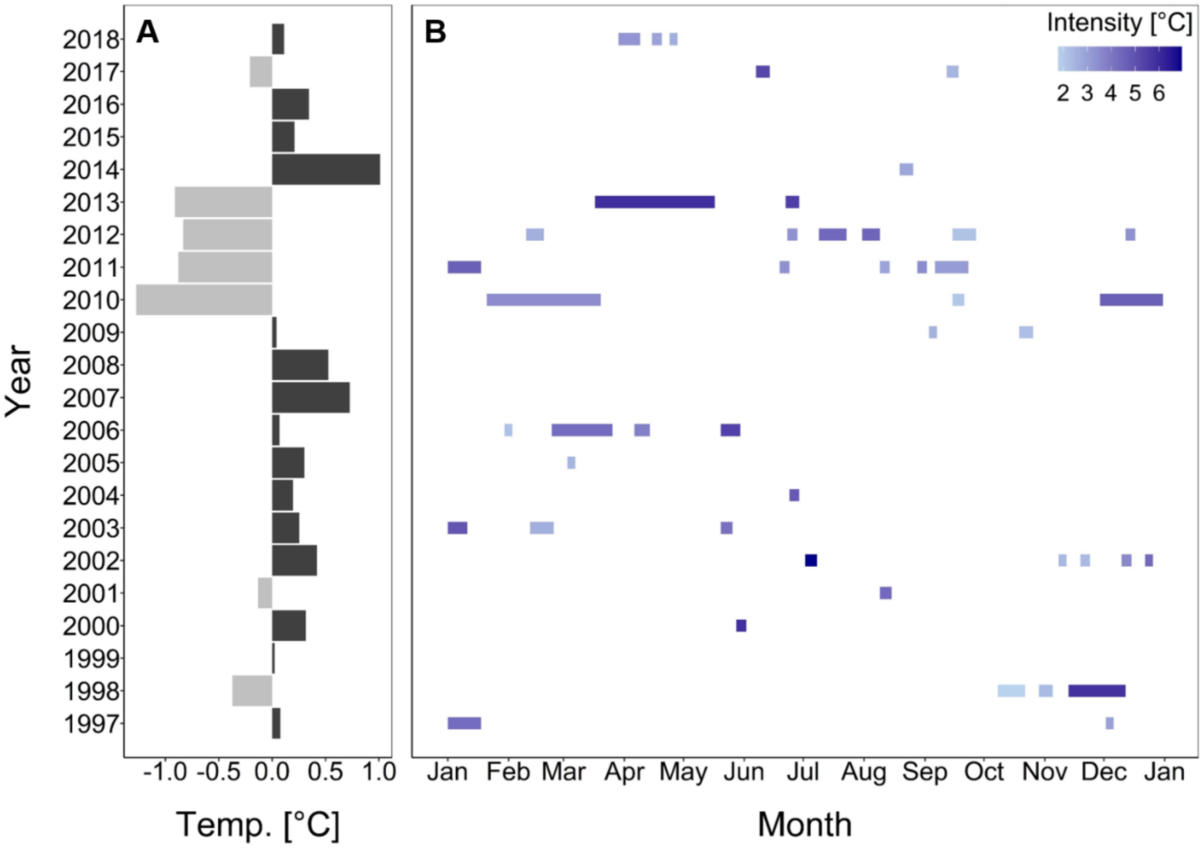

**Chapter I - Supplementary Figure 6:** Differences between the Generalized Additive Mixed-effect Models (GAMM) of different treatments (**A-F**) for feeding rate (mg mussel dry weight per day) of *Asterias rubens* during 68 days of incubation, under *No*, *Interrupted* (=Inter.), *Present-day* (=Pres.) and *Extended* (=Ext.) heatwave treatments (see Chapter I - Figure 1 for treatment descriptions). Data are represented as model (GAMM) differences (line) and as 95% confidence intervals (shaded areas) for n=12 (*Present-day* and *Extended*) and for n=11 (*No* and *Interrupted*). The red lines represent periods where the models differed.

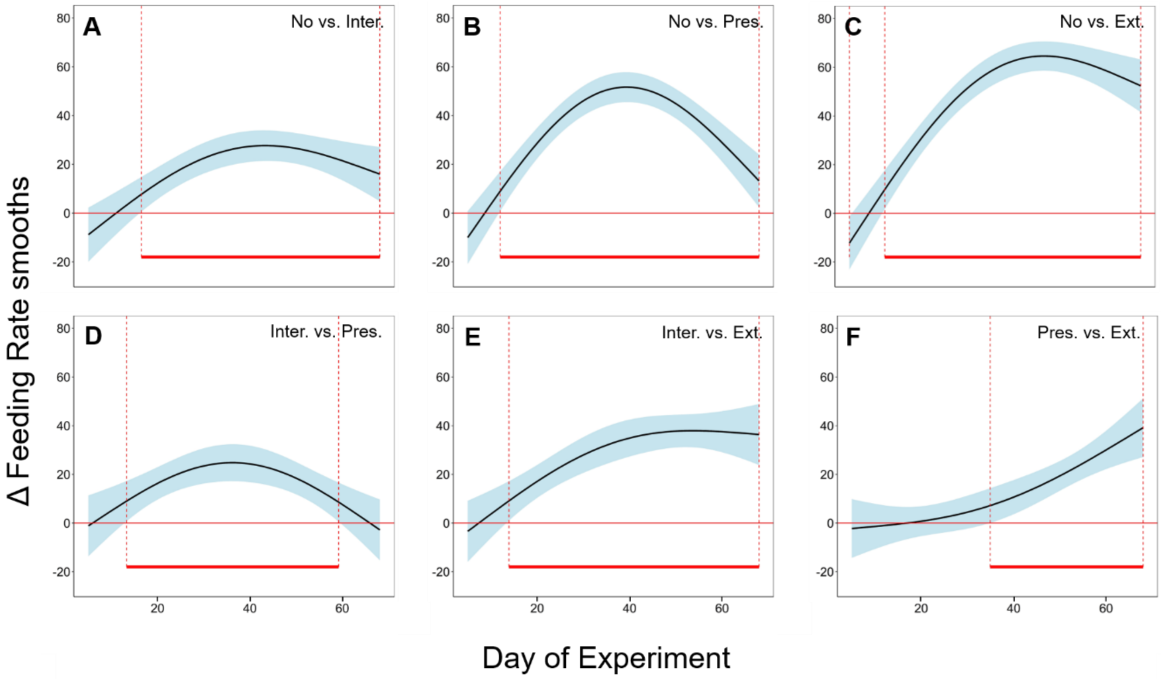

**Chapter I - Supplementary Figure 7:** Differences between the Generalized Additive Mixed-effect Models (GAMM) of different treatments (**A-F**) for righting time (min) of *Asterias rubens* during 68 days of incubation, under *No*, *Interrupted* (=Inter.), *Present-day* (=Pres.) and *Extended* (=Ext.) heatwave treatments (see Chapter I - Figure 1 for treatment descriptions). Data are represented as model (GAMM) differences (line) and as 95% confidence intervals (shaded areas) for n=12 (*Present-day* and *Extended*) and for n=11 (*No* and *Interrupted*). The red lines represent periods where the models differed.

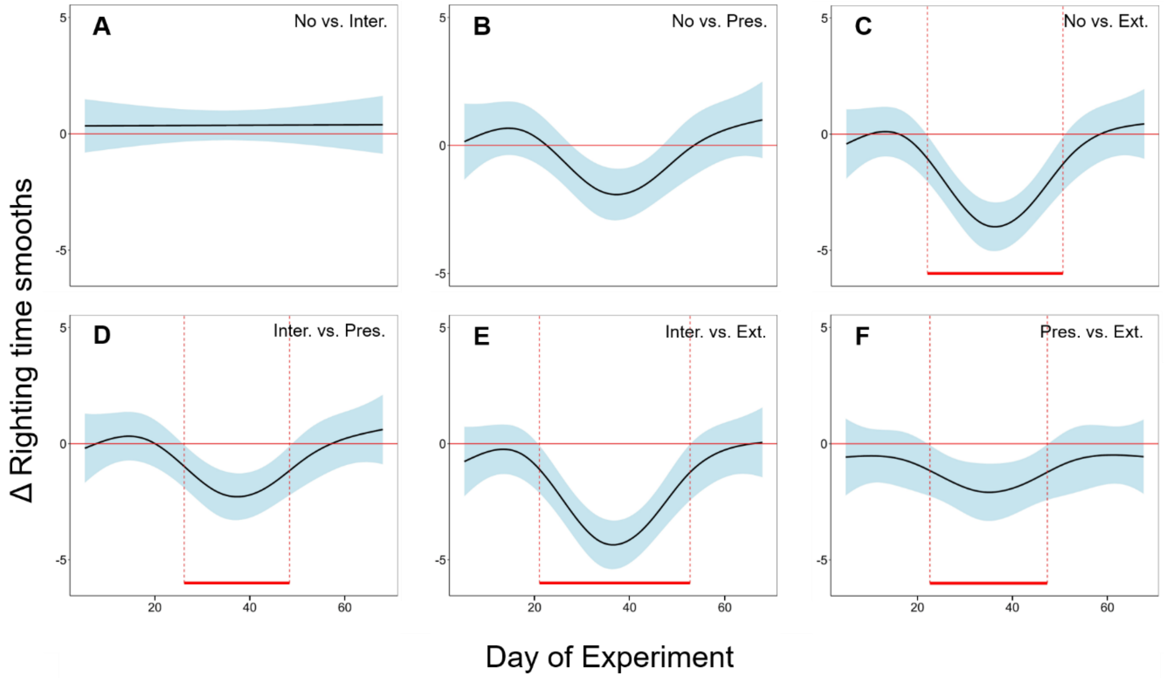

**Chapter I - Supplementary Figure 8:** Feeding rate of *Asterias rubens* over each three days (mg mussel dry weight per day) during 68 days of incubation under *No* (**A**), *Interrupted* (**B**), *Present-day* (**C**) and *Extended* (**D**) heatwave (MHW) treatments (see Chapter I - Figure 1 for treatment descriptions). Data are represented as means and 95% confidence intervals for n=12 (*Present-day* and *Extended*) and for n=11 (*No* and *Interrupted*). The different colors represent periods of applied heatwaves (orange = ramping to red = full treatment).

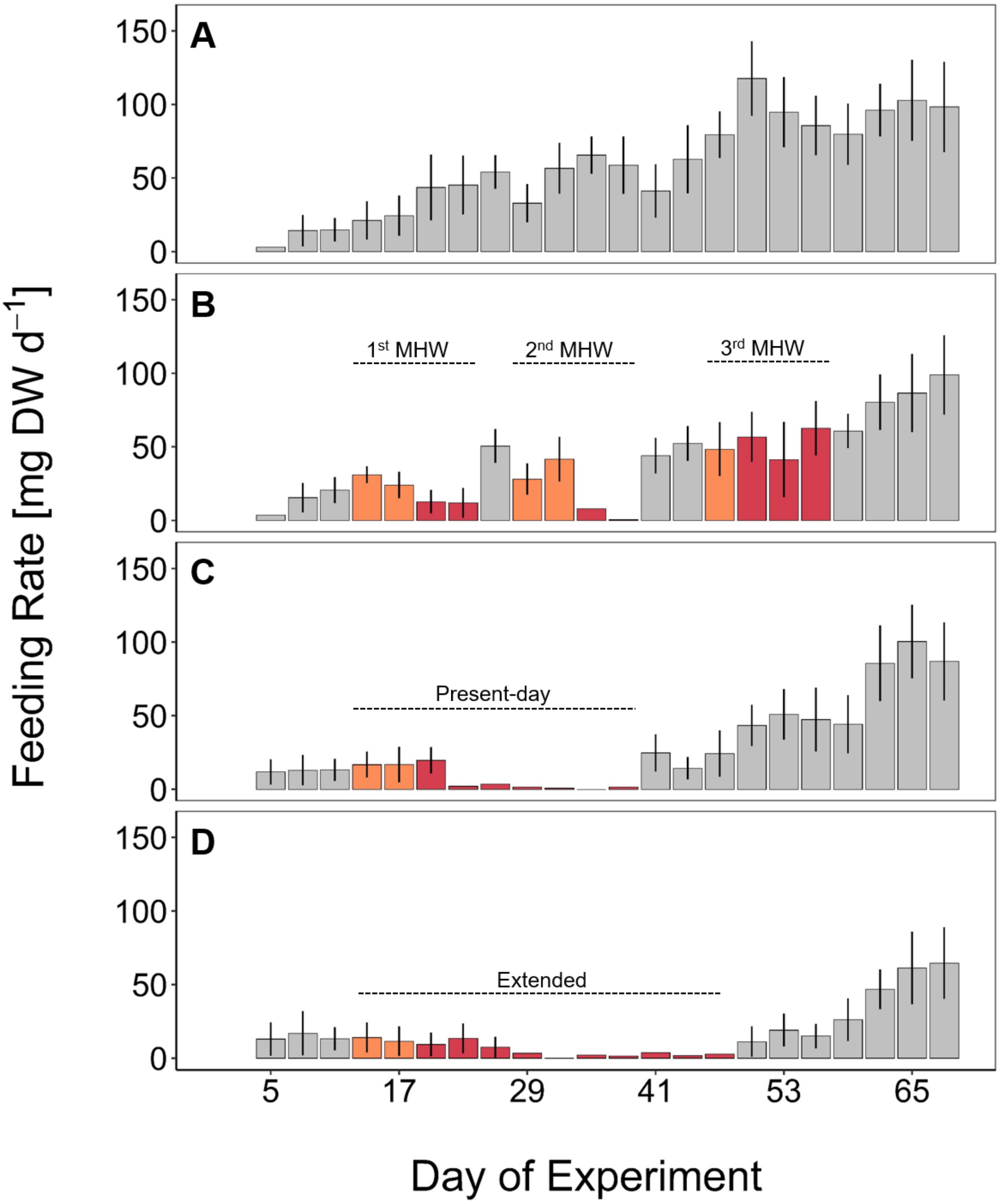

**Chapter I - Supplementary Figure 9:** Wet weight (g) of *Asterias rubens* during 68 days of incubation under *No* (**A**), *Interrupted* (**B**), *Present-day* (**C**) and *Extended* (**D**) heatwave (MHW) treatments (see Chapter I - Figure 1 for treatment descriptions). Data are represented as means and 95% confidence intervals for n=12 (*Present-day* and *Extended*) and for n=11 (*No* and *Interrupted*). Red bars represent measurements during heatwaves.

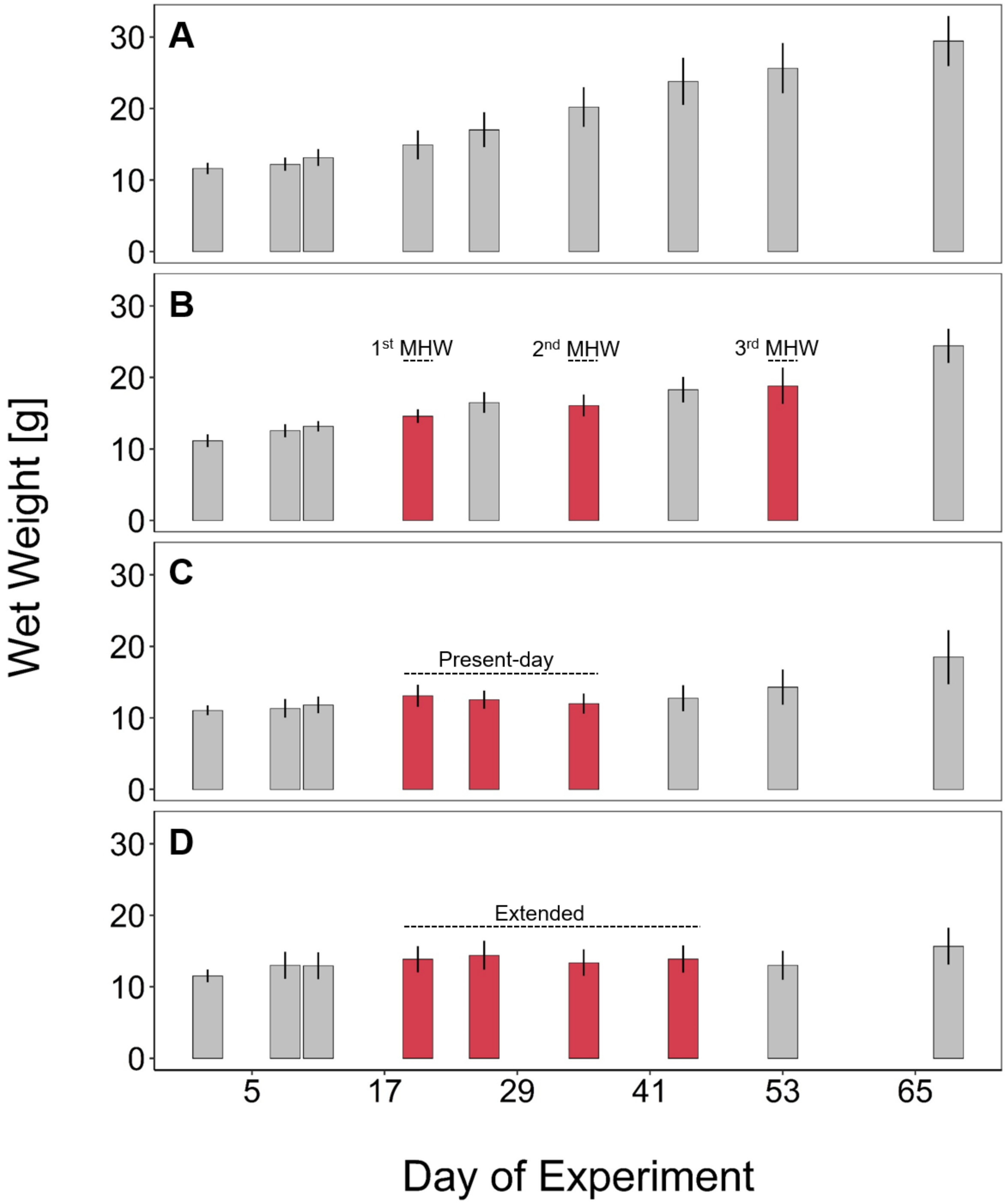

**Chapter I - Supplementary Figure 10:** Righting Time (minutes) of *Asterias rubens* during 68 days of incubation under *No* (**A**), *Interrupted* (**B**), *Present-day* (**C**) and *Extended* (**D**) heatwave (MHW) treatments (see Chapter I - Figure 1 for treatment descriptions). Data are represented as means and 95% confidence intervals for n=12 (*Present-day* and *Extended*) and for n=11 (*No* and *Interrupted*). Red bars represent measurements during heatwaves.

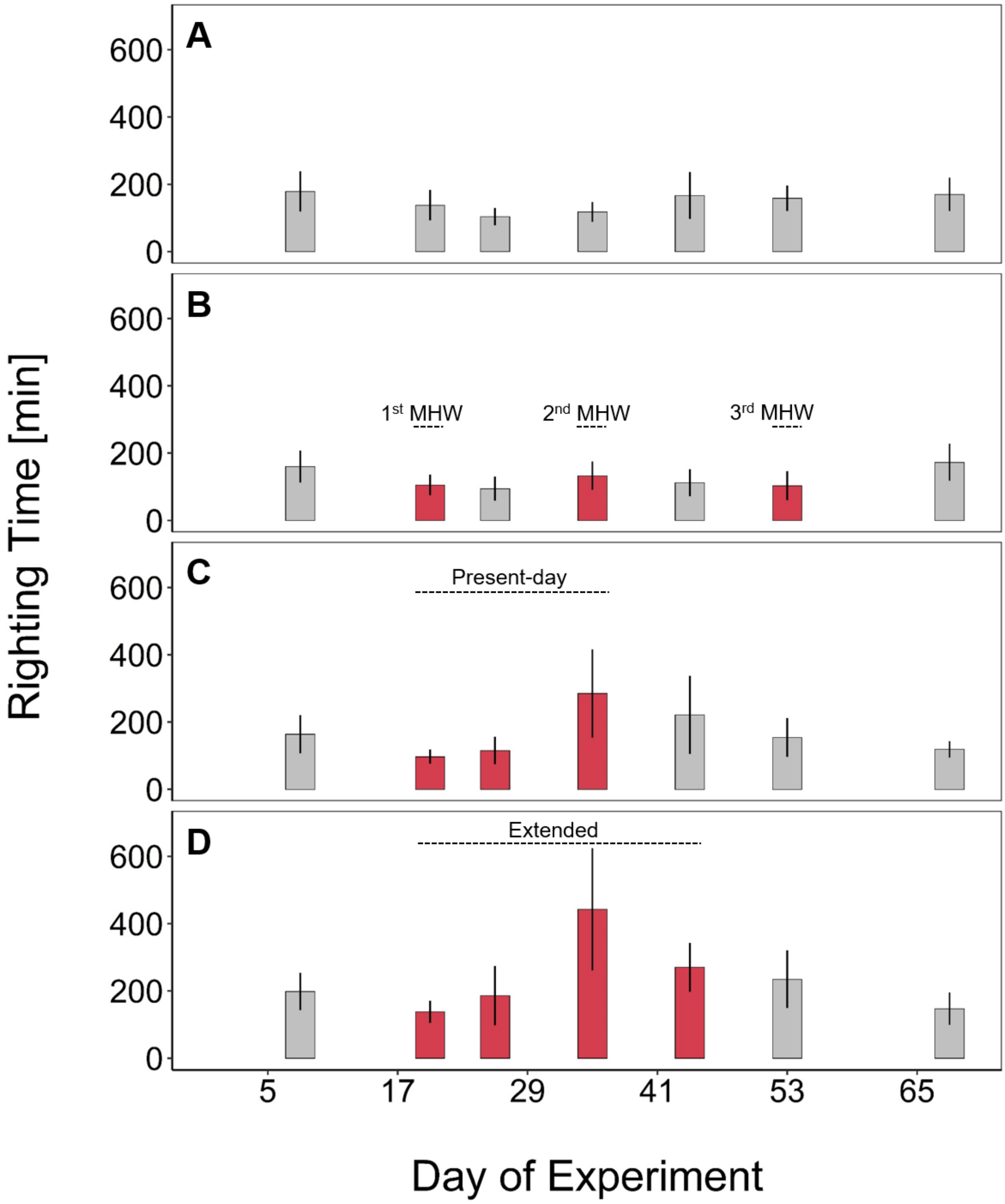

**Chapter I - Supplementary Figure 11:** Recorded Temperatures (°C; solid black lines) in 1.8 m depth in the Kiel Fjord, Germany at the GEOMAR pier (N54° 19' 45.97'' E10° 8' 58.582''; Wolf et al. 2020) of the years 1997 until 2018. This dataset was analyzed on the occurrences of heatwaves and cold spells after Hobday et al. (2016). Based on this modelling the 22-year climatological values are represented as grey solid line, whereas the thresholds for heatwaves (i.e., 90th percentile) and cold-spells (i.e., 10th percentile) are represented as dotted lines. Temperatures above the climatological values, but below the 90th percentile are shown in orange, whereas temperatures above the 90th percentile are shown in red. Temperatures below the climatological trend, but above the 10th percentile are shown in light-blue, whereas temperatures below the 10th percentile are shown in dark-blue.

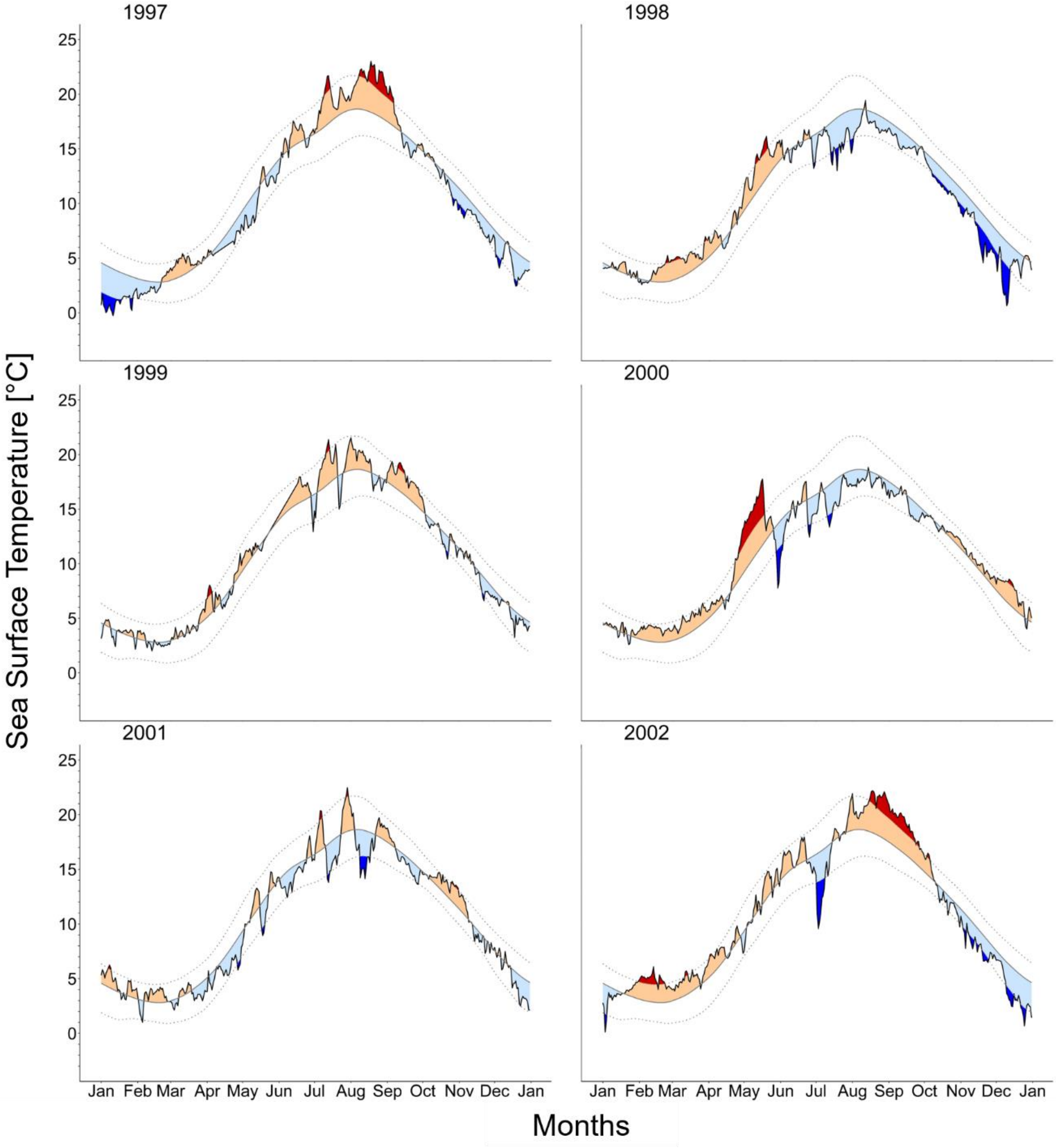

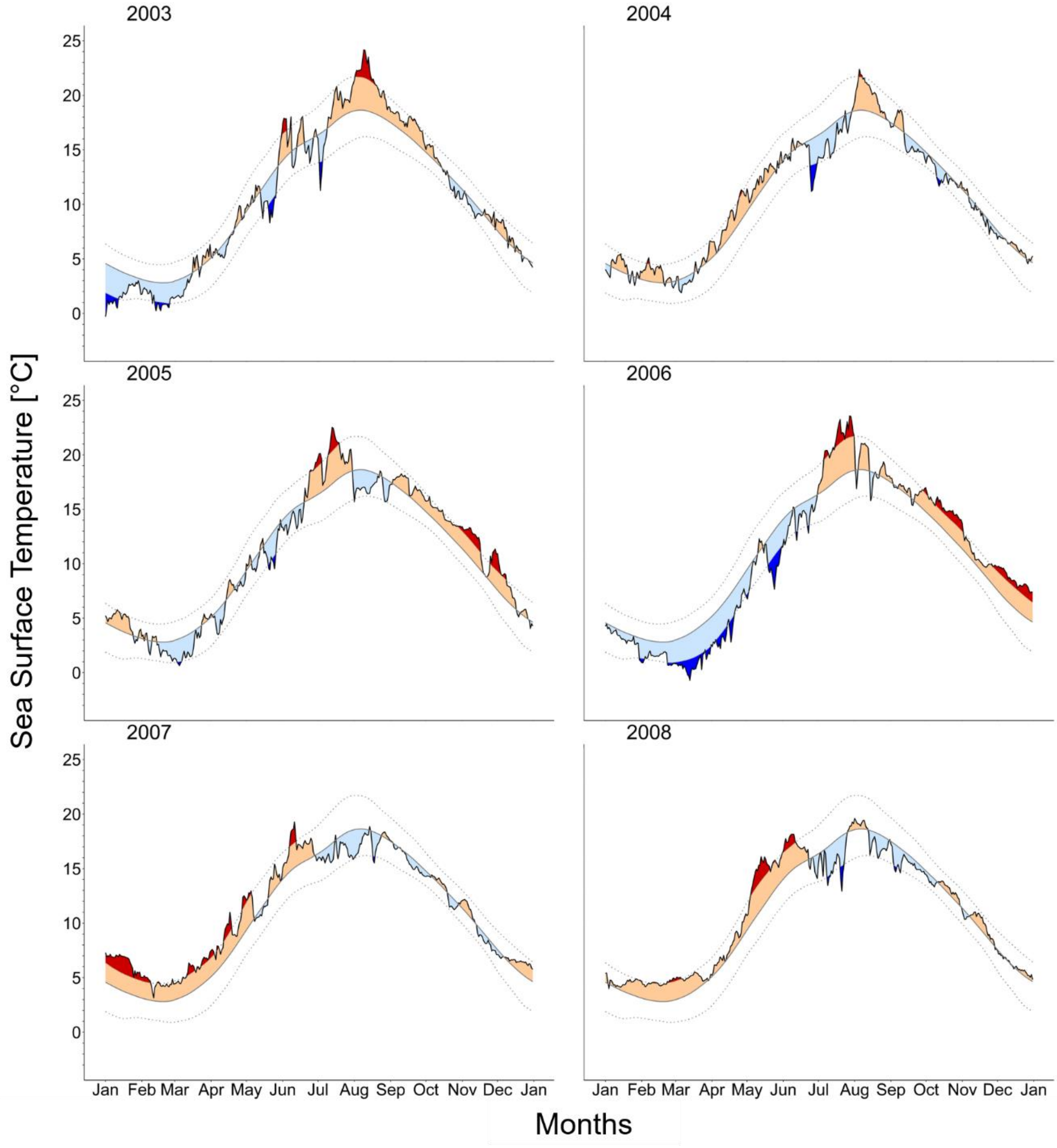
2003
2004
2005
2006
2007
2008
Sea Surface Temperature [°C]
0
5
10
15
20
25
Jan Feb Mar Apr May Jun Jul Aug Sep Oct Nov Dec Jan
Months

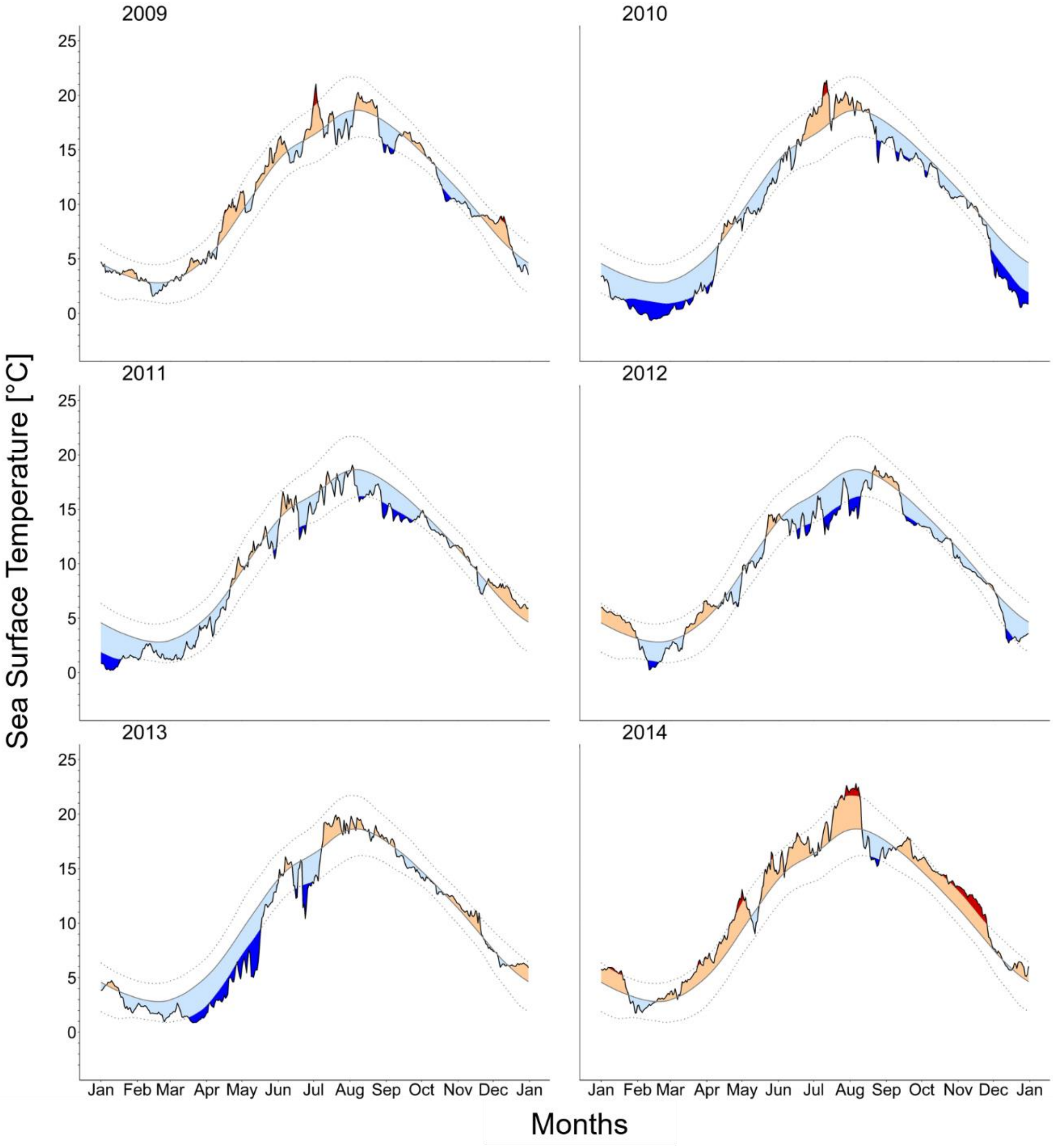
2009
2010
2011
2012
2013
2014
Sea Surface Temperature [°C]
25
20
15
10
5
0
Jan Feb Mar Apr May Jun Jul Aug Sep Oct Nov Dec Jan
Months

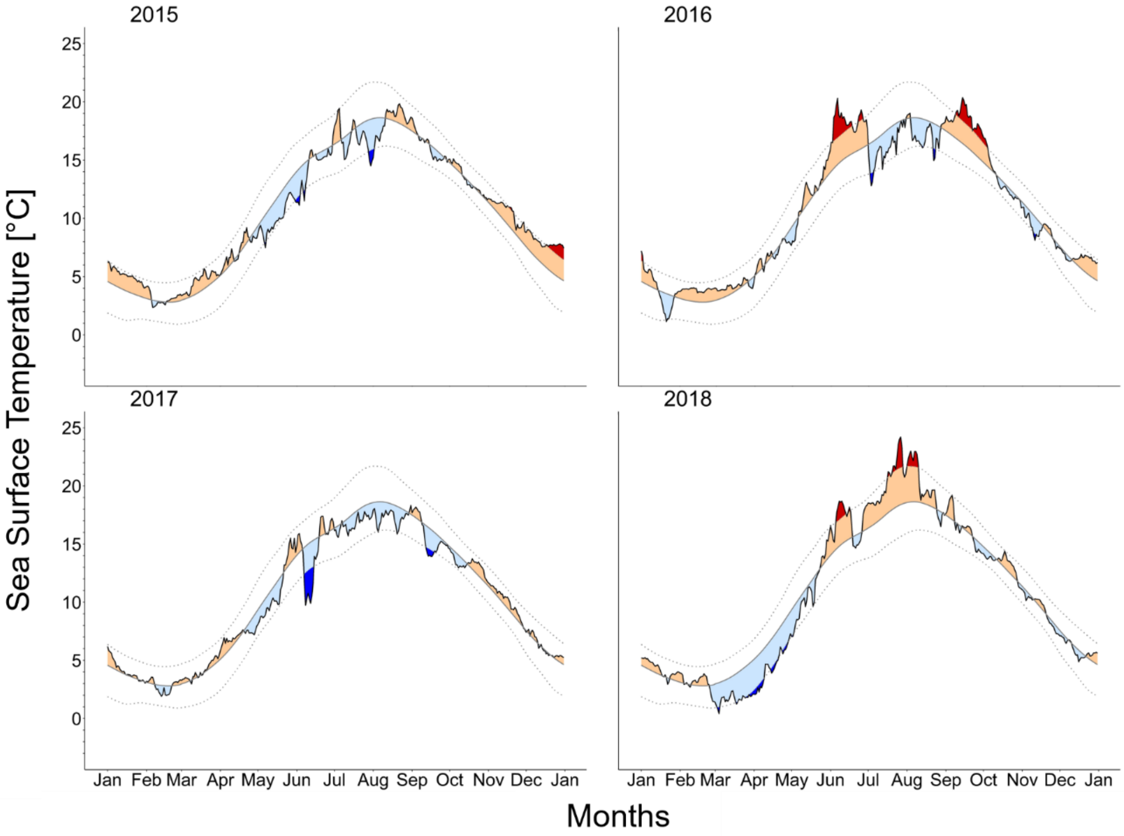
2015
2016
2017
2018
Sea Surface Temperature [°C]
25
20
15
10
5
0
Jan Feb Mar Apr May Jun Jul Aug Sep Oct Nov Dec Jan
Months

## *Supplementary Tables*

**Chapter I - Supplementary Table 1:** Heatwave characteristics (minimal, mean, and maximal values) modelled after Hobday et al. (2016) using published data (Wolf et al. 2020) separated after seasons or summarized over the year. Frequency represents the number of events per year or season, the duration represents the time of the events (days), intensity represents the amplitude above the climatological values (°C), onset rate represents the increase of temperature from the time crossing the 90th percentile until the maximum of the event (°C per day) and the decline rate represents the decrease of temperature from the maximum of the event until the time it crosses the 90th percentile (°C per day). For a detailed description of the traits see Figure 1 in Hobday et al. (2016). Bold numbers represent values used for creating the experimental heatwave treatments given in Chapter I - Figure 1.

| Heatwave trait | Trait parameter | Annual | Spring | Summer | Fall | Winter |
|---|---|---|---|---|---|---|
| Frequency | Minimal | 0 | 0 | 0 | 0 | 0 |
| | Mean | 1.8 | 0.4 | 0.7 | 0.3 | 0.4 |
| | Maximal | 6 | 4 | 3 | 2 | 2 |
| Duration | Minimal | 5 | 7 | **5** | 5 | 5 |
| | Mean | 14.9 | 10.8 | 13.6 | 18 | 18.2 |
| | Maximal | 75 | 22 | 39 | 32 | 75 |
| Intensity | Minimal | 1.7 | 2.4 | 3.5 | 1.8 | 1.7 |
| | Mean | 3.6 | 3.9 | **4.6** | 2.9 | 2.5 |
| | Maximal | 6 | 6 | 5.8 | 3.9 | 3.3 |
| Onset Rate | Minimal | 0 | 0.1 | 0.1 | 0.1 | 0 |
| | Mean | 0.3 | 0.4 | 0.4 | 0.2 | 0.1 |
| | Maximal | 1.2 | 1.2 | **0.7** | 0.4 | 0.4 |
| Decline Rate | Minimal | 0 | 0.1 | 0.1 | 0.1 | 0 |
| | Mean | 0.4 | 0.7 | 0.5 | 0.2 | 0.1 |
| | Maximal | 1.9 | 1.9 | **1.4** | 0.7 | 0.4 |

**Chapter I - Supplementary Table 2:** Cold-spell characteristics (minimal, mean, and maximal values) modelled after Hobday et al. (2016) using published data (Wolf et al. 2020) separated after seasons or summarized over the year. Frequency represents the number of events per year or season, the duration represents the time of the events (days), intensity represents the amplitude below the climatological values (°C), onset rate represents the decrease of temperature from the time crossing the 90th percentile until the maximum of the event (°C per day) and the decline rate represents the increase of temperature from the maximum of the event until the time it crosses the 90th percentile (°C per day).

| Trait | Trait Characteristic | Annual | Spring | Summer | Fall | Winter |
|---|---|---|---|---|---|---|
| Frequency | Minimal | 0 | 0 | 0 | 0 | 0 |
| | Mean | 2 | 0.5 | 0.5 | 0.5 | 0.5 |
| | Maximal | 6 | 3 | 3 | 2 | 2 |
| Duration | Minimal | 5 | 5 | **6** | 5 | 5 |
| | Mean | 12.7 | 15.5 | 7.8 | 9.2 | 18.3 |
| | Maximal | 62 | 62 | 15 | 18 | 59 |
| Intensity | Minimal | 1.8 | 2.5 | 2.8 | 1.8 | 2.2 |
| | Mean | 3.7 | 4.1 | **4.3** | 2.4 | 3.7 |
| | Maximal | 6.9 | 5.9 | 6.9 | 3.1 | 5.8 |
| Onset Rate | Minimal | 0 | 0.1 | 0.1 | 0 | 0.1 |
| | Mean | 0.7 | 0.6 | 1.3 | 0.3 | 0.4 |
| | Maximal | 3.1 | 2.5 | **3.1** | 0.7 | 1.4 |
| Decline Rate | Minimal | 0 | 0.1 | 0.1 | 0.1 | 0 |
| | Mean | 0.3 | 0.3 | 0.4 | 0.2 | 0.4 |
| | Maximal | 1.2 | 0.8 | **1.1** | 0.6 | 1.2 |

**Chapter I - Supplementary Table 3:** Generalized Additive Model (GAM) results for cold-spell frequency, duration, maximal intensity, cumulative intensity, onset rate and decline rate. The GAM for frequency, duration, maximal intensity, cumulative intensity, onset rate and decline rate had an explained deviance of 0.0%, -3.2%, 23.2%, -2.6%, 36.3% and 34.5%, respectively.

| **GAM Frequency** | | | | |
|---|---|---|---|---|
| ***Parametric Coefficients*** | ***Estimate*** | ***Std. Error*** | ***t-value*** | ***p-value*** |
| Intercept | 0.693 | 0.151 | 4.597 | **<0.001** |
| ***Smooth Terms*** | ***Estimated d.f.*** | ***Reference d.f.*** | ***F-value*** | ***p-value*** |
| s (Year) | 1.000 | 1.000 | 0.005 | 0.943 |
| **GAM Duration** | | | | |
| ***Parametric Coefficients*** | ***Estimate*** | ***Std. Error*** | ***t-value*** | ***p-value*** |
| Intercept | 14.909 | 3.112 | 4.792 | **<0.001** |
| ***Smooth Terms*** | ***Estimated d.f.*** | ***Reference d.f.*** | ***F-value*** | ***p-value*** |
| s (Peak Date) | 1.000 | 1.000 | 0.718 | 0.402 |
| s (Month) | 1.000 | 1.000 | 0.504 | 0.482 |
| **GAM Maximal Intensity** | | | | |
| ***Parametric Coefficients*** | ***Estimate*** | ***Std. Error*** | ***t-value*** | ***p-value*** |
| Intercept | 3.664 | 0.176 | 20.870 | **<0.001** |
| ***Smooth Terms*** | ***Estimated d.f.*** | ***Reference d.f.*** | ***F-value*** | ***p-value*** |
| s (Peak Date) | 1.000 | 1.000 | 3.861 | 0.057 |
| s (Month) | 2.636 | 2.907 | 3.168 | **0.042** |
| **GAM Cumulative Intensity** | | | | |
| ***Parametric Coefficients*** | ***Estimate*** | ***Std. Error*** | ***t-value*** | ***p-value*** |
| Intercept | 44.909 | 11.282 | 3.981 | **<0.001** |
| ***Smooth Terms*** | ***Estimated d.f.*** | ***Reference d.f.*** | ***F-value*** | ***p-value*** |
| s (Peak Date) | 1.000 | 1.000 | 0.473 | 0.496 |
| s (Month) | 1.000 | 1.000 | 0.393 | 0.535 |
| **GAM Onset Rate** | | | | |
| ***Parametric Coefficients*** | ***Estimate*** | ***Std. Error*** | ***t-value*** | ***p-value*** |
| Intercept | 0.688 | 0.095 | 7.236 | **<0.001** |
| ***Smooth Terms*** | ***Estimated d.f.*** | ***Reference d.f.*** | ***F-value*** | ***p-value*** |
| s (Peak Date) | 1.000 | 1.000 | 11.359 | **0.002** |
| s (Month) | 2.474 | 2.810 | 6.283 | **0.002** |
| **GAM Decline Rate** | | | | |
| ***Parametric Coefficients*** | ***Estimate*** | ***Std. Error*** | ***t-value*** | ***p-value*** |
| Intercept | 0.345 | 0.038 | 8.994 | **<0.001** |
| ***Smooth Terms*** | ***Estimated d.f.*** | ***Reference d.f.*** | ***F-value*** | ***p-value*** |
| s (Peak Date) | 1.887 | 2.338 | 2.942 | 0.051 |
| s (Month) | 2.577 | 2.868 | 2.822 | **0.031** |

**Chapter I - Supplementary Table 4:** Generalized Additive Model (GAM) results for heatwave frequency, duration, maximal intensity, cumulative intensity, onset rate and decline rate. The GAM for frequency, duration, maximal intensity, cumulative intensity, onset rate and decline rate had an explained deviance of 0.0%, 2.7%, 57.2%, -0.4%, 24.1% and 28.3%, respectively.

| | | | | |
|---|---|---|---|---|
| **GAM Frequency** | | | | |
| ***Parametric Coefficients*** | ***Estimate*** | ***Std. Error*** | ***t-value*** | ***p-value*** |
| Intercept | 0.573 | 0.160 | 3.575 | **<0.001** |
| ***Smooth Terms*** | ***Estimated d.f.*** | ***Reference d.f.*** | ***F-value*** | ***p-value*** |
| s (Year) | 1.000 | 1.000 | 0.000 | 0.992 |
| **GAM Duration** | | | | |
| ***Parametric Coefficients*** | ***Estimate*** | ***Std. Error*** | ***t-value*** | ***p-value*** |
| Intercept | 16.327 | 3.041 | 5.369 | **<0.001** |
| ***Smooth Terms*** | ***Estimated d.f.*** | ***Reference d.f.*** | ***F-value*** | ***p-value*** |
| s (Peak Date) | 1.000 | 1.000 | 0.019 | 0.891 |
| s (Month) | 1.712 | 2.040 | 1.892 | 0.177 |
| **GAM Maximal Intensity** | | | | |
| ***Parametric Coefficients*** | ***Estimate*** | ***Std. Error*** | ***t-value*** | ***p-value*** |
| Intercept | 3.642 | 0.130 | 27.980 | **<0.001** |
| ***Smooth Terms*** | ***Estimated d.f.*** | ***Reference d.f.*** | ***F-value*** | ***p-value*** |
| s (Peak Date) | 1.000 | 1.001 | 0.000 | 0.999 |
| s (Month) | 2.689 | 2.924 | 14.939 | **<0.001** |
| **GAM Cumulative Intensity** | | | | |
| ***Parametric Coefficients*** | ***Estimate*** | ***Std. Error*** | ***t-value*** | ***p-value*** |
| Intercept | 47.875 | 9.720 | 4.925 | **<0.001** |
| ***Smooth Terms*** | ***Estimated d.f.*** | ***Reference d.f.*** | ***F-value*** | ***p-value*** |
| s (Peak Date) | 1.000 | 1.000 | 0.299 | 0.588 |
| s (Month) | 1.669 | 1.993 | 1.795 | 0.200 |
| **GAM Onset Rate** | | | | |
| ***Parametric Coefficients*** | ***Estimate*** | ***Std. Error*** | ***t-value*** | ***p-value*** |
| Intercept | 0.291 | 0.035 | 8.323 | **<0.001** |
| ***Smooth Terms*** | ***Estimated d.f.*** | ***Reference d.f.*** | ***F-value*** | ***p-value*** |
| s (Peak Date) | 1.000 | 1.000 | 0.087 | 0.770 |
| s (Month) | 2.381 | 2.722 | 4.103 | **0.040** |
| **GAM Decline Rate** | | | | |
| ***Parametric Coefficients*** | ***Estimate*** | ***Std. Error*** | ***t-value*** | ***p-value*** |
| Intercept | 0.401 | 0.062 | 6.495 | **<0.001** |
| ***Smooth Terms*** | ***Estimated d.f.*** | ***Reference d.f.*** | ***F-value*** | ***p-value*** |
| s (Peak Date) | 1.000 | 1.000 | 0.017 | 0.899 |
| s (Month) | 2.615 | 2.885 | 4.849 | **0.023** |

*Supplementary References*

Hobday, A. J., Alexander, L. V., Perkins, S. E., Smale, D. A., Straub, S. C., Oliver, E. C. J. et al. (2016). A hierarchical approach to defining marine heatwaves. Progress in Oceanography 141, pp. 227–238. doi: 10.1016/j.pocean.2015.12.014

Wolf, Fabian; Bumke, Karl; Wahl, Sebastian; Nevoigt, Frauke; Hecht, Ute; Hiebenthal, Claas; Pansch, Christian (2020): High resolution water temperature data between January 1997 and December 2018 at the GEOMAR pier surface. PANGAEA. Available online at https://doi.org/10.1594/PANGAEA.919186.

# Supplement to Chapter II

## *Supplementary Introduction*

### Worldwide Distribution of *Asterias rubens* and temperature limits

The starfish *Asterias rubens* inhabits the inter- and subtidal zones of the North Atlantic region (Budd 2008; Clark and Downey 1992; Vevers 1949). More specifically, *A. rubens* is distributed along the West Coast of the Atlantic Ocean from Washington, D.C. (United States) to Newfoundland (Canada) and along the East Coast of the Atlantic Ocean from Lisbon (Portugal) to Vestfjorden (Norway), as well as in the Baltic Sea until Rügen (Germany) (SealifeBase).

Overall, *A. rubens* experiences a natural temperature range from -0.4 °C until 24.1 °C (Schlegel 2020). Seawater temperatures below 2 °C or above 22 °C (F. Melzner, personal communication; Agüera et al. 2012) can be physiological thresholds for this species' performance (ceasing of feeding activity). Hence, these conditions can delimit suitable habitats for *A. rubens*.

### Acidification and oxygen limits

*A. rubens* may experience acidification and hypoxia, across its range in e.g., Chesapeake Bay, St. Lawrence Bay, Long Island Sound (Fennel and Testa 2019) or in the North and Baltic Seas (Diaz 2001). Dissolved oxygen below 4.6 mg $L^{-1}$ was shown to be the median lethal concentration of marine species (Vaquer-Sunyer and Duarte 2008). As *A. rubens* cannot regulate their ceolomic fluid pH, *A. rubens* is potentially susceptible to low pH. Indeed, *A. rubens* was shown to decrease feeding rate at pH of 7.6 and oxygen concentrations below 3.5 mg $L^{-1}$ (Fontanini et al. 2018).

### Salinity limits

Low salinities can occur in coastal regions with high riverine inflow (e.g., Delaware Bay or Chesapeake Bay, New Jersey; Bureau of Marine Water Monitoring; Tassone et al. 2021). Furthermore, salinity in the Wadden Sea can fluctuate between 10 and 32.5 (van Aken 2008; Zimmerman 1976). In the Baltic Sea, as a semi-enclosed marginal sea, the salinity decreases from North to South and West to East (Leppäranta and Myrberg 2009). The common starfish A. rubens does not occur in salinities below 8 (Kautsky and Kautsky 2000).

To ensure that the experiment presented in the main manuscript is of global relevance, and not mainly driven by low-salinity effects, we also tested for the salinity tolerance of *A. rubens* under two different temperature scenarios (see Supplementary Methods). We found that although survival *A. rubens* from Kiel Fjord decreased at very low and very high salinities, adults of this species fed at salinities between 12 and 24. Only under high temperature (i.e., 22.6 °C) feeding rates were suppressed, illustrating an overriding temperature effect. Therefore, we conclude that adults of Kiel Fjord starfish were not significantly stressed by the salinities prevailing (14.1 to 19.8) during the current experiment, and that the salinity shifts during the imposed upwelling event (17.4 to 19.6) did not significantly affect *A. rubens* performance.

### Potential shifts in suitable habitat

In the ~15 m deep inner Kiel Fjord, South-Western Baltic Sea, suitable conditions for *A. rubens* can be found from the water surface down to a depth of 12.4 m during a typical summer (Chapter II - Supplementary Figure 1a). Yet, a present-day heatwave can push *A. rubens* from the surface to deeper areas (> 1.4 m depth; green area in Chapter II - Supplementary Figure 1b), while a projected end-of-century heatwave would even further limit the upper water depth range suitable for this starfish (6.2–9.4 m; the orange area in Chapter II - Supplementary Figure 1b). Such summer heatwaves typically occur five times per year, reaching a usual maximum intensity of 3.4 °C above the climatological trajectory (Pansch et al. 2018). Upwelling events would decrease such unfavorable surface water temperatures (Chapter II - Supplementary Figure 1c) while, at the same time, increasing salinity but reducing pH (increase in $pCO_2$) and oxygen availability for *A. rubens* (Chapter II - Supplementary Figure 1c).

## *Supplementary Methods*

### Experimental treatments

Marine heatwaves may be defined as conditions exceeding particular thresholds for specific amounts of time above which the temperature is anomalous (Hobday et al. 2016). As heatwaves can emerge quickly in shallow coastal habitats, these may also be defined by their onset rates. Following this, Pansch et al. (2018) defined a heatwave as the period with a temperature increase of more than 0.7 °C per day for at least two consecutive days and identified such events using 15 years of high-resolution temperature records from the Kiel Fjord (South-Western Baltic Sea). The *Present-day* heatwave treatment in the current study mirrored the peak summer heatwave applied in the experiment by Pansch et al. (2018) (5 °C above climatology, maximum 22.9 °C, duration 9 days; see Chapter II - Figure 1 and Chapter II - Supplementary Figure 4 for applied and attained temperatures). The underlying climatological trajectory (used for the re-creation of conditions without heatwaves, i.e., *No* heatwave treatment, and as a baseline for the simulation of the applied heatwaves) was defined using a generalised additive mixed model (GAMM; Pansch et al. 2018). The *Extende*d heatwave treatment was simulated by extending the duration of the *Present-day* heatwave to 13 days, representing 2100 conditions, based on a 17% increase of heatwave durations worldwide between the reference period 1925–1954 and the recent period 1987–2016 (Oliver et al. 2018). Based on the same end-of-century projections for marine heatwaves (Oliver et al. 2018), starfish in both *Amplified* and *Future* heatwave treatments (8 °C above the climatology, maximum 25.9 °C; see Chapter II - Figure 1 and Chapter II - Supplementary Figure 4 for applied and attained temperatures) experienced heatwaves with an intensity of 3 °C above *Present-day* and *Extended* heatwaves.

During the upwelling event (August 19th to August 29th), water flow-through and aeration were stopped. Half of the water was exchanged on three occasions (i.e., August 20th, August 21st, and August 23rd) with deep Fjord water (pumped up from below the pycnocline) to create stepwise upwelling conditions and to mix the water in the experimental units. Before the water exchange, temperature (16.3 ± 0.25 °C, mean and SD), salinity (20.2 ± 0.28), pH (7.5 ± 0.03), and oxygen concentration (3.3 ± 0.47 mg $L^{-1}$) of the pumped deep water was measured (Multi 3630 IDS, WTW, Germany). To ensure adequate water quality (measured Ammonium and Ammonia concentrations, JBL Ammonium/Ammonia test set, JBL GmbH & Co Kg, Germany) during the simulated upwelling, the 2 L Kautex® bottles were placed into larger 18 L acrylic glass cylinders. Water exchange between the Kautex® bottle and the cylinder was ensured by 32 holes (5 mm diameter) drilled into the Kautex® bottles' walls. Water flow-through started again on August 26th to allow a slow transition from upwelling back to ambient conditions.

## Data analysis

All analyses were performed using R (R Core Team 2021). Impacts of the applied treatments on the performance of *A. rubens* over time and their interplay were analysed using regression approaches. Changes in the feeding rate and wet weight of *A. rubens* throughout the experiment and in response to the simulated heatwaves and upwelling events were described through generalised additive mixed models (GAMMs) fitted with the function bam from the R package "mgcv" (Wood 2017). GAMMs were used as they provide the flexibility needed for modeling the non-linear changes in feeding rate and wet weight induced by the imposed stressors. The model was fitted assuming a Gaussian distribution of errors. Smooth terms for modelling the effects of different treatments in time were fitted using thin plate regression splines and the smoothing parameters estimated through Restricted Maximum Likelihood (REML; Wood 2017). Since feeding rate measurements were repeatedly performed on the same organisms, the identity of individuals was included as a random effect. Following parsimony and as identity of the tank did not significantly change the modelling outcomes (checked via AIC and ANOVA), identity of the tanks was not included as additional random factor in the final model.

GAMM trends in time obtained for the different treatments were compared using the function plot_diff from the package “itsadug” (van Rij et al. 2020).

Linear mixed models (LMM) were fitted using the function lmer from the “lme4” package (Bates et al. 2015) to evaluate the impact of heatwave treatments over time on righting time. Differential changes in this response variables over the experimental duration in individuals subjected to *No, Present-day* and *Extended* heatwave treatments were represented in the model by the interaction between treatment and time. Since the righting response exhibited abrupt changes that were not properly captured by smoothing and classic regression approaches, time was considered as a factor in the righting model and results were compared between discrete measuring events. REML was used to fit the models. For feeding rate and wet weight, an additional LMM was applied using REML to test for the overall effect of the applied treatments at the end of the experiment. Therefore, only treatment (as fixed effect) and the identity of individuals (as random effect) were included in the models. As explained above, the identity of the tank was not included as additional random factor due to the rule of parsimony and as the inclusion did not significantly change the modelling outcomes (checked via AIC and ANOVA). LMM outputs were generated using the function emmeans of the identically named package (Lenth 2020). The Tukey method was used for performing multiple comparisons.

For all models, assumptions were visually checked through a detailed inspection of the residual plots. Testing for it proofed that there was no autocorrelation in the GAMMs (i.e., using ACF and PACF).

### *Additional Experiment: Salinity tolerance of the investigated A. rubens population*

To ensure that the experiment presented in the main manuscript is of global relevance, and not mainly driven by low-salinity effects, we also tested for the salinity tolerance of *A. rubens* under two different temperature scenarios.

#### Methods

We tested the impact of a salinity gradient (i.e., salinity 8 – 30 in steps of 2) under two different temperatures (18.6 and 22.6 °C). These temperatures represent the long term maximum climatological summer temperature of the study region (Wolf et al. 2022) and a warming scenario of 4 °C for the Baltic Sea (HELCOM 2013). The experiment was conducted in the Kiel Indoor Benthocosms (KIBs; for further information see main manuscript and Pansch and Hiebenthal 2019) from June 5th until June 17th, 2019. 72 experimental units (2 L Kautex® bottles with 32 holes of 5 mm each hanging inside 18 L acrylic glass cylinders) were evenly distributed among eight 600 L tanks, which served as water baths. Each of the experimental units was separately supplied with air. The two temperature treatments were randomly attributed to the eight tanks (i.e., four tanks with the same temperature treatment). Three randomly chosen cylinders of each temperature treatment experienced the same salinity treatment. To ensure adequate alkalinity, the 12 salinities were set by diluting North Sea water with a mixture of 50% tap and 50% deionized water.

Starfish individuals (*A. rubens*) were collected near Möltenort, Kiel (N54° 22’57.54”, E10°12’8.81”) on June 3rd, 2019. Starfish were brought to a climate room and kept in a 600 L tank at conditions recorded at the collection site (i.e., 14 °C and a salinity of 14). After two days of acclimation to lab conditions, 72 starfish of similar weight (11.9 ± 1.5 g, mean and SD) were individually placed inside the experimental units and randomly distributed to the temperature and salinity treatments.

Every three days the feeding rate was determined as consumption of blue mussels (*Mytilus spp.*, size: 1.5 – 2.0 cm). At the same time, mortality of *A. rubens* was recorded. Blue mussels were freshly collected the day prior to the feeding in the Kiel Fjord at adjacent piers of GEOMAR (N54° 19’45.8”, E010° 08’56.4”). After three days of feeding (*ad libitum*), all mussels in the experimental units were exchanged with fresh mussels and shell lengths of the empty mussels were measured (Dial Caliper, Wiha Division KWB Switzerland). Based on a previously described relationship between shell size and tissue dry weight of blue mussels in the study area (Morón Lugo et al. 2020), the dry weight of consumed mussels was estimated.

To investigate the impact of salinity under two different temperature scenarios on the feeding rate, a factorial ANOVA was run using R (R Core Team 2021). Therefore, the interactive effect of the two factors salinity and temperature was included into the model. Assumptions were visually checked through a detailed inspection of residual plots. To test the impact of salinity, temperature and their interactive effect on starfish survival, separate Kruskal-Wallis tests was run using R (R Core Team 2021).

Findings

Salinities below 12 or 16 and above 24 or 20 decreased the survival of Kiel Fjord *Asterias rubens* significantly in temperatures of 18.6 °C or 22.6 °C, respectively (Chapter II - Supplementary Figure 2). Generally, mortality was significantly higher under high (22.6 °C) compared to low temperatures (18.6 °C; Chapter II - Supplementary Figure 2). Starfish in the thermal- and salinity range at which they can survive showed a significant reduction in feeding rate among individuals subjected to high temperatures (22.6 °C; Chapter II - Supplementary Figure 3). Salinity did not significantly influence the feeding rate of starfish (Chapter II - Supplementary Figure 3).

## *Supplementary Figures*

**Chapter II - Supplementary Figure 1:** Temperature (°C, in red) and oxygen (mg $L^{-1}$, in blue) profiles from surface to 15 m depth in the inner Kiel Fjord (adjacent to GEOMAR pier; 54°19'45.5"N 10°09'01.8"E; Wolf et al. 2021c). Depth profile during summer (August 28th, 2017, **a**), depth profile with present-day heatwave (left temperature profile, August 1st, 2018, **b**) and amplified heatwave (+3 °C, right temperature profile, projected for 2100 following RCP4.5 scenario, **b**) (Oliver et al. 2019), and depth profile during a hypoxic upwelling event (July 28th, 2020, **c**). The green areas represent the depth horizon suitable for *Asterias rubens*, i.e., temperatures < 22.0 °C (cessation of feeding activity; F. Melzner, personal communication) and oxygen concentrations > 4 mg $L^{-1}$ (hypoxia; Vaquer-Sunyer and Duarte 2008). Considering the same thresholds, the orange area in **b** represents the suitable depth range for *A. rubens* during the amplified heatwave.

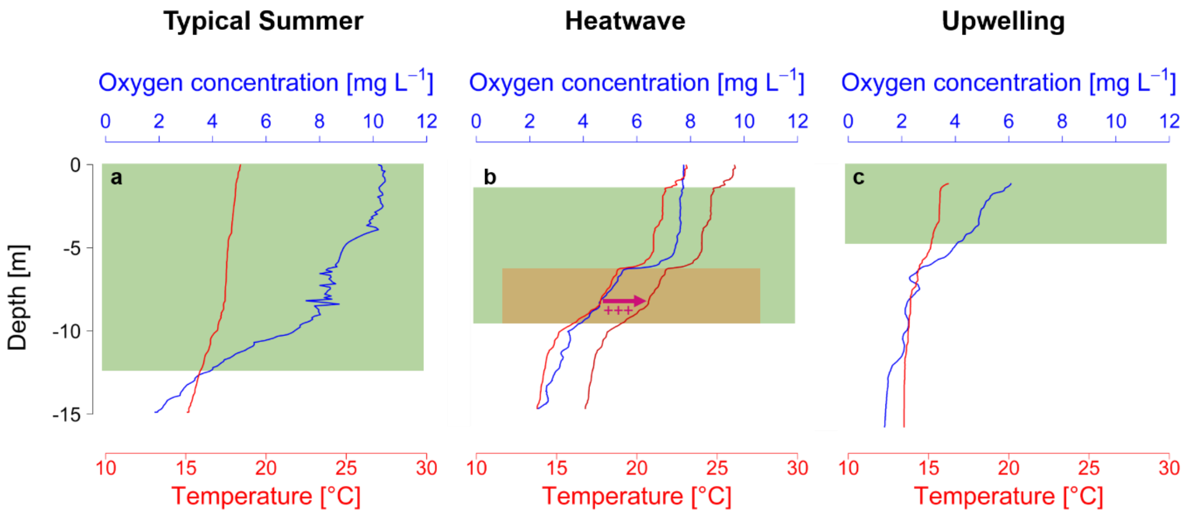

**Chapter II - Supplementary Figure 2:** Survival of starfish subjected to salinities between 8 and 30 (in steps of 2) and temperatures of 18.6 (blue line) or 22.6 °C (red line), with n = 3 replicates per treatment combination. For the statistical results see Chapter II - Supplementary Table 1.

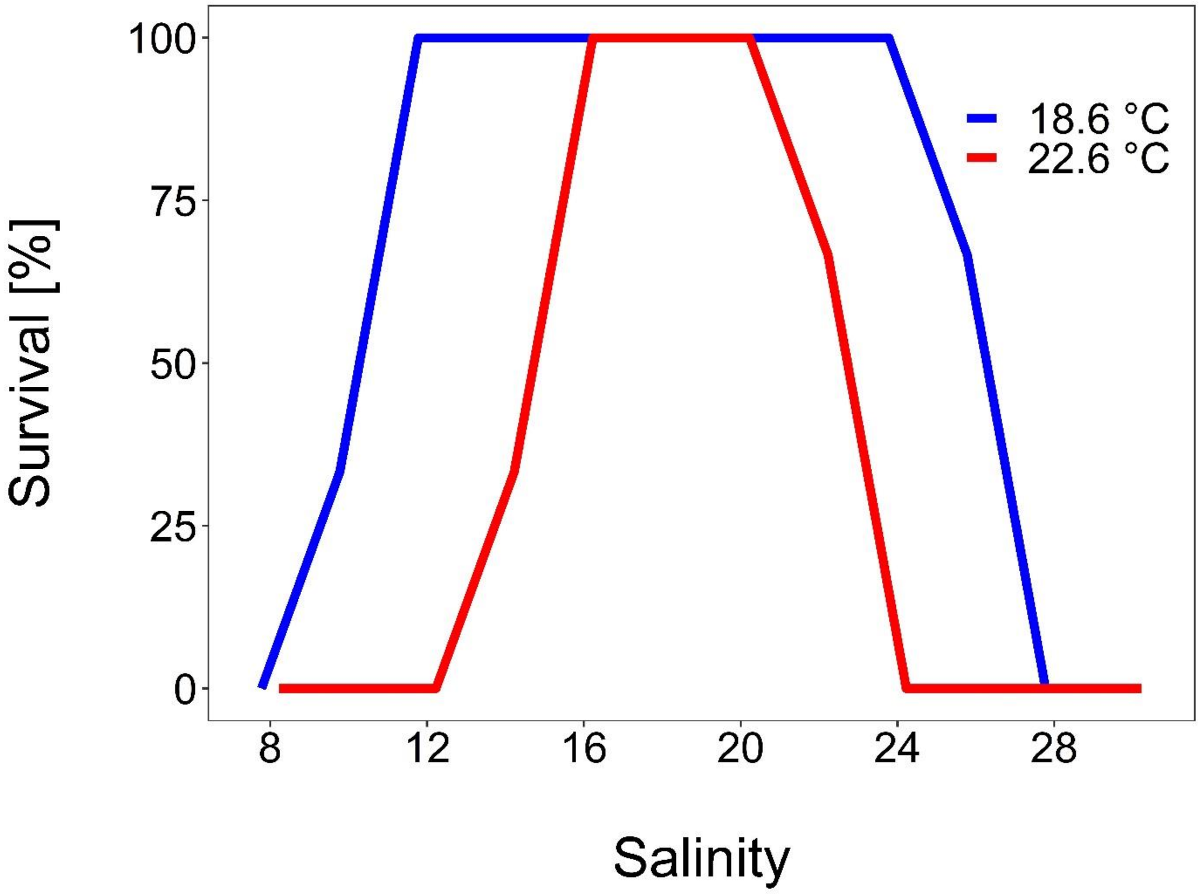

**Chapter II - Supplementary Figure 3:** Feeding rate of starfish (mg mussel dry weight day) subjected to salinities between 8 and 30 (in steps of 2) and temperatures of 18.6 (blue line) or 22.6 °C (red), with n = 3 replicates per treatment combination. For the statistical results see Chapter II - Supplementary Table 1.

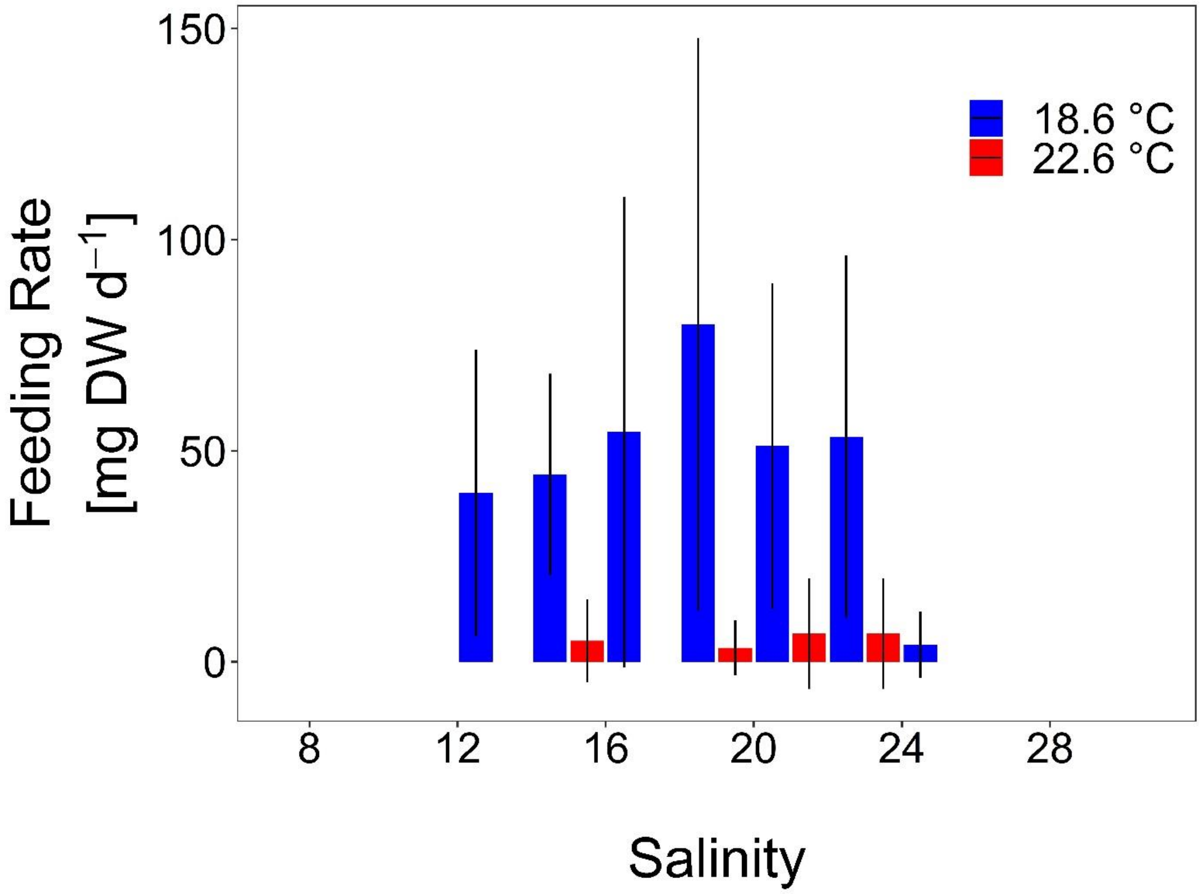

**Chapter II - Supplementary Figure 4:** Measured treatment temperatures in *No* (**a**, blue), *Present-day* (**b**, green), *Extended* (**c**, yellow), *Amplified* (**d**, pink) and *Future* (**e**, red) heatwave treatments. All treatments received an upwelling event towards the end of the experiment. Coloured points show mean temperatures measured across all units and standard deviations (n=6 for days 3–23 (except day 20: n=12) and n=12 for days 24–63 (except day 42: n=6); if numbers deviate, n is indicated in the plot). The grey line shows the implemented temperature profiles. All starfish died after 24 days in the *Amplified* treatments and the respective experimental units were terminated.

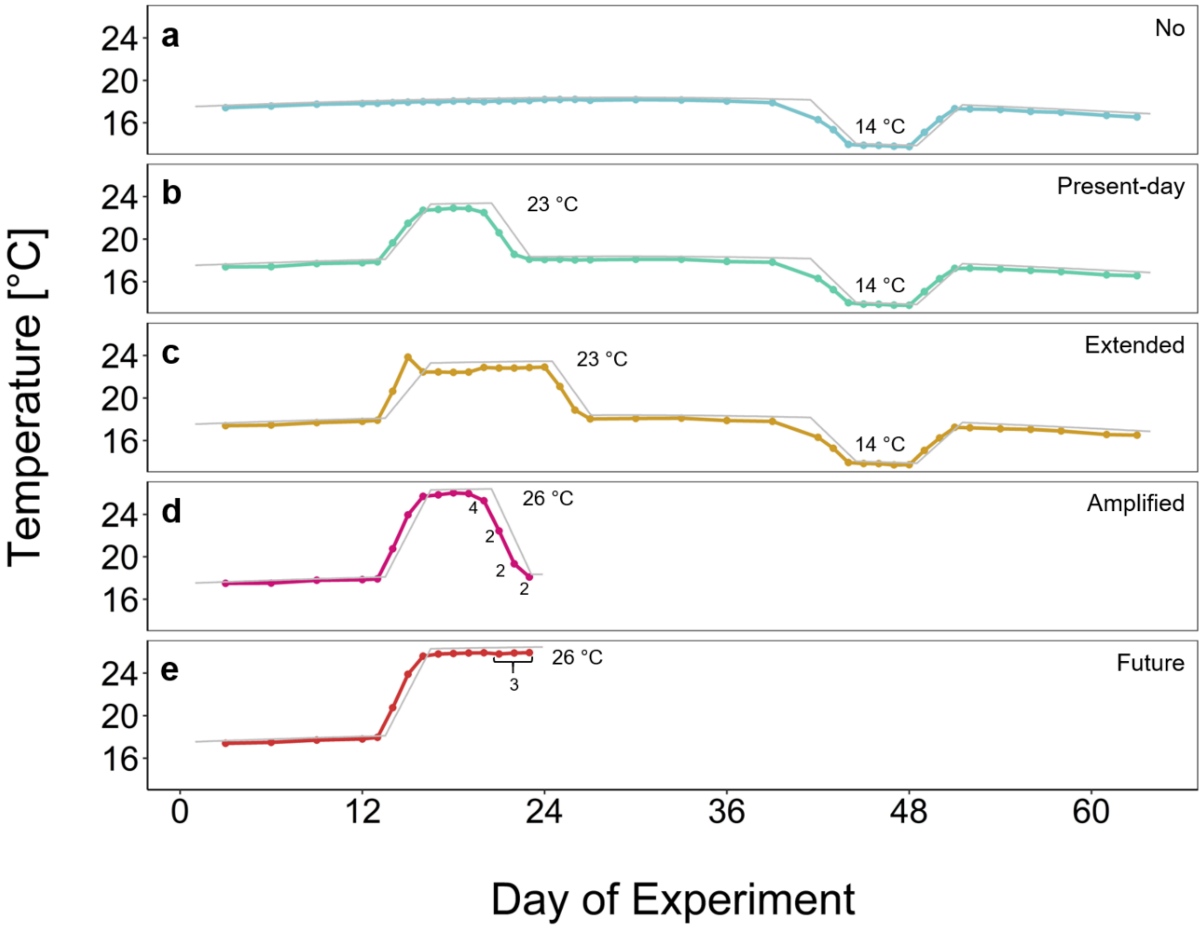

**Chapter II - Supplementary Figure 5:** Temperature (°C, **a**), salinity (**b**), $pH_{NBS}$ (**c**) and oxygen concentration (mg $L^{-1}$, **d**) during the upwelling event, following *No* (blue), *Present-day* (green), and *Extended* (yellow) heatwave treatments (see Chapter II - Figure 1 for treatment descriptions). Presented are means and standard deviations (n=12 (except day 42: n=6). Minimal (and maximal) values of the overall means (of all treatments) are given with standard deviations in the respective plots. Note that the *Amplified* treatments are not shown as all starfish died after 24 days in these treatments. The grey line shows the upwelling event recorded in September 2017 (September 11th to September 27th; Wolf et al. 2021a).

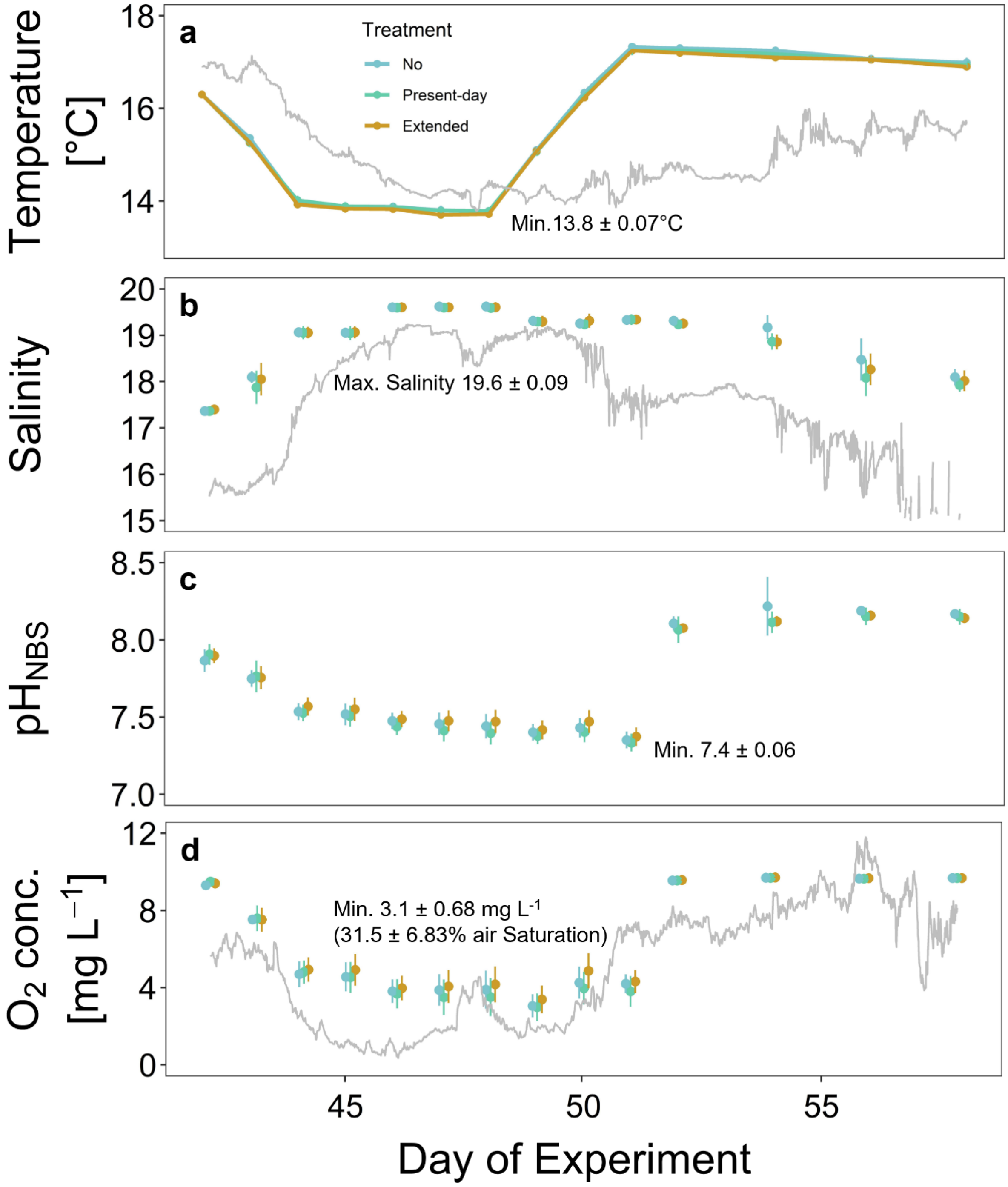

**Chapter II - Supplementary Figure 6:** Examples of starfish shape and condition without heatwave and hypoxic upwelling (**a**), during upwelling (**b**) or during both treatments of *Amplified* temperatures (**c**, **d**). See Chapter II - Figure 1 for treatment details.

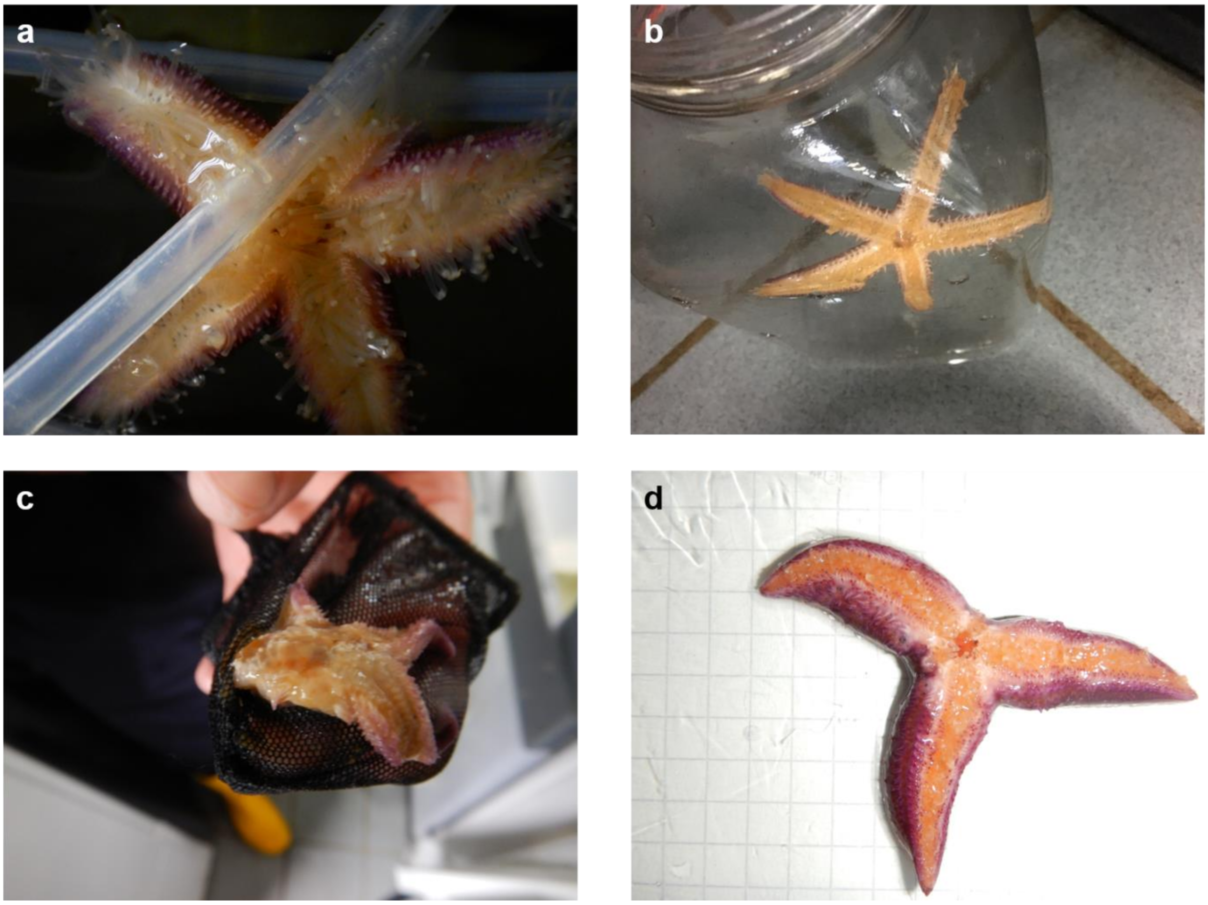

**Chapter II - Supplementary Figure 7:** Survival (%) of *Asterias rubens* over 63 days of incubation under *No* (blue), *Present-day* (green), *Extended* (yellow), *Amplified* (pink) and *Amplified & Extended* (red) heatwave treatments (periods indicated by red dashed lines; see Chapter II - Figure 1 for treatment descriptions). All treatments received an upwelling event towards the end of the experiment (indicated by blue dashed lines). By day 21, 83 and 75% of the starfish individuals had died when the temperature reached 25.9 °C for 2 and 3 days in the *Amplified* and the *Future* heatwave treatments, respectively.

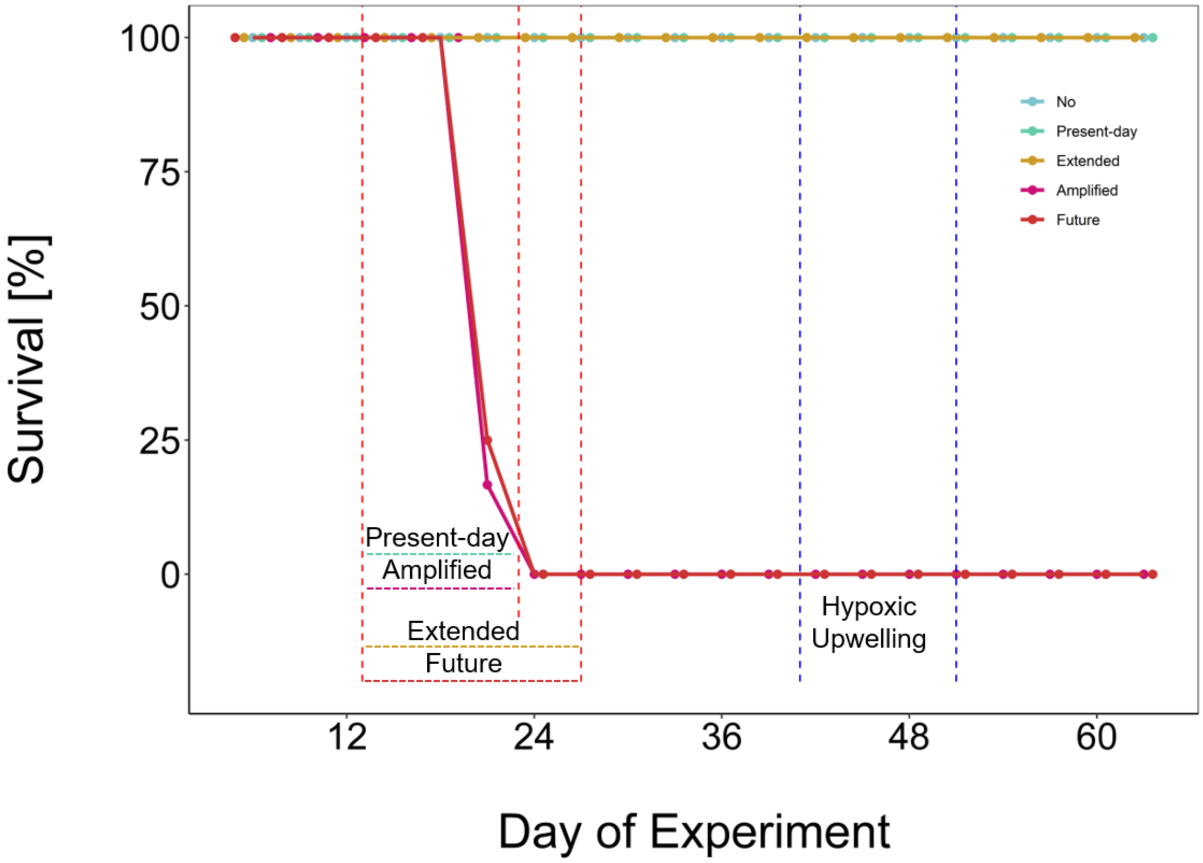

**Chapter II - Supplementary Figure 8:** Differences between the generalised additive mixed models (GAMM) of different treatments for feeding rate (mg mussel dry weight per day, **a-c**) and wet weight (**g**, **d-f**) of *Asterias rubens* during 63 days of incubation, under *No*, *Present-day* (=Pres.), *Extended* (=Ext.) heatwave treatments (see Chapter II - Figure 1 for treatment descriptions). All treatments received an upwelling event towards the end of the experiment. Data are represented as model (GAMM) differences (line) and as 95% confidence intervals (shaded areas; n=12). The red dotted lines mark periods where the models differed.

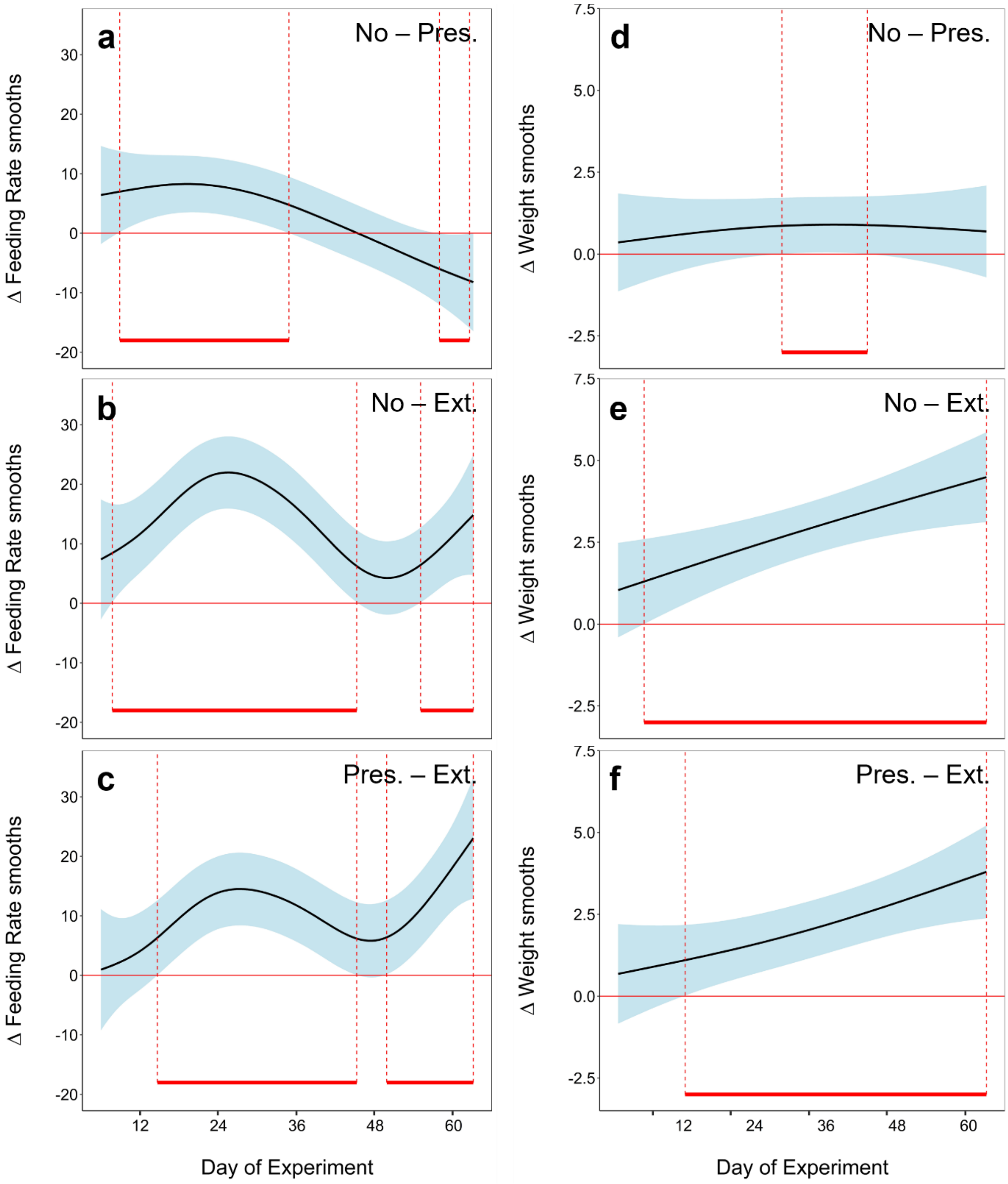

**Chapter II - Supplementary Figure 9:** Feeding Rate of *Asterias rubens* over each three days (mg mussel dry weight per day) during 63 days of incubation under *No* (**a**), *Present-day* (**b**), *Extended* (**c**), *Amplified* (**d**) and *Future* (**e**) heatwave treatments (see Chapter II - Figure 1 for treatment descriptions). All treatments received an upwelling event towards the end of the experiment. Data are presented as means and 95% confidence intervals (n=12, if number deviates, n is given in the plot in **d** and **e**). The different colours represent periods of applied heatwave (orange = ramping to red) and the hypoxic upwelling events (blue). All starfish died after 24 days in treatments of *Amplified* temperatures (**d**, **e**).

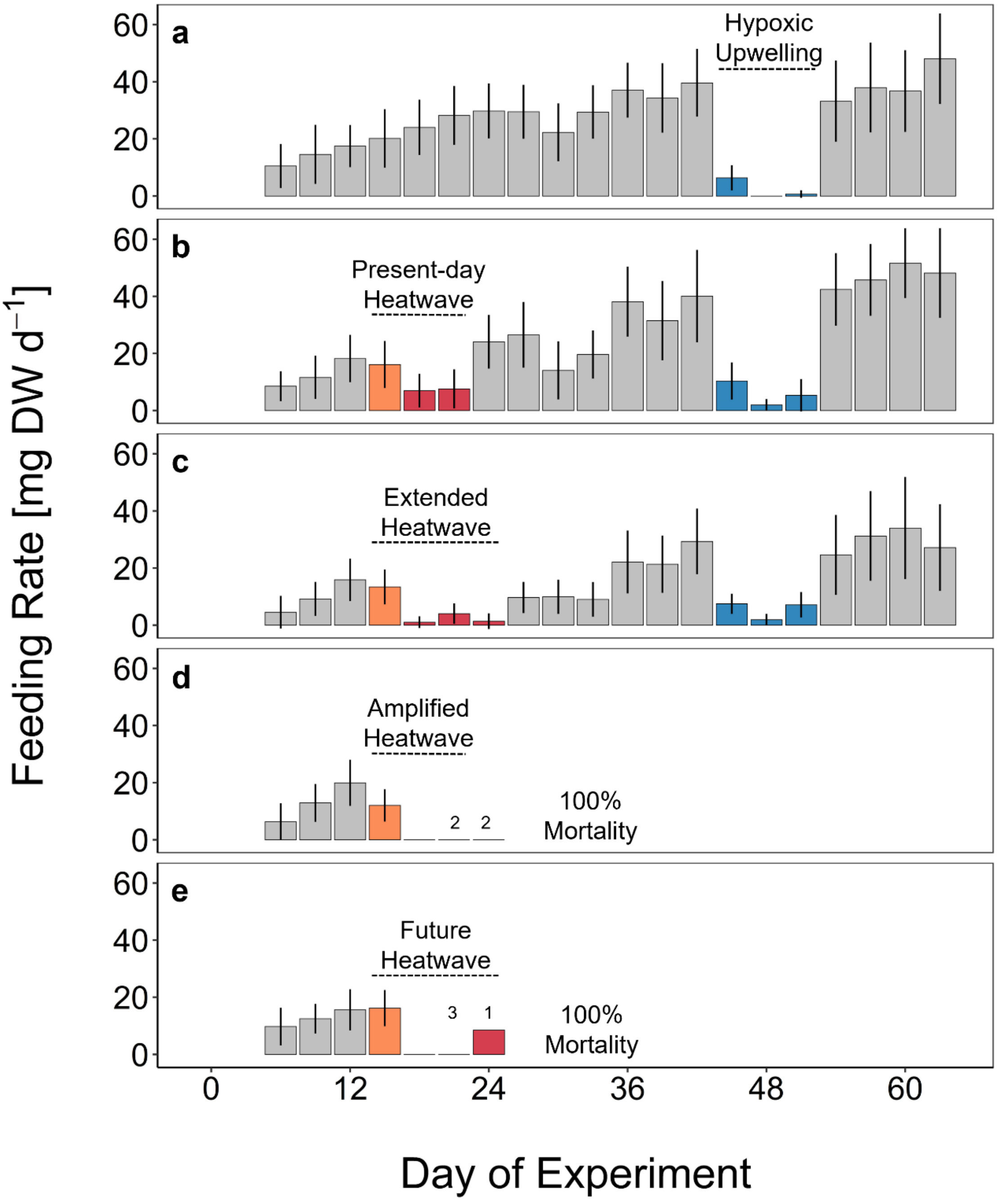

**Chapter II - Supplementary Figure 10:** Wet weight (g) of *Asterias rubens* during 63 days of incubation under *No* (**a**), *Present-day* (**b**), *Extended* (**c**), *Amplified* (**d**) and *Future* (**e**) heatwave treatments (see Chapter II - Figure 1 for treatment descriptions). All treatments received an upwelling event towards the end of the experiment. Data are presented as means and 95% confidence intervals (n=12, if number deviates, n is given in the plot in d and e). The different colours represent periods of the applied heatwave (red) and the hypoxic upwelling (blue) events. All starfish died after 24 days in treatments of *Amplified* temperatures (**d**, **e**).

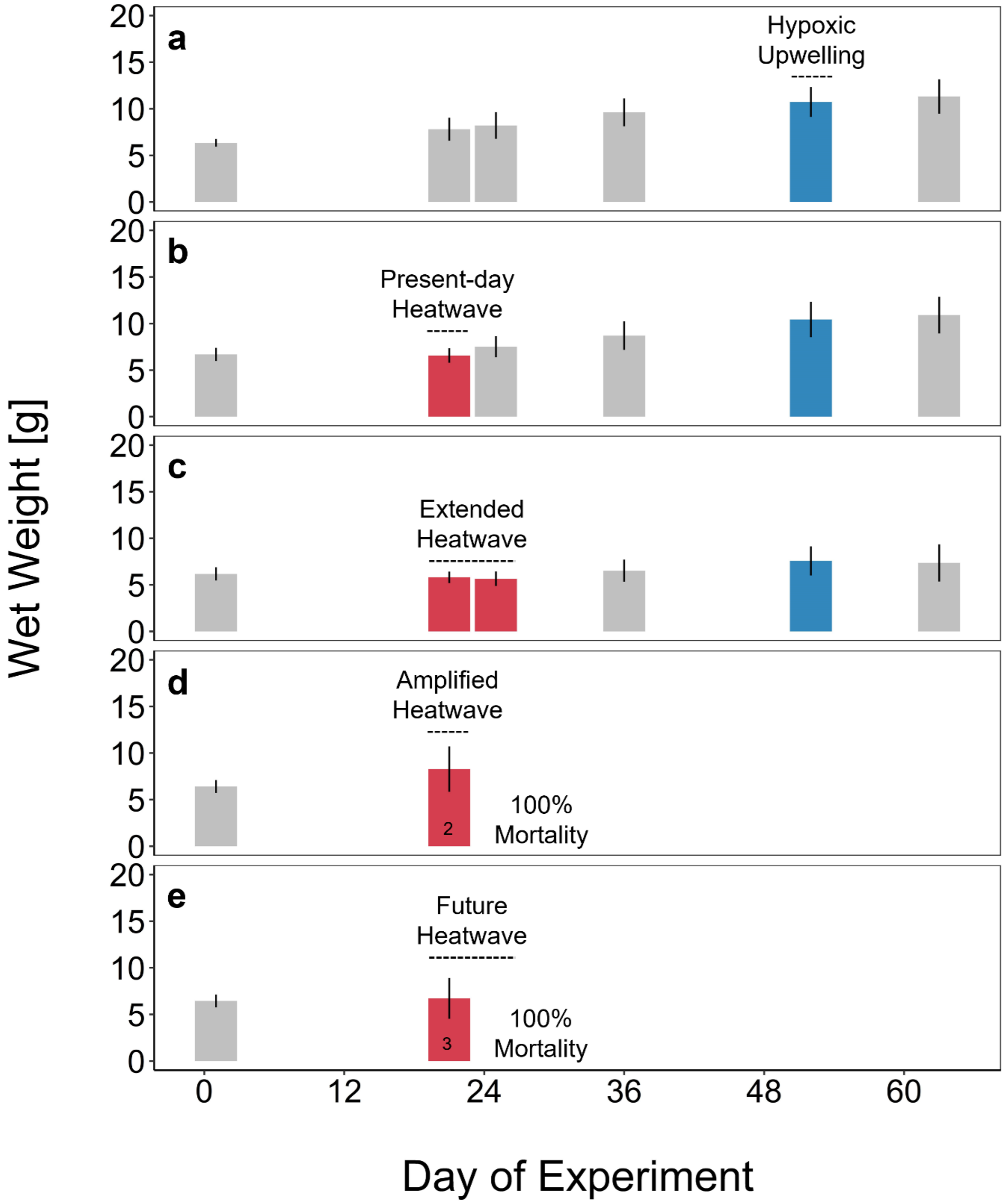

**Chapter II - Supplementary Figure 11:** Righting Time of *Asterias rubens* (minutes) during 63 days of incubation, under *No* (**a**), *Present-day* (**b**), *Extended* (**c**), *Amplified* (**d**) and *Future* (**e**) heatwave treatments (see Chapter II - Figure 1 for treatment descriptions). All treatments received an upwelling event towards the end of the experiment. Data are presented as means and 95% confidence intervals (n=12, if number deviates, n is given in the plot in d and e). The different colours represent periods of the applied heatwave (red) and the hypoxic upwelling (blue) events. All starfish died after 24 days in treatments of *Amplified* temperatures (**d**, **e**).

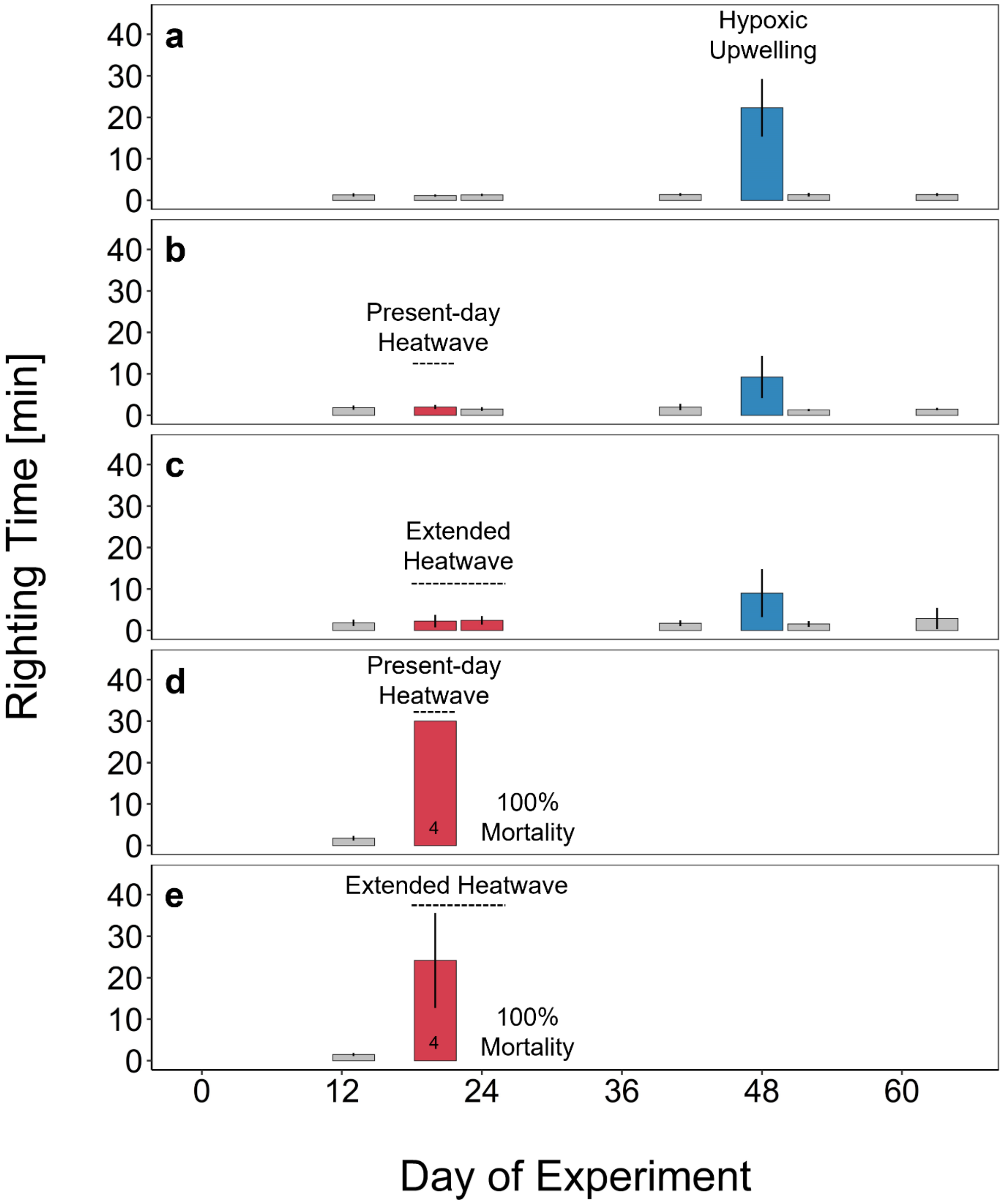

**Chapter II - Supplementary Figure 12:** Feeding rate (mg mussel dry weight per day) of *Asterias rubens* during different periods (**a**) of the 63 days experiment under *No* (blue), *Present-day* (green), and *Extended* (yellow) heatwave treatments (see Chapter II - Figure 1 for treatment descriptions). Periods represent distinct phases during the experiment, i.e., before the heatwaves (**b**), during the heatwaves (**c**), after the heatwaves (**d**), during the upwelling (**e**), and after the upwelling (f). Data are represented as means and 95% confidence intervals. Analysis of Variance (ANOVA) was used to evaluate the impact of heatwave treatments on feeding rates. The mean feeding rate of the *No* heatwave treatment was calculated for the respective period of the *Present-day* as well as for the *Extended* heatwave. These means of the *No* heatwave treatment were then averaged to account for different lengths of the period during the *Extended* and *Present-day* heatwave. To meet all assumptions, the square root of the feeding rate for the periods before and during the heatwave was applied. Detailed statistical outcomes are presented in Chapter II - Supplementary Table 4. All starfish died after 24 days in the *Amplified* treatments and were therefore excluded from the plots.

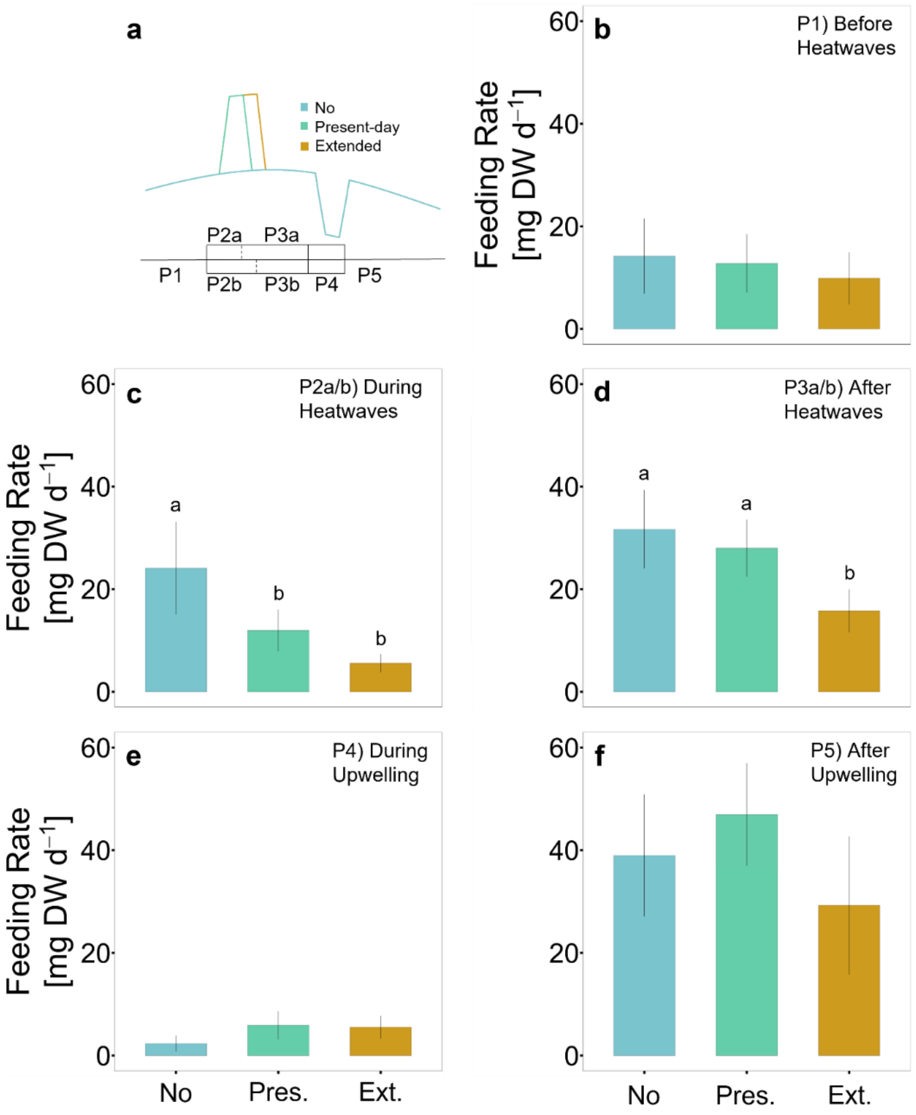

**Chapter II - Supplementary Figure 13:** Temperature (°C, **a**) and oxygen concentration (mg L$^{-1}$, **b**) measured biweekly over 14 years close to the GEOMAR pier (54°19'45.5"N 10°09'01.8"E; Wolf et al. 2021b) at the surface and in 18 m depth. The red and blue shaded areas show summer conditions at the surface or at 18 m depth, respectively (**a** and **b**). Extreme summer surface temperatures (i.e., heatwaves, **c**, red shaded area, °C; Wolf et al. 2021a) can be interrupted by cold, but hypoxic deep water being shoaled up to the surface (i.e., hypoxic upwelling, 18 days on average per year, **c**, blue shaded area, mg L$^{-1}$; Karstensen et al. 2014; Wolf et al. 2021a).

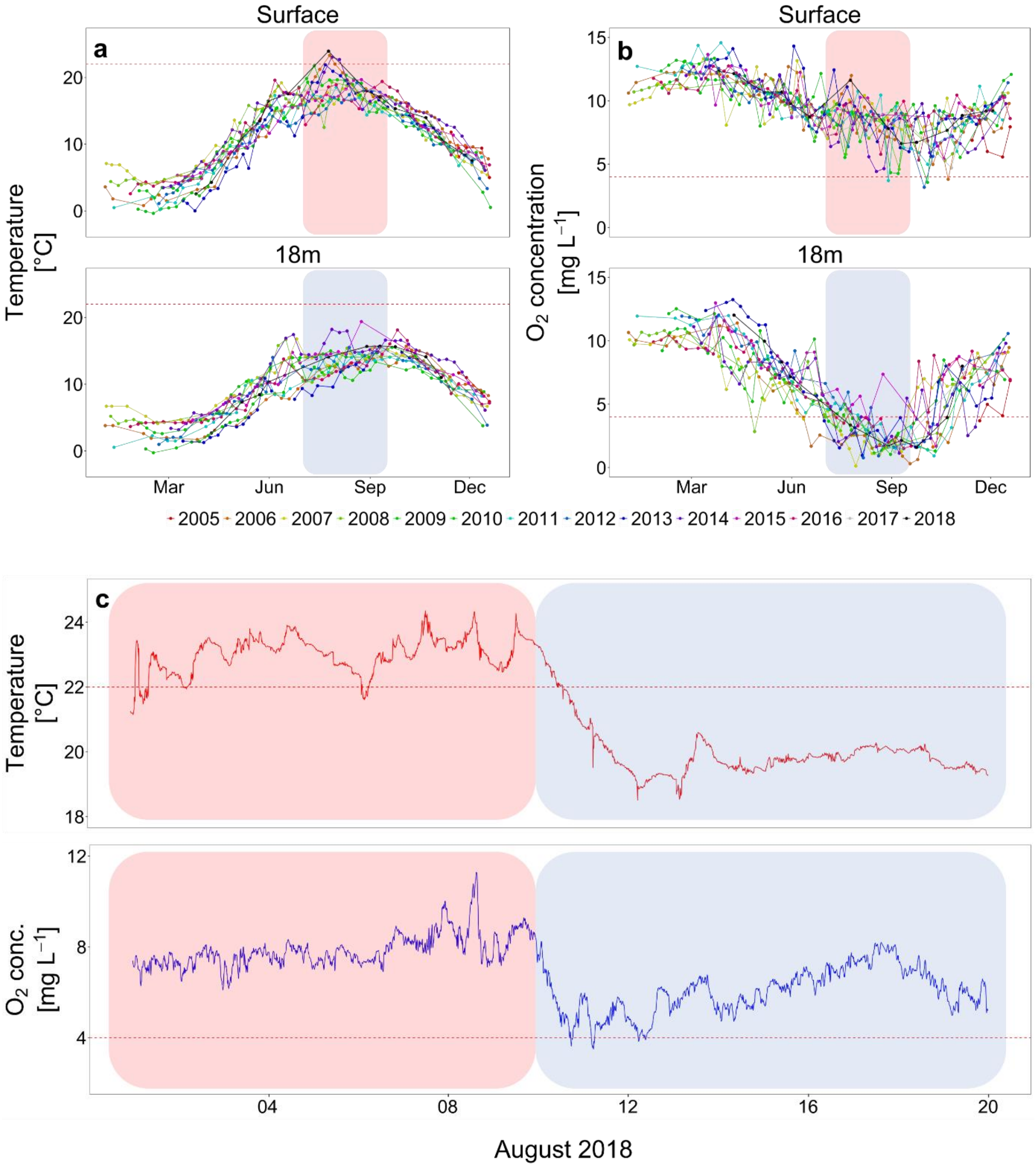

## *Supplementary Tables*

**Chapter II - Supplementary Table 1:** Kruskal-Wallis Test results for survival and ANOVA results for feeding rate of *Asterias rubens* subjected to salinities between 8 and 30 (in steps of 2) and temperatures of 18.6 or 22.6 °C.

| **Kruskal-Wallis Survival** | df | Chi sq | p-value | | |
|---|---|---|---|---|---|
| Temperature Treatment | 1 | 19.628 | **<0.001** | | |
| Salinity Treatment | 11 | 42.074 | **<0.001** | | |
| Temperature Treatment:Salinity Treatment | 11 | 60.481 | **<0.001** | | |
| **ANOVA Feeding rate** | | Sum sq | Mean sq | F-value | p-value |
| Temperature Treatment | 1 | 11801 | 11801.000 | 12.470 | **0.001** |
| Salinity Treatment | 9 | 14305 | 1589.000 | 1.680 | 0.141 |
| Temperature Treatment:Salinity Treatment | 6 | 5505 | 918.000 | 0.970 | 0.463 |
| Residuals | 28 | 26489 | 946.000 | | |

**Chapter II - Supplementary Table 2:** Generalised Additive Mixed Effect Model (GAMM) results for feeding rate (mg mussel dry weight per day) over 63 days of incubation in all treatments. The GAMM for feeding rate had an explained deviance of 37.6%. Linear Mixed-effect Model (LMM) results for feeding rate (mg mussel dry weight per day) of all treatments. P-values in the LMM were adjusted for multiple comparisons applying the Tukey method. Significant effects are shown in bold.

| **GAM Feeding Rate** | | | | |
|---|---|---|---|---|
| Parametric Coefficients | Estimate | Std. Error | t-value | p-value |
| Intercept | 21.163 | 1.390 | 15.224 | < **0.001** |
| Present-day | -2.623 | 1.617 | -1.622 | 0.105 |
| Extended | -12.899 | 1.663 | -7.755 | < **0.001** |
| Smooth Terms | edf | rdf | F-value | p-value |
| s (Day of Experiment) | 7.787 | 7.974 | 24.605 | < **0.001** |
| s (Day of Experiment): Present-day | 2.126 | 2.647 | 5.042 | **0.005** |
| s (Day of Experiment): Extended | 4.115 | 5.035 | 3.604 | **0.003** |
| s (Individual) | 0.958 | 1.000 | 22.573 | < **0.001** |

| **LMM Feeding Rate** | | | | | |
|---|---|---|---|---|---|
| Contrast | Estimate | Std. Error | df | t-value | p-value |
| No:Present-day | 1.550 | 3.700 | 33.000 | 0.420 | 0.908 |
| No:Extended | 10.760 | 3.700 | 33.000 | 2.909 | **0.017** |
| Present-day:Extended | 9.210 | 3.700 | 33.000 | 2.489 | **0.046** |

**Chapter II - Supplementary Table 3:** Generalised Additive Mixed Effect Model (GAMM) results for wet weight (g) over 63 days of incubation in all treatments. The GAMM for wet weight had an explained deviance of 40.5%. Linear Mixed-effect Model (LMM) results for wet weight (g) of all treatments. P-values in the LMM were adjusted for multiple comparisons applying the Tukey method. Significant effects are shown in bold.

| **AM Wet Weight** | | | | |
|---|---|---|---|---|
| Parametric Coefficients | Estimate | Std. Error | t-value | p-value |
| Intercept | 8.320 | 0.332 | 25.094 | < **0.001** |
| Present-day | -0.728 | 0.388 | -1.878 | 0.062 |
| Extended | -2.869 | 0.398 | -7.203 | < **0.001** |
| Smooth Terms | edf | rdf | F-value | p-value |
| s (Day of Experiment) | 1.006 | 1.010 | 39.589 | < **0.001** |
| s (Day of Experiment): Present-day | 1.420 | 1.663 | 0.240 | 0.705 |
| s (Day of Experiment): Extended | 1.126 | 1.236 | 6.532 | **0.006** |
| s (Individual) | 0.928 | 1.000 | 12.944 | < **0.001** |

| **LMM Wet Weight** | | | | | |
|---|---|---|---|---|---|
| Contrast | Estimate | Std. Error | df | t-value | p-value |
| No:Present-day | 0.537 | 0.832 | 33.000 | 0.645 | 0.796 |
| No:Extended | 2.487 | 0.832 | 33.000 | 2.990 | **0.014** |
| Present-day:Extended | 1.950 | 0.832 | 33.000 | 2.345 | 0.063 |

**Chapter II - Supplementary Table 4:** Linear Mixed-effect Model (LMM) for the righting time (min) over 63 days of incubation. P-values were adjusted for multiple comparisons applying the Tukey method. Significant effects are shown in bold.

| **LMM Righting Response** | | | | | |
|---|---|---|---|---|---|
| Parametric Coefficients | Estimate | Std. Error | df | t-value | p-value |
| Intercept | 77.417 | 73.335 | 229.668 | 1.056 | 0.292 |
| Present-day | 34.750 | 103.712 | 229.668 | 0.335 | 0.738 |
| Extended | 33.167 | 103.712 | 229.668 | 0.320 | 0.749 |
| Day of Experiment 20 | -9.750 | 102.902 | 197.053 | -0.095 | 0.925 |
| Day of Experiment 24 | 0.833 | 102.902 | 197.053 | 0.008 | 0.994 |
| Day of Experiment 41 | 6.333 | 102.902 | 197.053 | 0.062 | 0.951 |
| Day of Experiment 48 | 1261.917 | 102.902 | 197.053 | 12.263 | **< 0.001** |
| Day of Experiment 52 | 2.500 | 102.902 | 197.053 | 0.024 | 0.981 |
| Day of Experiment 63 | 4.917 | 102.902 | 197.053 | 0.048 | 0.962 |
| Present-day:Day of Experiment 20 | 20.083 | 145.525 | 197.053 | 0.138 | 0.890 |
| Extended:Day of Experiment 20 | 34.750 | 145.525 | 197.053 | 0.239 | 0.812 |
| Present-day:Day of Experiment 24 | -20.417 | 145.525 | 197.053 | -0.140 | 0.889 |
| Extended:Day of Experiment 24 | 36.250 | 145.525 | 197.053 | 0.249 | 0.804 |
| Present-day:Day of Experiment 41 | 1.667 | 145.525 | 197.053 | 0.011 | 0.991 |
| Extended:Day of Experiment 41 | -13.083 | 145.525 | 197.053 | -0.090 | 0.928 |
| Present-day:Day of Experiment 48 | -819.417 | 145.525 | 197.053 | -5.631 | **< 0.001** |
| Extended:Day of Experiment 48 | -832.083 | 145.525 | 197.053 | -5.718 | **< 0.001** |
| Present-day:Day of Experiment 52 | -38.333 | 145.525 | 197.053 | -0.263 | 0.793 |
| Extended:Day of Experiment 52 | -18.583 | 145.525 | 197.053 | -0.128 | 0.899 |
| Present-day:Day of Experiment 63 | -27.417 | 145.525 | 197.053 | -0.188 | 0.851 |
| Extended:Day of Experiment 63 | 56.664 | 147.193 | 198.209 | 0.385 | 0.701 |

**Chapter II - Supplementary Table 5:** Analysis-of-variance (ANOVA) results for feeding rate during five periods of 63 days of incubation (i.e., P1-before heatwaves, P2-during heatwaves, P3-after heatwaves, P4-during upwelling, P5-after upwelling). For significant treatment effects a Tukey-post-hoc-test was applied. Significant effects are shown in bold.

| **ANOVA Feeding Rate P1** | | | | | |
|---|---|---|---|---|---|
| | df | Sum-Sq | Mean-Sq | F -value | p-value |
| Heatwave Treatment | 2.000 | 1.590 | 0.796 | 0.226 | 0.799 |
| Residuals | 33.000 | 116.400 | 3.527 | | |
| **ANOVA Feeding Rate P2** | | | | | |
| | df | Sum-Sq | Mean-Sq | F -value | p-value |
| Heatwave Treatment | 2.000 | 52.160 | 26.080 | 9.292 | **<0.001** |
| Residuals | 57.000 | 159.980 | 2.807 | | |
| **Tukey-post hoc Test P2** | | | | | |
| Treatment Comparison | Mean Diff. | CI95 lwr | CI 95 upr | p-value | |
| No:Present-day | -1.574 | -2.999 | -0.148 | **0.027** | |
| No:Extended | -2.548 | -3.973 | -1.123 | **0.000** | |
| Present-day:Extended | 0.974 | -0.189 | 2.138 | 0.118 | |
| **ANOVA Feeding Rate P3** | | | | | |
| | df | Sum-Sq | Mean-Sq | F -value | p-value |
| Heatwave Treatment | 2.000 | 2709.000 | 1354.700 | 8.632 | **<0.001** |
| Residuals | 57.000 | 8945.000 | 156.900 | | |
| **Tukey-post hoc Test P3** | | | | | |
| Treatment Comparison | Mean Diff. | CI95 lwr | CI 95 upr | p-value | |
| No:Present-day | -3.683 | -14.341 | 6.975 | 0.685 | |
| No:Extended | -15.895 | -26.553 | -5.236 | **0.002** | |
| Present-day:Extended | 12.212 | 3.509 | 20.914 | **0.004** | |
| **ANOVA Feeding Rate P4** | | | | | |
| | df | Sum-Sq | Mean-Sq | F -value | p-value |
| Heatwave Treatment | 2.000 | 91.700 | 45.840 | 2.982 | 0.065 |
| Residuals | 33.000 | 507.200 | 15.370 | | |
| **ANOVA Feeding Rate P5** | | | | | |
| | df | Sum-Sq | Mean-Sq | F -value | p-value |
| Heatwave Treatment | 2.000 | 1892.000 | 945.800 | 2.150 | 0.132 |
| Residuals | 33.000 | 14513.000 | 439.800 | | |

*Supplementary References*

Agüera, Antonio; Trommelen, Michel; Burrows, Frances; Jansen, Jeroen M.; Schellekens, Tim; Smaal, Aad (2012): Winter feeding activity of the common starfish (Asterias rubens L.). The role of temperature and shading. In Journal of Sea Research 72, pp. 106–112. DOI: 10.1016/j.seares.2012.01.006.

Bates, Douglas; Mächler, Martin; Bolker, Ben; Walker, Steve (2015): Fitting Linear Mixed-Effects Models Using lme4. In J. Stat. Soft. 67 (1). DOI: 10.18637/jss.v067.i01.

Budd, G. C. (2008): Asterias rubens Common starfish. Edited by Tyler-Walters H., K. Hiscock. Marine Life Information Network: Biology and Sensitivity Key Infomation Reviews (online). Plymouth: Marine Biological Association of the United Kingdom. Available online at https://dx.doi.org/10.17031/marlinsp.1194.1.

Bureau of Marine Water Monitoring, New Jersey: Nutrient Monitoring Networks. Available online at https://www.nj.gov/dep/bmw/coastalwaterquality.htm.

Clark, Ailsa M.; Downey, Maureen E. (1992): Starfishes of the Atlantic. 1. ed. London: Chapman & Hall (Natural History Museum publications, 3).

Diaz, R. J. (2001): Overview of hypoxia around the world. In Journal of environmental quality 30 (2), pp. 275–281. DOI: 10.2134/jeq2001.302275x.

Fennel, Katja; Testa, Jeremy M. (2019): Biogeochemical Controls on Coastal Hypoxia. In Annual review of marine science 11, pp. 105–130. DOI: 10.1146/annurev-marine-010318-095138.

Fontanini, Aisling; Steckbauer, Alexandra; Dupont, Sam; Duarte, Carlos M. (2018): Variable metabolic responses of Skagerrak invertebrates to low O2 and high CO2 scenarios. In Biogeosciences 15 (12), pp. 3717–3729. DOI: 10.5194/bg-15-3717-2018.

HELCOM (2013): Climate Change in the Baltic Sea Area: A HELMCOM thematic assessment in 2013. In Balt. Sea Environ. Proc. 37.

Hobday, Alistair J.; Alexander, Lisa V.; Perkins, Sarah E.; Smale, Dan A.; Straub, Sandra C.; Oliver, Eric C.J. et al. (2016): A hierarchical approach to defining marine heatwaves. In Progress in Oceanography 141, pp. 227–238. DOI: 10.1016/j.pocean.2015.12.014.

Kautsky, Lena; Kautsky, Nils (2000): The Baltic Sea, including Bothnian Sea and Bothnian Bay. In Charles R. C. Sheppard (Ed.): Seas at the Millenium: An environmental Evaluation. Regional Chapters: Europe, The Amicas and West Africa: Pergamon (1).

Lenth, Russels V. (2020): emmeans: Estimated Marginal Means, aka Least Squares means. Available online at https://CRAN.R-project.org/package=emmeans.

Leppäranta, Matti; Myrberg, Kai (Eds.) (2009): Physical Oceanography of the Baltic Sea. Berlin, Heidelberg: Springer Berlin Heidelberg.

Morón Lugo, Sonia C.; Baumeister, Moritz; Nour, Ola Mohamed; Wolf, Fabian; Stumpp, Meike; Pansch, Christian (2020): Warming and temperature variability determine the performance of two invertebrate predators. In Scientific reports 10 (1), p. 6780. DOI: 10.1038/s41598-020-63679-0.

Oliver, Eric C. J.; Burrows, Michael T.; Donat, Markus G.; Sen Gupta, Alex; Alexander, Lisa V.; Perkins-Kirkpatrick, Sarah E. et al. (2019): Projected Marine Heatwaves in the 21st Century and the Potential for Ecological Impact. In Front. Mar. Sci. 6, p. 891. DOI: 10.3389/fmars.2019.00734.

Oliver, Eric C. J.; Donat, Markus G.; Burrows, Michael T.; Moore, Pippa J.; Smale, Dan A.; Alexander, Lisa V. et al. (2018): Longer and more frequent marine heatwaves over the past century. In Nature communications 9 (1), p. 1324. DOI: 10.1038/s41467-018-03732-9.

Pansch, Christian; Hiebenthal, Claas (2019): A new mesocosm system to study the effects of environmental variability on marine species and communities. In Limnol. Oceanogr. Methods 28, p. 16. DOI: 10.1002/lom3.10306.

Pansch, Christian; Scotti, Marco; Barboza, Francisco R.; Al-Janabi, Balsam; Brakel, Janina; Briski, Elizabeta et al. (2018): Heat waves and their significance for a temperate benthic community. A near-natural experimental approach. In Glob Change Biol. DOI: 10.1111/gcb.14282.

R Core Team (2021): R: A language and environment for statistical computing. Version 4.1.1. Vienna, Austria: R Foundation for Statistical Computing. Available online at https://www.R-project.org.

Schlegel, Robert W. (2020): Marine Heatwave Tracker. Available online at http://www.marineheatwaves.org/tracker.

SealifeBase: Asterias rubens (Linnaeus, 1758). Available online at https://www.sealifebase.se/summary/Asterias-rubens.html.

Tassone, Spencer J.; Besterman, Alice F.; Buelo, Cal D.; Walter, Jonathan A.; Pace, Michael L. (2021): Co-occurrence of Aquatic Heatwaves with Atmospheric Heatwaves, Low Dissolved Oxygen, and Low pH Events in Estuarine Ecosystems. In Estuaries and Coasts 7 (3), p. 1170. DOI: 10.1007/s12237-021-01009-x.

van Aken, Hendrik M. (2008): Variability of the salinity in the western Wadden Sea on tidal to centennial time scales. In Journal of Sea Research 59 (3), pp. 121–132. DOI: 10.1016/j.seares.2007.11.001.

van Rij, Jacolien; Wieling, Martijn; Baayen, R. Harald; van Rijn, Hedderik (2020): itsadug: Interpreting Time Series and Autocorrelated Data Using GAMMs. Available online at https://CRAN.R-project.org/package=itsadug.

Vaquer-Sunyer, Raquel; Duarte, Carlos M. (2008): Thresholds of hypoxia for marine biodiversity. In Proceedings of the National Academy of Sciences of the United States of America 105 (40), pp. 15452–15457. DOI: 10.1073/pnas.0803833105.

Vevers, H. G. (1949): The Biology of Asterias Rubens L. Growth And Reproduction. In J. Mar. Biol. Ass. 28 (1), pp. 165–187. DOI: 10.1017/S0025315400055272.

Wolf, Fabian; Clemmesen, Catriona; Hiebenthal, Claas (2021a): Continuous water temperature, salinity, oxygen and pH data in front of GEOMAR Pier, Kiel, Germany (2014-2019). PANGAEA. Available online at https://doi.org/10.1594/PANGAEA.930979.

Wolf, Fabian; Clemmesen, Catriona; Hiebenthal, Claas (2021b): Water temperature, salinity and oxygen data from 2005-2019 in front of GEOMAR Pier, Kiel, Germany. PANGAEA. Available online at https://doi.org/10.1594/PANGAEA.930974.

Wolf, Fabian; Seebass, Katja; Pansch, Christian (2022): The Role of Recovery Phases in Mitigating the Negative Impacts of Marine Heatwaves on the Sea Star Asterias rubens. In Front. Mar. Sci. 8, p. 1029. DOI: 10.3389/fmars.2021.790241.

Wolf, Fabian; Schütt, Renate; Wahl, Martin (2021c): Hydrography measured from June 2009 - October 2020 in the Kiel Fjord, Germany. PANGAEA. Available online at https://doi.org/10.1594/PANGAEA.931315.

Wood, Simon N. (2017): Generalized Additive Models: Chapman and Hall/CRC.

Zimmerman, J.T.F. (1976): Mixing and flushing of tidal embayments in the western Dutch Wadden Sea part I. Distribution of salinity and calculation of mixing time scales. In Netherlands Journal of Sea Research 10 (2), pp. 149–191. DOI: 10.1016/0077-7579(76)90013-2.

# Supplement to Chapter III

## *Supplementary Figures*

**Chapter III - Supplementary Figure 1:** Collection sites of *Zostera marina* for Experiment 1 and 2 in the Western Baltic Sea (**a**), more specifically in Kiel, Northern Germany (**b**) at Falckenstein Beach (**c**). For experiment 1, two populations from either inside or outside the sandbank (**d**) were collected. Images were taken from © Google Earth.

**Chapter III - Supplementary Figure 2:** Water temperatures (°C) logged nearby the collection site of the *Outside* (deep, blue) and *Inside* (shallow, red) population at Falckenstein beach (see Chapter III - Supplementary Figure 1) in summer 2017 over time (**a**) and summarized (**b**). The grey solid line and the grey dashed line in a show the climatological values and the 90th percentile threshold for marine heatwaves in the inner Kiel Fjord, respectively (Wolf et al. 2022).

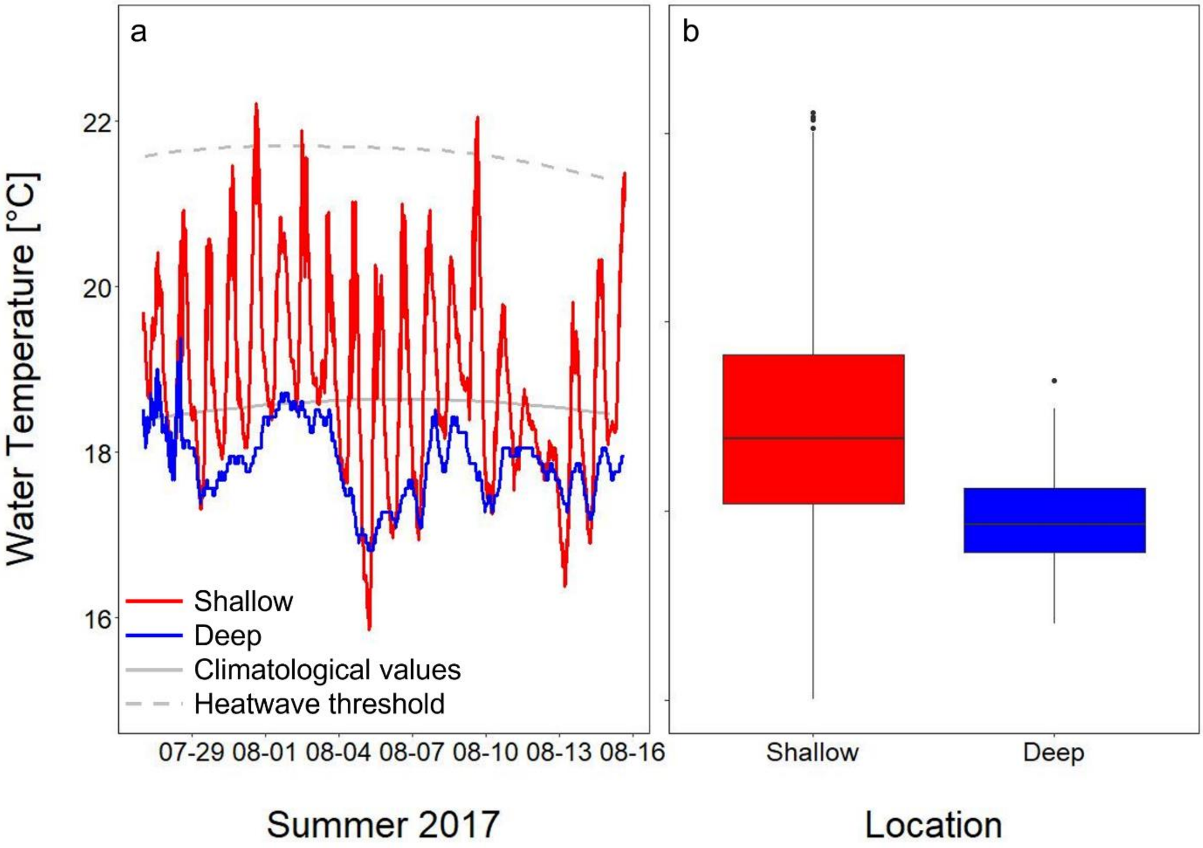

**Chapter III - Supplementary Figure 3:** Cardinal orientation of the Kiel Outdoor Benthocosm tanks and the eelgrass trays. Note that the eelgrasses are always placed on the western side of a tank. Colours indicate the *Ambient* (blue) and *Warming* (red) treatments (see also Chapter III - Figure 2 for treatment description). Eelgrass symbols are taken from https://ian.umces.edu/media-library/symbols/#download.

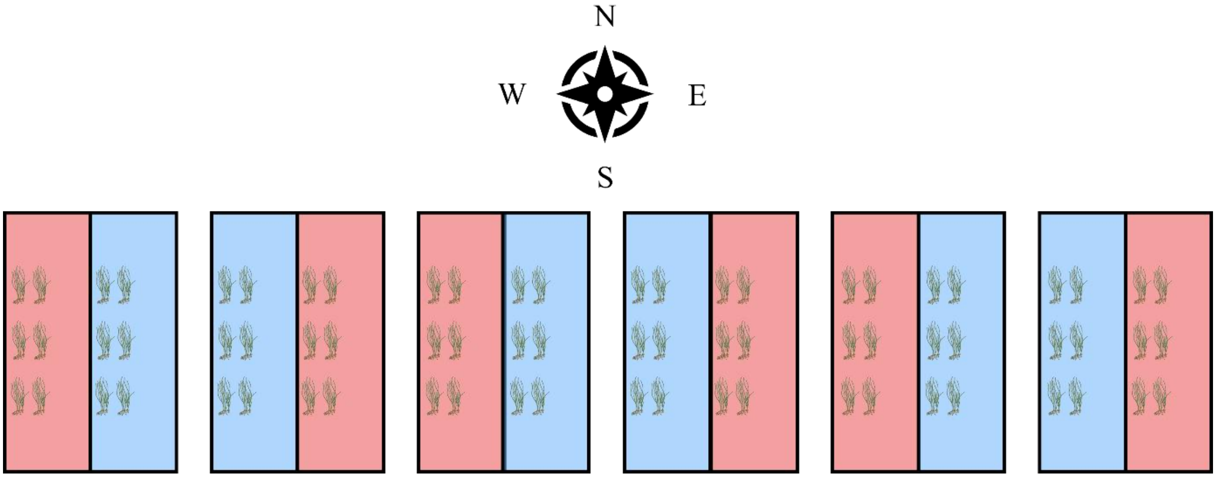

**Chapter III - Supplementary Figure 4:** Temperature (°C, **a**), Salinity (**b**), pH$_{NBS}$ (**c**), and Oxygen concentration (mg L$^{-1}$, **d**) in the Kiel Outdoor Benthocosms subjected to *Ambient* temperatures (blue) and a *Warming* scenario (red) of the Kiel Fjord from February 2019 until June 2020 (See Chapter III - Figure 1 for treatment description). Data are presented as means over all tanks and standard deviation.

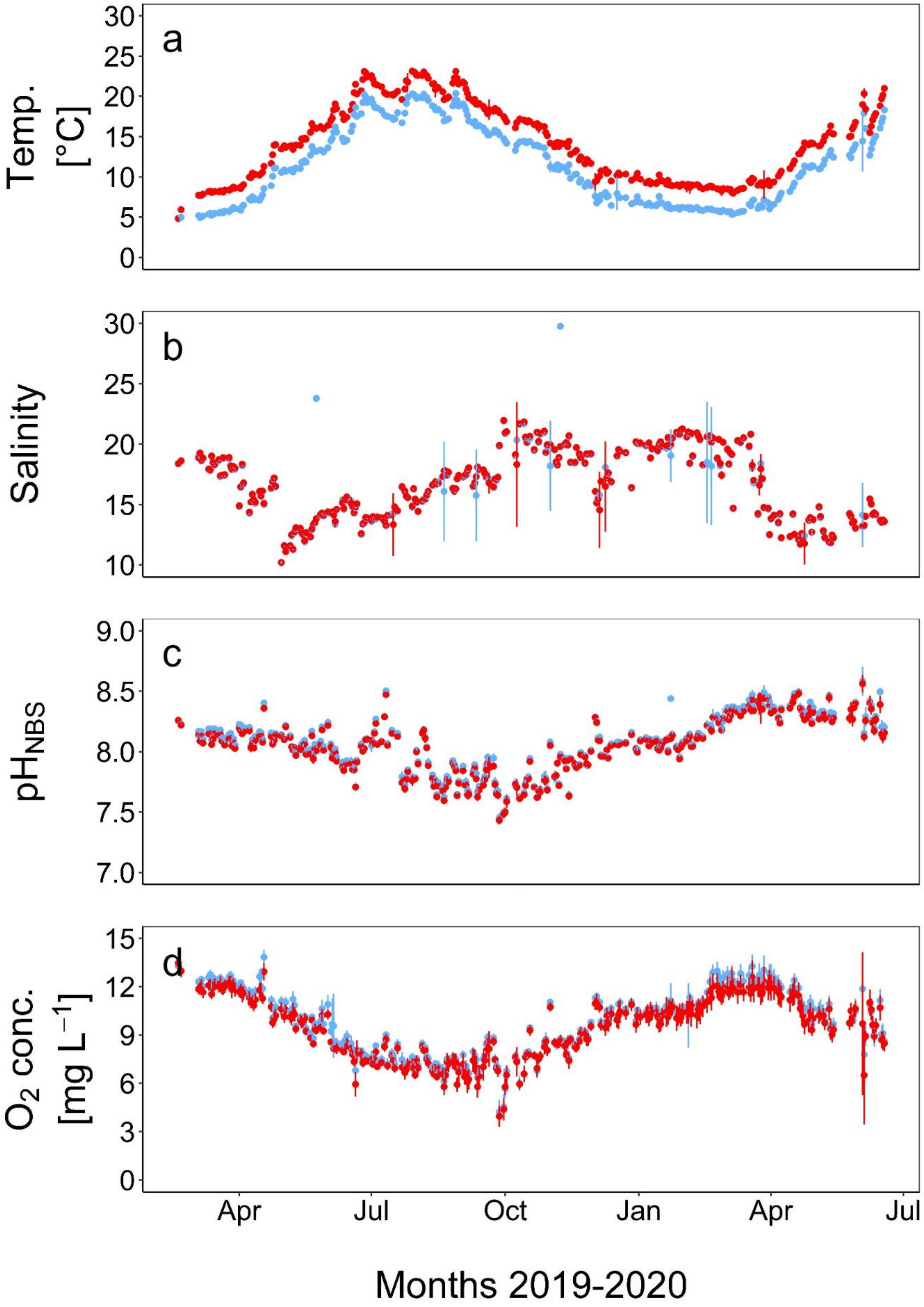

**Chapter III - Supplementary Figure 5:** Continuously logged treatment temperatures in *No* (grey, **a**), *Interrupted* (green, **b**), *Present-day* (red, **c**), and *Extended* (purple, **f**) heatwave treatments and additional hypoxic upwelling treatments without a preceding heatwave (*Upwelling*, blue, **d**) or with a preceding present-day heatwave (*Present-day & Upwelling*, orange, **e**) in the Kiel Indoor Benthocosms (see Chapter III - Figure 2 for treatment descriptions).

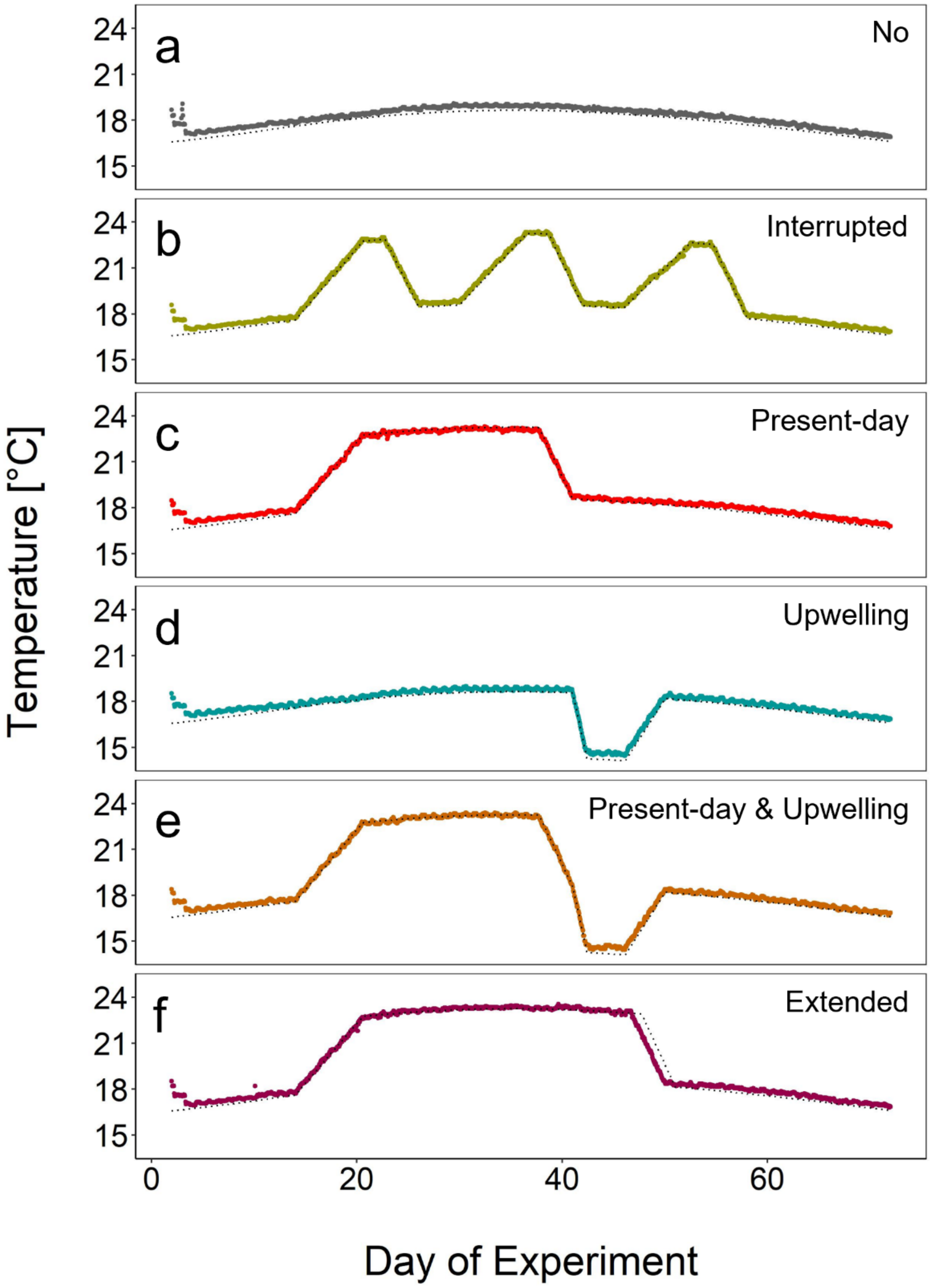

**Chapter III - Supplementary Figure 6:** Temperature (°C, **a**), salinity (**b**), pH (**c**) and oxygen concentration (mg $L^{-1}$, **d**), following *No* (grey), *Interrupted* (green), *Present-day* (red), and *Extended* (purple) heatwave treatments and additional hypoxic upwelling treatments without a preceding heatwave (*Upwelling*, blue) or with a preceding present-day heatwave (*Present-day & Upwelling*, orange) in the Kiel Indoor Benthocosms (see Chapter III - Figure 2 for treatment descriptions). Shown are means and standard deviations (n=12).

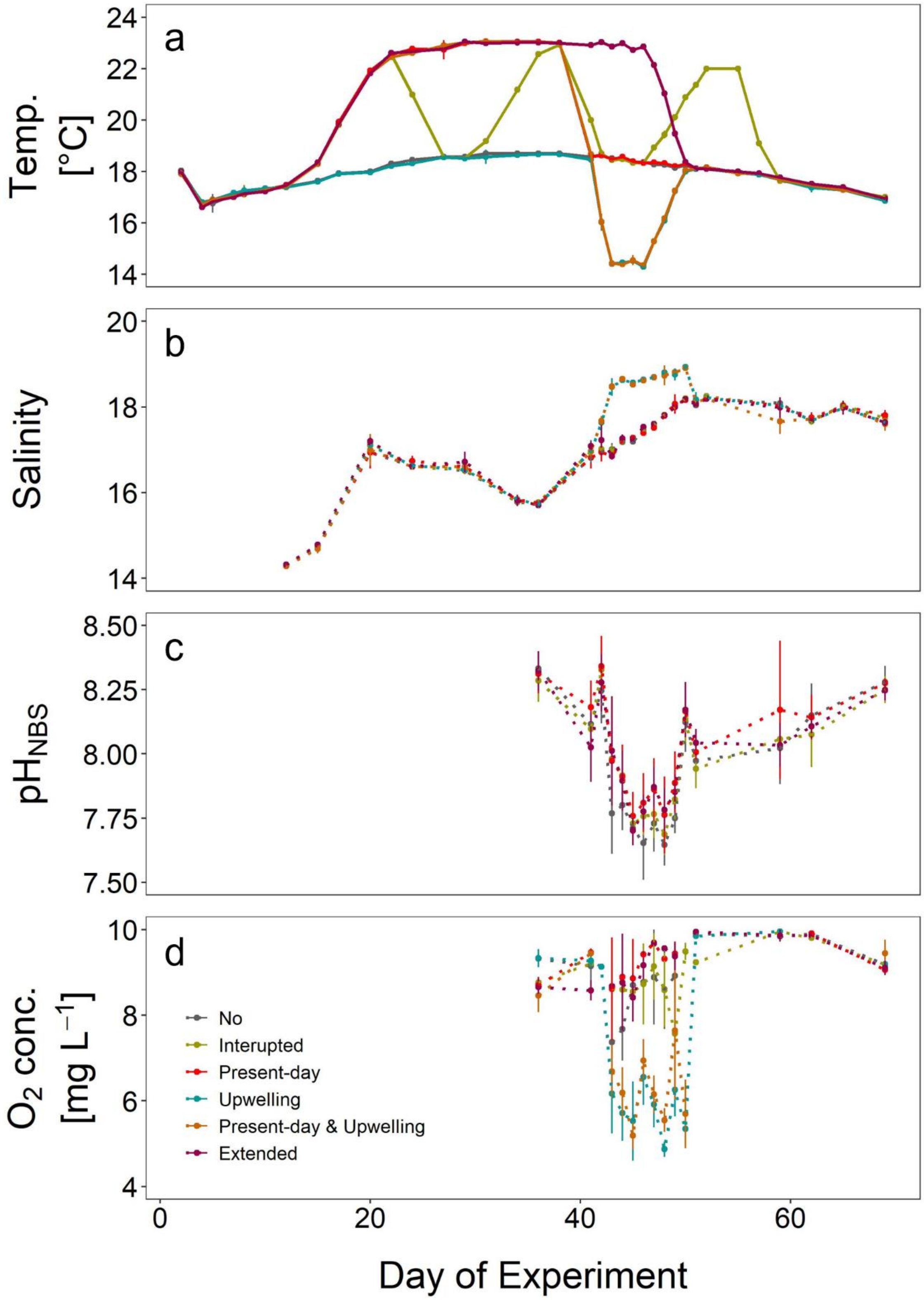

**Chapter III - Supplementary Figure 7:** Differences between the generalized additive mixed effect models (GAMM for absolute growth) of two *Zostera marina* populations coming from outside (**a**, **c**, **e**) and inside a sandbank (**b**, **d**, **f**) throughout 1.5 years of experiment in the Kiel Outdoor Benthocosms, under *Ambient* temperatures and a *Warming* scenario projected for the Kiel Fjord (see Chapter III - Figure 1 for treatment descriptions). Data are represented as model (GAMM) differences between *Ambient* and *Warming* temperature conditions (line) and as 95% confidence intervals (shaded areas; n=6). The red lines represent periods where the models differed.

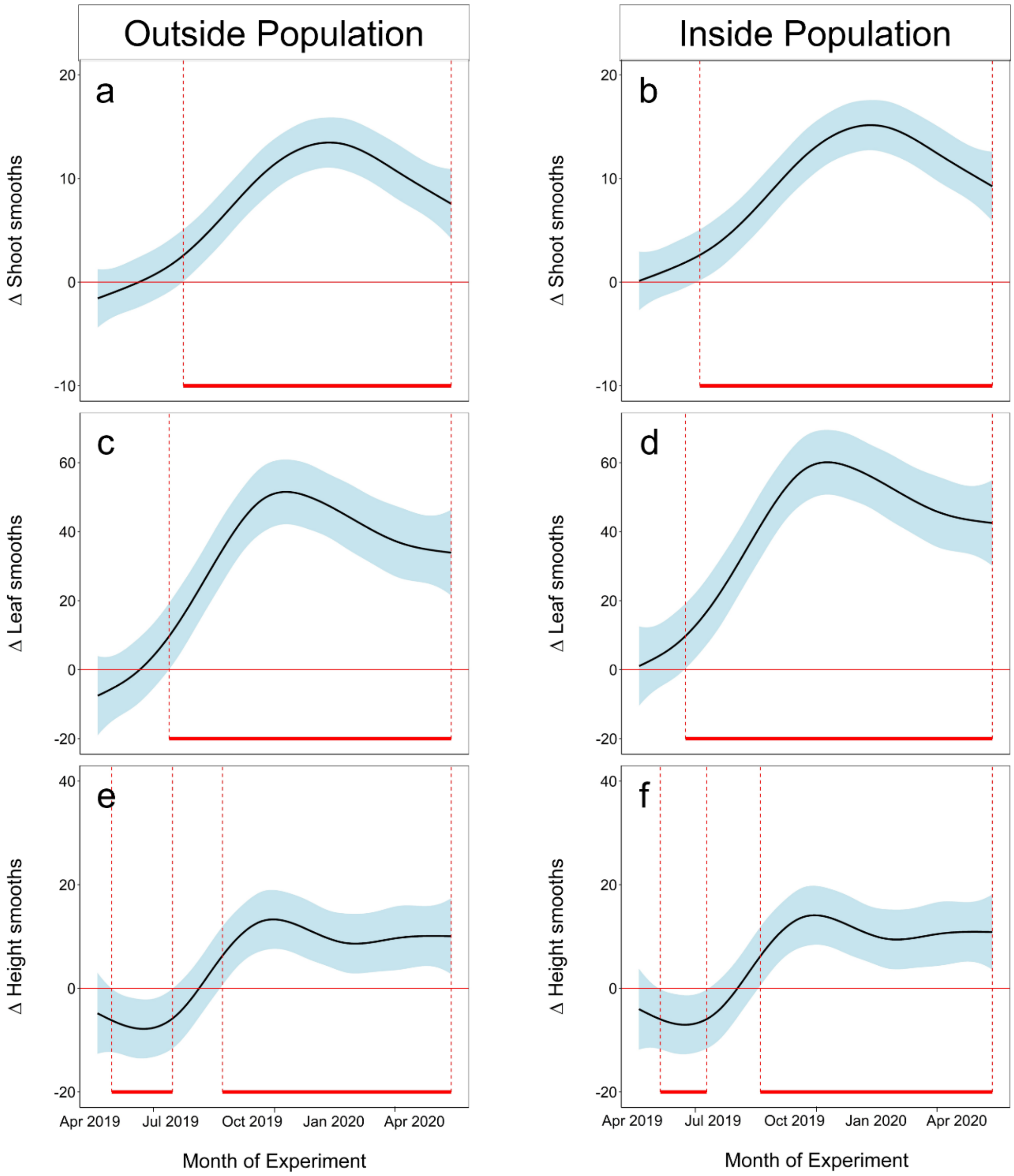

**Chapter III - Supplementary Figure 8:** Relative shoot number (%, **a** and **b**), relative leaf number (%, **c** and **d**), and relative height (%, **e** and **f**) of two *Zostera marina* populations coming from outside (**a**, **c**, **e**) and inside a sandbank (**b**, **d**, **f**) throughout 1.5 years of experiment in the Kiel Outdoor Benthocosms, under *Ambient* Kiel Fjord temperatures (blue for response variable and black solid line for temperature profile in °C) and a *Warming* scenario projected for Kiel Fjord (red for response variable and black dotted line for temperature profile in °C). All growth parameters are relative to the values at the start of the experiment. Data are represented as means (dots) of n=6 experimental tanks. Trends were modelled using generalized additive mixed models (GAMM, explained deviance for relative shoot number (**a-b**) = 79.1%, relative leaf number (**c-d**) = 75.6%, and relative height (**e-f**) = 84.7%). Solid lines show the mean fitted trends and the shaded areas the associated 95% confidence intervals. Differences between *Z. marina* responses subjected to *Ambient* and *Warming* temperature conditions are represented by dashed black lines placed at the bottom of the plots (see Chapter III - Supplementary Figure 9 for further details). Detailed statistical outcomes are presented in Chapter III - Supplementary Table 6.

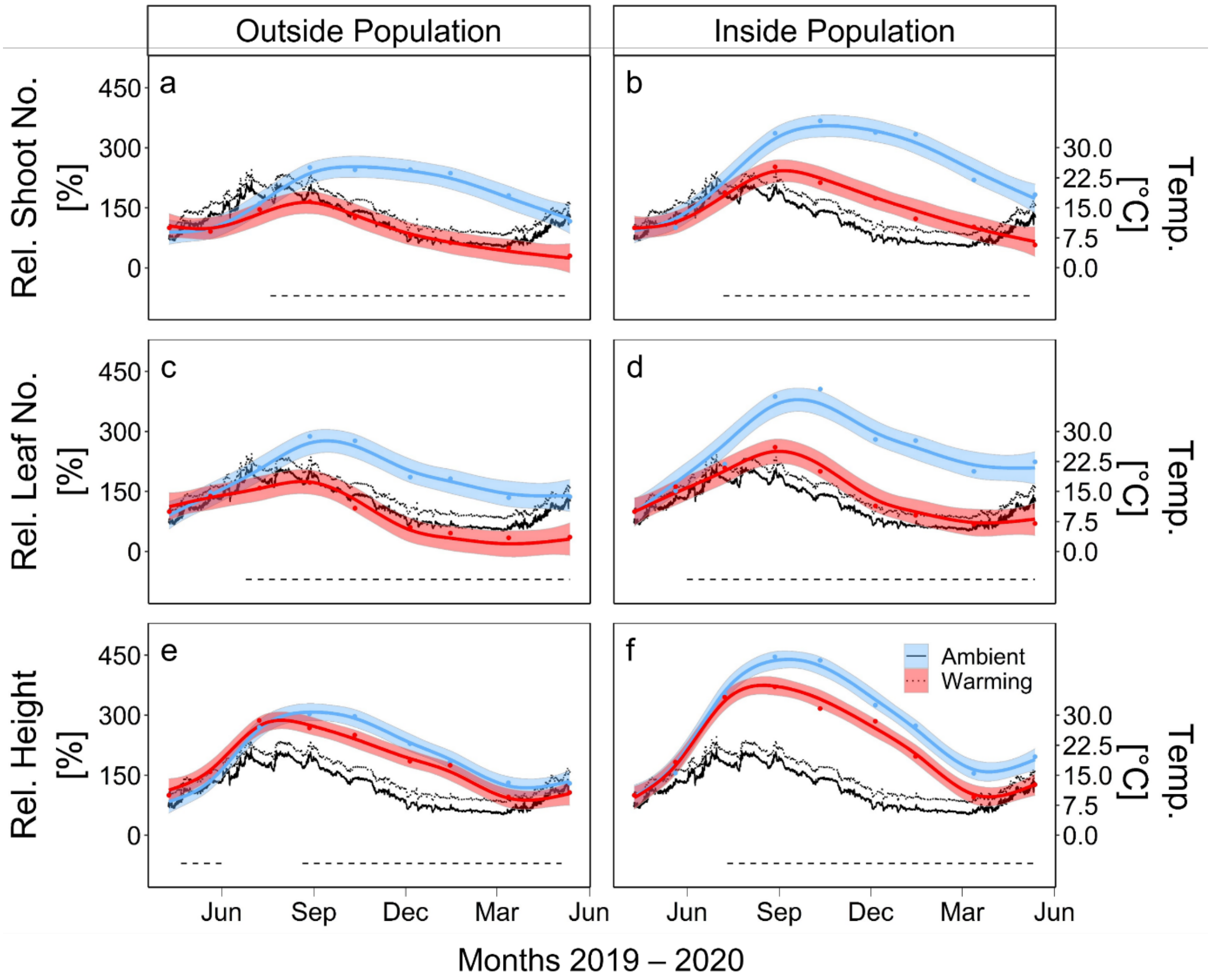

**Chapter III - Supplementary Figure 9:** Differences between the generalized additive mixed effect models (GAMM for relative growth) of two *Zostera marina* populations coming from outside (**a**, **c**, **e**) and inside a sandbank (**b**, **d**, **f**) throughout 1.5 years of experiment in the Kiel Outdoor Benthocosms, under *Ambient* and a *Warming* scenario projected for the Kiel Fjord (see Chapter III - Figure 1 for treatment descriptions). Data are represented as model (GAMM) differences between *Ambient* and *Warming* temperature conditions (line) and as 95% confidence intervals (shaded areas; n=6). The red lines represent periods where the models differed.

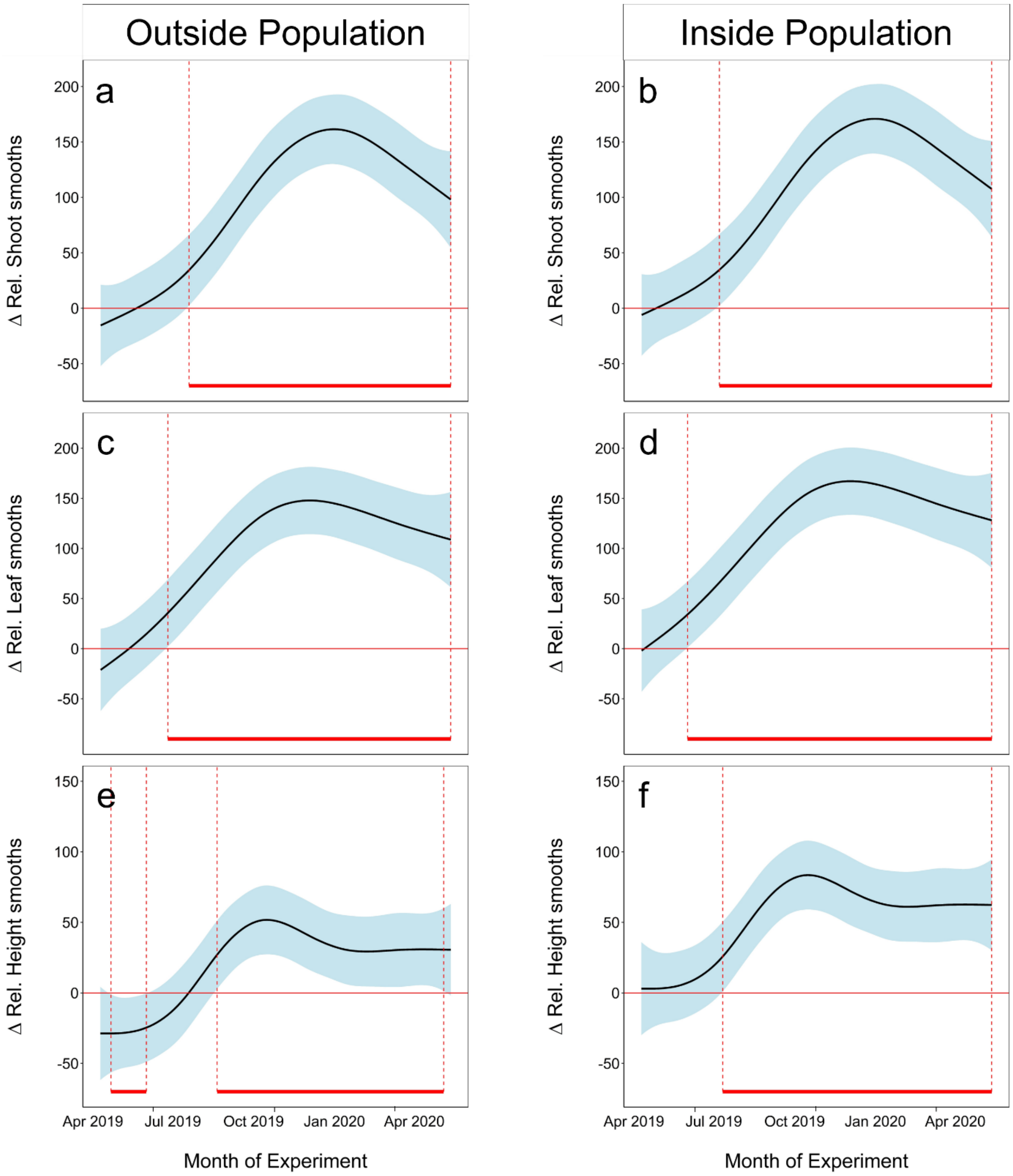

## *Supplementary Tables*

**Chapter III - Supplementary Table 1:** Linear mixed model (LMM) results for the height (cm), shoot number, and leaf number of *Zostera marina* over 68 days of incubation in all treatments in the Kiel Indoor Benthocosms and results of the analyses of variance (ANOVA) of the LMMs. Significant effects are shown in bold.

**LMM Shoot Number**

| | Estimate | Std. Error | df | t-value | p-value |
|---|---|---|---|---|---|
| Intercept | 1.500 | 0.083 | 66 | 18.105 | **<0.001** |
| Interrupted | -0.167 | 0.117 | 66 | -1.422 | 0.160 |
| Present-day | -0.271 | 0.117 | 66 | -2.312 | **0.024** |
| Upwelling | -0.208 | 0.117 | 66 | -1.778 | 0.080 |
| Present-day & Upwelling | -0.375 | 0.117 | 66 | -3.201 | **0.002** |
| Extended | -0.323 | 0.117 | 66 | -2.756 | **0.008** |

**LMM Leaf Number**

| | Estimate | Std. Error | df | t-value | p-value |
|---|---|---|---|---|---|
| Intercept | 6.906 | 0.345 | 66 | 20.032 | **<0.001** |
| Interrupted | -0.635 | 0.488 | 66 | -1.303 | **0.197** |
| Present-day | -1.313 | 0.488 | 66 | -2.692 | **0.009** |
| Upwelling | -0.802 | 0.488 | 66 | -1.645 | 0.105 |
| Present-day & Upwelling | -1.500 | 0.488 | 66 | -3.076 | **0.003** |
| Extended | -1.458 | 0.488 | 66 | -2.991 | **0.004** |

**LMM Height**

| | Estimate | Std. Error | df | t-value | p-value |
|---|---|---|---|---|---|
| Intercept | 41.947 | 2.857 | 282 | 14.682 | **<0.001** |
| Interrupted | -0.212 | 4.040 | 282 | -0.052 | 0.958 |
| Present-day | -0.959 | 4.040 | 282 | -0.237 | 0.812 |
| Upwelling | -3.712 | 4.040 | 282 | -0.919 | 0.359 |
| Present-day & Upwelling | 2.726 | 4.040 | 282 | 0.675 | 0.500 |
| Extended | -1.685 | 4.040 | 282 | -0.417 | 0.677 |

**ANOVA from LMM of Shoot Number**

| | Sum Sq. | Mean Sq. | df num. | df den. | F-value | p-value |
|---|---|---|---|---|---|---|
| Treatments | 0.824 | 0.165 | 5 | 66 | 2.578 | **0.034** |

**ANOVA from LMM of Leaf Number**

| | Sum Sq. | Mean Sq. | df num. | df den. | F-value | p-value |
|---|---|---|---|---|---|---|
| Treatments | 16.873 | 3.375 | 5 | 66 | 2.887 | **0.020** |

**ANOVA from LMM of Height**

| | Sum Sq. | Mean Sq. | df num. | df den. | F-value | p-value |
|---|---|---|---|---|---|---|
| Treatments | 1082.500 | 216.500 | 5 | 282 | 0.553 | 0.736 |

**Chapter III - Supplementary Table 2:** Results of Tukey post-hoc tests after significant analyses of variance (ANOVA) of linear mixed models (LMM) for the height (cm), shoot number, and leaf number of *Zostera marina* over 68 days of incubation in all treatments in the Kiel Indoor Benthocosms. Significant effects are shown in bold.

**Tukey Post-hoc Test Shoot Number**

| Contrast | Estimate | Std. Error | df | t-value | p-value |
|---|---|---|---|---|---|
| No:Interrupted | 0.167 | 0.117 | 66 | 1.422 | 0.713 |
| No:Present-day | 0.271 | 0.117 | 66 | 2.312 | 0.204 |
| No:Upwelling | 0.208 | 0.117 | 66 | 1.778 | 0.487 |
| No:Present-day&Upwelling | 0.375 | 0.117 | 66 | 3.201 | **0.025** |
| No:Extended | 0.323 | 0.117 | 66 | 2.756 | 0.078 |
| Interrupted:Present-day | 0.104 | 0.117 | 66 | 0.889 | 0.948 |
| Interrupted:Upwelling | 0.042 | 0.117 | 66 | 0.356 | 0.999 |
| Interrupted:Present-day&Upwelling | 0.208 | 0.117 | 66 | 1.778 | 0.487 |
| Interrupted:Extended | 0.156 | 0.117 | 66 | 1.334 | 0.765 |
| Present-day:Upwelling | -0.063 | 0.117 | 66 | -0.533 | 0.995 |
| Present-day:Present-day&Upwelling | 0.104 | 0.117 | 66 | 0.889 | 0.948 |
| Present-day:Extended | 0.052 | 0.117 | 66 | 0.445 | 0.998 |
| Upwelling:Present-day&Upwelling | 0.167 | 0.117 | 66 | 1.422 | 0.713 |
| Upwelling:Extended | 0.115 | 0.117 | 66 | 0.978 | 0.923 |
| Present-day&Upwelling:Extended | -0.052 | 0.117 | 66 | -0.445 | 0.998 |

**Tukey Post-hoc Test Leaf Number**

| Contrast | Estimate | Std. Error | df | t-value | p-value |
|---|---|---|---|---|---|
| No:Interrupted | 0.635 | 0.488 | 66 | 1.303 | 0.782 |
| No:Present-day | 1.313 | 0.488 | 66 | 2.692 | 0.091 |
| No:Upwelling | 0.802 | 0.488 | 66 | 1.645 | 0.572 |
| No:Present-day&Upwelling | 1.500 | 0.488 | 66 | 3.076 | **0.035** |
| No:Extended | 1.458 | 0.488 | 66 | 2.991 | **0.043** |
| Interrupted:Present-day | 0.677 | 0.488 | 66 | 1.389 | 0.734 |
| Interrupted:Upwelling | 0.167 | 0.488 | 66 | 0.342 | 0.999 |
| Interrupted:Present-day&Upwelling | 0.865 | 0.488 | 66 | 1.773 | 0.490 |
| Interrupted:Extended | 0.823 | 0.488 | 66 | 1.688 | 0.545 |
| Present-day:Upwelling | -0.510 | 0.488 | 66 | -1.047 | 0.900 |
| Present-day:Present-day&Upwelling | 0.188 | 0.488 | 66 | 0.385 | 0.999 |
| Present-day:Extended | 0.146 | 0.488 | 66 | 0.299 | 1.000 |
| Upwelling:Present-day&Upwelling | 0.698 | 0.488 | 66 | 1.431 | 0.708 |
| Upwelling:Extended | 0.656 | 0.488 | 66 | 1.346 | 0.758 |
| Present-day&Upwelling:Extended | -0.042 | 0.488 | 66 | -0.085 | 1.000 |

**Chapter III - Supplementary Table 3:** Linear mixed model (LMM) results for the $F_{min}$ and Yield of the pulse-amplitude-modulated (PAM) measurements of *Zostera marina* over 68 days of incubation in all treatments in the Kiel Indoor Benthocosms and results of the analyses of variance (ANOVA) of the LMMs. Significant effects are shown in bold.

| **LMM PAM f-min** | | | | | |
|---|---|---|---|---|---|
| | Estimate | Std. Error | df | t-value | p-value |
| Intercept | 444.047 | 13.172 | 570 | 33.712 | **< 0.001** |
| Interrupted | -3.458 | 18.628 | 570 | -0.186 | 0.853 |
| Present-day | 5.786 | 18.628 | 570 | 0.311 | 0.756 |
| Upwelling | 0.099 | 18.628 | 570 | 0.005 | 0.996 |
| Present-day & Upwelling | -14.604 | 18.628 | 570 | -0.784 | 0.433 |
| Extended | -38.422 | 18.628 | 570 | -2.063 | **0.040** |

| **LMM PAM Yield** | | | | | |
|---|---|---|---|---|---|
| | Estimate | Std. Error | df | t-value | p-value |
| Intercept | 781.583 | 2.059 | 66 | 379.604 | **< 0.001** |
| Interrupted | 3.250 | 2.912 | 66 | 1.116 | 0.268 |
| Present-day | -0.620 | 2.912 | 66 | -0.213 | 0.832 |
| Upwelling | -1.026 | 2.912 | 66 | -0.352 | 0.726 |
| Present-day & Upwelling | 3.151 | 2.912 | 66 | 1.082 | 0.283 |
| Extended | 0.958 | 2.912 | 66 | 0.329 | 0.743 |

| **ANOVA from LMM of PAM f-min** | | | | | | |
|---|---|---|---|---|---|---|
| | Sum Sq. | Mean Sq. | df num. | df den. | F-value | p-value |
| Treatments | 125594.000 | 25119.000 | 5 | 570 | 1.508 | 0.185 |

| **ANOVA from LMM of PAM Yield** | | | | | | |
|---|---|---|---|---|---|---|
| | Sum Sq. | Mean Sq. | df num. | df den. | F-value | p-value |
| Treatments | 1277.200 | 255.440 | 5 | 66 | 0.821 | 0.539 |

**Chapter III - Supplementary Table 4:** Linear mixed effect model (LMM) results for the survival, leaf dry weight (natural logarithm, g), and root dry weight (natural logarithm, g) of two *Zostera marina* populations (inside and outside a sandbank) after 1.5 years incubation under *Ambient* temperatures and a *Warming* scenario of the Kiel Fjord in the Kiel Outdoor Benthocosms and results of the analyses of variance (ANOVA) of the LMMs. Significant effects are shown in bold.

**LMM Survival**

| | Estimate | Std. Error | df | t-value | p-value |
|---|---|---|---|---|---|
| Intercept | 71.296 | 19.725 | 19.454 | 3.615 | **0.002** |
| Warming | -46.296 | 27.895 | 19.454 | -1.660 | 0.113 |
| Inside Population | 12.963 | 25.452 | 10.000 | 0.509 | 0.622 |
| Warming:Inside Population | 3.704 | 35.995 | 10.000 | 0.103 | 0.920 |

**LMM Dry weight of leaves**

| | Estimate | Std. Error | df | t-value | p-value |
|---|---|---|---|---|---|
| Intercept | 1.089 | 0.377 | 14.374 | 2.892 | **0.012** |
| Warming | -1.379 | 0.582 | 16.920 | -2.370 | **0.030** |
| Inside Population | -0.810 | 0.462 | 27.269 | -1.755 | 0.091 |
| Warming:Inside Population | 1.617 | 0.761 | 29.817 | 2.126 | **0.042** |

**LMM Dry weight of roots**

| | Estimate | Std. Error | df | t-value | p-value |
|---|---|---|---|---|---|
| Intercept | 0.518 | 0.441 | 13.848 | 1.177 | 0.259 |
| Warming | -1.366 | 0.672 | 15.746 | -2.034 | 0.059 |
| Inside Population | -0.702 | 0.473 | 26.721 | -1.484 | 0.150 |
| Warming:Inside Population | 1.702 | 0.788 | 28.765 | 2.160 | **0.039** |

**ANOVA from LMM Survival**

| | Sum. Sq. | Mean Sq. | df num. | df den. | F-value | p-value |
|---|---|---|---|---|---|---|
| Treatment | 8451.500 | 8451.500 | 1.000 | 10.000 | 4.349 | 0.064 |
| Population | 1316.900 | 1316.900 | 1.000 | 10.000 | 0.678 | 0.430 |
| Treatment:Population | 20.600 | 20.600 | 1.000 | 10.000 | 0.011 | 0.920 |

**ANOVA from LMM Dry weight of leaves**

| | Sum. Sq. | Mean Sq. | df num. | df den. | F-value | p-value |
|---|---|---|---|---|---|---|
| Treatment | 1.568 | 1.568 | 1.000 | 9.631 | 1.405 | 0.264 |
| Population | 0.000 | 0.000 | 1.000 | 29.817 | 0.000 | 0.996 |
| Treatment:Population | 5.043 | 5.043 | 1.000 | 29.817 | 4.518 | **0.042** |

**ANOVA from LMM Dry weight of roots**

| | Sum. Sq. | Mean Sq. | df num. | df den. | F-value | p-value |
|---|---|---|---|---|---|---|
| Treatment | 0.906 | 0.906 | 1.000 | 10.071 | 0.787 | 0.396 |
| Population | 0.165 | 0.165 | 1.000 | 28.765 | 0.143 | 0.708 |
| Treatment:Population | 5.369 | 5.369 | 1.000 | 28.765 | 4.667 | **0.039** |

**Chapter III - Supplementary Table 5:** Generalized additive mixed effect model (GAMM) results for the shoot number, leaf number, and height (cm) of two *Zostera marina* populations (inside and outside a sandbank) over 1.5 years incubation under *Ambient* temperatures and a *Warming* scenario of the Kiel Fjord in the Kiel Outdoor Benthocosms. The GAMM for the height, shoot number, and leaf number had an explained deviance of 86.6%, 78.0%, and 78.9%, respectively. Significant effects are shown in bold.

| **GAMM Shoot Number** | | | | |
|---|---|---|---|---|
| Parametric Coefficients | Estimate | Std. Error | t-value | p-value |
| Intercept | 2.866 | 0.049 | 59.083 | **< 0.001** |
| Warming | -0.604 | 0.059 | -10.194 | **< 0.001** |
| Inside Population | 0.101 | 0.048 | 2.097 | **0.036** |
| Warming:Inside Population | 0.029 | 0.079 | 0.371 | 0.711 |
| Smooth Terms | edf | rdf | F-value | p-value |
| s (Date) | 6.175 | 7.142 | 145.999 | **< 0.001** |
| s (Date):Warming | 2.612 | 3.255 | 107.130 | **< 0.001** |
| s (Date):Inside Population | 2.109 | 2.637 | 14.991 | **0.002** |
| s (Tank) | 0.951 | 1.000 | 19.471 | **< 0.001** |
| **GAMM Leaf Number** | | | | |
| Parametric Coefficients | Estimate | Std. Error | t-value | p-value |
| Intercept | 4.278 | 0.024 | 178.132 | **< 0.001** |
| Warming | -0.648 | 0.029 | -22.023 | **< 0.001** |
| Inside Population | 0.122 | 0.024 | 5.188 | **< 0.001** |
| Warming:Inside Population | -0.019 | 0.039 | -0.475 | 0.635 |
| Smooth Terms | edf | rdf | F-value | p-value |
| s (Date) | 7.402 | 7.845 | 527.426 | **< 0.001** |
| s (Date):Warming | 4.484 | 5.468 | 494.457 | **< 0.001** |
| s (Date):Inside Population | 3.111 | 3.851 | 97.121 | **< 0.001** |
| s (Tank) | 0.983 | 1.000 | 58.061 | **< 0.001** |
| **GAMM Height** | | | | |
| Parametric Coefficients | Estimate | Std. Error | t-value | p-value |
| Intercept | 68.242 | 1.218 | 56.018 | **< 0.001** |
| Warming | -4.546 | 1.730 | -2.628 | **0.009** |
| Inside Population | -13.472 | 1.736 | -7.759 | **< 0.001** |
| Warming:Inside Population | -0.801 | 2.435 | -0.329 | 0.743 |
| Smooth Terms | edf | rdf | F-value | p-value |
| s (Date) | 7.457 | 7.861 | 108.132 | **< 0.001** |
| s (Date):Warming | 4.756 | 5.744 | 7.266 | **< 0.001** |
| s (Date):Inside Population | 1.001 | 1.002 | 7.954 | **0.005** |
| s (Tank) | 0.000 | 1.000 | 0.000 | 0.631 |

**Chapter III - Supplementary Table 6:** Generalized additive mixed effect model (GAMM) results for the relative shoot number, relative leaf number, and relative height (%) of two *Zostera marina* populations (inside and outside a sandbank) over 1.5 years incubation under *Ambient* temperatures and a *Warming* scenario of the Kiel Fjord in the Kiel Outdoor Benthocosms. The GAMM for the relative height, relative shoot number, relative leaf number had an explained deviance of 84.7%, 79.1%, and 75.6%, respectively. Significant effects are shown in bold.

| **GAMM Relative Shoot Number** | | | | |
|---|---|---|---|---|
| Parametric Coefficients | Estimate | Std. Error | t-value | p-value |
| Intercept | 202.943 | 9.325 | 21.764 | **< 0.001** |
| Warming | -83.657 | 10.384 | -8.056 | **< 0.001** |
| Inside Population | 64.481 | 10.165 | 6.344 | **< 0.001** |
| Warming:Inside Population | -9.442 | 14.652 | -0.644 | 0.520 |
| Smooth Terms | edf | rdf | F-value | p-value |
| s (Date) | 5.502 | 6.475 | 16.000 | **< 0.001** |
| s (Date):Warming | 3.834 | 4.674 | 17.343 | **< 0.001** |
| s (Date):Inside Population | 3.118 | 3.833 | 6.317 | **< 0.001** |
| s (Tank) | 0.950 | 1.000 | 18.852 | **< 0.001** |
| **GAMM Relative Leaf Number** | | | | |
| Parametric Coefficients | Estimate | Std. Error | t-value | p-value |
| Intercept | 223.578 | 10.665 | 20.964 | **< 0.001** |
| Warming | -87.481 | 11.666 | -7.499 | **< 0.001** |
| Inside Population | 69.348 | 11.478 | 6.042 | **< 0.001** |
| Warming:Inside Population | -19.238 | 16.475 | -1.168 | 0.244 |
| Smooth Terms | edf | rdf | F-value | p-value |
| s (Date) | 5.532 | 6.515 | 11.878 | **< 0.001** |
| s (Date):Warming | 3.299 | 4.047 | 13.941 | **< 0.001** |
| s (Date):Inside Population | 3.157 | 3.881 | 4.607 | **0.002** |
| s (Tank) | 0.975 | 1.000 | 38.408 | **< 0.001** |
| **GAMM Relative Height** | | | | |
| Parametric Coefficients | Estimate | Std. Error | t-value | p-value |
| Intercept | 203.500 | 7.100 | 28.661 | **< 0.001** |
| Warming | -16.822 | 7.735 | -2.175 | **0.031** |
| Inside Population | 76.731 | 7.754 | 9.896 | **< 0.001** |
| Warming:Inside Population | -31.751 | 10.900 | -2.913 | **0.004** |
| Smooth Terms | edf | rdf | F-value | p-value |
| s (Date) | 6.978 | 7.593 | 37.143 | **< 0.001** |
| s (Date):Warming | 4.247 | 5.172 | 5.572 | **< 0.001** |
| s (Date):Inside Population | 4.610 | 5.570 | 9.368 | **< 0.001** |
| s (Tank) | 0.684 | 1.000 | 2.163 | 0.077 |

## *Supplementary References*

Wolf, Fabian; Seebass, Katja; Pansch, Christian (2022): The Role of Recovery Phases in Mitigating the Negative Impacts of Marine Heatwaves on the Sea Star Asterias rubens. In Front. Mar. Sci. 8, p. 1029. DOI: 10.3389/fmars.2021.790241.

## Supplement to General Discussion

### *Supplementary Figures*

**Discussion - Supplementary Figure 1:** Modelled yearly heatwave frequency (**a**), duration (**b**), maximal intensity (**c**), cumulative intensity (**d**), onset (**e**) and decline rate (**f**) after Hobday et al. (2016), using published data (Wolf et al. 2020) and additional temperature data from 2019-2021 obtained from GEOMAR meteorology department, Sebastian Wahl. The heatwave threshold, however, is based on only the years 1997-2018 (Methods in CHAPTER ). Trends were modelled using Generalized Additive Models (GAMs). Shaded areas represent 95% confidence intervals. Detailed statistical results are given in Discussion - Supplementary Table 1.

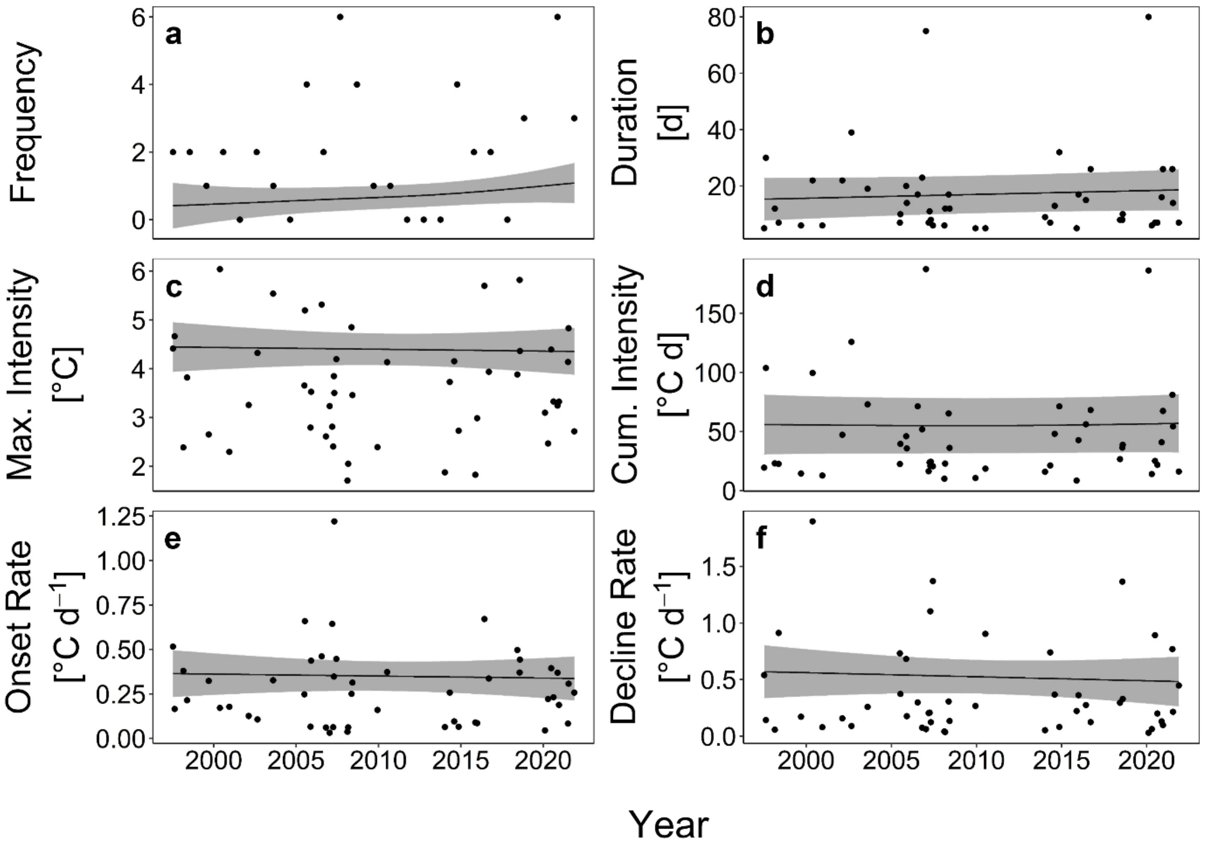

**Discussion - Supplementary Figure 2:** Modelled yearly cold-spell frequency (**a**), duration (**b**), maximal intensity (**c**), cumulative intensity (**d**), onset (**e**) and decline rate (**f**) after Hobday et al. (2016), using published data (Wolf et al. 2020) and additional temperature data from 2019-2021 obtained from GEOMAR meteorology department, Sebastian Wahl. The cold-spell threshold, however, is based on only the years 1997-2018 (Methods in CHAPTER ). Trends were modelled using Generalized Additive Models (GAMs). Shaded areas represent 95% confidence intervals. Detailed statistical results are given in Discussion - Supplementary Table 2.

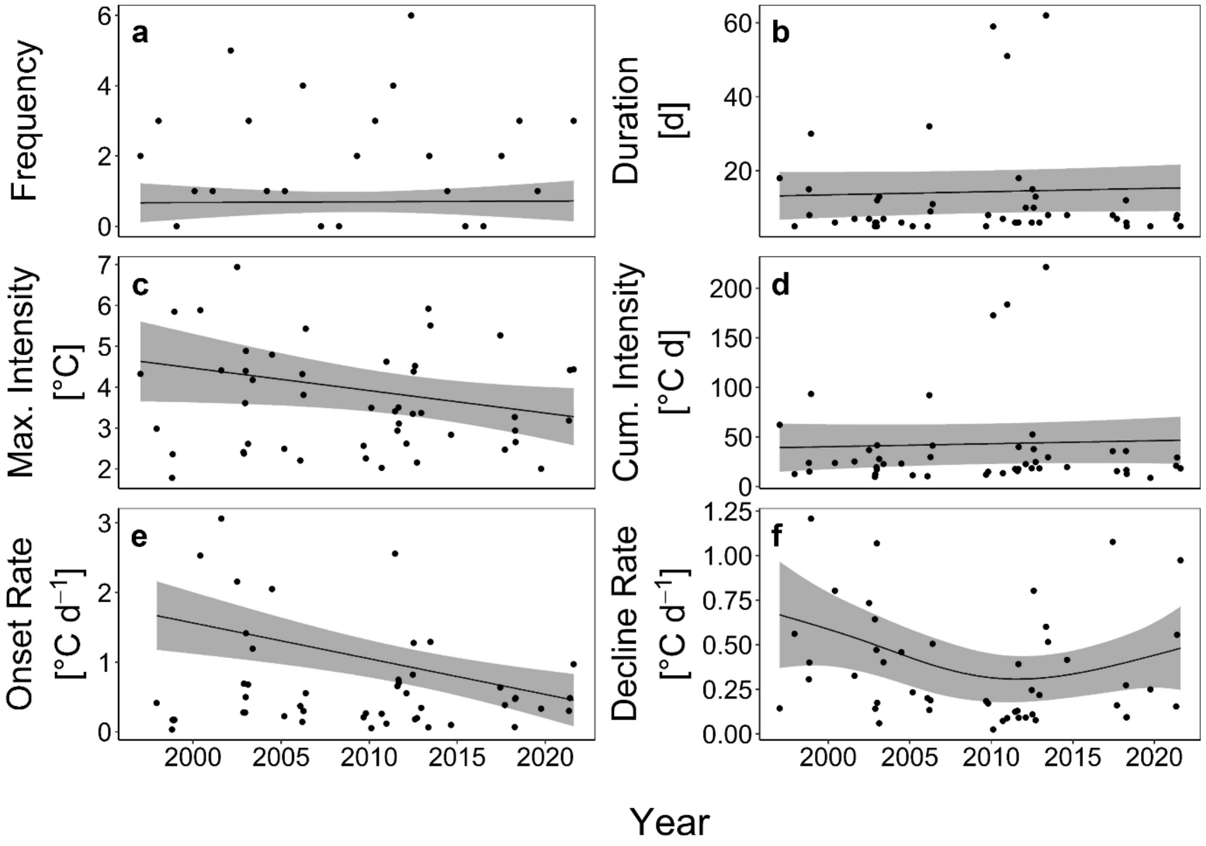

**Discussion - Supplementary Figure 3:** Recorded Temperatures (°C; solid black lines) in 1.8 m depth in the Kiel Fjord, Germany at the GEOMAR pier (N54° 19' 45.97" E10° 8' 58.582"; Wolf et al. 2020 and additional temperature data from 2019-2021 obtained from GEOMAR meteorology department, Sebastian Wahl) of the years 1997 until 2021. This dataset was analysed on the occurrences of heatwaves and cold spells after Hobday et al. (2016). Based on this modelling the 25-year climatological values are represented as grey solid line, whereas the thresholds for heatwaves (i.e., 90th percentile) and cold-spells (i.e., 10th percentile) are represented as dotted lines. Temperatures above the climatological values, but below the 90th percentile are shown in orange, whereas temperatures above the 90th percentile are shown in red. Temperatures below the climatological trend, but above the 10th percentile are shown in light-blue, whereas temperatures below the 10th percentile are shown in dark-blue.

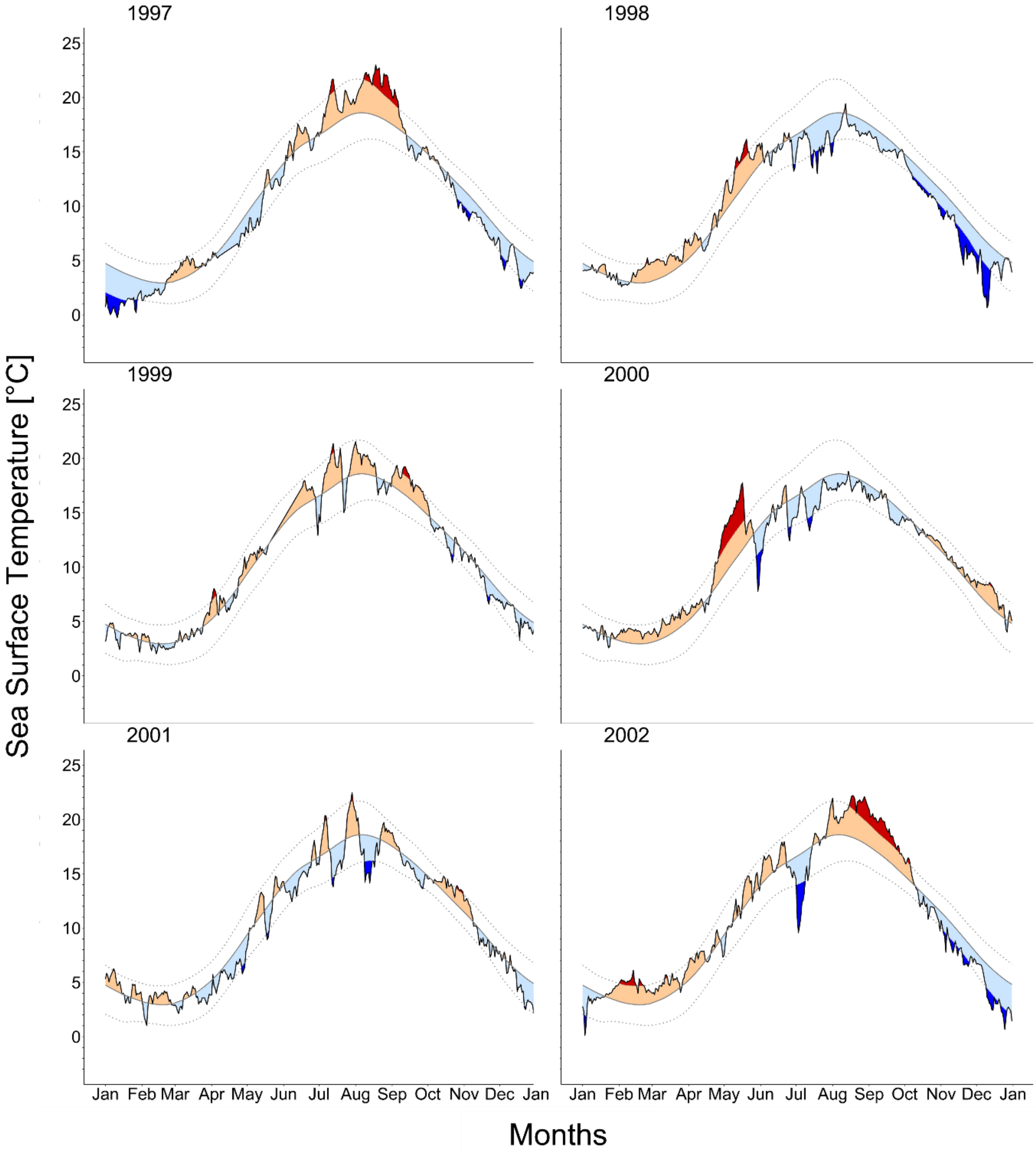

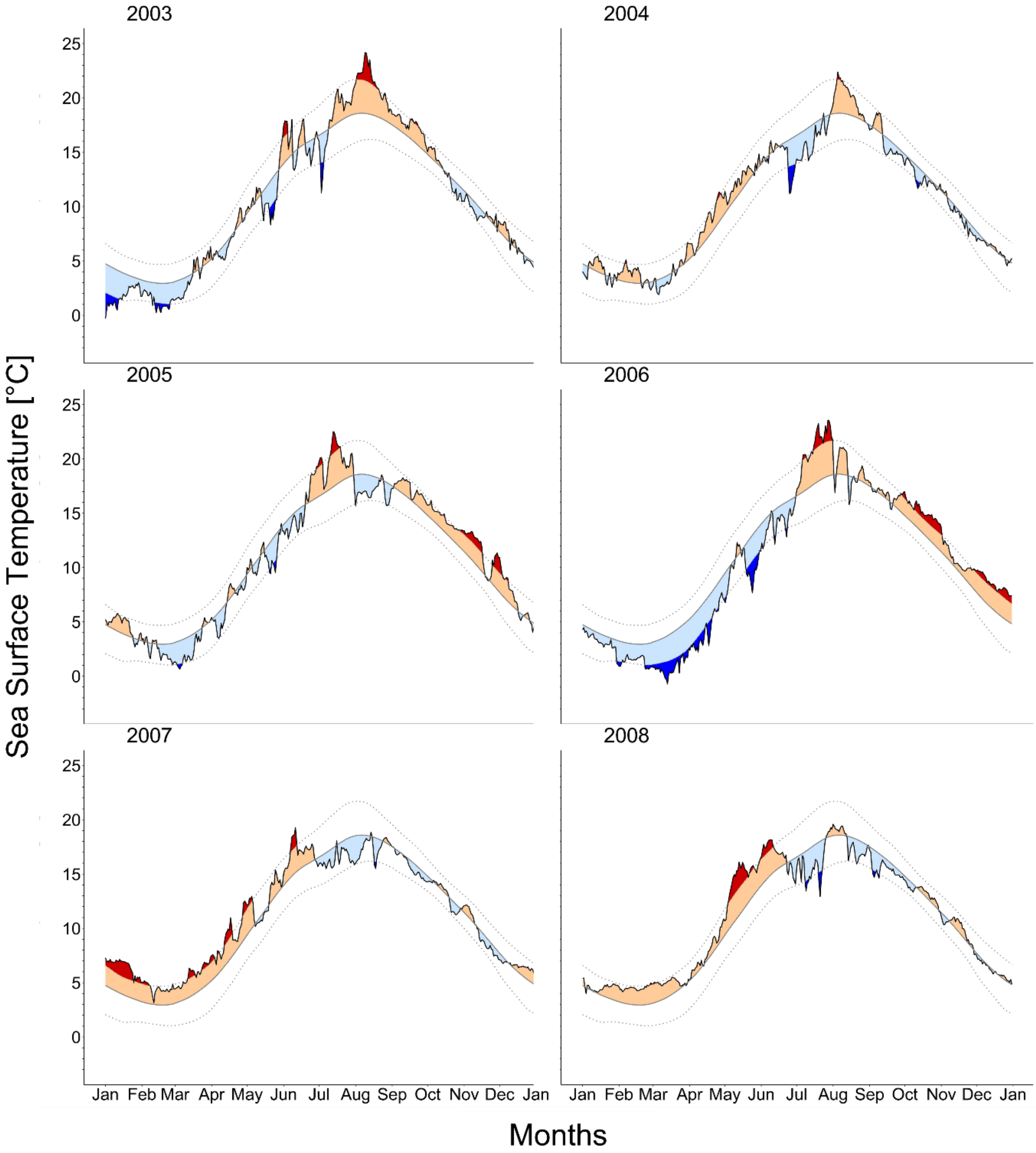
2003
2004
2005
2006
2007
2008
25
20
15
10
5
0
Sea Surface Temperature [°C]
Jan Feb Mar Apr May Jun Jul Aug Sep Oct Nov Dec Jan
Months

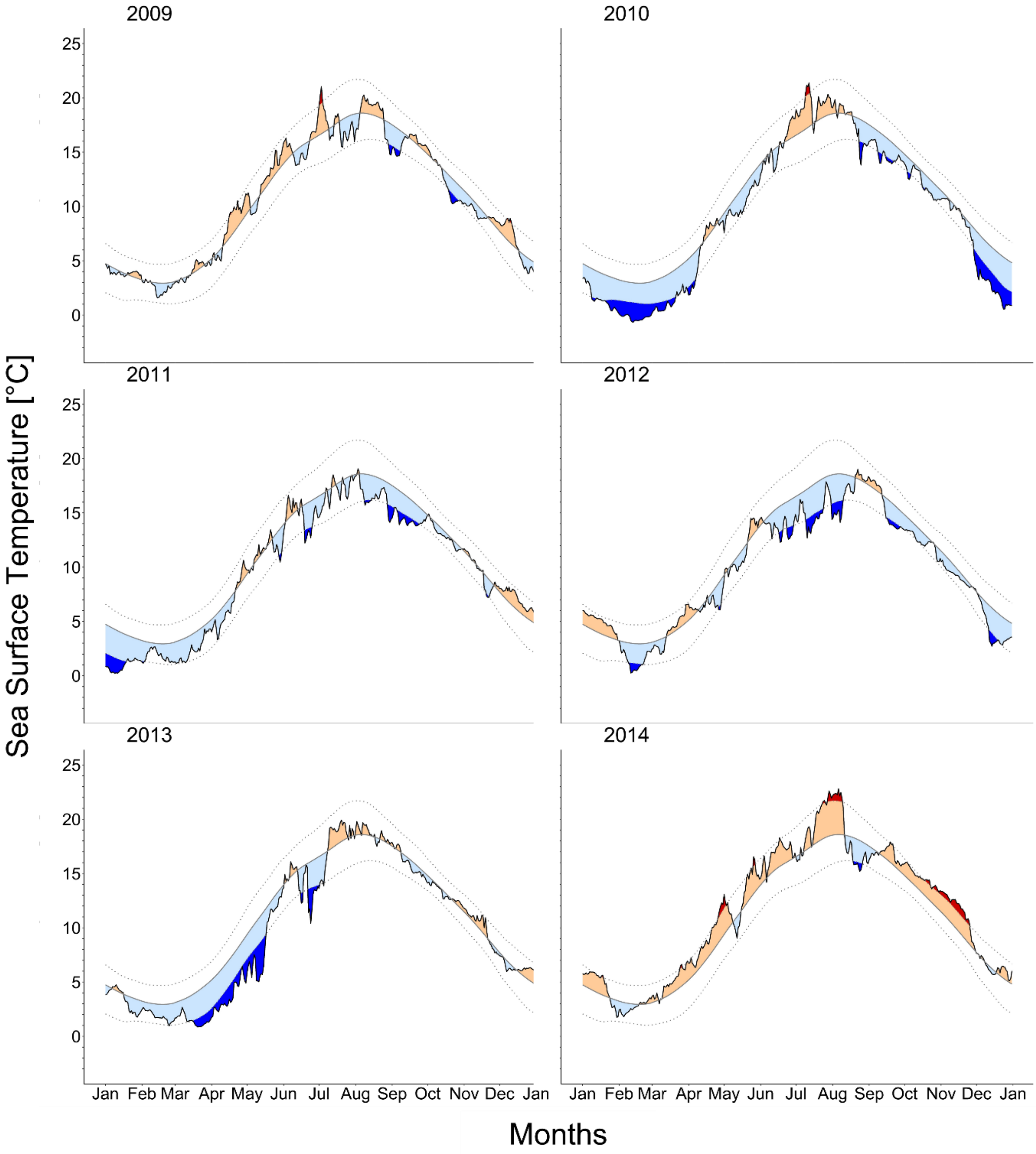
2009
2010
2011
2012
2013
2014
25
20
15
10
5
0
Sea Surface Temperature [°C]
Jan Feb Mar Apr May Jun Jul Aug Sep Oct Nov Dec Jan
Months

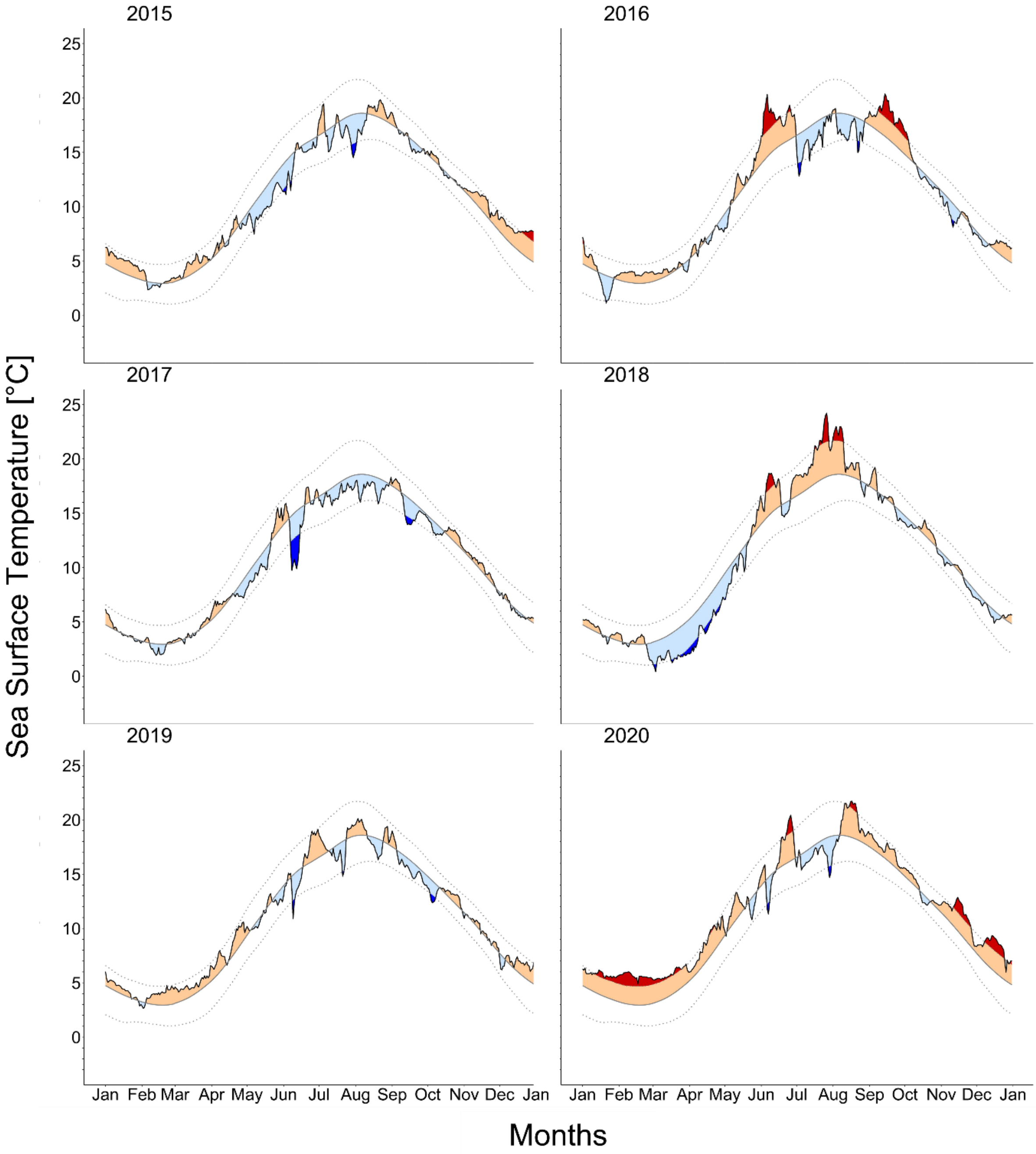
2015
2016
2017
2018
2019
2020
Sea Surface Temperature [°C]
0
5
10
15
20
25
Jan Feb Mar Apr May Jun Jul Aug Sep Oct Nov Dec Jan
Months

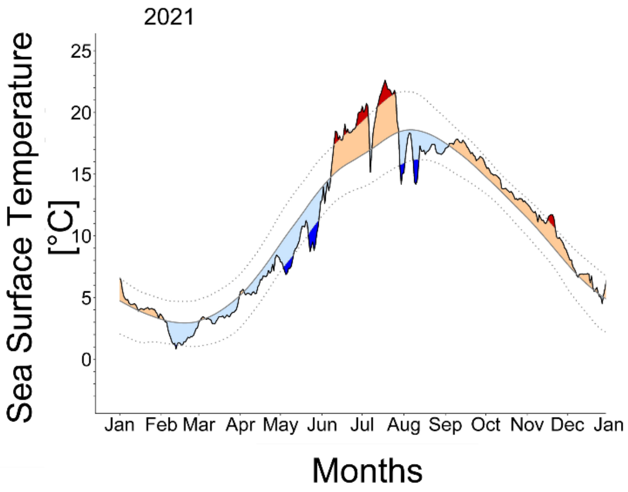
2021
Sea Surface Temperature [°C]
25
20
15
10
5
0
Jan
Feb
Mar
Apr
May
Jun
Jul
Aug
Sep
Oct
Nov
Dec
Jan
Months

## *Supplementary Tables*

**Discussion - Supplementary Table 1:** Generalized Additive Model (GAM) results for heatwave frequency, duration, maximal intensity, cumulative intensity, onset rate and decline rate. Heatwave characteristics are based on the analysis of 25-years of temperature data, while the threshold for heatwaves is based on 22-years. The GAM for frequency, duration, maximal intensity, cumulative intensity, onset rate and decline rate had an explained deviance of 5.8%, 4.7%, 53.6%, -2.4%, 20.7% and 28.3%, respectively.

| **GAM Frequency** | | | | |
|---|---|---|---|---|
| ***Parametric Coefficients*** | ***Estimate*** | ***Std. Error*** | ***t-value*** | ***p-value*** |
| Intercept | 0.675 | 0.147 | 4.598 | **<0.001** |
| ***Smooth Terms*** | ***Estimated d.f.*** | ***Reference d.f.*** | ***F-value*** | ***p-value*** |
| s (Year) | 1.344 | 1.608 | 2.291 | 0.303 |
| **GAM Duration** | | | | |
| ***Parametric Coefficients*** | ***Estimate*** | ***Std. Error*** | ***t-value*** | ***p-value*** |
| Intercept | 17.942 | 3.284 | 5.463 | **<0.001** |
| ***Smooth Terms*** | ***Estimated d.f.*** | ***Reference d.f.*** | ***F-value*** | ***p-value*** |
| s (Peak Date) | 1.000 | 1.000 | 0.970 | 0.330 |
| s (Month) | 1.636 | 1.961 | 2.141 | 0.103 |
| **GAM Maximal Intensity** | | | | |
| ***Parametric Coefficients*** | ***Estimate*** | ***Std. Error*** | ***t-value*** | ***p-value*** |
| Intercept | 3.616 | 0.114 | 31.751 | **<0.001** |
| ***Smooth Terms*** | ***Estimated d.f.*** | ***Reference d.f.*** | ***F-value*** | ***p-value*** |
| s (Peak Date) | 1.000 | 1.000 | 0.059 | 0.810 |
| s (Month) | 2.694 | 2.926 | 16.378 | **<0.001** |
| **GAM Cumulative Intensity** | | | | |
| ***Parametric Coefficients*** | ***Estimate*** | ***Std. Error*** | ***t-value*** | ***p-value*** |
| Intercept | 52.066 | 11.515 | 4.522 | **<0.001** |
| ***Smooth Terms*** | ***Estimated d.f.*** | ***Reference d.f.*** | ***F-value*** | ***p-value*** |
| s (Peak Date) | 1.203 | 1.373 | 0.095 | 0.912 |
| s (Month) | 1.944 | 2.281 | 3.503 | **0.036** |
| **GAM Onset Rate** | | | | |
| ***Parametric Coefficients*** | ***Estimate*** | ***Std. Error*** | ***t-value*** | ***p-value*** |
| Intercept | 0.280 | 0.030 | 9.463 | **<0.001** |
| ***Smooth Terms*** | ***Estimated d.f.*** | ***Reference d.f.*** | ***F-value*** | ***p-value*** |
| s (Peak Date) | 1.000 | 1.000 | 0.076 | 0.784 |
| s (Month) | 2.431 | 2.758 | 4.186 | **0.039** |
| **GAM Decline Rate** | | | | |
| ***Parametric Coefficients*** | ***Estimate*** | ***Std. Error*** | ***t-value*** | ***p-value*** |
| Intercept | 0.385 | 0.052 | 7.340 | **<0.001** |
| ***Smooth Terms*** | ***Estimated d.f.*** | ***Reference d.f.*** | ***F-value*** | ***p-value*** |
| s (Peak Date) | 1.000 | 1.000 | 0.252 | 0.618 |
| s (Month) | 2.657 | 2.907 | 6.022 | **0.007** |

**Discussion - Supplementary Table 2:** Generalized Additive Model (GAM) results for cold-spell frequency, duration, maximal intensity, cumulative intensity, onset rate and decline rate. Cold-spell characteristics are based on the analysis of 25-years of temperature data, while the threshold for cold-spells is based on 22-years. The GAM for frequency, duration, maximal intensity, cumulative intensity, onset rate and decline rate had an explained deviance of 0.0%, -3.93%, 22.4%, -3.12%, 34.5% and 31.1%, respectively.

| | | | | |
|---|---|---|---|---|
| **GAM Frequency** | | | | |
| ***Parametric Coefficients*** | ***Estimate*** | ***Std. Error*** | ***t-value*** | ***p-value*** |
| Intercept | 0.651 | 0.145 | 4.506 | **<0.001** |
| ***Smooth Terms*** | ***Estimated d.f.*** | ***Reference d.f.*** | ***F-value*** | ***p-value*** |
| s (Year) | 1.000 | 1.000 | 0.116 | 0.734 |
| **GAM Duration** | | | | |
| ***Parametric Coefficients*** | ***Estimate*** | ***Std. Error*** | ***t-value*** | ***p-value*** |
| Intercept | 14.290 | 2.913 | 4.906 | **<0.001** |
| ***Smooth Terms*** | ***Estimated d.f.*** | ***Reference d.f.*** | ***F-value*** | ***p-value*** |
| s (Peak Date) | 1.000 | 1.000 | 0.589 | 0.447 |
| s (Month) | 1.000 | 1.000 | 0.498 | 0.484 |
| **GAM Maximal Intensity** | | | | |
| ***Parametric Coefficients*** | ***Estimate*** | ***Std. Error*** | ***t-value*** | ***p-value*** |
| Intercept | 3.652 | 0.166 | 22.028 | **<0.001** |
| ***Smooth Terms*** | ***Estimated d.f.*** | ***Reference d.f.*** | ***F-value*** | ***p-value*** |
| s (Peak Date) | 1.000 | 1.000 | 3.941 | 0.054 |
| s (Month) | 2.635 | 2.908 | 3.480 | **0.032** |
| **GAM Cumulative Intensity** | | | | |
| ***Parametric Coefficients*** | ***Estimate*** | ***Std. Error*** | ***t-value*** | ***p-value*** |
| Intercept | 42.930 | 10.298 | 4.169 | **<0.001** |
| ***Smooth Terms*** | ***Estimated d.f.*** | ***Reference d.f.*** | ***F-value*** | ***p-value*** |
| s (Peak Date) | 1.000 | 1.001 | 0.339 | 0.563 |
| s (Month) | 1.000 | 1.000 | 0.347 | 0.559 |
| **GAM Onset Rate** | | | | |
| ***Parametric Coefficients*** | ***Estimate*** | ***Std. Error*** | ***t-value*** | ***p-value*** |
| Intercept | 0.674 | 0.089 | 7.611 | **<0.001** |
| ***Smooth Terms*** | ***Estimated d.f.*** | ***Reference d.f.*** | ***F-value*** | ***p-value*** |
| s (Peak Date) | 1.000 | 1.000 | 11.944 | **0.001** |
| s (Month) | 2.499 | 2.830 | 6.286 | **0.002** |
| **GAM Decline Rate** | | | | |
| ***Parametric Coefficients*** | ***Estimate*** | ***Std. Error*** | ***t-value*** | ***p-value*** |
| Intercept | 0.357 | 0.038 | 9.354 | **<0.001** |
| ***Smooth Terms*** | ***Estimated d.f.*** | ***Reference d.f.*** | ***F-value*** | ***p-value*** |
| s (Peak Date) | 2.336 | 2.861 | 2.555 | 0.059 |
| s (Month) | 2.315 | 2.695 | 4.003 | 0.057 |

**Discussion - Supplementary Table 3:** Generalized Additive Model (GAM) results for heatwave frequency, duration, maximal intensity, cumulative intensity, onset rate and decline rate. Heatwave characteristics and thresholds are based on the analysis of 25-years of temperature data. The GAM for frequency, duration, maximal intensity, cumulative intensity, onset rate and decline rate had an explained deviance of 36.2%, 40.9%, 37.4%, 6.6%, 16.4% and 23.7%, respectively.

| **GAM Frequency** | | | | |
|---|---|---|---|---|
| ***Parametric Coefficients*** | ***Estimate*** | ***Std. Error*** | ***t-value*** | ***p-value*** |
| Intercept | 0.573 | 0.160 | 3.575 | **<0.001** |
| ***Smooth Terms*** | ***Estimated d.f.*** | ***Reference d.f.*** | ***F-value*** | ***p-value*** |
| s (Year) | 1.000 | 1.000 | 0.000 | 0.992 |
| **GAM Duration** | | | | |
| ***Parametric Coefficients*** | ***Estimate*** | ***Std. Error*** | ***t-value*** | ***p-value*** |
| Intercept | 16.327 | 3.041 | 5.369 | **<0.001** |
| ***Smooth Terms*** | ***Estimated d.f.*** | ***Reference d.f.*** | ***F-value*** | ***p-value*** |
| s (Peak Date) | 1.000 | 1.000 | 0.019 | 0.891 |
| s (Month) | 1.712 | 2.040 | 1.892 | 0.177 |
| **GAM Maximal Intensity** | | | | |
| ***Parametric Coefficients*** | ***Estimate*** | ***Std. Error*** | ***t-value*** | ***p-value*** |
| Intercept | 3.642 | 0.130 | 27.980 | **<0.001** |
| ***Smooth Terms*** | ***Estimated d.f.*** | ***Reference d.f.*** | ***F-value*** | ***p-value*** |
| s (Peak Date) | 1.000 | 1.001 | 0.000 | 0.999 |
| s (Month) | 2.689 | 2.924 | 14.939 | **<0.001** |
| **GAM Cumulative Intensity** | | | | |
| ***Parametric Coefficients*** | ***Estimate*** | ***Std. Error*** | ***t-value*** | ***p-value*** |
| Intercept | 47.875 | 9.720 | 4.925 | **<0.001** |
| ***Smooth Terms*** | ***Estimated d.f.*** | ***Reference d.f.*** | ***F-value*** | ***p-value*** |
| s (Peak Date) | 1.000 | 1.000 | 0.299 | 0.588 |
| s (Month) | 1.669 | 1.993 | 1.795 | 0.200 |
| **GAM Onset Rate** | | | | |
| ***Parametric Coefficients*** | ***Estimate*** | ***Std. Error*** | ***t-value*** | ***p-value*** |
| Intercept | 0.291 | 0.035 | 8.323 | **<0.001** |
| ***Smooth Terms*** | ***Estimated d.f.*** | ***Reference d.f.*** | ***F-value*** | ***p-value*** |
| s (Peak Date) | 1.000 | 1.000 | 0.087 | 0.770 |
| s (Month) | 2.381 | 2.722 | 4.103 | **0.040** |
| **GAM Decline Rate** | | | | |
| ***Parametric Coefficients*** | ***Estimate*** | ***Std. Error*** | ***t-value*** | ***p-value*** |
| Intercept | 0.401 | 0.062 | 6.495 | **<0.001** |
| ***Smooth Terms*** | ***Estimated d.f.*** | ***Reference d.f.*** | ***F-value*** | ***p-value*** |
| s (Peak Date) | 1.000 | 1.000 | 0.017 | 0.899 |
| s (Month) | 2.615 | 2.885 | 4.849 | **0.023** |

**Discussion - Supplementary Table 4:** Generalized Additive Model (GAM) results for cold-spell frequency, duration, maximal intensity, cumulative intensity, onset rate and decline rate. Cold-spell characteristics and thresholds are based on the analysis of 25-years of temperature data. The GAM for frequency, duration, maximal intensity, cumulative intensity, onset rate and decline rate had an explained deviance of 0.1%, -3.4%, 18.9%, -2.8%, 32.6% and 30.7%, respectively.

| **GAMM Frequency** | | | | |
|---|---|---|---|---|
| ***Parametric Coefficients*** | ***Estimate*** | ***Std. Error*** | ***t-value*** | ***p-value*** |
| Intercept | 0.693 | 0.144 | 4.800 | **<0.001** |
| ***Smooth Terms*** | ***Estimated d.f.*** | ***Reference d.f.*** | ***F-value*** | ***p-value*** |
| s (Year) | 1.000 | 1.000 | 0.021 | 0.885 |
| **GAMM Duration** | | | | |
| ***Parametric Coefficients*** | ***Estimate*** | ***Std. Error*** | ***t-value*** | ***p-value*** |
| Intercept | 16.463 | 3.520 | 4.677 | **<0.001** |
| ***Smooth Terms*** | ***Estimated d.f.*** | ***Reference d.f.*** | ***F-value*** | ***p-value*** |
| s (Peak Date) | 1.573 | 1.949 | 1.907 | 0.204 |
| s (Month) | 1.000 | 1.000 | 0.179 | 0.675 |
| **GAMM Maximal Intensity** | | | | |
| ***Parametric Coefficients*** | ***Estimate*** | ***Std. Error*** | ***t-value*** | ***p-value*** |
| Intercept | 3.709 | 0.170 | 21.781 | **<0.001** |
| ***Smooth Terms*** | ***Estimated d.f.*** | ***Reference d.f.*** | ***F-value*** | ***p-value*** |
| s (Peak Date) | 1.000 | 1.000 | 3.029 | 0.089 |
| s (Month) | 2.547 | 2.857 | 2.768 | 0.065 |
| **GAMM Cumulative Intensity** | | | | |
| ***Parametric Coefficients*** | ***Estimate*** | ***Std. Error*** | ***t-value*** | ***p-value*** |
| Intercept | 49.079 | 14.418 | 3.404 | **0.001** |
| ***Smooth Terms*** | ***Estimated d.f.*** | ***Reference d.f.*** | ***F-value*** | ***p-value*** |
| s (Peak Date) | 1.001 | 1.003 | 1.754 | 0.192 |
| s (Month) | 1.000 | 1.000 | 0.022 | 0.884 |
| **GAMM Onset Rate** | | | | |
| ***Parametric Coefficients*** | ***Estimate*** | ***Std. Error*** | ***t-value*** | ***p-value*** |
| Intercept | 0.661 | 0.090 | 7.312 | **<0.001** |
| ***Smooth Terms*** | ***Estimated d.f.*** | ***Reference d.f.*** | ***F-value*** | ***p-value*** |
| s (Peak Date) | 1.000 | 1.000 | 9.774 | **0.003** |
| s (Month) | 2.453 | 2.794 | 5.878 | **0.002** |
| **GAMM Decline Rate** | | | | |
| ***Parametric Coefficients*** | ***Estimate*** | ***Std. Error*** | ***t-value*** | ***p-value*** |
| Intercept | 0.353 | 0.038 | 9.234 | **<0.001** |
| ***Smooth Terms*** | ***Estimated d.f.*** | ***Reference d.f.*** | ***F-value*** | ***p-value*** |
| s (Peak Date) | 2.402 | 2.934 | 2.903 | 0.061 |
| s (Month) | 2.208 | 2.600 | 1.977 | 0.083 |

**Discussion - Supplementary Table 5:** Heatwave characteristics (minimal, mean, and maximal values) modelled after Hobday et al. (2016) using published data (Wolf et al. 2020) and additional temperature data from 2019-2021 obtained from GEOMAR meteorology department, Sebastian Wahl, separated after seasons or summarized over the year. Frequency represents the number of events per year or season, the duration represents the time of the events (days), intensity represents the amplitude above the climatological values (°C), onset rate represents the increase of temperature from the time crossing the 90th percentile until the maximum of the event (°C per day) and the decline rate represents the decrease of temperature from the maximum of the event until the time it crosses the 90th percentile (°C per day). For a detailed description of the traits see Figure 1 in Hobday et al. (2016).

| Trait | Trait Characteristic | Annual | Spring | Summer | Fall | Winter |
|---|---|---|---|---|---|---|
| Frequency | Minimal | 0.0 | 0.0 | 0.0 | 0.0 | 0.0 |
| | Mean | 1.8 | 0.4 | 0.8 | 0.4 | 0.2 |
| | Maximal | 6.0 | 4.0 | 3.0 | 2.0 | 2.0 |
| Duration | Minimal | 5.0 | 2.3 | 3.3 | 1.8 | 2.8 |
| | Mean | 15.6 | 10.8 | 12.2 | 14.9 | 39.6 |
| | Maximal | 74.0 | 22.0 | 40.0 | 32.0 | 74.0 |
| Intensity | Minimal | 1.8 | 2.3 | 3.3 | 1.8 | 2.8 |
| | Mean | 3.7 | 3.7 | 4.4 | 2.7 | 3.0 |
| | Maximal | 6.1 | 6.1 | 5.8 | 3.9 | 3.2 |
| Onset Rate | Minimal | 0.0 | 0.1 | 0.1 | 0.1 | 0.0 |
| | Mean | 0.3 | 0.4 | 0.4 | 0.3 | 0.1 |
| | Maximal | 1.2 | 1.2 | 0.8 | 0.5 | 0.2 |
| Decline Rate | Minimal | 0.0 | 0.1 | 0.1 | 0.1 | 0.0 |
| | Mean | 0.4 | 0.6 | 0.5 | 0.2 | 0.1 |
| | Maximal | 1.9 | 1.9 | 1.4 | 0.7 | 0.4 |

**Discussion - Supplementary Table 6:** Heatwave characteristics (minimal, mean, and maximal values) modelled after Hobday et al. (2016) using published data (Wolf et al. 2020) and additional temperature data from 2019-2021 obtained from GEOMAR meteorology department, Sebastian Wahl, separated after seasons or summarized over the year. Frequency represents the number of events per year or season, the duration represents the time of the events (days), intensity represents the amplitude above the climatological values (°C), onset rate represents the increase of temperature from the time crossing the 90th percentile until the maximum of the event (°C per day) and the decline rate represents the decrease of temperature from the maximum of the event until the time it crosses the 90th percentile (°C per day). For a detailed description of the traits see Figure 1 in Hobday et al. (2016).

| Trait | Trait Characteristic | Annual | Spring | Summer | Fall | Winter |
|---|---|---|---|---|---|---|
| Frequency | Minimal | 0.0 | 0.0 | 0.0 | 0.0 | 0.0 |
| | Mean | 2.0 | 0.5 | 0.7 | 0.4 | 0.5 |
| | Maximal | 6.0 | 3.0 | 3.0 | 2.0 | 2.0 |
| Duration | Minimal | 5.0 | 2.6 | 2.8 | 1.8 | 2.3 |
| | Mean | 13.6 | 16.1 | 9.4 | 8.4 | 21.4 |
| | Maximal | 63.0 | 63.0 | 28.0 | 15.0 | 63.0 |
| Intensity | Minimal | 1.8 | 2.6 | 2.8 | 1.8 | 2.3 |
| | Mean | 3.7 | 4.0 | 4.3 | 2.3 | 3.9 |
| | Maximal | 7.1 | 5.9 | 7.1 | 2.6 | 6.0 |
| Onset Rate | Minimal | 0.0 | 0.1 | 0.1 | 0.0 | 0.0 |
| | Mean | 0.7 | 0.6 | 1.2 | 0.3 | 0.4 |
| | Maximal | 3.1 | 2.5 | 3.1 | 0.7 | 1.4 |
| Decline Rate | Minimal | 0.0 | 0.0 | 0.1 | 0.1 | 0.0 |
| | Mean | 0.4 | 0.3 | 0.4 | 0.3 | 0.4 |
| | Maximal | 1.2 | 0.8 | 1.1 | 0.6 | 1.2 |

**Discussion - Supplementary Table 7:** Results of a linear model for temperature over the years 1997-2018 and 1997-2021.

| **LM Temperature 1997-2018** | | | | | |
|---|---|---|---|---|---|
| Parametric Coefficients | Estimate | Std. Error | df | t-value | p-value |
| Intercept | 10.490 | 0.168 | 20 | 62.289 | 0.000 |
| Year | -0.054 | 0.161 | 20 | -0.334 | 0.742 |
| **LM Temperature 1997-2021** | | | | | |
| Parametric Coefficients | Estimate | Std. Error | df | t-value | p-value |
| Intercept | 10.562 | 0.167 | 23 | 63.265 | 0.000 |
| Year | 0.061 | 0.160 | 23 | 0.378 | 0.709 |

**Discussion - Supplementary Table 8:** Start and end dates for potential upwelling events in the Kiel Fjord, Western Baltic Sea, over a 22-year long sea surface temperature data set (Wolf et al. 2020) covering the years 1997 until 2018. Potential upwelling events (i.e., sharp decrease in water temperature) were identified by visual inspection of heatwave and cold-spell plots of the respective years (Chapter I - Supplementary Figure 11**)**.

| Start Potential Upwelling | End Potential Upwelling | Start Potential Upwelling | End Potential Upwelling |
|---|---|---|---|
| 1997-07-13 | 1997-07-31 | 2007-07-22 | 2007-07-31 |
| 1997-09-04 | 1997-09-25 | 2008-07-06 | 2008-07-09 |
| 1998-06-27 | 1998-06-29 | 2008-07-18 | 2008-07-21 |
| 1998-07-12 | 1998-07-19 | 2008-08-12 | 2008-08-14 |
| 1998-11-15 | 1998-11-20 | 2008-08-31 | 2008-09-05 |
| 1998-12-04 | 1998-12-10 | 2009-07-03 | 2009-07-10 |
| 1999-06-25 | 1999-06-30 | 2009-07-17 | 2009-07-21 |
| 1999-07-19 | 1999-07-23 | 2009-08-24 | 2009-08-31 |
| 1999-08-11 | 1999-08-20 | 2010-07-12 | 2010-07-18 |
| 2000-05-16 | 2000-05-30 | 2010-08-17 | 2010-08-25 |
| 2000-06-22 | 2000-06-25 | 2011-06-16 | 2011-06-19 |
| 2000-07-05 | 2000-07-13 | 2011-08-03 | 2011-08-09 |
| 2001-05-14 | 2001-05-18 | 2011-08-25 | 2011-08-30 |
| 2001-07-07 | 2001-07-13 | 2012-06-30 | 2012-07-10 |
| 2001-07-29 | 2001-08-06 | 2012-07-26 | 2012-07-31 |
| 2002-06-21 | 2002-07-03 | 2013-06-12 | 2013-06-16 |
| 2003-06-08 | 2003-06-10 | 2013-06-20 | 2013-06-24 |
| 2003-06-18 | 2003-06-24 | 2014-05-07 | 2014-05-12 |
| 2003-07-01 | 2003-07-03 | 2014-08-08 | 2014-08-24 |
| 2004-06-23 | 2004-06-25 | 2015-07-05 | 2015-07-09 |
| 2004-09-11 | 2004-09-15 | 2015-07-24 | 2015-07-30 |
| 2005-07-03 | 2005-07-05 | 2016-06-25 | 2016-07-03 |
| 2005-07-29 | 2005-08-01 | 2016-08-19 | 2016-08-26 |
| 2005-11-15 | 2005-11-22 | 2017-06-03 | 2017-06-12 |
| 2006-05-14 | 2006-05-25 | 2017-09-29 | 2017-10-13 |
| 2006-07-29 | 2006-08-03 | 2018-06-12 | 2018-06-21 |
| 2006-08-13 | 2006-08-16 | 2018-07-27 | 2018-08-12 |
| 2007-05-05 | 2007-05-08 | 2018-08-23 | 2018-08-28 |

### *Supplementary References*

Hobday, Alistair J.; Alexander, Lisa V.; Perkins, Sarah E.; Smale, Dan A.; Straub, Sandra C.; Oliver, Eric C.J. et al. (2016): A hierarchical approach to defining marine heatwaves. In Progress in Oceanography 141, pp. 227–238. DOI: 10.1016/j.pocean.2015.12.014.

Wolf, Fabian; Bumke, Karl; Wahl, Sebastian; Nevoigt, Frauke; Hecht, Ute; Hiebenthal, Claas; Pansch, Christian (2020): High resolution water temperature data between January 1997 and December 2018 at the GEOMAR pier surface. PANGAEA. DOI: 10.1594/PANGAEA.919186

# Acknowledgements

First of all, I would like to thank **Associate Prof. Dr. Christian Pansch-Hattich** for his great supervision throughout the past years. I am very happy that **Christian** guided me through my doctoral project and helped me with his constructive comments that improved me as a scientist. Furthermore, I would like to thank **Prof. Dr. Martin Wahl** for his support of my doctoral project and thesis. Moreover, I acknoweledge my further advisors **Dr. Frank Melzner** and **Dr. Florian Weinberger** for helpful disccusions and realisation of my experiments.

I further thank the **Deutsche Bundesstitftung Umwelt** (DBU) for funding my doctoral project through a granted Promotionsstipendium (20018/553).

Moreover, I am very happy for the good times in Hohenbergstraße with everyone of the **Benthic Ecology Group**. I really enjoyed the supporting environment and knew that there was always an open ear for any problems or concerns I had. Particularly, I want to thank **Dr. Jahan Vajedsamiei** and **Dr. Francisco Rafael Barboza** for their help with my statistical analyses. Apart from just being good colleagues, I became friends with many of you (you all know who I mean). Thank you for the great time.

Furthermore, I want to thank **all my friends** for supporting me when needed and making my time as a doctoral researcher a fun and enjoyable time. Finally, I want to say thank you to my **parents and brother** for all the love and support I received from you during the last years. I am extremely grateful to have such a cool family. And last but not least, I want to thank **Chantal Mudlaff** for all the love, emotional support, and just being the best partner, I could wish for. Thank you all.

# Declaration

I, Fabian Jeldrik Wolf, hereby declare that the dissertation submitted, entitled "**Extreme events and warming in the Baltic Sea: relevance for coastal benthic communities**" was written independently by me and only using the sources listed. The content and design of this thesis, apart from the supervisor's guidance, is my own work. The thesis has not been submitted either partially or wholly as a part of a doctoral degree to another examining body and is my first and only doctoral procedure. In time of defence, **Chapter I** of this thesis is published in *Frontiers in Marine Science*, **Chapter II** of this thesis is resubmitted to *Proceedings of the Royal Society B*, and its state is under review, while **Chapter III** of this thesis is not yet submitted to a scientific peer-reviewed journal. The authors' share of the manuscripts is explained in the subsection Chapters and authors contributions (pages 26-27). This work has been prepared respecting the Rules of Good Scientific Practice of the German Research Foundation. I have not been deprived of an academic degree.

Kiel, 19.05.2022

Wolf
……………………
Fabian Jeldrik Wolf